

Thermal Properties of 1847 WISE-observed Asteroids

DENISE HUNG,¹ JOSEF HANUŠ,² JOSEPH R. MASIERO,³ AND DAVID J. THOLEN¹

¹*Institute for Astronomy, University of Hawai'i, 2680 Woodlawn Drive, Honolulu, HI 96822, USA*

²*Charles University, Faculty of Mathematics and Physics, Institute of Astronomy, V Holešovičkách 2, 18000 Prague, Czech Republic*

³*Caltech/IPAC, 1200 E. California Boulevard, MC 100-22, Pasadena, CA 91125, USA*

ABSTRACT

We present new thermophysical model (TPM) fits of 1847 asteroids, deriving thermal inertia, diameter, and Bond and visible geometric albedo. We use thermal flux measurements obtained by the Wide-field Infrared Survey Explorer (WISE; Wright et al. 2010; Mainzer et al. 2011) during its fully cryogenic phase, when both the 12 μ m (*W3*) and 22 μ m (*W4*) bands were available. We take shape models and spin information from the Database of Asteroid Models from Inversion Techniques (DAMIT; Āurech et al. 2010) and derive new shape models through lightcurve inversion and combining WISE photometry with existing DAMIT lightcurves. When we limit our sample to the asteroids with the most reliable shape models and thermal flux measurements, we find broadly consistent thermal inertia relations with recent studies. We apply fits to the diameters D (km) and thermal inertia Γ (J m⁻² s^{-0.5} K⁻¹) normalized to 1 au with a linear relation of the form $\log[\Gamma] = \alpha + \beta \log[D]$, where we find $\alpha = 2.667 \pm 0.059$ and $\beta = -0.467 \pm 0.044$ for our sample alone and $\alpha = 2.509 \pm 0.017$ and $\beta = -0.352 \pm 0.012$ when combined with other literature estimates. We find little evidence of any correlation between rotation period and thermal inertia, owing to the small number of slow rotators to consider in our sample. While the large uncertainties on the majority of our derived thermal inertia only allow us to identify broad trends between thermal inertia and other physical parameters, we can expect a significant increase in high-quality thermal flux measurements and asteroid shape models with upcoming infrared and wide-field surveys, enabling even more thermophysical modeling of higher precision in the future.

Keywords: minor planets, asteroids: general

1. INTRODUCTION

Thermal inertia is the measure of a material's resistance to changes in its temperature and can be a useful tool for inferring the surface properties of asteroids. The thermal inertia Γ of a material increases with the thermal conductivity κ , density ρ , and specific heat capacity c by $\Gamma = \sqrt{\kappa\rho c}$. Low thermal inertia values are consistent with high porosity or loose regolith, while high values can suggest the presence of conductive materials such as compact rocks and metals. Thermal inertia also governs the Yarkovsky effect, which is a net force that arises from anisotropic thermal emission that perturbs the orbits of asteroids over time (see the reviews by Bottke et al. 2006; Vokrouhlický et al. 2015). Because of nonzero thermal inertia, an asteroid will absorb the most heat from the Sun at its subsolar point but only rera-

diate it some time later in its rotation. The transverse component of the resulting recoil will cause a prograde rotating asteroid to spiral outwards, while a retrograde rotating asteroid will spiral inwards (Bottke et al. 2006). The Yarkovsky effect is in part responsible for how asteroid populations are distributed across the solar system today and is important to consider when assessing the impact probabilities of potentially hazardous asteroids (e.g., Farnocchia et al. 2013).

Asteroid surfaces have been found to have lower than expected thermal inertia values than their material counterparts on Earth, suggesting high porosity. Using a sample of 85 Centaurs and trans-Neptunian objects (TNOs) with thermal observations from Herschel and Spitzer, Lellouch et al. (2013) derived thermal inertia that were two to three orders of magnitude smaller

than expected for compact ice. Early results from the sample return missions Origins, Spectral Interpretation, Resource Identification, Security, Regolith Explorer (OSIRIS-REx) to (101955) Bennu (Lauretta et al. 2019) and Hayabusa-2 to (162173) Ryugu (Okada et al. 2020) have found both asteroids to have thermal inertia between 300 and 350 $\text{J m}^{-2} \text{s}^{-0.5} \text{K}^{-1}$, or much smaller than expected for solid rock. As in situ measurements are presently very few in number, it is unclear whether the subkilometer near-Earth asteroids (NEAs) such as (101955) Bennu and (162173) Ryugu are representative of other B- and C-type asteroids or not.

It is difficult to comment on the average thermal inertia representative of various asteroid subpopulations as existing thermal inertia estimates only number in the few hundreds and cover a wide range in values, from 0 to nearly 1500 $\text{J m}^{-2} \text{s}^{-0.5} \text{K}^{-1}$ (see Table 3). Previous studies have attempted to identify how thermal inertia might correlate with other physical properties such as spectral type, rotation period, and size (e.g., Delbo' et al. 2015; Hanuš et al. 2018a; Alí-Lagoa et al. 2020). Due to the inverse dependency of skin depth with rotation speed, the heat from solar radiation can penetrate the thin topmost regolith layers of slowly rotating asteroids and reach the denser, more highly thermally conductive subsurface material. It was thus hypothesized that slow rotators (i.e., rotation periods longer than 12 hours) should on average present higher thermal inertia than those of fast rotators. While early studies such as Harris & Drube (2016) and Marciniak et al. (2018) appeared to confirm this trend, later studies with larger samples of slow rotators (e.g., Marciniak et al. 2019; Alí-Lagoa et al. 2020; Marciniak et al. 2021) found no such relation.

The inverse correlation between asteroid thermal inertia and size was first identified by Delbo' et al. (2007). We would expect large asteroids to have low thermal inertia values as their weathered surfaces have accumulated several layers of regolith over hundreds of millions of years. On airless bodies, heat can only be transported through direct conduction or inefficient radiation (Gundlach & Blum 2013). As the grain size of the regolith decreases (e.g., the finer grains in mature regolith), the area of contact between grains also decreases, reducing the thermal conductivity of the material and thus the thermal inertia. The thermal conductivity of the finely powdered lunar regolith is three orders of magnitude lower than that of compact rock (Delbo' et al. 2015), corresponding to a low thermal inertia of around 50 $\text{J m}^{-2} \text{s}^{-0.5} \text{K}^{-1}$ (e.g., Hayne et al. 2017).

Simple thermal models such as the widely used Near-Earth Asteroid Thermal Model (NEATM; Harris 1998) can derive diameters and albedos in the many cases where various physical properties of the asteroids are unknown. However, the thermal inertia can only be constrained using more sophisticated models, such as thermophysical models (TPMs) which numerically solve the heat transfer equation on a large number of plane surface facets to fully represent an asteroid's surface temperature distribution, generating synthetic flux values to compare with observations (e.g., Spencer et al. 1989; Lagerros 1996; Delbo' et al. 2007; Rozitis & Green 2011). Whereas simple thermal models assume a spherical asteroid so that they can be widely applied to any thermal data set, TPMs require shape models as input, which are unknown for the vast majority of asteroids. The absence of shape information or thermal data precludes the use of a TPM, and large uncertainties on the derived thermal inertia estimates is common due to the scarcity of high-quality data (see, e.g., Hanuš et al. 2018a).

The accuracy of physical properties derived with a TPM improves with greater detailed shape models and higher precision multiband infrared data. However, it is not uncommon to see large reduced χ^2 values in TPM fits, due to systematic uncertainties that might be introduced in both thermal observations (e.g., as a result of flux offsets between different instruments) and thermophysical modeling. The recent rise of high-precision thermal infrared surveys of asteroids such as the Wide-field Infrared Survey Explorer (WISE; Wright et al. 2010) has motivated the need for further optimization in TPMs, as the scale of model uncertainties are now comparable to that of measured flux uncertainties (Delbo' et al. 2015). The accuracy of shape models is now in some cases a limiting factor, where differences between the assumed shape model and the asteroid's true shape can lead to poor fits (e.g., Rozitis & Green 2014). In addition, current TPMs are largely limited to using convex models with an average albedo and roughness rather than detailed surfaces. However, asteroid shape models have become more common in recent years due to both the public availability of fast, robust lightcurve inversion codes (Kaasalainen & Torppa 2001) and a growing archive of photometric data (Warner et al. 2009).

The lightcurve inversion code works best with temporally dense photometry, where there are hundreds of measurements over one revolution. However, the code can also be successful with combined independent internally calibrated data sets of temporally sparse photometry, such as measurements obtained by all-sky surveys that only have a few measurements per night. These all-

sky surveys provide the largest quantity of photometric data, though unique spin and shape solutions can be difficult to find due to high noise in the data. Āurech et al. (2019) combined the Lowell Observatory photometric database with the more accurate sparse photometry in Gaia Data Release 2 (DR2; Gaia Collaboration et al. 2018), which were both available for over 5000 asteroids. However, the authors were only able to derive roughly 1000 unique shape models through lightcurve inversion due to limitations imposed by the poor photometric accuracy of the Lowell data as well as the small number of Gaia DR2 data points. The latter issue will resolve itself once the final Gaia catalog is released, and more powerful upcoming all-sky surveys will enable even more accurate spin and shape models. As our knowledge of the physical properties of asteroids increases, the better insight we will have on both individual asteroids and on the population as a whole.

2. DATA AND METHODOLOGY

For our TPM, we use the C++ code developed by Delbo’ et al. (2007), which is publicly available¹ and one of the most commonly used standard implementations in the field. The TPM takes input information about the asteroid in terms of thermal flux, an ephemeris, a shape model, rotation period, and pole orientation. Our selection criteria for each parameter are chosen largely following the methodology of Hanuř et al. (2015) and references therein, which we summarize here.

2.1. Thermophysical Modeling Inputs

For the flux observations, we use the thermal infrared data taken by the Wide-field Infrared Survey Explorer (WISE; Wright et al. 2010; Mainzer et al. 2011) during its fully cryogenic phase between 2010 January 14 to August 6 where both the $12\mu\text{m}$ ($W3$) and $22\mu\text{m}$ ($W4$) bands were available. Asteroids in this time period were at most observed by WISE in two epochs, with many only having observations in a single epoch. We restrict the TPM application to WISE-observed asteroids with both $W3$ and $W4$ band data. By doing so, we avoid the complications of the presence of reflected sunlight in the $3.4\mu\text{m}$ ($W1$) and $4.6\mu\text{m}$ ($W2$) bands, which our TPM cannot properly model, though a number of past studies using WISE data with other models have made some use of these bands (e.g., Alı-Lagoa et al. 2013; Myhrvold 2018; Rozitis et al. 2018; Jiang et al. 2019;

Yu & Ip 2021). The inclusion of two bands additionally places greater constraints on the TPM fit and size scaling, allowing us to determine properties such as the asteroid’s thermal inertia.

We select which WISE data to use in the TPM largely following the methodology of Masiero et al. (2011). We first obtain R.A./decl./time values from the Minor Planet Center (MPC) observation file² by selecting all observations submitted from observatory code C51. We then use these ephemerides as input to query the WISE All-Sky Single Exposure (L1b) Source Table through the Gator tool provided by the Infrared Science Archive (IRSA; WISE Team 2012).³ We limit our search radius to within 2 s and $0.3''$ of the time and position of the MPC reported detections in order to minimize the inclusion of unrelated observations. We search for possible star and galaxy contaminants using the positions of the L1b catalog to query the AllWISE Atlas Metadata Table (also served by IRSA) within a search radius of $6.5''$, which is equivalent to the $W1$, $W2$, and $W3$ beam sizes. We discard all asteroid observations at positions where a source was found.

We only include observations with artifact flags of `cc.flags=0` or `p`, which indicate no or possible contamination. The calibration software was found to be overly aggressive in artifact flagging, with `cc.flags=0` and `cc.flags=p` detections having similar fluxes, so the majority of the latter can be treated as reliable (Masiero et al. 2011). We use quality flags `ph.qual=A`, `B`, or `C`, which respectively correspond to signal-to-noise (S/N) ratios of $S/N \geq 10$, $3 < S/N < 10$, and $2 < S/N < 3$. We impose a constraint of a frame quality score `qual.frame=10` to ensure we do not include observations corrupted by image artifacts or electronic noise. We require a South Atlantic Anomaly (SAA) separation value of `saa.sep > 0`, which indicates that WISE was outside of the SAA boundary. Due to concerns regarding nonlinearity and saturation for very bright objects, we exclude observations brighter than $W3 = -2$ and $W4 = -6$ in Vega magnitudes (Cutri et al. 2012).

As a precaution against contamination from spurious sources, we only include observations with $W3$ and $W4$ band errors of $\sigma \leq 0.25$ mag. However, if we have an observation with $\sigma_{W3} \leq 0.25$ mag, we also include the $W4$ observation even if its error is larger than our cutoff.

² <http://www.minorplanetcenter.net/iau/ECS/MPCAT-OBS/MPCAT-OBS.html>

³ <https://irsa.ipac.caltech.edu/cgi-bin/Gator/nph-scan?mission=irsa&submit=Select&projshort=WISE>

¹ https://www.oca.eu/images/LAGRANGE/pages_perso/delbo/thermops.tar.gz

The TPM benefits greatly from the inclusion of multiple bands. The WISE photometric software simultaneously fits a profile to all four bands, using information from each to find the center. The higher S/N observation will control the fit centroid, so we can be confident that the source is present, with the profile scaled to the observed flux. To further ensure that we have two bands to use in our thermophysical modeling, we only include asteroids that have total observations in the $W3$ or $W4$ band of at least 40% of the other band after our data use cuts, with a minimum of five observations per band. The WISE catalog uncertainties do not include the 0.03 mag systematic internal repeatability component found in comparisons with other catalogs⁴ (Cutri et al. 2012). To account for this, we add 0.03 mag in quadrature to all reported errors. We convert from magnitudes to flux density with the zero-points in Wright et al. (2010) modified for red sources: 306.681 Jy for $W1$, 170.663 Jy for $W2$, 31.3684 Jy for $W3$, and 7.9525 Jy for $W4$. The central wavelengths for $W3$ and $W4$ are shifted to $\lambda_{0,W3} = 11.0984 \mu\text{m}$ and $\lambda_{0,W4} = 22.6405 \mu\text{m}$ to correct for the discrepancy observed in photometric calibration tests between blue- and red-spectrum objects. We apply the Wright et al. (2010) color corrections for the $W3$ and $W4$ fluxes when passing the thermal data into the TPM.

The asteroid ephemerides used in the TPM are generated such that they span 50 rotations (or a minimum of 10 days) before the first observation to a few days after the last observation in one-day steps. The initial value of the temperature is set at a value given by the first ephemeris point, so setting the start of the ephemerides earlier gives the TPM time to find a more realistic temperature by the time it reaches the first observing epoch. We use the IMCCE Miriade service⁵ for its ease of extracting computed ephemerides via HTTP requests. The dates are then corrected for the light travel time before being passed into the TPM.

The TPM uses a convex polyhedron with triangular facets for the shape model. The shape models and spin information we use are sourced from the Database of Asteroid Models from Inversion Techniques (DAMIT; Āurech et al. 2010)⁶, last retrieved on 2020 November 1. DAMIT also provides its public lightcurve inversion code, which we discuss in §2.3. For many of the asteroids, the pole orientation is ambiguous, resulting in

multiple (usually two) possible shape models and associated spin information for one asteroid. In these cases, we run the TPM on each shape model.

2.2. Thermophysical Modeling Application

We apply the TPM following the methodology of Hanuš et al. (2015). The TPM is run over a grid of three free parameters: the thermal inertia Γ , Bond albedo A , and the surface roughness. The presence of craters on an asteroid will have an effect on its thermal infrared flux due to the interplay between the craters' shadows and heat transfer on the asteroid's surface. In our TPM application, the effects of the surface roughness are described by two parameters, the crater opening angle γ_c and crater density ρ_c (Table 1). For a given pair of γ_c and ρ_c , the TPM computes the Hapke (1984) mean surface slope $\bar{\theta}$, which represents the macroscopic roughness angle and is defined by

$$\tan \bar{\theta} = \frac{2}{\pi} \int_0^{\pi/2} \tan \theta a(\theta) d\theta \quad (1)$$

where θ is the angle of a given facet from horizontal and $a(\theta)$ is the distribution of the surface slopes, which are respectively analogous to γ_c and ρ_c . The thermal emission spectrum depends only on $\bar{\theta}$, for which different combinations of γ_c and ρ_c can yield the same value. Any two surfaces with the same value of $\bar{\theta}$ will produce similar disk-integrated thermal emission spectra. The exact values for γ_c and ρ_c thus do not matter for the TPM application beyond the effective overall roughness they produce (Emery et al. 1998).

We fix the bolometric emissivity ϵ at 0.9, which is the typical average spectral emissivity for the WISE band wavelengths we are using. The TPM is also run using the Lagerros (1996, 1997, 1998) approximation, which uses a simplified heat diffusion model for the craters and is suitable for small phase angle observations, saving significant computational time over the full solution.

We run the TPM on 10 loops, one for each surface roughness profile. At the start of each loop, we set the Bond albedo to 0.08 and the thermal inertia to $10^4 \text{ J m}^{-2} \text{ s}^{-0.5} \text{ K}^{-1}$ to find an initial diameter estimate. The loop then runs the thermal inertia through progressively lower values down to $0 \text{ J m}^{-2} \text{ s}^{-0.5} \text{ K}^{-1}$, using progressively finer steps as the TPM fit may become more sensitive to low thermal inertia values. Most asteroids are expected to have significantly lower thermal inertia than

⁴ https://wise2.ipac.caltech.edu/docs/release/allsky/expsup/sec6_3b.html

⁵ <http://vo.imcce.fr/webservices/miriade/>

⁶ <https://astro.troja.mff.cuni.cz/projects/damit/>

Table 1. Surface Roughness

Opening Angle (°)	Crater Density	Hapke Mean Surface Slope (°)	Qualitative Roughness
γ_c	ρ_c	$\bar{\theta}$	
0	0.0	0.0	None
30	0.3	3.9	Low
40	0.7	12.6	Moderate
41	0.9	16.5	Moderate
50	0.5	12.0	Moderate
60	0.9	26.7	High
70	0.7	27.3	High
88	0.5	35.8	High
89	0.7	46.8	Extreme
90	0.9	55.4	Extreme

NOTE—This table contains the 10 pairs of opening angles and crater densities we use to approximate the surface roughness in the TPM. The relationship between the opening angle and crater density can produce degenerate overall roughness profiles, described by the Hapke mean surface slope, so these pairs were chosen with only the effective roughness in mind.

our initial value, so we run the thermal inertia from high to low values to give the TPM a few iterations to reach a realistic albedo and size estimate for the asteroid. The TPM scales the surface equivalent size, i.e., the diameter of a sphere with the same surface as the shape model, and from it computes the volume equivalent diameter D . The albedo is updated for each iteration based on the previously found diameter. The H and G parameters are used to convert the diameter from one TPM iteration to a more realistic albedo to use on the proceeding iteration. The relation between the diameter D in kilometers and the visible geometric albedo p_V (Harris & Lagerros 2002) is

$$D = \frac{1329}{\sqrt{p_V}} 10^{-0.2H} \quad (2)$$

The Bond albedo A is then obtained using the phase integral q (Bowell et al. 1989) with

$$A \approx qp_V \approx (0.290 + 0.684G)p_V \quad (3)$$

The values for the absolute magnitude H and slope G are taken from the Asteroid Absolute Magnitudes and Slopes (AAMS; Muinonen et al. 2010; Oszkiewicz et al. 2011) in the Planetary Data System. We do not account for the uncertainty in the H and G values. We note that the thermal inertia has been found to not be strongly dependent on H (Hanuš et al. 2018a). In addition, changes of $\Delta 0.5$ mag in H are compensated by

a change in A (and therefore p_V), resulting in a similar D in Equation 2 (Hanuš et al. 2018a). There is no information on G for the majority of objects, and thus it is assumed to be 0.15 for many of the asteroids in our sample.

The TPM calculates a χ^2 value for each iteration with

$$\chi^2 = \sum_i^N \frac{(F_{\text{obs},i} - F_{\text{mod},i}s^2 - F_{\text{ref},i})^2}{\sigma_{\text{obs},i}^2} \quad (4)$$

where N is the total number of observations over all bands, F_{obs} is the observed flux, F_{mod} is the modeled flux, s is the mesh scaling factor, F_{ref} is the observed reflected flux (assumed to be zero in our application), and σ_{obs} is the uncertainty in the observed flux (Fig. 1).

We caution the reader that this χ^2 value only directly accounts for the uncertainties in the thermal fluxes. The TPM does not account for any uncertainties in either the shape model or the rotation state of the asteroid, so the uncertainties on the derived parameters are best taken to be lower limits. We find the best fit by the TPM solution that yields the smallest χ^2 value. We then estimate the uncertainties in the parameters found by the TPM, the thermal inertia Γ , diameter D , and Bond albedo A .

We use an empirical approach to obtain the approximate 1σ upper and lower bounds of each parameter, where the error bars span all parameter values corre-

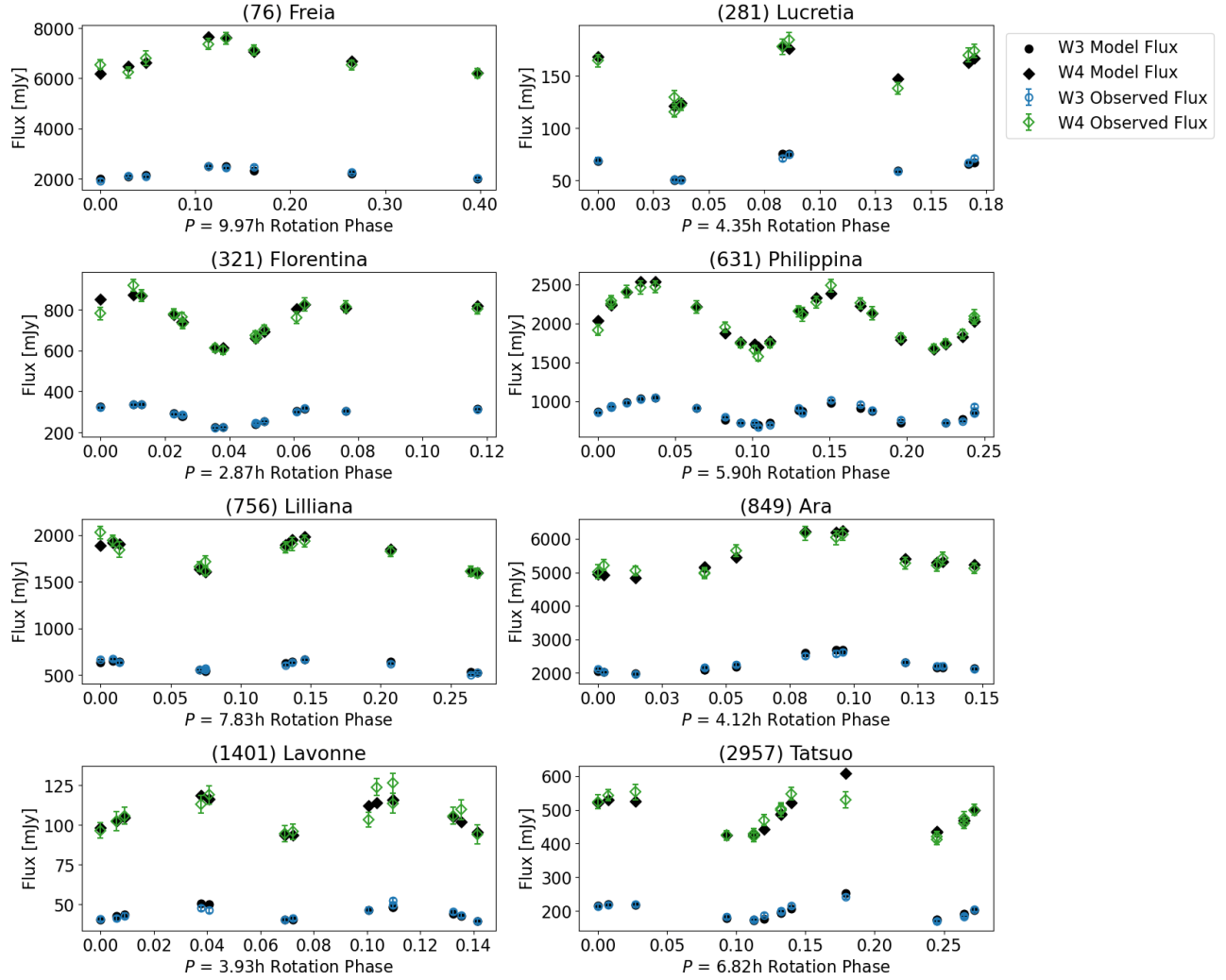


Figure 1. Example TPM fits to WISE thermal data for eight asteroids, folded on the rotation phase. The vast majority of asteroids in our sample were only observed by WISE over one to two days. Due to the cadence and the small number of WISE observations, the rotation phase is usually only sparsely sampled with large gaps in coverage (Wright et al. 2010).

sponding to solutions with $\chi_{\text{red}}^2 < \chi_{\text{min}}^2 (1 + \sigma)$, where $\sigma = \sqrt{2\nu}/\nu$ and ν is the number of degrees of freedom (Press et al. 1986). This approach has been commonly used for TPM studies (e.g., Emery et al. 2014; Hanuš et al. 2015) and gives reliable uncertainties where $\chi_{\text{red}}^2 \sim 1$, though this condition is often not met. As we do not know the exact roughness of the asteroid’s surface, all solutions here include all roughness profiles to provide more robust uncertainty ranges for each parameter. In the few cases where we see more than one local minimum, we estimate each parameter’s uncertainty from the contiguous roughness profile curves containing the best-fit solution.

2.3. Shape Models

Shape models are derived using the lightcurve inversion method and codes developed by Kaasalainen & Torppa (2001) and Kaasalainen et al. (2001), which are publicly available on DAMIT. Many of the lightcurves found on DAMIT can be sourced back to the Asteroid Lightcurve Data Exchange Format database⁷ (ALCDEF; Warner et al. 2011). We largely follow the methodology of Hanuš et al. (2011) using the same code. We summarize this process below.

As input, the code takes any number of lightcurves for an asteroid. As with the TPM files, we take the ephemerides from the IMCCE Miriade service, which serve to correct the data for light travel time. In cases where the lightcurves are calibrated, we transform the

⁷ <http://alcdef.org/>

photometry to intensity, corrected so the asteroid is 1 au from the Sun and 1 au from the observer. If the calibration is not pertinent, such as for the WISE data, we simply normalize the intensity to a mean value of 1. In the case of sparse data, i.e., those from all-sky surveys, we treat the photometry as calibrated. The code does not take into account any flux uncertainties in the lightcurve data.

Obtaining a model first requires finding the correct period for the asteroid. To do this, we make use of a gradient-based algorithm known as convex inversion (CI), which converges to a local minimum given by the initial values of the rotation state parameters: the sidereal rotation period and pole direction. The smallest separation ΔP between two neighboring local minima in the period spectrum of the lightcurve fit can be approximated by a simple relation:

$$\frac{\Delta P}{P} = \frac{1}{2} \frac{P}{T} \quad (5)$$

where P is the rotation period and T is the temporal coverage of the optical data. After each step, ΔP is recomputed from the previous period. Using $0.5\Delta P$ as our period step ensures that we sample all local minima within a given period interval no matter what initial P value is used. For each sample period, we run the CI with 10 different pole orientations isotropically distributed on a sphere. A unique period is found if there are no other solutions with a χ_{LC}^2 below a user-defined threshold multiplied by the χ_{LC}^2 minimum. If the period search is successful, we run the CI with the unique period on a finer grid of pole orientations and look for pole solutions below a new user-defined χ_{LC}^2 cutoff. Due to ambiguities in pole orientation, the search may yield multiple accepted pole solutions, therefore leading to multiple shape models, one for each pole. We identify the pole solution as unique if there are at most two solutions below our defined threshold: the pole and its mirror counterpart. If there is a unique pole solution, we run the CI for each set of unique rotation state parameters and obtain the global shape solution in the representation of a Gaussian image. We then compute the convex polyhedron from the Gaussian image with the Minkowski algorithm, which helps to stabilize the shape solution (Kaasalainen et al. 2001). This polyhedron can then be converted to a shape model with triangular facets that is compatible with the TPM code we use.

One of our goals in this paper is to improve existing shape models from the DAMIT database with WISE observations. In order to accomplish this, we derive

new shape models by taking the existing lightcurves and appending WISE data onto them. We select the WISE data again in the cryogenic phase of the mission so that we minimize the temporal gap between the optical lightcurve data and thermal data. In addition to the $W3$ and $W4$ bands, we now also include the $W1$ and $W2$ bands for the purpose of the lightcurve inversion in deriving a shape model. The lightcurve inversion method is best suited for optical lightcurves such as the reflected sunlight component in the $W1$ and $W2$ bands. However, the shapes of thermal lightcurves have been found to be similar enough to that of optical lightcurves that we can use the $W3$ and $W4$ data as well for our application (Durech et al. 2018a).

The $W1$ and $W2$ data fall under the same constraints we placed on the $W3$ and $W4$ data in §2.1, although now we do not explicitly impose a minimum number of observations per band. Each WISE band is a separate lightcurve, so we get a total of four lightcurves out of one observing epoch if data are available in every band. The WISE data we use fall under the same constraints for keeping observations as in §2.1, with the only change being that we now only keep observations with errors of $\sigma \leq 0.25$ mag as a precaution against including spurious sources. While the TPM uses multiple bands and can control the fit centroid with a higher S/N data point in one band, the lightcurve inversion treats each band independently.

The reader might wonder if we lose some information about the thermal properties by treating the thermal data lightcurves (in this case, the $W1$, $W2$, $W3$, and $W4$ bands) as optical. The presence of a nonzero thermal inertia will introduce a phase offset between the thermal and optical lightcurves, which will in turn shift the lightcurve inversion code’s best-fit rotation period to compensate. However, a unique period often cannot be determined with sparse data alone. The addition of supplemental data such as the WISE photometry will better constrain the rotation state and the shape, particularly for shape solutions that were based only on sparse data or very few dense optical lightcurves. The period is likely to be better constrained by both the abundance of lightcurve coverage around the WISE photometry as well as the fits to the primarily reflected light $W1$ and $W2$ data points. Simultaneously applying the inversion to both optical and thermal infrared data has been shown to provide more realistic estimates of thermophysical parameter uncertainties (Durech et al. 2017).

We set the χ_{LC}^2 threshold in the period search at 5% better than any other χ_{LC}^2 in the period search inter-

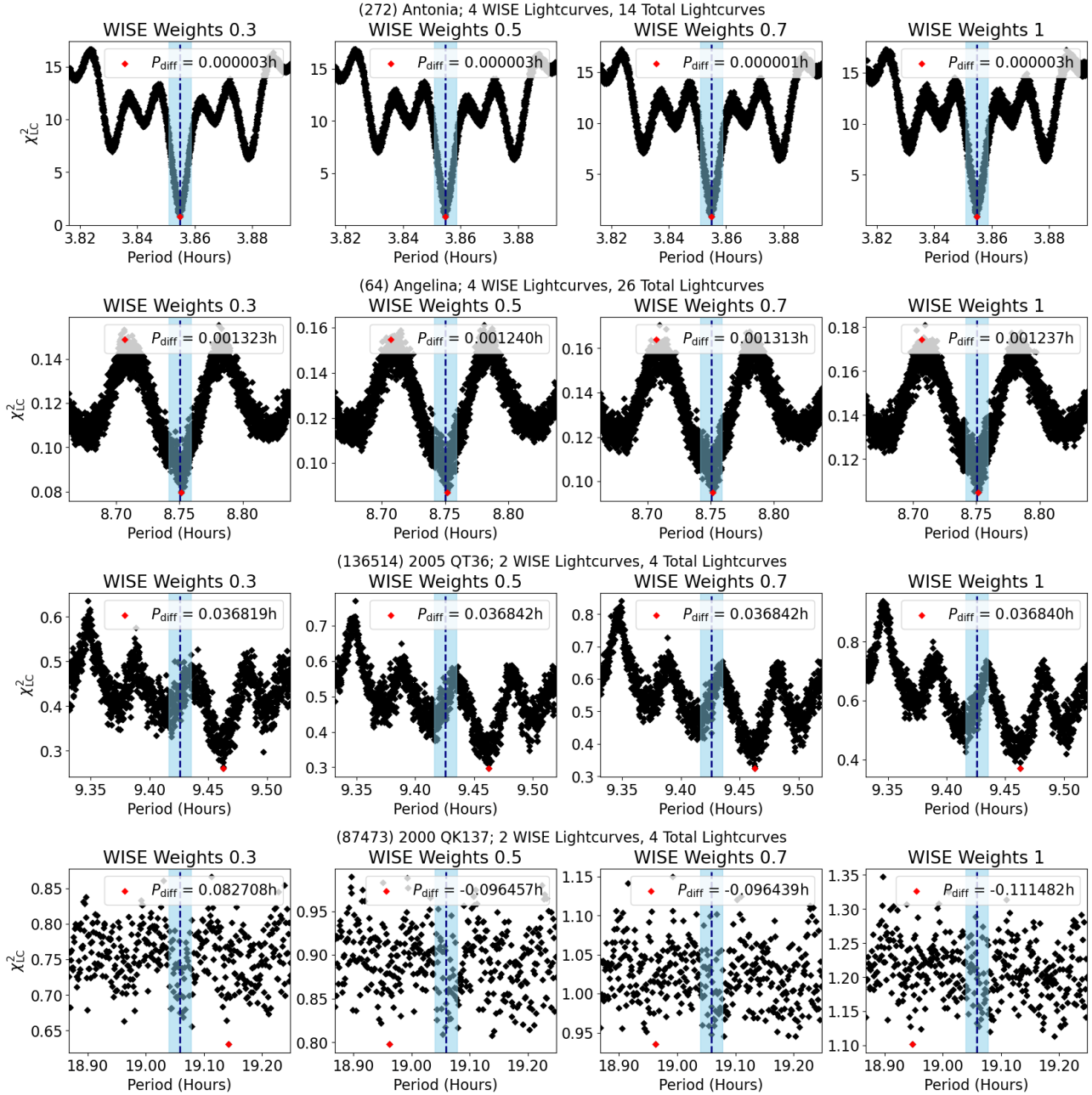


Figure 2. Example outputs of period searches conducted for (272) Antonia, (64) Angelina, (136514) 2005 QT36, and (87473) 2000 QK137. Each period search was conducted four times in total, using weights of 0.3, 0.5, 0.7, and 1 for the WISE lightcurves we supplemented to the DAMIT data set. The original DAMIT period is denoted by the vertical dashed line. The shaded region covers $\pm 0.1\%$ of the original DAMIT period. The period associated with the smallest χ^2_{LC} in the search range is marked in red. The difference between it and the DAMIT period is labeled P_{diff} in each legend. The period search for (271) Antonia shows the ideal periodogram: a strong, tight V-shape with a clear single χ^2_{LC} minimum. Its unique period was automatically identified as there were no other solutions with a χ^2_{LC} under the threshold of $1.05 \chi^2_{LC,\text{min}}$. (64) Angelina is an example of a case where we manually identified the unique period. Like for (272) Antonia, the period search shows a clear V-shape and χ^2_{LC} minimum. However, there were a few other solutions under the χ^2_{LC} threshold with periods differing by a total range of 0.004 hour. (136514) 2005 QT36 is an example of where a unique period was automatically identified, but we rejected the period for its large offset relative to the original DAMIT period—in this case by over 0.3%. Finally, (87473) 2000 QK137 is an example of a periodogram that is mostly flat and shows large scatter, and thus no unique period could be recovered.

val, while we use a 10% cutoff for the finer pole search. If a unique period is automatically identified with our χ_{LC}^2 threshold, we visually inspect the periodograms and reject the period if it is inconsistent with the DAMIT solution (i.e., a period difference of greater than 0.1%). For the period searches where no unique period is automatically identified, we take the period associated with the smallest χ_{LC}^2 if the periodogram has a clear single minimum in χ_{LC}^2 and the period is consistent with the DAMIT solution. This manual inspection allows us to recover unique periods that happened to have a few other solutions that fell under our set χ_{LC}^2 threshold (Fig. 2). Our imposed consistency check with the DAMIT solution is deliberately conservative. While the rotation periods in DAMIT may not necessarily be correct, we lack the compelling evidence in the form of new dense lightcurve data to support significantly discrepant results, and thus we err on the side of caution in our approach.

Though we use the same lightcurves as DAMIT to generate our shape models, DAMIT itself does not list any explicit weighting information. We thus adopt a simple scheme of treating the sparse survey telescope lightcurves with a weight of 0.1, while denser, more classical lightcurves are given a weight of 1. We give the WISE lightcurves a weight of 0.5, as their uncertainties, particularly in the *W1* and *W2* bands, are much larger than the uncertainties of dense optical lightcurves. We also run period searches using weights of 0.3, 0.7, and 1 with the WISE lightcurves to check for consistency, though the results are often largely identical outside of minor overall scaling differences in χ_{LC}^2 . The WISE lightcurves have around an order of magnitude fewer data points than the dense optical lightcurves, so even if the weights were to be overestimated, the data do not dominate in the χ_{LC}^2 calculations. Though ideally the nonsurvey lightcurves should have hundreds of measurements over the entire rotational phase of the asteroid, we note that the existing lightcurves in DAMIT can vary wildly in terms of accuracy, period coverage, and sampling.

3. RESULTS

3.1. TPM Fits with DAMIT Shape Models

In the fully cryogenic WISE data, we identified a total of 97,657 asteroids with sufficient observations meeting our criteria in §2.1 for our thermophysical modeling, but only 2551 among them had existing DAMIT shape models. Of these, 1843 asteroids had two shape models, leaving us with a total of 4935 shape models to use in

the TPM fitting. The vast majority of this set is made up of main-belt asteroids (MBAs), with a small number of Mars crossers, Trojans, and NEAs. For each asteroid, we record the minimum reduced χ^2 of the grid of parameters tested in the TPM run (Fig. 3). We run each TPM fit separately and independently in the cases of asteroids with multiple shape models. We can consider the thermophysical properties derived by the TPM to be well constrained if the TPM fit shows a clear minimum in its χ^2 curve, even if the reduced χ^2 is conventionally considered large (i.e., > 5). Conversely, the thermophysical properties are unconstrained for TPM fits without a clear minimum, even if the reduced χ^2 is small (Fig. 4). Such cases are usually the result of poor thermal data (either too few measurements or large uncertainties), asteroid rotation periods greater than 15 hours, or close to pole-on observing geometries (Hanuš et al. 2018a). A nonzero thermal inertia will introduce an offset between the points of maximum thermal absorption and emission, but this difference is small for slow rotators. In such cases, it is difficult to detect the thermal inertia signal, and therefore the offset is also difficult to constrain. Pole-on observations only show the same region on the asteroid, so the thermal lightcurve remains flat for any combination of thermophysical parameters, and so once again the parameters are difficult to constrain.

For our analysis, we reject all TPM fits where any thermal parameter was found to have zero uncertainty. The TPM code calculates zero and nonzero thermal inertia differently, and very rarely this presents itself as a conspicuous discontinuity in χ^2 between thermal inertia of 0 and $1 \text{ J m}^{-2} \text{ s}^{-0.5} \text{ K}^{-1}$. Out of the 4935 shape models we applied the TPM to, a total of 12 fits were rejected in this manner. In each case, the shape model was derived from very sparse lightcurve data, which was often wholly comprised of only photometry from survey telescopes. In terms of χ^2 cuts, we reject all TPM fits with reduced $\chi^2 > 10$. Additionally, we reject TPM fits with an overall flat distribution in χ^2 . For such cases, the thermal parameters are only poorly constrained at best. We identify these poorly constrained TPM fits by taking note of the ratio between the maximum and minimum χ^2 in the TPM fit and rejecting fits where the ratio is less than 20. We measure this ratio based on the single roughness profile curve that gives the minimum χ^2 in the thermal inertia range $\Gamma < 9000 \text{ J m}^{-2} \text{ s}^{-0.5} \text{ K}^{-1}$ to remove the initial few steps of the TPM before it has reached a realistic albedo and size estimate. Of the 2551 asteroids we modeled with existing DAMIT shape models, 2152 met our initial reduced χ^2 cutoff, while 1811 passed our χ^2 ratio cut.

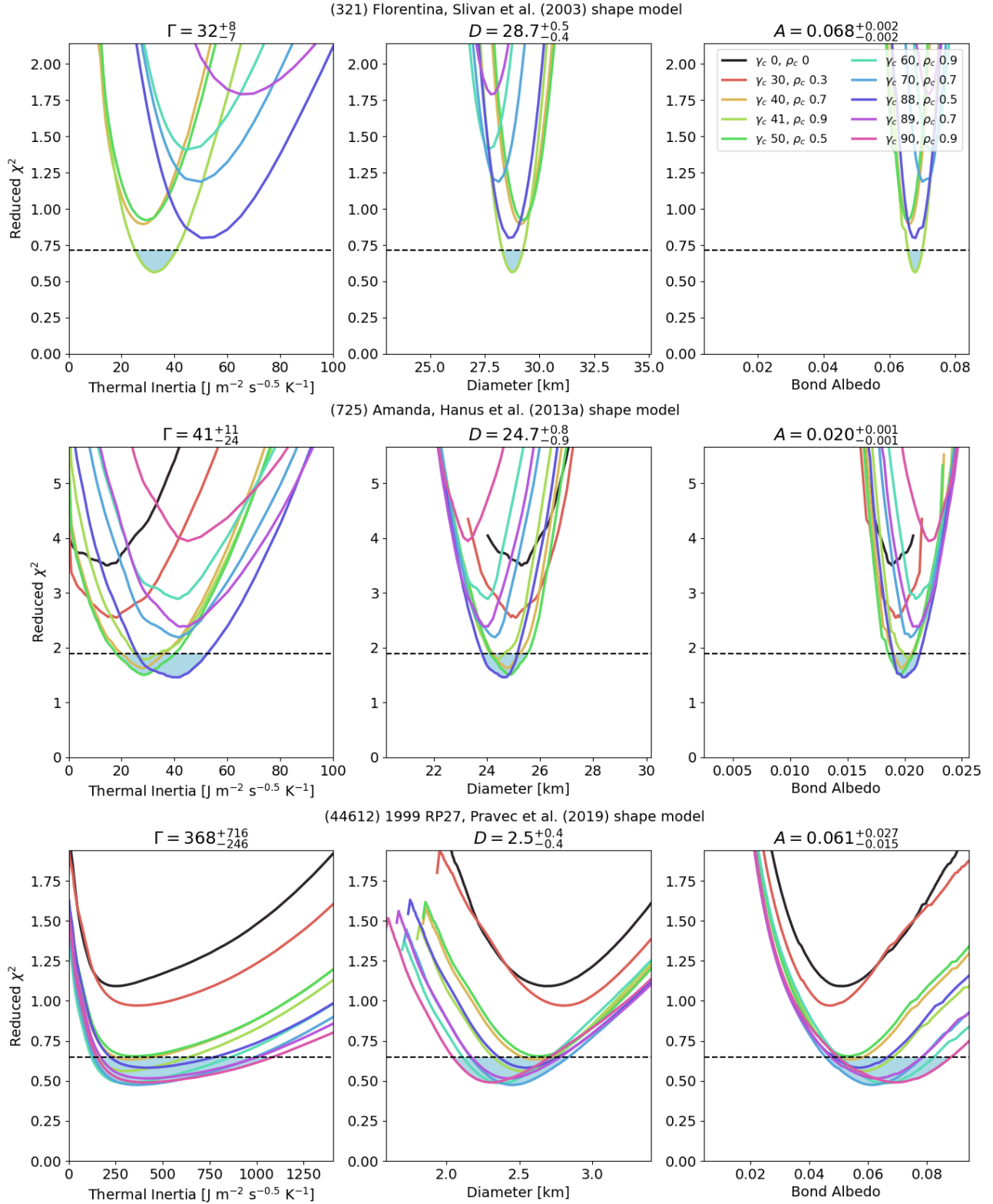


Figure 3. TPM example outputs for (321) Florentina, (725) Amanda, and (44612) 1999 RP27 and their respective best-fit thermal inertia, diameters, and Bond albedos found in Table 4. Each curve represents a different roughness profile as a pair of the crater opening angle γ_c and crater density ρ_c as denoted in Table 1. The dashed horizontal line is drawn at $\chi^2_{\min} (1 + \sigma)$, where σ is related to the degrees of freedom ν by $\sigma = \sqrt{2\nu/\nu}$, and its intersection with the χ^2 curves approximates the TPM fit's 1σ uncertainty bounds of the best-fit thermal parameters found. The shaded region shows the contiguous regions around the χ^2 minimum we use to identify the uncertainty ranges for each parameter.

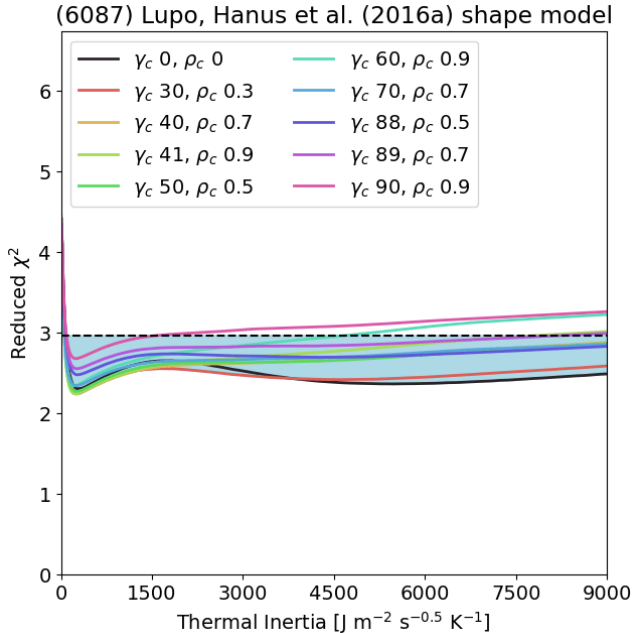


Figure 4. An example of what we consider a poorly constrained TPM fit for (6087) Lupo. Though the minimum reduced χ^2 is not very large at 2.3, the overall flatness of the χ^2 curve leaves the thermal inertia completely unconstrained.

In Figure 5, we plot the fitted thermal inertia, diameters, and albedos for the total of 1722 asteroids in our sample that passed both of our χ^2 cuts. In the cases where an asteroid has multiple shape models, we plot the derived parameters of the TPM fit associated with the smaller χ^2 . The visible geometric albedos are calculated from the Bond albedos using Equation 3. The distributions of diameter and albedo are similar in shape to the distributions found in a much larger set of over 100,000 WISE-observed asteroids through NEATM modeling by Masiero et al. (2011), where the number of asteroids decreases with increasing diameter and the albedo distribution is bimodal. Though we have a fair number of TPM fits with $\Gamma > 1000 \text{ J m}^{-2} \text{ s}^{-0.5} \text{ K}^{-1}$, such values are both physically unrealistic and much higher than most thermal inertia estimates in the literature, as we will discuss further in detail in §4.2. We see no clear trend between each parameter and χ^2 other than in diameter, where there appears to be a χ^2 boundary that decreases with diameter. However, this is primarily a consequence of the larger relative flux uncertainties in WISE observations of smaller asteroids, which drops the χ^2 in the TPM calculations.

3.2. TPM Fits with Revised Shape Models

In our initial TPM results, many of the asteroids have very high minimum χ^2 values, suggesting that the TPM was unable to constrain any parameters with the given input data. One method available to us for improving the TPM results is to improve the shape models. We attempted to derive revised shape models for the 2551 asteroids in our sample by supplementing their lightcurves with WISE data following the methods outlined in §2.3. We obtained a total of 1282 new shape models for 696 asteroids. Due to the sparse lightcurve data available for the majority of our asteroids, we were often unable to resolve the ambiguities in an asteroid’s pole orientation. In such cases, we have two derived shape models for a single asteroid, one each for each pole solution. Due to our selection criteria, the periods of our new shape models are very similar to their original DAMIT counterparts, though there are sometimes large differences in the pole orientation (Fig. 6).

As with the DAMIT shape models, we again reject all TPM fits where any one thermal parameter was found to have zero uncertainty due to concerns with the TPM’s boundary conditions, removing a total of five TPM fits from consideration, including the single revised shape model available for two asteroids, bringing our total number down to 694 unique asteroids. In Figure 7, we plot our asteroids’ χ^2 of the TPM fits obtained with their revised shape models (where we use the best χ^2 among them if there are multiple models for one asteroid) against the χ^2 obtained from fits using their original shape models. The majority of asteroids appear to fall into either of two groups: one where there is little change between the two shape models and one where the improved reduced χ^2 drops below 10, regardless of the original value. Even among the cases where the χ^2 of the TPM fit worsened with the change in shape model, the χ^2 was still less than 10 for the majority of asteroids. Of the 694 total asteroids, we saw improvements in χ^2 in the TPM fit for 540 asteroids with their revised shape models. Among the asteroids with revised shape models, 205 had their TPM fits originally rejected by our χ^2 cuts in §3.1. The improvements in χ^2 were enough to add 124 of these asteroids to our final sample of derived thermal parameters.

Our input data and results are given in an abridged form in Tables 4 and 5, and the full data sets are available online on the VizieR database of astronomical catalogues at the Centre de Données astronomiques de Stras-

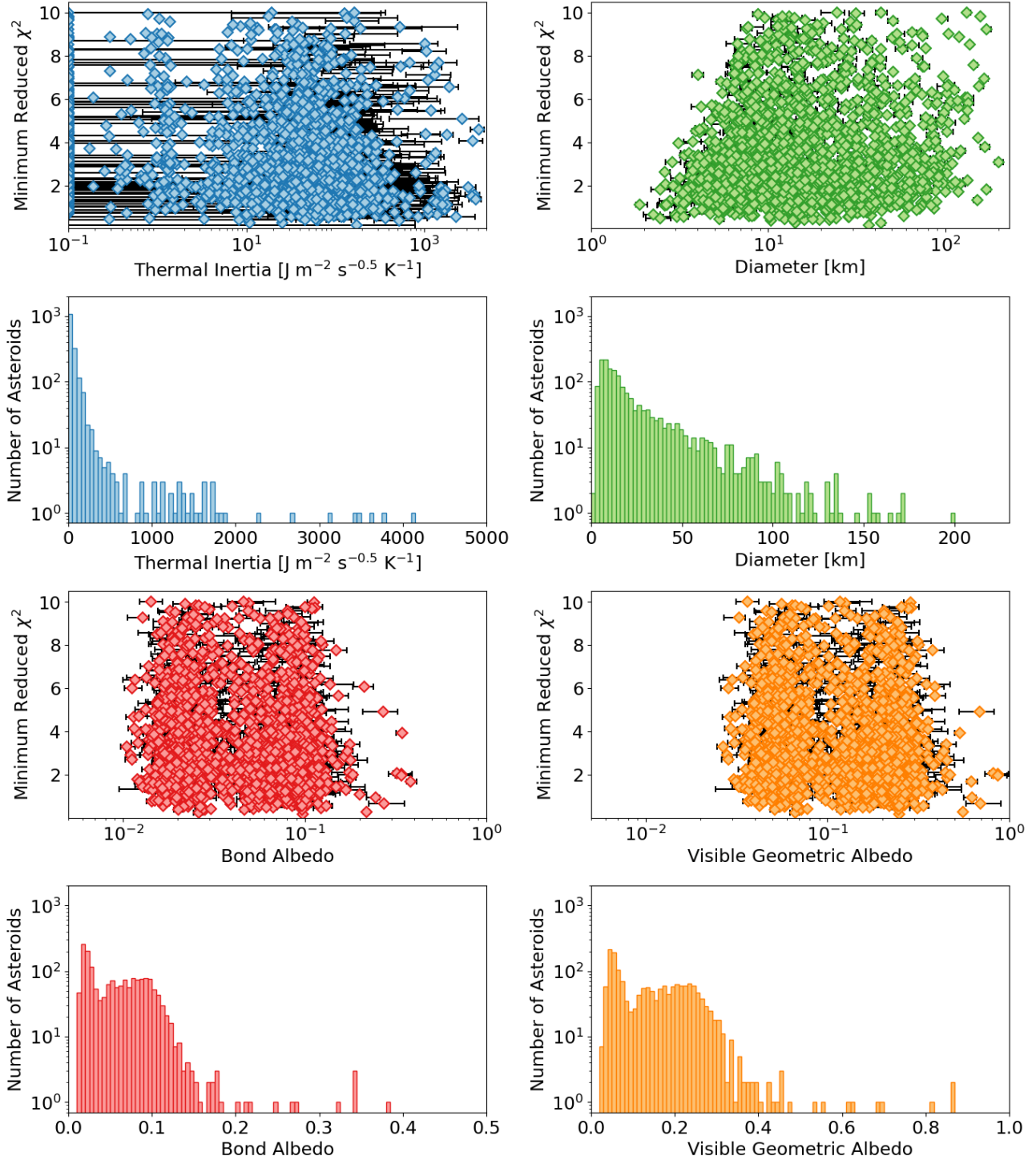


Figure 5. The thermal inertia, diameters, and albedos of our selected 1722 asteroids are shown with their uncertainties plotted against the reduced χ^2 of their TPM fits. The distributions of each parameter, ignoring their uncertainties, are shown in the accompanying histograms. Asteroids with a best-fit thermal inertia of 0 J m⁻² s^{-0.5} K⁻¹ are instead represented here with a value of 0.1 for the sake of the logarithmic scale. Error bars are only plotted for a best-fit thermal inertia of 50 J m⁻² s^{-0.5} K⁻¹ or above in order to avoid visual clutter. We see in the top right panel that there appears to be a χ^2 boundary that decreases with diameter, but this is primarily a consequence of the larger relative flux uncertainties in observations of smaller asteroids. The albedo distribution is clearly bimodal, with a sharp peak at around $A = 0.03/p_V = 0.06$ and a second peak at $A = 0.09/p_V = 0.23$. While there are a few thermal inertia values recorded over 1000 J m⁻² s^{-0.5} K⁻¹, such cases should be treated with caution, as they are physically unrealistic and exceed nearly all other literature thermal inertia estimates.

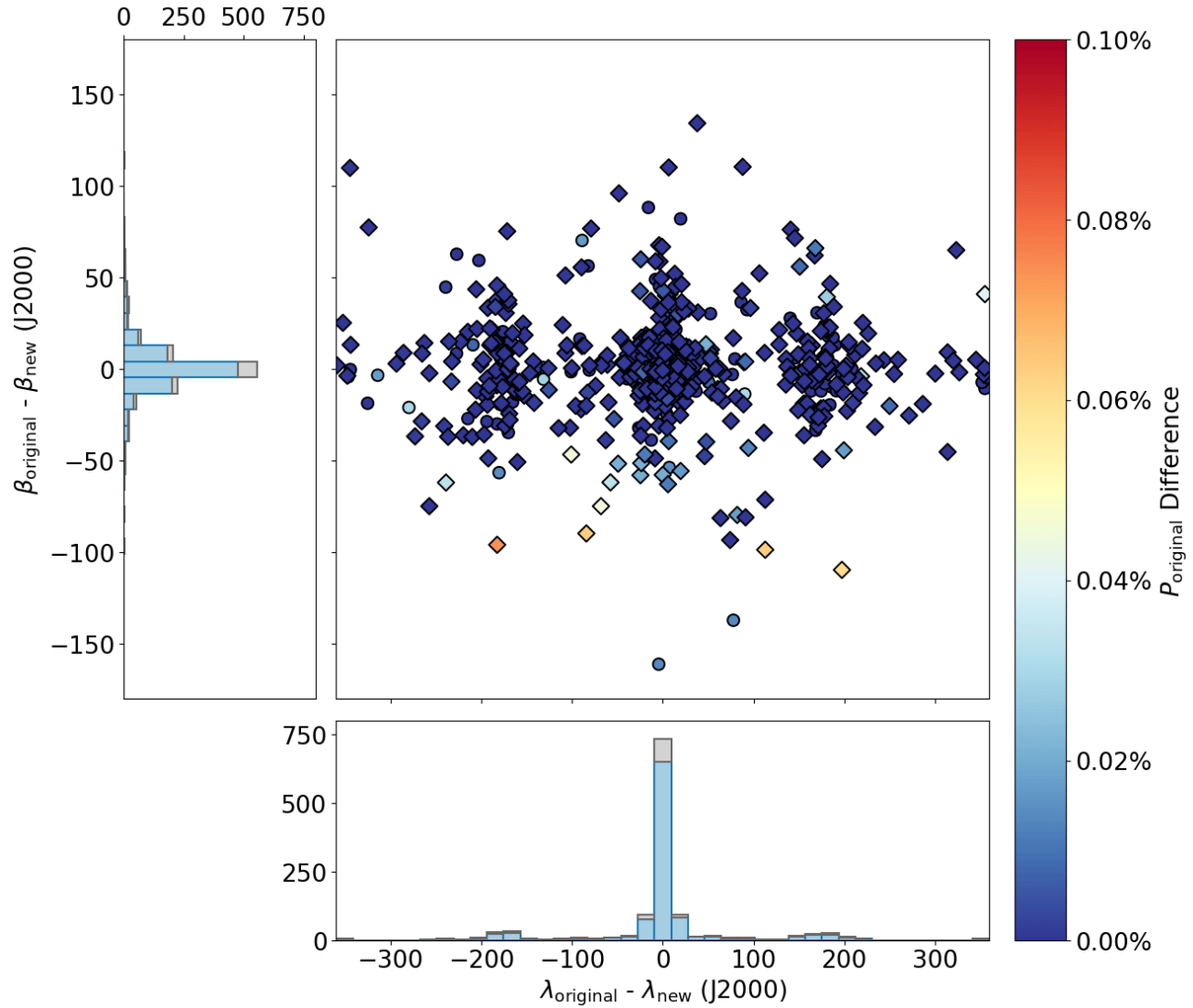


Figure 6. The differences in pole orientation in ecliptic coordinates and period between the original DAMIT shape models and revised shape models for each asteroid. The periods are reported as a percentage difference from the original DAMIT period. The diamond points and colored histograms represent revised shape models where the χ^2 of the associated TPM fits fell into acceptable bounds by our criteria, while the circular points and grayscale histograms represent rejected TPM fits. We obtained a total of 1282 models for 696 asteroids. Of these, 63 asteroids had 1 DAMIT shape model and 1 revised shape model, 148 asteroids had 1 DAMIT shape model and 2 revised shape models, 43 asteroids had 2 DAMIT shape models and 1 revised shape model, and 440 asteroids had 2 DAMIT shape models and 2 revised shape models. In the cases where we had multiple DAMIT shape models, we only report the difference in the revised shape model with the closer DAMIT pole. The majority of revised shape models have poles which fall very closely to the DAMIT solutions with period differences of less than 0.01%. Due to the ambiguities in the pole orientation, we also see the mirror solutions that show up in the local maxima in λ at around $\pm 180^\circ$.

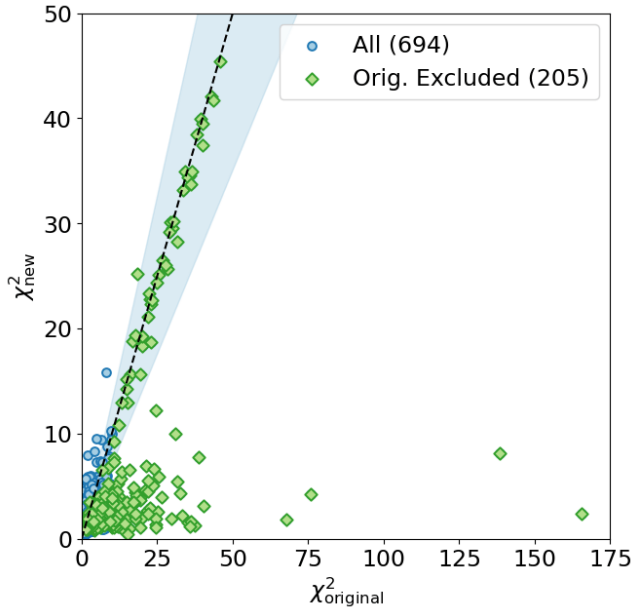


Figure 7. Our TPM fits’ minimum reduced χ^2 values, using both the nominal DAMIT shape models, $\chi^2_{original}$, and our new revised shape models, χ^2_{new} . The points in green show asteroids that were initially removed with the χ^2 cuts in §3.1. The dashed line denotes where the two axes are equal. The shaded region shows where the values of the two axes are within 30% of each other. Of the 694 asteroids with revised shape models, we saw improvements in the χ^2 of their TPM fits for 540 asteroids compared to the fits using their DAMIT shape models. For the majority of asteroids, we either saw little change or slightly larger χ^2 when switching to the revised shape models, but we also had several instances of dramatically improved TPM fits with the revised shape models.

bourg (CDS) website⁸. We report the TPM fit for each shape model used that passed our χ^2 cuts.

It is important to remember that the accuracy of TPM-derived physical properties will depend on the quality of the thermal flux measurements and shape models, particularly in the case of the thermal inertia (Delbo’ et al. 2015). We advise readers to regard any atypical derived thermal inertia values among our results with caution. For example, we find the best-fit thermal inertia of several asteroids to be equal or close to zero. Zero thermal inertia, however, is unphysical in nature. Such derived values may be the product of inaccuracies in the TPM fitting, whether they be in the thermal flux measurements, the shape model, the H and G parameters, or the TPM itself. The derived thermal inertia value is also dependent on the assumed degree

of surface roughness. While we note the best fitting Hapke (1984) mean surface slope for each TPM fit, we remind the reader that our roughness model is both very crude and not evenly sampled in parameter space, and thus should not be taken at face value. Moreover, the majority of asteroids in our sample were only observed by WISE in a single epoch, and the WISE observations for MBAs in general only cover a small total range in solar phase angles (14°–32°; Masiero et al. 2011). The thermal inertia and roughness may therefore share some degeneracy in the thermophysical modeling that we are unable to break due to the lack of infrared observations at multiple phase angles. Wider coverage in terms of wavelength, phase, rotational, and aspect angle would offer greater constraints for the TPM fitting that we do not have access to.

In Figure 8, we identify the best fit for each asteroid between the DAMIT and revised shape models by the χ^2 of the fits, switching to using the revised shape model for 543 asteroids in our sample. Applying the same χ^2 criteria we used in §3.1, we now have 2239 asteroids with reduced $\chi^2 < 10$, 1914 asteroids with a χ^2 ratio greater than 20, and 1847 asteroids meeting both conditions. Of these, we have 476 asteroids where the TPM fits used their revised shape models. The distributions of the thermal inertia, diameters, and albedos are largely unchanged from our original sample. The majority of the revised shape model TPM fits have a thermal inertia of less than $1000 \text{ J m}^{-2} \text{ s}^{-0.5} \text{ K}^{-1}$, which are values more in line with the literature thermal inertia estimates reported in Table 3. In contrast, the revised shape model TPM fits are more evenly distributed over the total ranges of the diameter and albedo.

4. DISCUSSION

4.1. Comparison with NEATM Results

Because many of the asteroids in our sample have previously estimated diameters, we can check the reliability of our results by comparing the diameters found by our best-fit TPM runs with the WISE diameters obtained with NEATM (Harris 1998) and reported in the Planetary Data System (Mainzer et al. 2019). Both sets of diameters were derived using the WISE thermal infrared data, so any significant discrepancies between the two arise from the differences in the models used, i.e., TPM versus NEATM. Of our 1847 asteroid sample, there are 1822 WISE diameters with which we can compare. We plot the WISE and TPM diameters against each other in Figure 9 where we see that 1746 asteroids fall within a 20% agreement, and 1360 of those fall within 10%. We

⁸ <https://cds.u-strasbg.fr/>

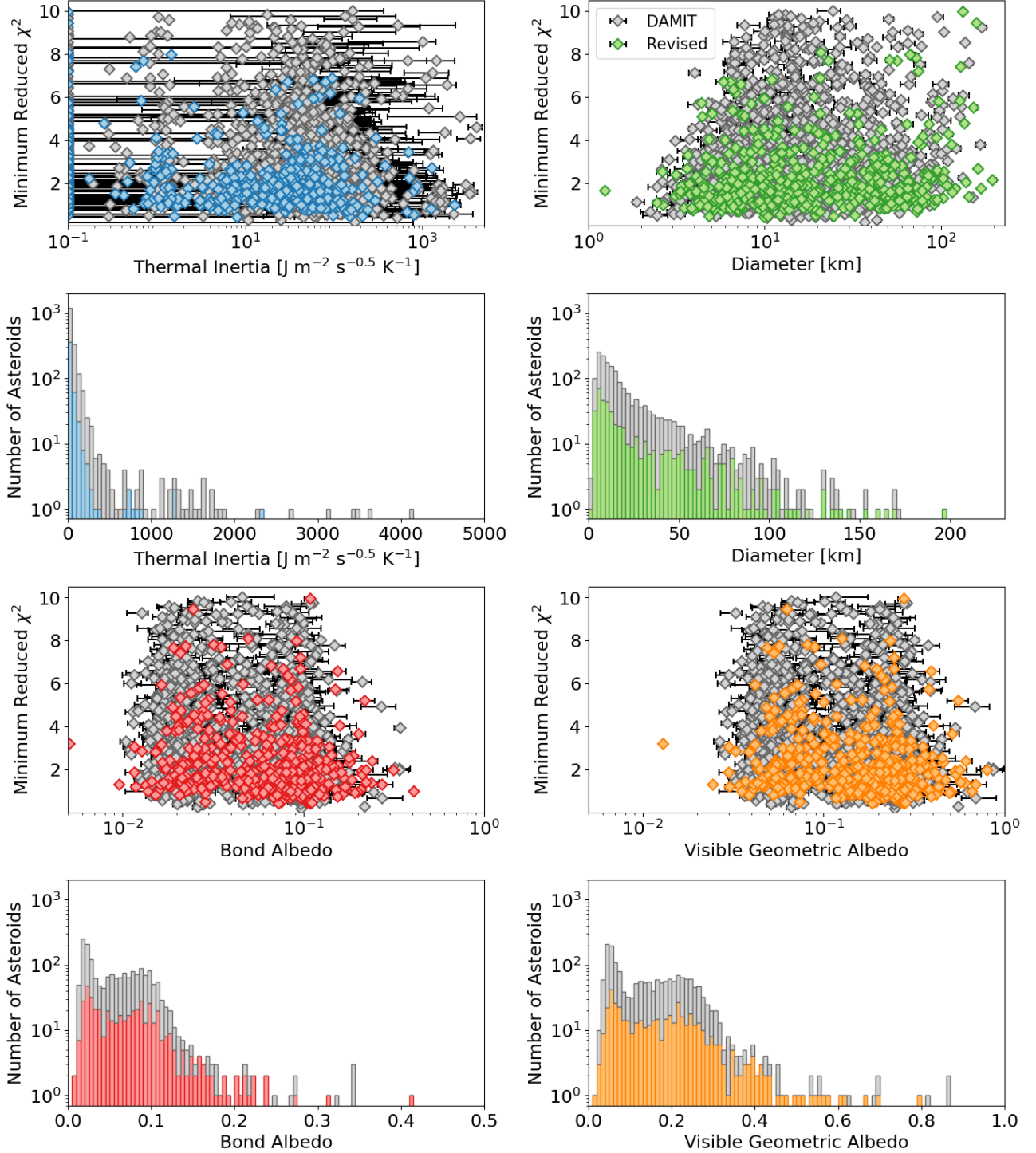


Figure 8. Thermal inertia, diameters, and albedos of our selected 1847 asteroid sample with their associated uncertainties. The visible geometric albedos are calculated from the Bond albedos using Equation 3. As with Figure 5, asteroids with a best-fit thermal inertia of $0 \text{ J m}^{-2} \text{ s}^{-0.5} \text{ K}^{-1}$ are instead represented here with a value of 0.1 to accommodate the logarithmic scale. Error bars are only plotted for best-fit thermal inertia of $50 \text{ J m}^{-2} \text{ s}^{-0.5} \text{ K}^{-1}$ or above in order to avoid visual clutter. The DAMIT points in grayscale refer to the TPM fits using the original shape model and are unchanged from Figure 5. The colored points indicate the 476 cases in this sample where we obtained better TPM fits with the new shape models. Similarly, the colored portions of the histograms represent the fraction of total TPM fits that used the revised shape models. While the majority of the revised shape model TPM fits find thermal inertia values of less than $1000 \text{ J m}^{-2} \text{ s}^{-0.5} \text{ K}^{-1}$, the diameter and albedo values are more evenly distributed throughout their respective total ranges. The smallest asteroid shown in this figure is the 1.2 km NEA (1865) Cerberus, which is conspicuous here only as a result of the very few NEAs in our sample. The very low albedo at $A = 0.005$ and $p_V = 0.013$ belongs to the B-type MBA (1484) Postrema. Such low values for asteroid albedo are extremely rare (see, e.g., Masiero et al. 2011), but our derived estimate agrees within 1σ of the existing estimate derived through NEATM fitting of WISE data by Masiero et al. (2014).

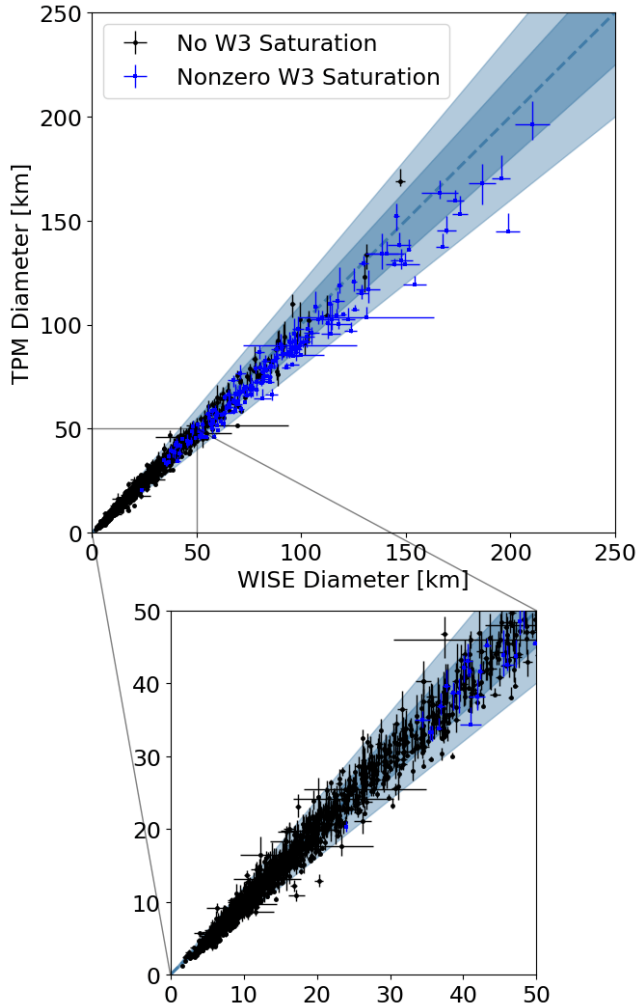


Figure 9. WISE diameters determined by NEATM and the diameters derived by our TPM fits. The inset shows an enlarged range between 0 and 50 km. The dashed line denotes where the two axes are equal, and the darker and lighter shaded regions show where the axes are respectively within 10% and 20% of each other. The asteroids plotted are separated based on the median saturation in their $W3$ band thermal flux measurements. We find that the 1652 nonsaturated asteroids have TPM diameters on average 95% the size of the WISE diameters, while the difference for the 170 saturated asteroids is at 91%. While our TPM fits only model the $W3$ and $W4$ bands, the NEATM fits have the benefit of also modeling the $W2$ band observation at high S/N, which downweights the significance of the $W3$ observation. We thus recommend readers to treat our derived thermophysical parameters for our $W3$ saturated asteroids with caution.

expect that disagreements between the two mainly come about due to the nonrotating spherical shape model assumed by NEATM, which becomes a cruder approximation for more elongated asteroids.

However, we also see that the sizes of the larger asteroids, particularly above 100 km in diameter, show a slight, yet persistent underestimation by the TPM fits compared with the WISE diameters. Due to their size, these asteroids have the brightest thermal flux measurements, which causes partial saturation in the $W3$ band, leading to decreased accuracy in the reported magnitudes. The uncertainty on $W3$ for bright objects is known not to be dominated by random noise but by the systematic component from point-spread function (PSF)-wing fitting of saturated sources, which results in fluxes that are slightly overestimated (Cutri et al. 2012). Among the 170 asteroids in our sample with a nonzero median $W3$ band saturation, the typical saturation is around 15%, with the highest reaching just under 30%. The $W3$ saturated asteroids have TPM diameters 9% smaller than the WISE diameters on average, while the TPM diameters are only smaller by 5% for the nonsaturated asteroids. Whereas in our TPM fits we only model the $W3$ and $W4$ bands, the NEATM fits for large asteroids typically also model the $W2$ band, which can shift the determined sizes (Masiero et al. 2014). Because we do not make any correction for the partial $W3$ saturation nor do we use the measurements in the $W2$ band, we thus advise readers to treat our derived thermophysical parameters with caution for the $W3$ saturated asteroids in our sample.

We can do the same comparison with the WISE NEATM-derived visible geometric albedos (Mainzer et al. 2019), where we once again have 1824 values to compare with (Fig. 10). We see markedly fewer matches between the two albedo estimates relative to the diameter comparison, with only 967 asteroids falling within a 20% agreement and 496 within a 10% agreement. The poorer agreement here is unsurprising due to the larger uncertainty on albedo. The albedo has about twice the uncertainty of the diameter as it is proportional to D^2 (Eq. 2), and we will also have added contributions to the individual uncertainties from the unreported uncertainties on the H and G parameters. As with the diameters, the WISE albedos are also subject to the NEATM spherical shape model assumption. Whereas our $W3$ saturated asteroids were found to be 9% smaller in size, we found albedos greater than the WISE values by about the same magnitude, at 11%. For the nonsaturated asteroids, the albedos are smaller by only 2% on average compared with the WISE albedos.

4.2. Interpretation of Thermal Inertia

4.2.1. Relationship with Size

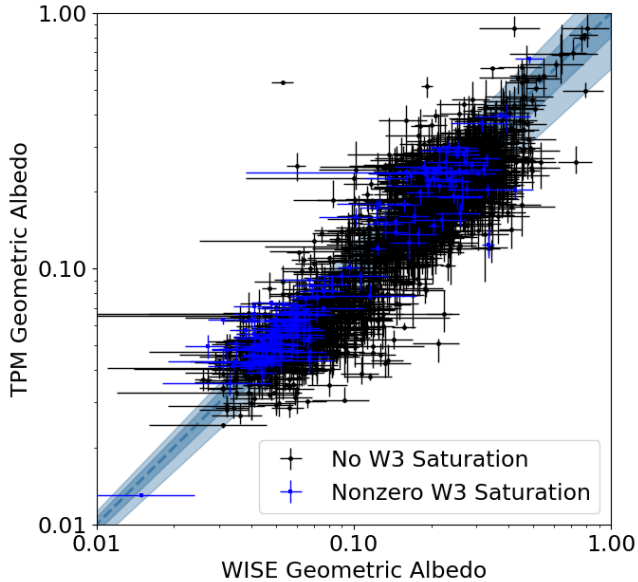


Figure 10. WISE albedos determined by NEATM and the albedos derived by our TPM fits, converted from Bond to visible geometric with Equation 3. The dashed line denotes where the two axes are equal, and the darker and lighter shaded regions show where the axes are, respectively, within 20% and 40% of each other. There is a greater discrepancy between the two data sets relative to the diameter comparison in Figure 9. The larger uncertainty on albedo is expected as it is proportional to D^2 and is also subject to the unreported uncertainties on the H and G parameters. We find that the 1652 asteroids without any saturation in their $W3$ band thermal flux measurements have albedos on average 98% the value of the WISE albedos. The 170 saturated asteroids however are much higher, at 111% the value of the WISE albedos.

While diameter and albedo can be fairly robustly determined in thermophysical modeling even with only an assumed spherical shape model, the same is not true for the determination of the thermal inertia. Shape models based on rich optical lightcurve data sets are closer to reality and tend to be smoother and have fewer planar regions. Shape models based only on sparse optical lightcurve data are crude approximations, often characterized by large planar facets that come together at sharp edges. Such shape models are physically unrealistic and thus are more likely to introduce inaccuracies into the thermophysical model. Additionally, asteroids in our sample with the highest thermal inertia estimates ($\Gamma > 1000 \text{ J m}^{-2} \text{ s}^{-0.5} \text{ K}^{-1}$) are among those with the fewest optical lightcurve data. We consider these thermal inertia extremely high to the point of physical implausibility, and other thermophysical modeling studies have found very few equally high thermal inertia estimates (see Table 3). In order to ensure greater reliability

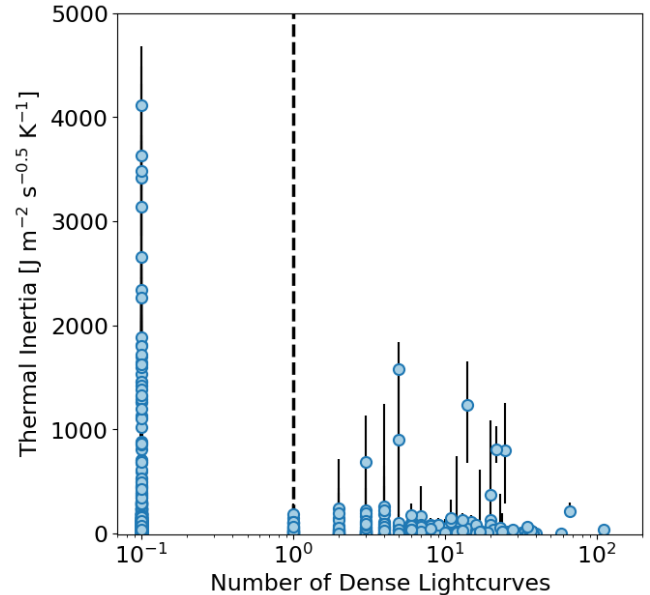


Figure 11. We plot the number of dense lightcurves included in each asteroid’s optical lightcurve data used to derive their shape models against their thermal inertia estimates for our 1847 asteroid sample. Zero dense optical lightcurves are represented here as 0.1 to accommodate the logarithmic axis. The physically implausibly high thermal inertia estimates of $\Gamma > 1000 \text{ J m}^{-2} \text{ s}^{-0.5} \text{ K}^{-1}$ are among the asteroids with the fewest optical lightcurve data. Limiting our sample to the shape models derived from data sets with at least one dense optical lightcurve, denoted by the vertical dashed line, is enough to remove nearly all cases with a best-fit thermal inertia of $\Gamma > 1000 \text{ J m}^{-2} \text{ s}^{-0.5} \text{ K}^{-1}$.

from our thermal inertia analysis in this section, we limit our sample to the asteroids with shape models derived from data sets with at least one dense optical lightcurve, so chosen as to eliminate all of the physically implausibly high thermal inertia values (Fig. 11). Here we define an optical lightcurve as dense if it satisfies three conditions: (1) includes at least 30 data points, (2) data points span 20% or more of the asteroid’s rotation phase, and (3) the mean separation between the data points is at most 2% of the rotation phase. We consider lightcurves that meet all three of these conditions to be well sampled and free of large gaps in the portions of the rotation phase covered, and thus such lightcurves are more likely to yield more accurate shape models derived through lightcurve inversion. This cut reduces the sample down to TPM fits of 270 asteroids in total. We also exclude the TPM fits using partially saturated $W3$ observations, which further removes another 79 asteroids.

In Figure 12, we plot the diameter against the normalized thermal inertia of our sample. As a function of

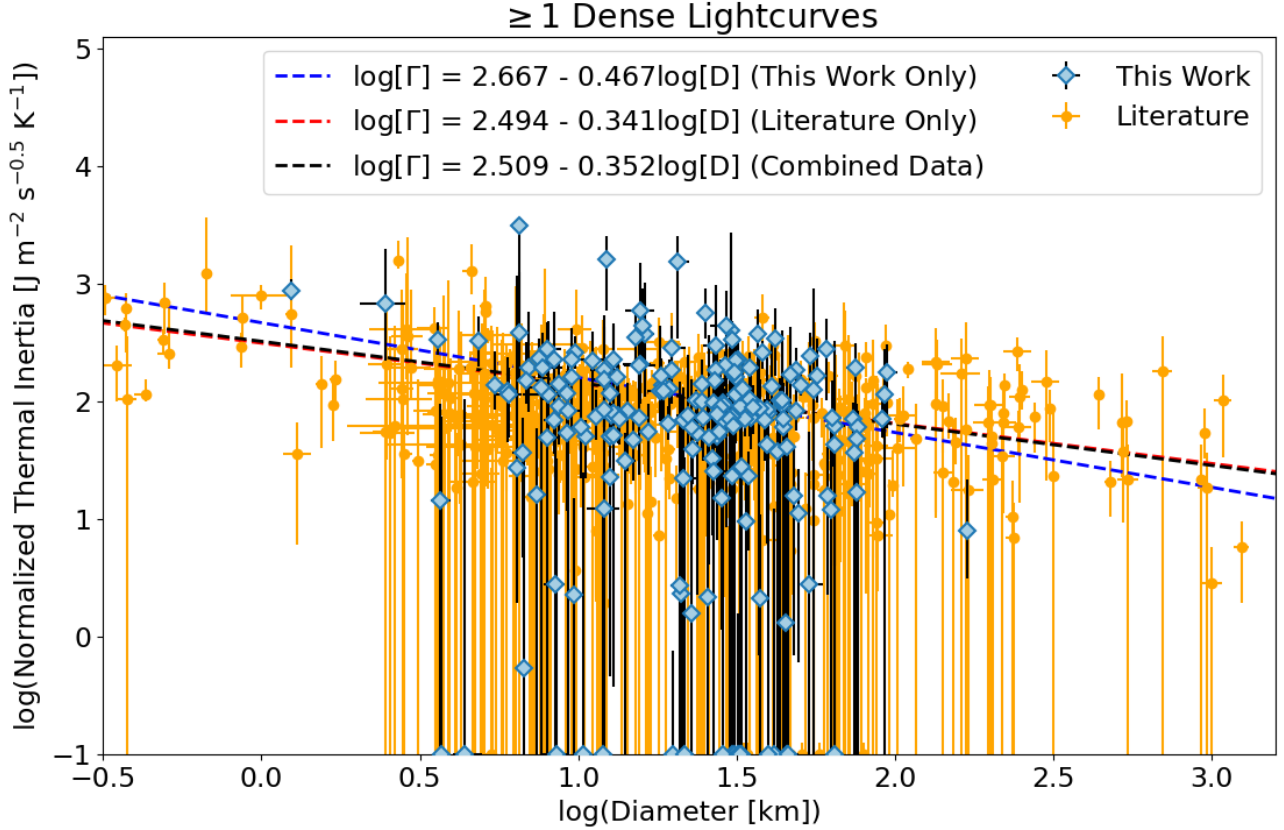


Figure 12. Our 191 asteroid sample’s diameters and thermal inertia normalized to 1 au are shown here along with the 502 thermophysically derived literature values referenced in Table 3. The literature numbers include multiple instances of the same asteroid in order to account for the differences between independently derived parameters. Thermal inertia of $0 \text{ J m}^{-2} \text{ s}^{-0.5} \text{ K}^{-1}$ are represented here with values of 0.1 for the convenience of the logarithmic scale. When we apply linear fits to the data of the form $\log[\Gamma] = \alpha + \beta \log[D]$, we find the most similarity between the literature-only and combined data sets as we have nearly twice as many literature data points as we do of our sample. We also see that the fit to our sample alone prefers a larger α and steeper β mainly due to the lack of large diameter data points, where we only have one larger than 100 km. Overall, we find good agreement between our results and the literature, with all terms within $1-2\sigma$ of each other.

the temperature T , thermal inertia will vary with heliocentric distance r_{hel} as $\Gamma \propto T^{3/2} \propto r_{\text{hel}}^{-3/4}$ (Delbo’ et al. 2015). To account for this temperature dependency in our comparisons, we normalize all thermal inertia values to $r_{\text{h}} = 1$ au, using the median r_{hel} from all thermal observations of each asteroid. Although this relation assumes that all observations of an asteroid were conducted at similar r_{hel} , of the 2551 asteroids in total we thermophysically modeled, 286 were observed by WISE in two epochs, and therefore at two different r_{hel} . However, as the vast majority of our asteroids are MBAs, the differences in r_{hel} are typically small, so this only introduces a small inaccuracy. The largest change in r_{hel} in our sample is 0.7 au, and the total ranges for 70% of the two epoch asteroids are smaller than 0.2 au.

The inverse correlation between size and thermal inertia was first identified by Delbo’ et al. (2007). With our sample limited to the 191 asteroids with dense optical

lightcurve data and no saturation in the $W3$ observations, we confirm the dependence between diameter and thermal inertia to be broadly consistent with literature results (Table 3). Nearly 25% of the 502 literature estimates listed are taken from Hanuš et al. (2018a) who similarly modeled roughly 300 MBAs with cryogenic observations by WISE using the same thermophysical modeling code as in our work, albeit using slightly different data cuts. Our 191 asteroid sample includes 93 asteroids with a previously estimated thermal inertia in the literature, and 70 among them were estimated by Hanuš et al. (2018a), for which we largely see similar best-fit values and uncertainty ranges.

We fit the data with a linear relation of the form $\log[\Gamma] = \alpha + \beta \log[D]$ using the `curve_fit` routine in the Python library SciPy. Γ values of zero are approximated as equal to 0.1 for the sake of the logarithmic convention. The uncertainties on the diameters are ignored as

negligibly small for the fit. We run the fitting procedure several times to account for the asymmetric uncertainties on Γ . For the initial fit, we use the uncertainty of each data point averaged between the upper and lower bounds, which gives us our first α and β values. We then use the linear fit to determine whether to use the upper or lower uncertainty bound for each data point. In other words, we take the upper uncertainty bound if the data point is lower than what is predicted by the fit, and vice versa. We then apply the fit again using these revised uncertainties. We repeat the fitting procedure in this manner until we see no more variation in the fit's α and β values, which takes a total of three loops.

For our sample alone, we find $\alpha = 2.667 \pm 0.059$ and a slope of $\beta = -0.467 \pm 0.044$, with an associated reduced χ_{fit}^2 of 0.916. The literature estimates alone give $\alpha = 2.494 \pm 0.018$ and a slightly less shallow slope of $\beta = -0.341 \pm 0.013$, with an associated reduced χ_{fit}^2 of 1.664. Combining our data with the literature, we see $\alpha = 2.509 \pm 0.017$ and an overall slope very similar to the literature-only subset of $\beta = -0.352 \pm 0.012$, and an overall reduced χ_{fit}^2 of 1.455 (Fig. 12). While we see an offset of about 2σ in both α and β with our sample and the literature-only data set, the combined data set agrees within 1σ of the literature-only data set. As there are around twice as many literature data points as there are data points from our sample, the literature data dominate in the fit of the combined data set. Our larger α and steeper β terms with our sample's data compared to the literature-only data set can be explained by the lack of large asteroids in our sample, as we only have one data point with a diameter larger than 100 km. Though many of the literature estimates we fit use several different thermophysical models and thermal data sources, such as observations from the Spitzer Space Telescope (e.g., Lamy et al. 2008; Marchis et al. 2012) and the Herschel Space Observatory (e.g., O'Rourke et al. 2012; Fornasier et al. 2013; Alí-Lagoa et al. 2020), we see an overall strong consistency with our Γ - D relation compared to the literature as a whole. Because our error bars are so large, however, it is difficult to draw any more definitive conclusions about thermal inertia's relationship with size.

4.2.2. Relationship with Rotation Period

Some earlier studies (e.g., Harris & Drube 2016) have suggested that slow rotators should present higher thermal inertia due to thermal observations being able to probe more deeply into an asteroid's surface. Other more recent studies (e.g., Marciniak et al. 2019; Alí-Lagoa et al. 2020; Marciniak et al. 2021) have found

no excess of high thermal inertia values among slow rotators (conventionally defined as asteroids with $P > 12$ hr), nor for low thermal inertia values among fast rotators. In our sample, we likewise find thermal inertia values greater than $100 \text{ J m}^{-2} \text{ s}^{-0.5} \text{ K}^{-1}$ to be generally present across our entire rotation period range, though we note that our sample is sparsely populated with rotation periods longer than 30 hours (Fig. 13).

Applying a linear fit to the sample of the form $\log[\Gamma] = \alpha + \beta \log[P]$, we find $\alpha = 1.957 \pm 0.063$ and a small positive slope of $\beta = 0.132 \pm 0.074$, with an associated reduced χ_{fit}^2 of 1.004. However, the sample may in fact be better described by a constant. If we fix the slope to be zero, we instead find $\alpha = 2.066 \pm 0.018$, with an associated reduced χ_{fit}^2 of 0.986. Because of the small sample size of rotation periods longer than 30 hours, the large scatter in the data, and large uncertainties on the thermal inertia, however, we cannot reliably state whether there is a trend between thermal inertia and the rotation period or not.

4.2.3. High Thermal Inertia in the Main Belt

While MBAs have generally been found to have low thermal inertia (Table 3), there are over 30 literature thermal inertia estimates for MBAs higher than $100 \text{ J m}^{-2} \text{ s}^{-0.5} \text{ K}^{-1}$, albeit many with large uncertainties. The highest literature thermal inertia estimate reported for an MBA is $250 \pm 150 \text{ J m}^{-2} \text{ s}^{-0.5} \text{ K}^{-1}$ for (277) Elvira (Delbo' & Tanga 2009). We have five MBAs with best-fit thermal inertia greater than $250 \text{ J m}^{-2} \text{ s}^{-0.5} \text{ K}^{-1}$ among our 191 most reliable TPM fits with no $W3$ saturation listed in Table 4. If we include the upper uncertainty bound on the thermal inertia for this threshold, we have another 17 MBAs in the high thermal inertia range. In each instance, the thermal inertia is associated with a large uncertainty and is thus not very well constrained (Fig. 14).

Indeed, for all but one MBA, the lower uncertainty bound on the thermal inertia is less than $250 \text{ J m}^{-2} \text{ s}^{-0.5} \text{ K}^{-1}$, placing the asteroids within the ranges of other MBA thermal inertia in the literature. The remaining MBA, (951) Gaspra, has a derived thermal inertia of $798_{-508}^{+453} \text{ J m}^{-2} \text{ s}^{-0.5} \text{ K}^{-1}$, which falls within the error bars of the estimate reported for (277) Elvira. Our other high thermal inertia case of interest is the Apollo NEA (1865) Cerberus, where we derive a best-fit thermal inertia of $809_{-134}^{+219} \text{ J m}^{-2} \text{ s}^{-0.5} \text{ K}^{-1}$, which is not atypical when compared with the thermal inertia of other NEAs in the literature.

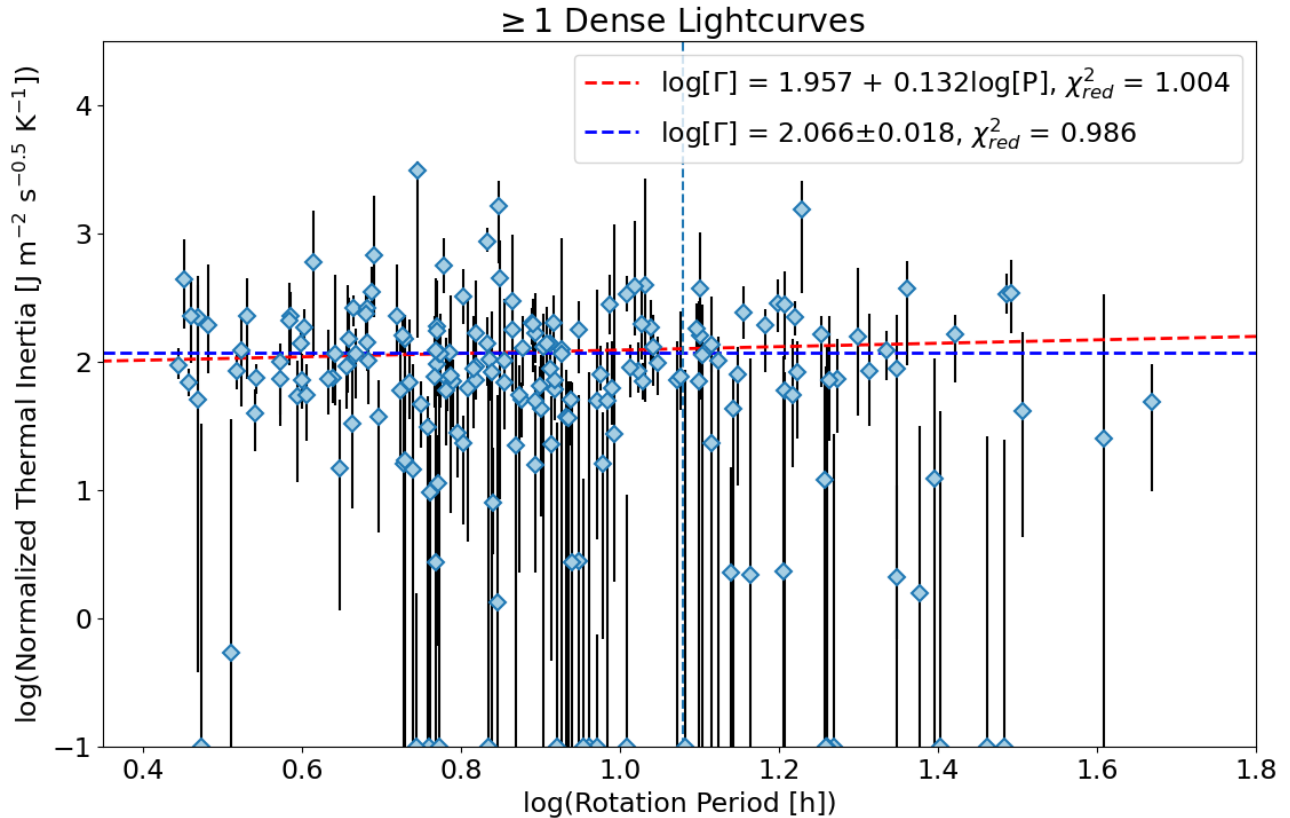


Figure 13. Our 191 asteroid sample’s rotation periods are shown here plotted against their thermal inertia normalized to 1 au. Thermal inertia of $0 \text{ J m}^{-2} \text{ s}^{-0.5} \text{ K}^{-1}$ are represented here with values of 0.1 for the convenience of the logarithmic scale. The dashed vertical line shows the 12 hour period separation into the 143 fast and 48 slow rotators. By applying a linear fit and a constant fit to the data, we find that any evidence of a positive correlation is very weak and difficult to substantiate due to the small number of data points at $P > 30 \text{ h}$, the large scatter in the relation, and the large uncertainties on thermal inertia.

While our derived high thermal inertia fits may not necessarily be discrepant with previous studies, it is possible that the high thermal inertia estimates for MBAs reported in the literature are themselves the results of poor TPM fits and untrustworthy. However, the high thermal inertia found in our sample are all associated with large uncertainties. Such values are thus best to be considered with caution. We do not recommend taking our findings as evidence of unusually high thermal inertia in the main belt.

4.3. Thermal Parameters and Taxonomy

To assess how the thermal parameters might differ depending on taxonomy, we sort the taxonomic classes into three main categories: C-group asteroids which include C-, B-, F-, G-, D-, and T-types, S-group asteroids which include S-, V-, A-, Q-, R-, K-, and L-types, and X-group asteroids which include X-, M-, P-, and E-types. For our 191 asteroids with the most reliable TPM fits (i.e., at least one dense optical lightcurve and no saturation in the thermal flux measurements), we have 20

C-group asteroids, 65 S-group asteroids, 30 X-group asteroids, and 77 asteroids with unknown taxonomy (Fig. 15). For these groupings, the Small Main-Belt Asteroid Spectroscopic Survey (SMASS) II (Bus & Binzel 2002) taxonomy is preferentially used over the Tholen (1984) taxonomy where available. Some asteroids in the Tholen (1984) taxonomy have multiple spectral types assigned due to ambiguities in the color analyses. In these cases, we adopt the best-fitting spectral type, which denoted by the first letter in the sequence.

Taxonomy appears to be no strong predictor of thermal inertia or size, with each group of asteroids being about as equally common over the same parameter space for both parameters derived in our work and in the literature estimates. In principle, metal-rich regolith should present higher thermal inertia due to the higher thermal conductivity of the material, as can be seen in iron meteorites compared with ordinary and carbonaceous chondrites (Opeil et al. 2010). However, taxonomy alone is far from a strong indicator of metal content. Although M-types are traditionally regarded as

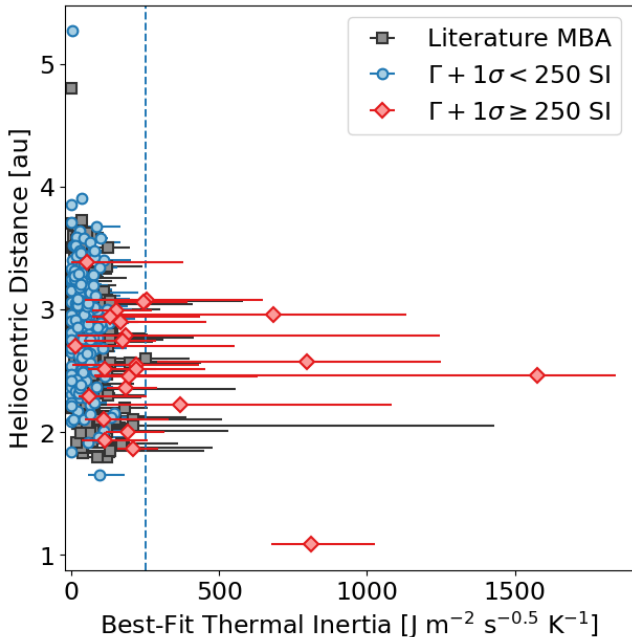


Figure 14. Best-fit thermal inertia for our 191 most reliable TPM fits with no $W3$ saturation listed in Table 4, along with the 425 unique (or 442 total) MBAs reported in the literature (Table 3). Especially high thermal inertia cases are denoted by TPM fits where the upper uncertainty on the best-fit thermal inertia exceeds $250 \text{ J m}^{-2} \text{ s}^{-0.5} \text{ K}^{-1}$, marked by the vertical dashed line, which is equal to the Delbo’ & Tanga (2009) thermal inertia estimate for (277) Elvira, the highest thermal inertia estimate reported for an MBA in Table 3. Our high thermal inertia estimates overlap in values with the estimates in the literature. However, our work can only provide tenuous evidence of unusually high thermal inertia in the main belt due to the consistently large associated uncertainties.

the metallic taxonomic class, the results of radar observations have suggested metal-poor compositions for some M-type asteroids (e.g., Magri et al. 1999, 2007; Shepard et al. 2015), while spectroscopic studies of M-type asteroids have found cases of spectral features inconsistent with metallic compositions (e.g., Clark et al. 2004; Hardersen et al. 2005). Relatively high radar albedos, which are consistent with high metal content, have also been found for some S- and C-type asteroids, suggesting that metal-rich compositions may not be limited to M-type objects (e.g., Magri et al. 2007). It is important to note, however, that the effects of composition are difficult to distinguish from other factors that will affect the thermal inertia, such as the average grain size or degree of compaction (Gundlach & Blum 2013). A high thermal inertia may not necessarily be the product of a metal-rich surface.

The geometric albedo distribution is consistent with the previous observations of each group of asteroids, where C-group asteroids are most common for albedos of $p_V < 0.10$, while S-group asteroids are most common for $p_V > 0.10$ (e.g., Gradie & Tedesco 1982; Tholen 1984). There are a few instances of unusual albedos per taxonomic class that may warrant further investigation into whether or not they were correctly classified.

We have two S-group asteroids with albedos fainter than $p_V = 0.10$ in our sample. The lowest albedo S-group asteroid is (1332) Marconia, which is classified as an Ld-type under the SMASS II (Bus & Binzel 2002) taxonomy. We estimate its geometric albedo to be $p_V = 0.044^{+0.002}_{-0.005}$, which is several sigma fainter than the WISE NEATM-derived estimate of $p_V = 0.063 \pm 0.008$, reported in the Planetary Data System (Mainzer et al. 2019). The second lowest albedo S-group asteroid is (673) Edda, which is classified as an S-type under both the SMASS II (Bus & Binzel 2002) and Tholen (1984) taxonomies. We estimate its geometric albedo to be $p_V = 0.097^{+0.001}_{-0.002}$, which agrees within 1σ of the WISE NEATM-derived estimate of $p_V = 0.092 \pm 0.034$.

We have three C-group asteroids with albedos brighter than $p_V = 0.15$. (1317) Silvretta has an estimated geometric albedo of $p_V = 0.199^{+0.057}_{-0.024}$, which is slightly fainter than the WISE NEATM-derived estimate of $p_V = 0.275 \pm 0.047$. (1317) Silvretta may however be better described as an X-type. The classification for (1317) Silvretta is particularly tenuous. Its full Tholen (1984) type is given as CX:, where the trailing colon signifies an uncertain classification. Our other bright C-group albedos belong to (390) Alma and (531) Zerlina. (390) Alma is denoted as a DT-type in the Tholen (1984) taxonomy. Our geometric albedo estimate of $p_V = 0.188^{+0.015}_{-0.015}$ is several sigma fainter than the WISE NEATM-derived estimate of $p_V = 0.268 \pm 0.011$. (531) Zerlina is a B-type under the SMASS II (Bus & Binzel 2002) taxonomy. Unlike the other bright C-group albedos, our geometric albedo estimate of $p_V = 0.151^{+0.009}_{-0.008}$ for this asteroid is several sigma brighter than the WISE NEATM-derived estimate of $p_V = 0.101 \pm 0.007$.

X-group asteroids cover a wide range in reflectivity and can be split into three types in the Tholen (1984) taxonomy based on albedo: P ($p_V < 0.10$), M ($0.10 < p_V < 0.30$), and E ($p_V > 0.30$). These subdivisions in albedo are cleanly recovered for the cases where a particular one of these types was specified. Our four P-types had albedos between $0.03 < p_V < 0.05$, our six M-types had albedos between $0.11 < p_V < 0.27$, and our three E-types had albedos between $0.42 < p_V < 0.69$.

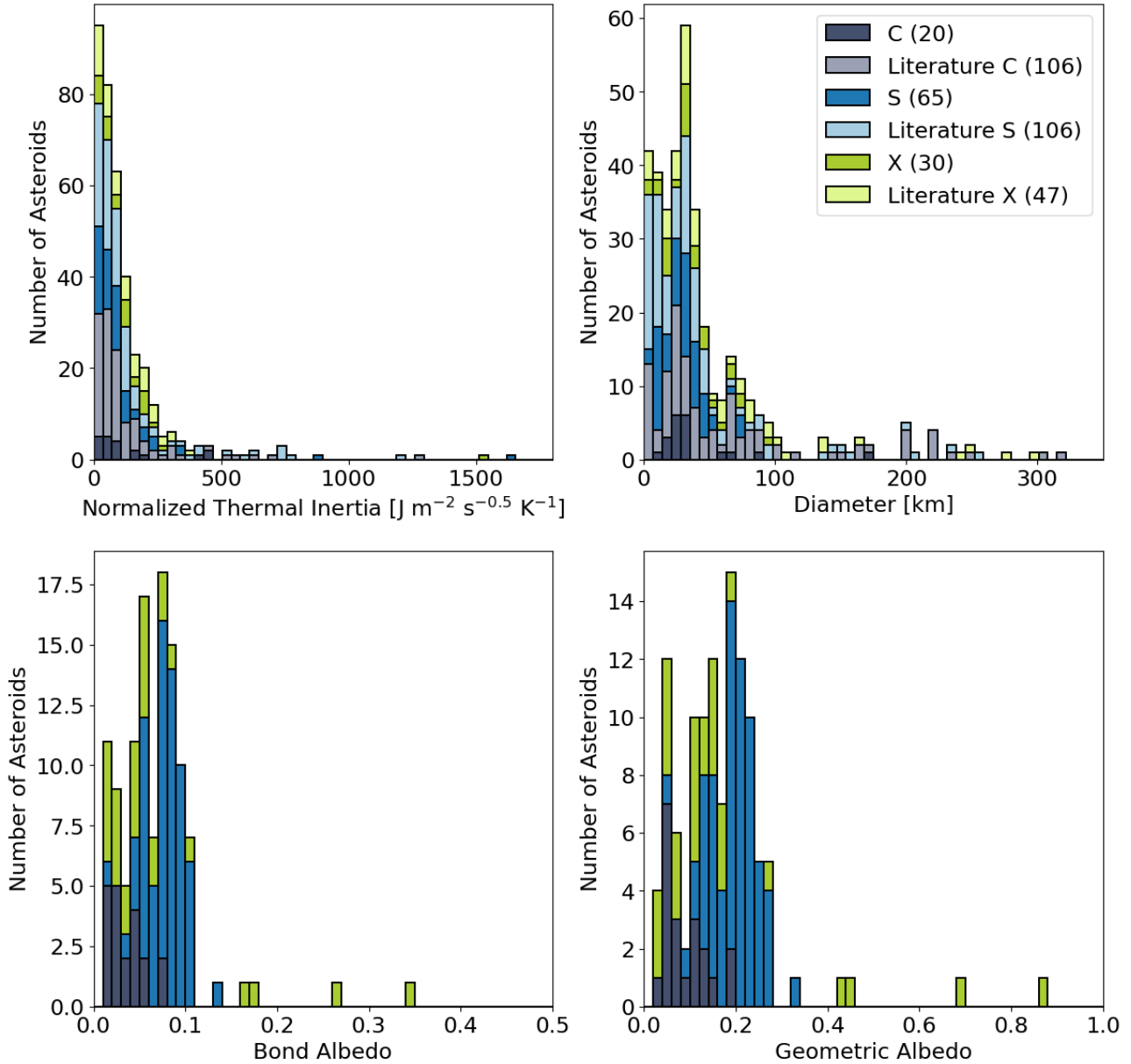


Figure 15. Thermal inertia (normalized to 1 au), diameter, and albedo represented as stacked histograms for our 191 asteroids with our most reliable TPM fits. The taxonomic types are sorted into three categories accordingly: C-, B-, F-, G-, D-, and T-types in the C-group, S-, V-, A-, Q-, R-, K-, and L-types in the S-group, and X-, M-, P-, and E-types in the X-group. The remaining 77 asteroids have unknown taxonomy and are not included here. Literature estimates for thermal inertia and diameter are included from Table 3. Note that the literature numbers count each duplicate asteroid in the table separately in order to account for the differences between independently derived parameters. The thermal inertia and size distributions are roughly equal when split by taxonomic class. The geometric albedo distribution is consistent with past observations of each taxonomic class, where C-group asteroids are most common among albedos of $p_V < 0.10$ and S-group asteroids are most common for brighter albedos, while X-group asteroids are scattered across the entire albedo range (e.g., [Gradie & Tedesco 1982](#); [Tholen 1984](#)).

4.4. Yarkovsky Follow-up

If an asteroid had no thermal inertia, it would absorb and release heat from the Sun immediately, making its temperature distribution symmetrical around its subsolar point. The net force acting on the asteroid would thus only be radially outward from the Sun. With a thermal inertia component, however, there is a delay between the thermal absorption and emission. This Yarkovsky force introduces a transverse component to the net force that will induce a secular change to the asteroid’s semimajor axis. However, the magnitude of the Yarkovsky effect also decreases at very high thermal inertia. If no heat is transferred over one rotation cycle, the temperature distribution is once again uniform and the Yarkovsky effect drops to zero. Moreover, while having some thermal inertia is necessary for the Yarkovsky effect, its magnitude also depends on an asteroid’s heliocentric distance, axial tilt, size, shape, and rotation period (Bottke et al. 2006). The majority of asteroids in our sample have diameters under 30–40 km, which is the maximum size range where we can theoretically expect asteroids to undergo possible Yarkovsky acceleration (Vokrouhlický et al. 2015). At larger sizes, the acceleration induced by the Yarkovsky effect becomes vanishingly small (Fig. 16). Because the Yarkovsky effect decreases with increasing heliocentric distance and larger asteroid size, the vast majority of asteroids with a measured nongravitational transverse acceleration parameter (A_2) are subkilometer NEAs.

As of this writing, there are published A_2 values for 244 NEAs on the JPL Small-Body Database. Yarkovsky drift rate detections for an additional 149 NEAs have also been reported in Greenberg et al. (2020). The largest reported diameters among these asteroids belong to the 6.25 km (3200) Phaethon and 5.4 km (4179) Toutatis⁹. (3200) Phaethon’s size was derived from 2007 and 2017 radar data from Arecibo and Goldstone (Taylor et al. 2019) but may be overestimated. Past thermophysical modeling efforts have derived a diameter of 5.1 km for (3200) Phaethon (Hanuš et al. 2016a), and more recent work using the same radar data set in combination with stellar occultations and multiple apparition lightcurves has revised the size down to 5.3 km (Marshall et al. 2021). In our sample, only (1685) Toro has an A_2 value explicitly determined¹⁰, where $A_2 = -3.339 \pm 0.6433 \times 10^{-15}$ au day⁻². We also note that one other asteroid in our sample, (1865) Cerberus,

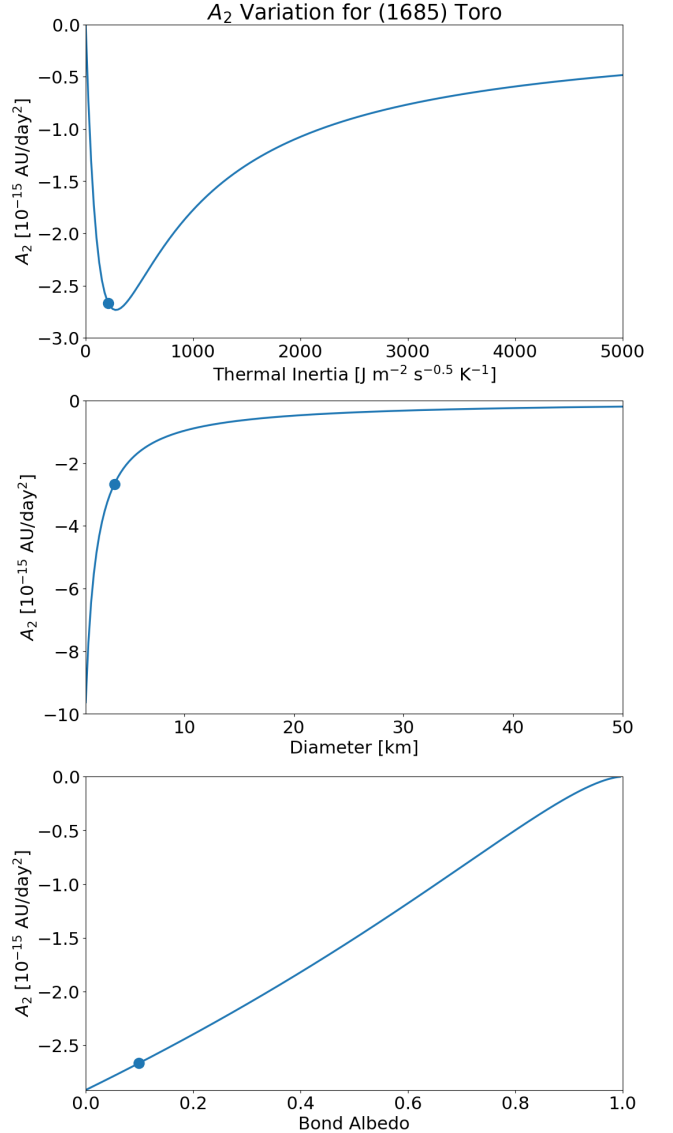


Figure 16. An example of how the transverse acceleration parameter A_2 changes as a function of thermal inertia, diameter, and Bond albedo respectively for (1685) Toro. Parameters not being varied are otherwise held constant at the best-fit values our TPM found for the asteroid, denoted by the single scatter point in each panel. While A_2 is inversely proportional with diameter and albedo, its magnitude drops off both for very low and very high thermal inertia values.

has a measured orbit-averaged semimajor axis drift rate of $\langle da/dt \rangle = -3.75 \pm 1.8 \times 10^{-4}$ au My⁻¹ (Greenberg et al. 2020), which is related to A_2 by Equation 5 in Farnocchia et al. (2013)

$$\langle da/dt \rangle = \frac{2A_2(1 - e^2)}{n} \left(\frac{1 \text{ au}}{r_{\text{hel}}} \right)^d \quad (6)$$

⁹ https://ssd.jpl.nasa.gov/tools/sbdb_query.html

¹⁰ https://ssd.jpl.nasa.gov/tools/sbdb_lookup.html#/?sstr=1685

where e is the eccentricity, n is the mean motion, and r_{hel} is the heliocentric distance. d is a value that depends upon the object’s thermal properties. For the extreme cases, d can be as low as 0.5 or as high as 3.5, though it is more typically between 2 to 3 (Farnocchia et al. 2013).

In order to identify the most promising Yarkovsky candidates for observational follow-up, we compute a rudimentary Yarkovsky acceleration prediction for every asteroid in our sample using Equation 10 in Farnocchia et al. (2013)

$$A_2 = \frac{4(1-A)}{9} \Phi(1 \text{ au}) f(\Theta) \cos(\gamma) \quad (7)$$

where A is the Bond albedo and γ is the spin obliquity. $\Phi(1 \text{ au})$ is the standard radiation force factor, equal to

$$\Phi(1 \text{ au}) = \frac{3G_S}{2\rho Dc} \quad (8)$$

where G_S is equal to 1361 W m^{-2} (Kopp & Lean 2011) and is the solar constant at 1 au, ρ is the bulk density, D is the mean diameter, and c is the speed of light. $f(\Theta)$ is the function of the thermal parameter Θ , which is equal to

$$f(\Theta) = \frac{0.5\Theta}{1 + \Theta + 0.5\Theta^2} \quad (9)$$

Θ is given by

$$\Theta = \frac{\Gamma}{\epsilon\sigma_{SB}T_*^3} \sqrt{\frac{2\pi}{P}} \quad (10)$$

where Γ is the thermal inertia, ϵ is the bolometric emissivity, σ_{SB} is the Stefan-Boltzmann constant, and P is the rotational period. T_* is the subsolar temperature, given by

$$T_* = \sqrt[4]{\frac{(1-A)G_S}{\epsilon\sigma_{SB}p^2}} \quad (11)$$

p is the semi latus rectum, given by

$$p = a(1 - e^2) \quad (12)$$

where a is the semimajor axis and e is the eccentricity.

For each asteroid, we estimate the uncertainty ranges on A_2 by choosing values of Γ , D , and A in their respective 1σ uncertainty bounds such that they minimize or

maximize A_2 . As in §2.2, we assume $\epsilon = 0.9$. We use the bulk densities reported in Carry (2012) if they are not denoted as unreliable, but such estimates are only available for fewer than 300 asteroids. For the asteroids in our sample that do not have existing estimates for ρ , if the SMASS II (Bus & Binzel 2002) taxonomy is known, we assume values equal to the average bulk densities with 20% accuracy in Table 3 of Carry (2012). If only the Tholen (1984) taxonomy is known, we use the average bulk densities of Krasinsky et al. (2002) following their classification scheme. The average bulk densities for each scenario is given in Table 2. In the cases where the taxonomic class is unknown, we reference the typical visible geometric albedo ranges for each composition type and treat the asteroid as a C-type for $p_V < 0.10$ and an S-type otherwise (Tholen 1984), then apply the Krasinsky et al. (2002) average bulk densities.

With our simplified approach, we found an A_2 estimate of $-2.6_{-0.2}^{+0.3} \times 10^{-15} \text{ au day}^{-2}$ for (1685) Toro, which is within a 1σ agreement with the JPL Small-Body Database value of $-3.339 \pm 0.6433 \times 10^{-15} \text{ au day}^{-2}$. We compile the 57 asteroids in our sample with an acceleration greater in magnitude than $A_2 = 1.9 \times 10^{-15} \text{ au day}^{-2}$ in Table 6 using the best-fit values for Γ , D , and A . This cutoff in A_2 is the same as the smallest published A_2 value on the JPL Small-Body Database, which is for the asteroid (35107) 1991 VH. Among the asteroids with dense optical lightcurve data, we have a total of four asteroids, 1 NEA and 3 MBAs, other than (1685) Toro in this parameter space. These asteroids are the best candidates in our sample for observational follow-up to measure their orbital drifts directly with astrometry. If successful, independent Yarkovsky measurements can also help further constrain the thermal inertia values derived through thermophysical modeling. However, we caution the reader that 11 of these 57 Yarkovsky candidate asteroids have an unconstrained lower bound on their thermal inertia, and so the lower bound on their A_2 estimate is similarly unconstrained. These asteroids may have undetectably small drift rates in reality (Fig. 17).

5. CONCLUSIONS AND FUTURE PROSPECTS

Using thermal observations from WISE (Wright et al. 2010; Mainzer et al. 2011) taken during its fully cryogenic phase and convex shape models from DAMIT (Đurech et al. 2010), we have thermophysically modeled a total of 2551 asteroids. With the addition of WISE photometry to the optical lightcurve data sets for each asteroid, we were able to derive revised shape models for

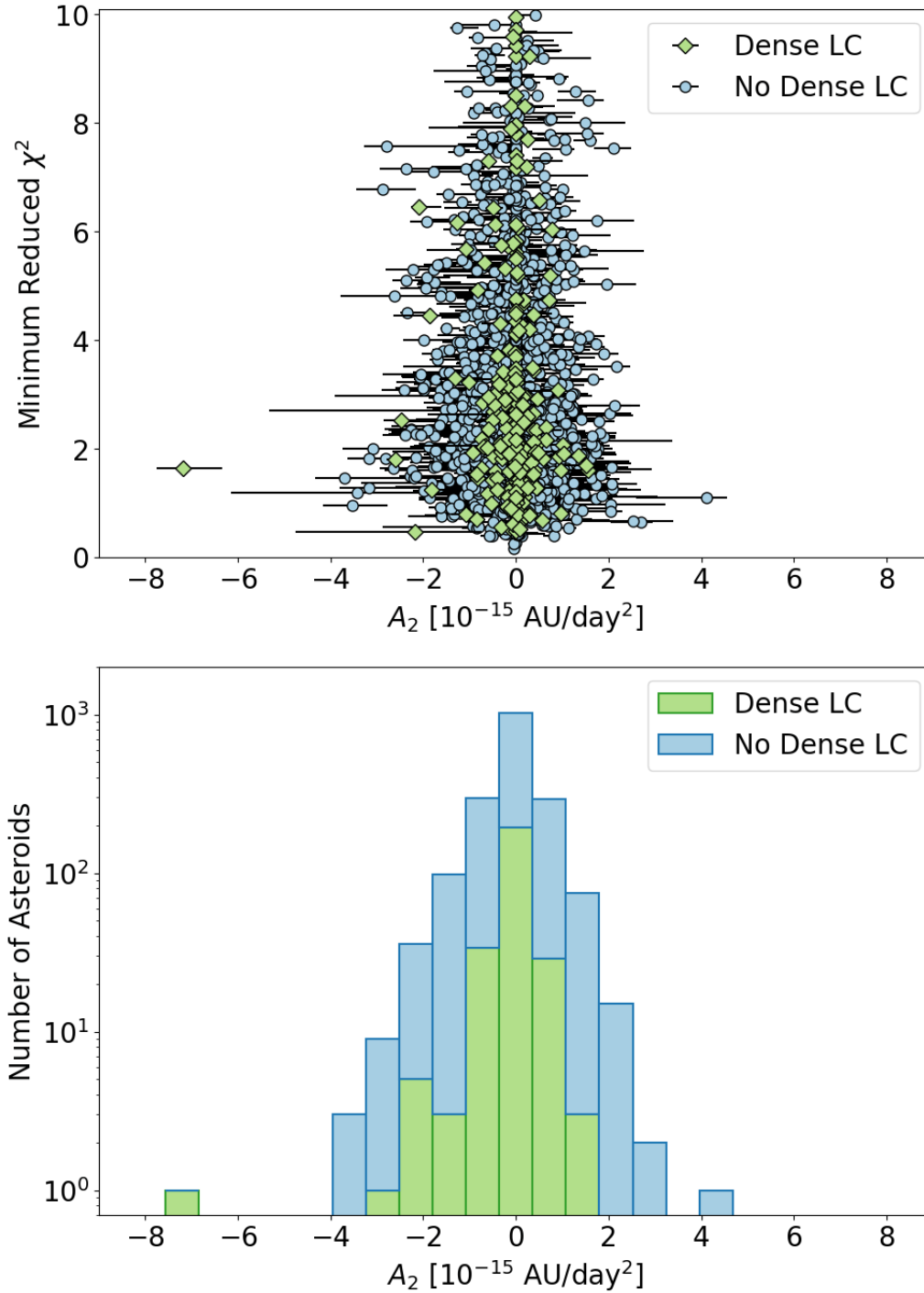


Figure 17. The top panel plots the estimated nongravitational transverse acceleration parameter A_2 for every asteroid in our sample against the χ^2 of their best TPM fit, while the bottom panel shows the histogram of the same data. We estimated an A_2 value for each asteroid following the procedure outlined in §4.4. The data points are distinguished between asteroids which, for the purposes of deriving their shape models, had at least one dense optical lightcurve in their data set and those that did not. In our sample, we have 57 asteroids with an A_2 larger in magnitude than the smallest published A_2 value on the JPL Small-Body Database ($A_2 = 1.9 \times 10^{-15}$ au day $^{-2}$), with 10 also having at least 1 dense optical lightcurve. These asteroids are the most promising for direct observational follow-up to confirm their Yarkovsky drift rates. However, because the lower bound on thermal inertia is unconstrained for 11 of these 57 best Yarkovsky candidates, the lower bound on A_2 here is also unconstrained, and as such the drift rates of these asteroids may be undetectably small.

Table 2. Average Bulk Density by Taxonomic Class

Taxonomic Class	Bulk Density ρ [g cm ⁻³]	Number of Asteroids
SMASS II (Bus & Binzel 2002) Taxonomy		
S	2.72	105
Sq	3.43	13
B	2.38	18
C	1.33	30
Cb	1.25	4
Ch	1.41	23
X	1.85	35
Xc	4.86	10
Xe	2.60	10
Xk	4.22	11
K	3.54	12
V	1.93	4
Tholen (1984) Taxonomy		
C, D, P, T, B, G, F	1.38	46
S, K, Q, V, R, A, E	2.71	86
M	5.32	9

NOTE—Average bulk densities based on taxonomic class, adapted from Table 3 in Carry (2012) for the SMASS II (Bus & Binzel 2002) classes and Table 1 in Krasinsky et al. (2002) for the Tholen (1984) classes. In the latter case, several classes were grouped together and regarded respectively as compositional C- and S-types. The Carry (2012) bulk densities were given in three forms for the level of accuracy considered: 20%, 50%, and no precision restriction; we adopt the 20% accuracy values here. Note that not every SMASS II taxonomic class has a listed density. For each row, we also give the number of asteroids where we took the associated average bulk density. The Krasinsky et al. (2002) densities are only used in cases where the Carry (2012) densities were not available. These numbers do not include asteroids where the taxonomic class was not available and only assumed based on the geometric albedo.

nearly 700 asteroids through lightcurve inversion, producing 540 TPM fits with an improved χ^2 compared with the DAMIT shape models. We set two conditions for what fits to include in our final sample: a reduced $\chi^2 < 10$ and a χ^2 ratio of at least 20. The purpose of the second condition is to quantify what we consider a well-defined minimum in the χ^2 curve of the TPM fit which is needed to constrain the derived thermal parameters. Our final sample consists of TPM fits for 1847 asteroids.

Currently, there are published thermal inertia estimates for only a few hundred asteroids (Table 3). Thanks largely in part to the sharp increase in asteroid shape models in recent years, we have derived through thermophysical modeling thermal inertia estimates for 1847 asteroids, though only 191 have both sufficient optical lightcurve data and nonsaturated thermal flux measurements for the derived thermal inertia to be reliable. However, even within this limited sample, we have 98 asteroids that did not previously have a thermal inertia estimate in the literature, which increases the number of asteroids with thermal inertia estimates by around 20%.

We found our derived diameters and albedos to be broadly consistent with the NEATM-derived values with the WISE thermal data set (Mainzer et al. 2019). Our derived thermal inertia were broadly consistent with the trends found with diameter (e.g., Delbo’ et al. 2007) and rotation period (e.g., Marciniak et al. 2019; Alí-Lagoa et al. 2020; Marciniak et al. 2021) in the literature, though in both cases the large uncertainties on thermal inertia limit the conclusions we were able to draw from the data. We applied a linear fit to the diameters and thermal inertia normalized to 1 au of the form $\log[\Gamma] = \alpha + \beta \log[D]$, finding best-fit values of $\alpha = 2.667 \pm 0.059$ and $\beta = -0.467 \pm 0.044$ for our sample alone and $\alpha = 2.509 \pm 0.017$ and $\beta = -0.352 \pm 0.012$ when combined with literature estimates. We applied a linear fit to the rotation periods and normalized thermal inertia and found a slightly positive trend between the two parameters. However, we also found that the data were similarly well described by a constant. Given the small sample size of rotation periods longer than 30 hours, the large scatter in the data, and large uncertainties on the thermal inertia, we were unable to reliably state whether there is a trend between thermal inertia and the rotation period or not. We found the thermal parameters when split by asteroid taxonomic class to be about equally distributed in terms of thermal inertia and diameter, and the albedo distribution was consistent with past studies (e.g., Gradie & Tedesco 1982; Tholen 1984). Finally, we used our derived thermal parameters to compute a rudimentary Yarkovsky acceleration for every asteroid in our sample, identifying the 57 best candidates for confirmation via observational follow-up.

Of the 2551 asteroids we thermophysically modeled, 71% use shape models derived by Āurech et al. (2018a, 2019, 2020), which take advantage of using incidental sparse photometry from survey telescopes such as the Asteroid Terrestrial-impact Last Alert System (ATLAS; Tonry et al. 2018) instead of having to conduct time-intensive targeted campaigns to obtain dense optical

lightcurves for individual asteroids. We can anticipate similar success with the large volume of data expected from upcoming all-sky surveys, such as the Vera Rubin Observatory Legacy Survey of Space and Time (LSST; Ivezić et al. 2019). LSST is a ground-based survey with full science operations planned by 2023. Its field of view covers nearly 10 square degrees of sky. It will cover the entire visible sky twice a week by taking nearly a thousand 30 s observations each night. With a light-gathering power equivalent to that of a 6.7 m diameter primary mirror, its limiting magnitude will eclipse those of current all-sky surveys such as the 0.5 m telescopes used by ATLAS and the 1.8 m Panoramic Survey Telescope and Rapid Response System (Pan-STARRS1) telescope (Chambers et al. 2016). The photometric data gathered by all-sky surveys will be bolstered by the European Space Agency mission Gaia¹¹ (Gaia Collaboration et al. 2016), which was launched in 2013 December with the goal of obtaining accurate astrometry and photometry for more than a billion stars. By scanning the entire sky, Gaia will also incidentally observe thousands of asteroids. DR2 (Gaia Collaboration et al. 2018) contained astrometric and photometric data for around 14,000 asteroids. Although the number of measurements per individual asteroids was small, DR2 has already enabled derivations of hundreds of new shape models (Ďurech et al. 2019). We can expect a greater number of more accurate shape models with the upcoming Gaia DR3 catalog, which is anticipated to become available on 2022 June 13.

Thermophysical modeling benefits greatly from the additional constraints granted by having multiple epochs of observations in order to probe the thermal emission across the asteroid’s diurnal temperature distribution. The seven-month fully cryogenic WISE mission, however, was limited to observing asteroids at a maximum of two epochs, and of our 2551 asteroids, 89% were only observed at one epoch. Thermal infrared data of asteroids have traditionally been limited in quantity due to the challenges of observing at such longer wavelengths from the ground. However, we will soon see much more plentiful thermal data with the upcoming Near-Earth Object Surveyor¹², a space-based survey with a planned launch in 2026. Its two infrared channels, which span 4–5.2 and 6–10 μm respectively, were designed to constrain the typical thermal emission curve expected for NEAs. The telescope will be passively cooled over its planned five-year mission, thus re-

quiring no cryogen. Within its nominal mission length, the telescope is expected to detect millions of asteroids, with the majority having several epochs of observations.

In the interest of saving significant computational time and labor, we do not account for the uncertainties in the shape models, and thus the error bars on our derived parameters are essentially lower limits. The effects of incorporating shape uncertainty into thermophysical modeling have been largely unexplored. Hanuš et al. (2015) introduced a method of generating several shape models for each asteroid by bootstrapping the photometric data used for lightcurve inversion, which was later applied to a larger sample of roughly 300 WISE-observed asteroids by Hanuš et al. (2018a). Asteroids where the TPM solutions differed among the set of shape models pointed to the shape model as the primary source of uncertainty, which was the case for roughly 35% of their asteroid sample. Improvements to the shape model can mainly come about with more data, such as additional optical photometry.

One of the longstanding challenges of thermophysical modeling is the lack of benchmark tests to verify the accuracy of the derived parameters. The earliest TPMs were made to model thermal observations of the lunar surface and were later adapted by Spencer et al. (1989) for general planetary bodies with an assumed spherical shape. The most commonly used thermophysical models used for asteroids today (e.g., Lagerros 1996; Delbo’ et al. 2007; Rozitis & Green 2011) are all variations of the Spencer et al. (1989) model. Lunar regolith is made up of fine grains and has an extremely low thermal conductivity (Winter & Krupp 1971), which is very different from the surfaces of many asteroids, particularly for the smallest in size. Ground truth information can be highly valuable as an independent check for TPM-derived parameters, but missions to individual asteroids are so far very few in number due to their enormous costs and several years of planning required. Meteorite studies are more accessible but do not investigate the same environment as TPMs, as asteroid fragments are unlikely to survive unchanged through ejection from their parent body and atmospheric entry. The orbital perturbation induced by the Yarkovsky effect is dependent on thermal inertia, and direct measurement of an asteroid’s orbital drift can serve to place constraints on the TPM-derived thermal inertia. However, this is complicated by the Yarkovsky drift’s dependency on several other physical parameters that we may not have any knowledge of, such as the asteroid’s bulk density. In the near future, we will see more and more asteroid thermal data and shape models become available, which will translate to

¹¹ <https://www.cosmos.esa.int/web/gaia>

¹² <https://neos.arizona.edu/>

a growth in the number of asteroids with thermophysically derived parameters. Large-scale independent verification of such parameters, however, is likely a long way off yet.

ACKNOWLEDGEMENTS

We would like to thank the anonymous referees for the valuable and thorough comments. The work of D.H. and D.J.T. are supported by NASA grant Nos. NNX13AI64G and 80NSSC21K0807. The work of J.H. has been supported by INTER-EXCELLENCE grant LTAUSA18093 from the Czech Ministry of Education, Youth, and Sports and by the grant GA20-04431S of the Czech

Science Foundation. This publication makes use of data products from the Wide-field Infrared Survey Explorer, which is a joint project of the University of California, Los Angeles, and the Jet Propulsion Laboratory/California Institute of Technology, funded by the National Aeronautics and Space Administration. This publication also makes use of data products from NEOWISE, which is a project of the Jet Propulsion Laboratory/California Institute of Technology, funded by the Planetary Science Division of the National Aeronautics and Space Administration. The technical support and advanced computing resources from University of Hawaii Information Technology Services – Cyberinfrastructure, funded in part by the National Science Foundation MRI award #1920304, are gratefully acknowledged.

REFERENCES

- Alí-Lagoa, V., de León, J., Licandro, J., et al. 2013, *A&A*, 554, A71, doi: [10.1051/0004-6361/201220680](https://doi.org/10.1051/0004-6361/201220680)
- Alí-Lagoa, V., Lionni, L., Delbo', M., et al. 2014, *A&A*, 561, A45, doi: [10.1051/0004-6361/201322215](https://doi.org/10.1051/0004-6361/201322215)
- Alí-Lagoa, V., Müller, T. G., Kiss, C., et al. 2020, *A&A*, 638, A84, doi: [10.1051/0004-6361/202037718](https://doi.org/10.1051/0004-6361/202037718)
- Bottke, William F., J., Vokrouhlický, D., Rubincam, D. P., & Nesvorný, D. 2006, *Annual Review of Earth and Planetary Sciences*, 34, 157, doi: [10.1146/annurev.earth.34.031405.125154](https://doi.org/10.1146/annurev.earth.34.031405.125154)
- Bowell, E., Hapke, B., Domingue, D., et al. 1989, in *Asteroids II*, ed. R. P. Binzel, T. Gehrels, & M. S. Matthews, 524–556
- Bus, S. J., & Binzel, R. P. 2002, *Icarus*, 158, 146, doi: [10.1006/icar.2002.6856](https://doi.org/10.1006/icar.2002.6856)
- Carry, B. 2012, *Planet. Space Sci.*, 73, 98, doi: [10.1016/j.pss.2012.03.009](https://doi.org/10.1016/j.pss.2012.03.009)
- Chambers, K. C., Magnier, E. A., Metcalfe, N., et al. 2016, arXiv e-prints, arXiv:1612.05560. <https://arxiv.org/abs/1612.05560>
- Clark, B. E., Bus, S. J., Rivkin, A. S., Shepard, M. K., & Shah, S. 2004, *AJ*, 128, 3070, doi: [10.1086/424856](https://doi.org/10.1086/424856)
- Cruikshank, D. P., Stansberry, J. A., Emery, J. P., et al. 2005, *ApJL*, 624, L53, doi: [10.1086/430420](https://doi.org/10.1086/430420)
- Cutri, R. M., Wright, E. L., Conrow, T., et al. 2012, Explanatory Supplement to the WISE All-Sky Data Release Products, Explanatory Supplement to the WISE All-Sky Data Release Products
- Delbo', M., dell'Oro, A., Harris, A. W., Mottola, S., & Mueller, M. 2007, *Icarus*, 190, 236, doi: [10.1016/j.icarus.2007.03.007](https://doi.org/10.1016/j.icarus.2007.03.007)
- Delbo', M., Mueller, M., Emery, J. P., Rozitis, B., & Capria, M. T. 2015, *Asteroid Thermophysical Modeling*, 107–128, doi: [10.2458/azu_uapress.9780816532131-ch006](https://doi.org/10.2458/azu_uapress.9780816532131-ch006)
- Delbo', M., & Tanga, P. 2009, *Planet. Space Sci.*, 57, 259, doi: [10.1016/j.pss.2008.06.015](https://doi.org/10.1016/j.pss.2008.06.015)
- Descamps, P., Marchis, F., Āurech, J., et al. 2009, *Icarus*, 203, 88, doi: [10.1016/j.icarus.2009.04.032](https://doi.org/10.1016/j.icarus.2009.04.032)
- Āurech, J., Delbo', M., Carry, B., Hanuš, J., & Alí-Lagoa, V. 2017, *A&A*, 604, A27, doi: [10.1051/0004-6361/201730868](https://doi.org/10.1051/0004-6361/201730868)
- Āurech, J., Hanuš, J., & Alí-Lagoa, V. 2018a, *A&A*, 617, A57, doi: [10.1051/0004-6361/201833437](https://doi.org/10.1051/0004-6361/201833437)
- Āurech, J., Hanuš, J., Oszkiewicz, D., & Vančo, R. 2016, *A&A*, 587, A48, doi: [10.1051/0004-6361/201527573](https://doi.org/10.1051/0004-6361/201527573)
- Āurech, J., Hanuš, J., & Vančo, R. 2019, *A&A*, 631, A2, doi: [10.1051/0004-6361/201936341](https://doi.org/10.1051/0004-6361/201936341)
- Āurech, J., Sidorin, V., & Kaasalainen, M. 2010, *A&A*, 513, A46, doi: [10.1051/0004-6361/200912693](https://doi.org/10.1051/0004-6361/200912693)
- Āurech, J., Tonry, J., Erasmus, N., et al. 2020, *A&A*, 643, A59, doi: [10.1051/0004-6361/202037729](https://doi.org/10.1051/0004-6361/202037729)
- Āurech, J., Kaasalainen, M., Marciniak, A., et al. 2007, *A&A*, 465, 331, doi: [10.1051/0004-6361:20066347](https://doi.org/10.1051/0004-6361:20066347)
- Āurech, J., Kaasalainen, M., Warner, B. D., et al. 2009, *A&A*, 493, 291, doi: [10.1051/0004-6361:200810393](https://doi.org/10.1051/0004-6361:200810393)
- Āurech, J., Kaasalainen, M., Herald, D., et al. 2011, *Icarus*, 214, 652, doi: [10.1016/j.icarus.2011.03.016](https://doi.org/10.1016/j.icarus.2011.03.016)
- Āurech, J., Vokrouhlický, D., Pravec, P., et al. 2018b, *A&A*, 609, A86, doi: [10.1051/0004-6361/201731465](https://doi.org/10.1051/0004-6361/201731465)
- Āurech, J., Hanuš, J., Brož, M., et al. 2018c, *Icarus*, 304, 101, doi: [10.1016/j.icarus.2017.07.005](https://doi.org/10.1016/j.icarus.2017.07.005)
- Emery, J. P., Sprague, A. L., Witteborn, F. C., et al. 1998, *Icarus*, 136, 104, doi: [10.1006/icar.1998.6012](https://doi.org/10.1006/icar.1998.6012)
- Emery, J. P., Fernández, Y. R., Kelley, M. S. P., et al. 2014, *Icarus*, 234, 17, doi: [10.1016/j.icarus.2014.02.005](https://doi.org/10.1016/j.icarus.2014.02.005)
- Farnocchia, D., Chesley, S. R., Vokrouhlický, D., et al. 2013, *Icarus*, 224, 1, doi: [10.1016/j.icarus.2013.02.004](https://doi.org/10.1016/j.icarus.2013.02.004)
- Fernández, Y. R., Jewitt, D. C., & Sheppard, S. S. 2002, *AJ*, 123, 1050, doi: [10.1086/338436](https://doi.org/10.1086/338436)

- Fernández, Y. R., Sheppard, S. S., & Jewitt, D. C. 2003, *AJ*, 126, 1563, doi: [10.1086/377015](https://doi.org/10.1086/377015)
- Fornasier, S., Lellouch, E., Müller, T., et al. 2013, *A&A*, 555, A15, doi: [10.1051/0004-6361/201321329](https://doi.org/10.1051/0004-6361/201321329)
- Franco, L., Klinglesmith, Daniel A., I., DeHart, A., Hendrickx, S., & Hanowell, J. 2015, *Minor Planet Bulletin*, 42, 198
- Franco, L., Marchini, A., Galdies, C., Brincat, S. M., & Grech, W. 2019, *Minor Planet Bulletin*, 46, 269
- Gaia Collaboration, Prusti, T., de Bruijne, J. H. J., et al. 2016, *A&A*, 595, A1, doi: [10.1051/0004-6361/201629272](https://doi.org/10.1051/0004-6361/201629272)
- Gaia Collaboration, Spoto, F., Tanga, P., et al. 2018, *A&A*, 616, A13, doi: [10.1051/0004-6361/201832900](https://doi.org/10.1051/0004-6361/201832900)
- Gradie, J., & Tedesco, E. 1982, *Science*, 216, 1405, doi: [10.1126/science.216.4553.1405](https://doi.org/10.1126/science.216.4553.1405)
- Greenberg, A. H., Margot, J.-L., Verma, A. K., Taylor, P. A., & Hodge, S. E. 2020, *AJ*, 159, 92, doi: [10.3847/1538-3881/ab62a3](https://doi.org/10.3847/1538-3881/ab62a3)
- Groussin, O., Lamy, P., & Jorda, L. 2004, *A&A*, 413, 1163, doi: [10.1051/0004-6361:20031564](https://doi.org/10.1051/0004-6361:20031564)
- Gundlach, B., & Blum, J. 2013, *Icarus*, 223, 479, doi: [10.1016/j.icarus.2012.11.039](https://doi.org/10.1016/j.icarus.2012.11.039)
- Hanuš, J., Delbo', M., Ďurech, J., & Alí-Lagoa, V. 2015, *Icarus*, 256, 101, doi: [10.1016/j.icarus.2015.04.014](https://doi.org/10.1016/j.icarus.2015.04.014)
- . 2018a, *Icarus*, 309, 297, doi: [10.1016/j.icarus.2018.03.016](https://doi.org/10.1016/j.icarus.2018.03.016)
- Hanuš, J., Marchis, F., & Ďurech, J. 2013a, *Icarus*, 226, 1045, doi: [10.1016/j.icarus.2013.07.023](https://doi.org/10.1016/j.icarus.2013.07.023)
- Hanuš, J., Ďurech, J., Brož, M., et al. 2011, *A&A*, 530, A134, doi: [10.1051/0004-6361/201116738](https://doi.org/10.1051/0004-6361/201116738)
- . 2013b, *A&A*, 551, A67, doi: [10.1051/0004-6361/201220701](https://doi.org/10.1051/0004-6361/201220701)
- Hanuš, J., Brož, M., Ďurech, J., et al. 2013c, *A&A*, 559, A134, doi: [10.1051/0004-6361/201321993](https://doi.org/10.1051/0004-6361/201321993)
- Hanuš, J., Delbo', M., Vokrouhlický, D., et al. 2016a, *A&A*, 592, A34, doi: [10.1051/0004-6361/201628666](https://doi.org/10.1051/0004-6361/201628666)
- Hanuš, J., Ďurech, J., Oszkiewicz, D. A., et al. 2016b, *A&A*, 586, A108, doi: [10.1051/0004-6361/201527441](https://doi.org/10.1051/0004-6361/201527441)
- Hanuš, J., Delbo', M., Alí-Lagoa, V., et al. 2018b, *Icarus*, 299, 84, doi: [10.1016/j.icarus.2017.07.007](https://doi.org/10.1016/j.icarus.2017.07.007)
- Hapke, B. 1984, *Icarus*, 59, 41, doi: [10.1016/0019-1035\(84\)90054-X](https://doi.org/10.1016/0019-1035(84)90054-X)
- Hardersen, P. S., Gaffey, M. J., & Abell, P. A. 2005, *Icarus*, 175, 141, doi: [10.1016/j.icarus.2004.10.017](https://doi.org/10.1016/j.icarus.2004.10.017)
- Harris, A. W. 1998, *Icarus*, 131, 291, doi: [10.1006/icar.1997.5865](https://doi.org/10.1006/icar.1997.5865)
- Harris, A. W., & Drube, L. 2016, *ApJ*, 832, 127, doi: [10.3847/0004-637X/832/2/127](https://doi.org/10.3847/0004-637X/832/2/127)
- Harris, A. W., & Lagerros, J. S. V. 2002, *Asteroids in the Thermal Infrared*, 205–218
- Hayne, P. O., Bandfield, J. L., Siegler, M. A., et al. 2017, *Journal of Geophysical Research (Planets)*, 122, 2371, doi: [10.1002/2017JE005387](https://doi.org/10.1002/2017JE005387)
- Horner, J., Müller, T. G., & Lykawka, P. S. 2012, *MNRAS*, 423, 2587, doi: [10.1111/j.1365-2966.2012.21067.x](https://doi.org/10.1111/j.1365-2966.2012.21067.x)
- Ivezić, Ž., Kahn, S. M., Tyson, J. A., et al. 2019, *ApJ*, 873, 111, doi: [10.3847/1538-4357/ab042c](https://doi.org/10.3847/1538-4357/ab042c)
- Jiang, H., & Ji, J. 2021, *AJ*, 162, 40, doi: [10.3847/1538-3881/ac01c8](https://doi.org/10.3847/1538-3881/ac01c8)
- Jiang, H., Ji, J., & Yu, L.-L. 2020, *AJ*, 159, 264, doi: [10.3847/1538-3881/ab8af5](https://doi.org/10.3847/1538-3881/ab8af5)
- Jiang, H., Yu, L.-L., & Ji, J. 2019, *AJ*, 158, 205, doi: [10.3847/1538-3881/ab46b4](https://doi.org/10.3847/1538-3881/ab46b4)
- Kaasalainen, M., & Torppa, J. 2001, *Icarus*, 153, 24, doi: [10.1006/icar.2001.6673](https://doi.org/10.1006/icar.2001.6673)
- Kaasalainen, M., Torppa, J., & Muinonen, K. 2001, *Icarus*, 153, 37, doi: [10.1006/icar.2001.6674](https://doi.org/10.1006/icar.2001.6674)
- Kaasalainen, M., Torppa, J., & Piironen, J. 2002a, *Icarus*, 159, 369, doi: [10.1006/icar.2002.6907](https://doi.org/10.1006/icar.2002.6907)
- . 2002b, *A&A*, 383, L19, doi: [10.1051/0004-6361:20020015](https://doi.org/10.1051/0004-6361:20020015)
- Kaasalainen, M., Pravec, P., Krugly, Y. N., et al. 2004, *Icarus*, 167, 178, doi: [10.1016/j.icarus.2003.09.012](https://doi.org/10.1016/j.icarus.2003.09.012)
- Kopp, G., & Lean, J. L. 2011, *Geophysical Research Letters*, 38, doi: [10.1029/2010gl045777](https://doi.org/10.1029/2010gl045777)
- Krasinsky, G. A., Pitjeva, E. V., Vasilyev, M. V., & Yagudina, E. I. 2002, *Icarus*, 158, 98, doi: [10.1006/icar.2002.6837](https://doi.org/10.1006/icar.2002.6837)
- Lagerros, J. S. V. 1996, *A&A*, 310, 1011
- . 1997, *A&A*, 325, 1226
- Lagerros, J. S. V. 1998, *A&A*, 332, 1123
- Lamy, P. L., Jorda, L., Fornasier, S., et al. 2008, *A&A*, 487, 1187, doi: [10.1051/0004-6361:20078996](https://doi.org/10.1051/0004-6361:20078996)
- Lauretta, D. S., Dellagiustina, D. N., Bennett, C. A., et al. 2019, *Nature*, 568, 55, doi: [10.1038/s41586-019-1033-6](https://doi.org/10.1038/s41586-019-1033-6)
- Lellouch, E., Santos-Sanz, P., Lacerda, P., et al. 2013, *A&A*, 557, A60, doi: [10.1051/0004-6361/201322047](https://doi.org/10.1051/0004-6361/201322047)
- Leyrat, C., Barucci, A., Mueller, T., et al. 2012, *A&A*, 539, A154, doi: [10.1051/0004-6361/201117793](https://doi.org/10.1051/0004-6361/201117793)
- Leyrat, C., Coradini, A., Erard, S., et al. 2011, *A&A*, 531, A168, doi: [10.1051/0004-6361/201116529](https://doi.org/10.1051/0004-6361/201116529)
- Lim, L. F., Emery, J. P., & Moskovitz, N. A. 2011, *Icarus*, 213, 510, doi: [10.1016/j.icarus.2010.12.006](https://doi.org/10.1016/j.icarus.2010.12.006)
- MacLennan, E. M., & Emery, J. P. 2021, *PSJ*, 2, 161, doi: [10.3847/PSJ/ac1591](https://doi.org/10.3847/PSJ/ac1591)
- Magri, C., Nolan, M. C., Ostro, S. J., & Giorgini, J. D. 2007, *Icarus*, 186, 126, doi: [10.1016/j.icarus.2006.08.018](https://doi.org/10.1016/j.icarus.2006.08.018)
- Magri, C., Ostro, S. J., Rosema, K. D., et al. 1999, *Icarus*, 140, 379, doi: [10.1006/icar.1999.6130](https://doi.org/10.1006/icar.1999.6130)
- Mainzer, A., Bauer, J., Grav, T., et al. 2011, *ApJ*, 731, 53, doi: [10.1088/0004-637X/731/1/53](https://doi.org/10.1088/0004-637X/731/1/53)

- Mainzer, A. K., Bauer, J. M., Cutri, R. M., et al. 2019, NASA Planetary Data System, doi: [10.26033/18S3-2Z54](https://doi.org/10.26033/18S3-2Z54)
- Marchis, F., Kaasalainen, M., Hom, E. F. Y., et al. 2006, *Icarus*, 185, 39, doi: [10.1016/j.icarus.2006.06.001](https://doi.org/10.1016/j.icarus.2006.06.001)
- Marchis, F., Enriquez, J. E., Emery, J. P., et al. 2012, *Icarus*, 221, 1130, doi: [10.1016/j.icarus.2012.09.013](https://doi.org/10.1016/j.icarus.2012.09.013)
- Marciniak, A., Michałowski, T., Kaasalainen, M., et al. 2007, *A&A*, 473, 633, doi: [10.1051/0004-6361:20077694](https://doi.org/10.1051/0004-6361:20077694)
- . 2008, *A&A*, 478, 559, doi: [10.1051/0004-6361:20078930](https://doi.org/10.1051/0004-6361:20078930)
- Marciniak, A., Michałowski, T., Hirsch, R., et al. 2009a, *A&A*, 508, 1503, doi: [10.1051/0004-6361/200912741](https://doi.org/10.1051/0004-6361/200912741)
- . 2009b, *A&A*, 498, 313, doi: [10.1051/0004-6361/200811078](https://doi.org/10.1051/0004-6361/200811078)
- Marciniak, A., Michałowski, T., Polińska, M., et al. 2011, *A&A*, 529, A107, doi: [10.1051/0004-6361/201015365](https://doi.org/10.1051/0004-6361/201015365)
- Marciniak, A., Bartczak, P., Santana-Ros, T., et al. 2012, *A&A*, 545, A131, doi: [10.1051/0004-6361/201219542](https://doi.org/10.1051/0004-6361/201219542)
- Marciniak, A., Bartczak, P., Müller, T., et al. 2018, *A&A*, 610, A7, doi: [10.1051/0004-6361/201731479](https://doi.org/10.1051/0004-6361/201731479)
- Marciniak, A., Alí-Lagoa, V., Müller, T. G., et al. 2019, *A&A*, 625, A139, doi: [10.1051/0004-6361/201935129](https://doi.org/10.1051/0004-6361/201935129)
- Marciniak, A., Ďurech, J., Alí-Lagoa, V., et al. 2021, *A&A*, 654, A87, doi: [10.1051/0004-6361/202140991](https://doi.org/10.1051/0004-6361/202140991)
- Marshall, S., McGlasson, R., Repp, D., et al. 2021, in *AAS/Division for Planetary Sciences Meeting Abstracts*, Vol. 53, AAS/Division for Planetary Sciences Meeting Abstracts, 306.12
- Masiero, J. R., Grav, T., Mainzer, A. K., et al. 2014, *ApJ*, 791, 121, doi: [10.1088/0004-637X/791/2/121](https://doi.org/10.1088/0004-637X/791/2/121)
- Masiero, J. R., Wright, E. L., & Mainzer, A. K. 2019, *AJ*, 158, 97, doi: [10.3847/1538-3881/ab31a6](https://doi.org/10.3847/1538-3881/ab31a6)
- Masiero, J. R., Mainzer, A. K., Grav, T., et al. 2011, *ApJ*, 741, 68, doi: [10.1088/0004-637X/741/2/68](https://doi.org/10.1088/0004-637X/741/2/68)
- Matter, A., Delbo', M., Carry, B., & Ligorì, S. 2013, *Icarus*, 226, 419, doi: [10.1016/j.icarus.2013.06.004](https://doi.org/10.1016/j.icarus.2013.06.004)
- Matter, A., Delbo', M., Ligorì, S., Crouzet, N., & Tanga, P. 2011, *Icarus*, 215, 47, doi: [10.1016/j.icarus.2011.07.012](https://doi.org/10.1016/j.icarus.2011.07.012)
- Michałowski, T., Kaasalainen, M., Marciniak, A., et al. 2005, *A&A*, 443, 329, doi: [10.1051/0004-6361:20053656](https://doi.org/10.1051/0004-6361:20053656)
- Mueller, M. 2012, arXiv e-prints, arXiv:1208.3993. <https://arxiv.org/abs/1208.3993>
- Mueller, M., Marchis, F., Emery, J. P., et al. 2010, *Icarus*, 205, 505, doi: [10.1016/j.icarus.2009.07.043](https://doi.org/10.1016/j.icarus.2009.07.043)
- Mueller, T. G., & Lagerros, J. S. V. 1998, *A&A*, 338, 340
- Muñonen, K., Belskaya, I. N., Cellino, A., et al. 2010, *Icarus*, 209, 542, doi: [10.1016/j.icarus.2010.04.003](https://doi.org/10.1016/j.icarus.2010.04.003)
- Müller, T. G., Hasegawa, S., & Usui, F. 2014a, *PASJ*, 66, 52, doi: [10.1093/pasj/psu034](https://doi.org/10.1093/pasj/psu034)
- Müller, T. G., Kiss, C., Scheirich, P., et al. 2014b, *A&A*, 566, A22, doi: [10.1051/0004-6361/201423841](https://doi.org/10.1051/0004-6361/201423841)
- Müller, T. G., Ďurech, J., Hasegawa, S., et al. 2011, *A&A*, 525, A145, doi: [10.1051/0004-6361/201015599](https://doi.org/10.1051/0004-6361/201015599)
- Müller, T. G., O'Rourke, L., Barucci, A. M., et al. 2012, *A&A*, 548, A36, doi: [10.1051/0004-6361/201220066](https://doi.org/10.1051/0004-6361/201220066)
- Müller, T. G., Miyata, T., Kiss, C., et al. 2013, *A&A*, 558, A97, doi: [10.1051/0004-6361/201321664](https://doi.org/10.1051/0004-6361/201321664)
- Müller, T. G., Ďurech, J., Ishiguro, M., et al. 2017, *A&A*, 599, A103, doi: [10.1051/0004-6361/201629134](https://doi.org/10.1051/0004-6361/201629134)
- Myhrvold, N. 2018, *Icarus*, 303, 91, doi: [10.1016/j.icarus.2017.12.024](https://doi.org/10.1016/j.icarus.2017.12.024)
- Okada, T., Fukuhara, T., Tanaka, S., et al. 2020, *Nature*, 579, 518, doi: [10.1038/s41586-020-2102-6](https://doi.org/10.1038/s41586-020-2102-6)
- Opeil, C. P., Consolmagno, G. J., & Britt, D. T. 2010, *Icarus*, 208, 449, doi: [10.1016/j.icarus.2010.01.021](https://doi.org/10.1016/j.icarus.2010.01.021)
- O'Rourke, L., Müller, T., Valtchanov, I., et al. 2012, *Planet. Space Sci.*, 66, 192, doi: [10.1016/j.pss.2012.01.004](https://doi.org/10.1016/j.pss.2012.01.004)
- Oszkiewicz, D. A., Muñonen, K., Bowell, E., et al. 2011, *JQSRT*, 112, 1919, doi: [10.1016/j.jqsrt.2011.03.003](https://doi.org/10.1016/j.jqsrt.2011.03.003)
- Pál, A., Kiss, C., Müller, T. G., et al. 2012, *A&A*, 541, L6, doi: [10.1051/0004-6361/201218874](https://doi.org/10.1051/0004-6361/201218874)
- Polishook, D. 2009, *Minor Planet Bulletin*, 36, 119
- Pravec, P., Fatka, P., Vokrouhlický, D., et al. 2019, *Icarus*, 333, 429, doi: [10.1016/j.icarus.2019.05.014](https://doi.org/10.1016/j.icarus.2019.05.014)
- Press, W. H., Flannery, B. P., & Teukolsky, S. A. 1986, *Numerical recipes. The art of scientific computing*
- Rozitis, B., Duddy, S. R., Green, S. F., & Lowry, S. C. 2013, *A&A*, 555, A20, doi: [10.1051/0004-6361/201321659](https://doi.org/10.1051/0004-6361/201321659)
- Rozitis, B., & Green, S. F. 2011, *MNRAS*, 415, 2042, doi: [10.1111/j.1365-2966.2011.18718.x](https://doi.org/10.1111/j.1365-2966.2011.18718.x)
- . 2014, *A&A*, 568, A43, doi: [10.1051/0004-6361/201323090](https://doi.org/10.1051/0004-6361/201323090)
- Rozitis, B., Green, S. F., MacLennan, E., & Emery, J. P. 2018, *MNRAS*, 477, 1782, doi: [10.1093/mnras/sty640](https://doi.org/10.1093/mnras/sty640)
- Rozitis, B., MacLennan, E., & Emery, J. P. 2014, *Nature*, 512, 174, doi: [10.1038/nature13632](https://doi.org/10.1038/nature13632)
- Shepard, M. K., Taylor, P. A., Nolan, M. C., et al. 2015, *Icarus*, 245, 38, doi: [10.1016/j.icarus.2014.09.016](https://doi.org/10.1016/j.icarus.2014.09.016)
- Slivan, S. M., Binzel, R. P., Crespo da Silva, L. D., et al. 2003, *Icarus*, 162, 285, doi: [10.1016/S0019-1035\(03\)00029-0](https://doi.org/10.1016/S0019-1035(03)00029-0)
- Spencer, J. R., Lebofsky, L. A., & Sykes, M. V. 1989, *Icarus*, 78, 337, doi: [10.1016/0019-1035\(89\)90182-6](https://doi.org/10.1016/0019-1035(89)90182-6)
- Stephens, R. D., Warner, B. D., Megna, R., & Coley, D. 2012, *Minor Planet Bulletin*, 39, 2
- Taylor, P. A., Rivera-Valentín, E. G., Benner, L. A. M., et al. 2019, *Planet. Space Sci.*, 167, 1, doi: [10.1016/j.pss.2019.01.009](https://doi.org/10.1016/j.pss.2019.01.009)
- Tholen, D. J. 1984, PhD thesis, University of Arizona, Tucson

- Tonry, J. L., Denneau, L., Heinze, A. N., et al. 2018, *PASP*, 130, 064505, doi: [10.1088/1538-3873/aabadf](https://doi.org/10.1088/1538-3873/aabadf)
- Torppa, J., Kaasalainen, M., Michałowski, T., et al. 2003, *Icarus*, 164, 346, doi: [10.1016/S0019-1035\(03\)00146-5](https://doi.org/10.1016/S0019-1035(03)00146-5)
- Vokrouhlický, D., Bottke, W. F., Chesley, S. R., Scheeres, D. J., & Statler, T. S. 2015, *The Yarkovsky and YORP Effects*, 509–531, doi: [10.2458/azu_uapress.9780816532131-ch027](https://doi.org/10.2458/azu_uapress.9780816532131-ch027)
- Vokrouhlický, D., Ďurech, J., Pravec, P., et al. 2016a, *A&A*, 585, A56, doi: [10.1051/0004-6361/201526953](https://doi.org/10.1051/0004-6361/201526953)
- . 2016b, *AJ*, 151, 56, doi: [10.3847/0004-6256/151/3/56](https://doi.org/10.3847/0004-6256/151/3/56)
- Warner, B. D. 2008, *Minor Planet Bulletin*, 35, 171
- Warner, B. D., Harris, A. W., & Pravec, P. 2009, *Icarus*, 202, 134, doi: [10.1016/j.icarus.2009.02.003](https://doi.org/10.1016/j.icarus.2009.02.003)
- Warner, B. D., Stephens, R. D., & Harris, A. W. 2011, *Minor Planet Bulletin*, 38, 172
- Warner, B. D., Ďurech, J., Fauerbach, M., & Marks, S. 2008, *Minor Planet Bulletin*, 35, 167
- Winter, D. F., & Krupp, J. A. 1971, *Moon*, 2, 279, doi: [10.1007/BF00561881](https://doi.org/10.1007/BF00561881)
- WISE Team. 2012, *WISE All-Sky Single Exposure (L1b) Source Table*, IPAC, doi: [10.26131/IRSA139](https://doi.org/10.26131/IRSA139)
- Wolters, S. D., Rozitis, B., Duddy, S. R., et al. 2011, *MNRAS*, 418, 1246, doi: [10.1111/j.1365-2966.2011.19575.x](https://doi.org/10.1111/j.1365-2966.2011.19575.x)
- Wright, E. L., Eisenhardt, P. R. M., Mainzer, A. K., et al. 2010, *AJ*, 140, 1868, doi: [10.1088/0004-6256/140/6/1868](https://doi.org/10.1088/0004-6256/140/6/1868)
- Yu, L.-L., & Ip, W.-H. 2021, *ApJ*, 913, 96, doi: [10.3847/1538-4357/abf4c9](https://doi.org/10.3847/1538-4357/abf4c9)
- Yu, L.-L., & Ji, J. 2015, *MNRAS*, 452, 368, doi: [10.1093/mnras/stv1270](https://doi.org/10.1093/mnras/stv1270)
- Yu, L.-L., Ji, J., & Ip, W.-H. 2017a, *Research in Astronomy and Astrophysics*, 17, 070, doi: [10.1088/1674-4527/17/7/70](https://doi.org/10.1088/1674-4527/17/7/70)
- Yu, L.-L., Ji, J., & Wang, S. 2014, *MNRAS*, 439, 3357, doi: [10.1093/mnras/stu164](https://doi.org/10.1093/mnras/stu164)
- Yu, L. L., Yang, B., Ji, J., & Ip, W.-H. 2017b, *MNRAS*, 472, 2388, doi: [10.1093/mnras/stx2089](https://doi.org/10.1093/mnras/stx2089)

6. APPENDIX

Table 3. Literature TPM/ATPM-derived Properties

Asteroid	D (km)	Γ ($\text{J m}^{-2} \text{s}^{-0.5} \text{K}^{-1}$)	Taxonomy	r_h (au)	Orbit	Reference
1 Ceres	923_{-20}^{+20}	10_{-10}^{+10}	C	2.767	MBA	[1]
1 Ceres	951_{-7}^{+9}	25_{-10}^{+15}	C	2.80	MBA	[2]
2 Pallas	544_{-43}^{+43}	10_{-10}^{+10}	B	2.772	MBA	[1]
2 Pallas	536_{-5}^{+5}	30_{-15}^{+15}	B	2.95	MBA	[2]
3 Juno	234_{-11}^{+11}	5_{-5}^{+5}	S	2.671	MBA	[1]
3 Juno	252_{-3}^{+2}	60_{-20}^{+25}	S	2.70	MBA	[2]
4 Vesta	525_{-1}^{+1}	20_{-15}^{+15}	V	2.3	MBA	[3]
4 Vesta	520_{-6}^{+12}	35_{-23}^{+55}	V	2.36	MBA	[2]
8 Flora	142_{-2}^{+2}	50_{-30}^{+35}	S	2.20	MBA	[2]
10 Hygiea	441_{-4}^{+7}	50_{-25}^{+20}	C	3.02	MBA	[2]
16 Psyche	244_{-25}^{+25}	125_{-40}^{+40}	M	2.7	MBA	[4]
91 Aegina	$101.4_{-13.85}^{+13.85}$	19_{-19}^{+31}	CP	2.604–2.772	MBA	[5]
18 Melpomene	135_{-1}^{+4}	50_{-44}^{+15}	S	2.35	MBA	[2]
19 Fortuna	219_{-2}^{+3}	40_{-15}^{+30}	Ch	2.45	MBA	[2]
20 Massalia	147_{-2}^{+2}	35_{-10}^{+25}	S	2.40	MBA	[2]
21 Lutetia	96_{-1}^{+1}	5_{-5}^{+5}	M	2.8	MBA	[6]
21 Lutetia	98_{-1}^{+1}	10_{-2}^{+10}	M	2.40	MBA	[2]
22 Kalliope	167_{-17}^{+17}	125_{-125}^{+125}	M	2.3	MBA	[7]
29 Amphitrite	202_{-2}^{+3}	25_{-13}^{+10}	S	2.55	MBA	[2]
32 Pomona	85_{-1}^{+1}	70_{-50}^{+50}	S	2.8	MBA	[8]
41 Daphne	202_{-7}^{+7}	25_{-25}^{+25}	Ch	2.1	MBA	[9]
44 Nysa	81_{-1}^{+1}	120_{-40}^{+40}	E	2.5	MBA	[8]
45 Eugenia	198_{-20}^{+20}	45_{-45}^{+45}	C	2.6	MBA	[7]
52 Europa	317_{-3}^{+4}	10_{-10}^{+25}	C	3.05	MBA	[2]
54 Alexandra	153_{-2}^{+2}	10_{-10}^{+22}	C	2.60	MBA	[2]
62 Erato	$81.064_{-3.011}^{+5.528}$	55_{-12}^{+12}	B	3.1286	MBA	[10]
63 Ausonia	$94.595_{-2.483}^{+2.343}$	50_{-24}^{+12}	S	2.113–2.694	MBA	[11]
65 Cybele	277_{-2}^{+4}	30_{-15}^{+10}	Xc	3.30	OMB	[2]
73 Klytia	$44.1_{-2.1}^{+2.1}$	13_{-12}^{+12}	S	2.8	MBA	[12]
82 Alkmene	$58.6_{-1.2}^{+1.2}$	32_{-12}^{+12}	S	3.3	MBA	[12]
87 Sylvia	300_{-30}^{+30}	70_{-60}^{+60}	P	2.7	OMB	[7]
88 Thisbe	221_{-2}^{+2}	60_{-25}^{+15}	B	3.00	MBA	[2]
93 Minerva	167_{-3}^{+3}	25_{-10}^{+30}	C	3.01	MBA	[2]
99 Dike	$66.5_{-0.9}^{+0.9}$	35_{-19}^{+19}	C	3.2	MBA	[12]
100 Hekate	87_{-4}^{+5}	4_{-2}^{+66}	S	3.10	MBA	[13]
107 Camilla	245_{-25}^{+25}	25_{-10}^{+10}	P	3.2	OMB	[7]
108 Hecuba	69_{-1}^{+3}	35_{-30}^{+25}	S	3.18	OMB	[14]

Table 3 continued

Table 3 (continued)

Asteroid		D	Γ	Taxonomy	r_h	Orbit	Reference
		(km)	($\text{J m}^{-2} \text{s}^{-0.5} \text{K}^{-1}$)		(au)		
109	Felicitas	85_{-5}^{+7}	40_{-40}^{+100}	Ch	3.15	MBA	[13]
110	Lydia	$93.5_{-3.5}^{+3.5}$	135_{-65}^{+65}	M	2.9	MBA	[8]
115	Thyra	92_{-2}^{+2}	62_{-38}^{+38}	S	2.5	MBA	[8]
121	Hermione	220_{-22}^{+22}	30_{-25}^{+25}	Ch	2.9	OMB	[7]
125	Liberatrix	$50.1_{-1.3}^{+1.3}$	60_{-15}^{+15}	M	2.9	MBA	[12]
130	Elektra	197_{-20}^{+20}	30_{-30}^{+30}	Ch	2.9	MBA	[7]
152	Atala	$57.5_{-1.8}^{+1.8}$	0_{-0}^{+0}	I	2.9	MBA	[12]
155	Scylla	$39.0_{-0.8}^{+0.8}$	30_{-10}^{+10}	XFC	3.1	MBA	[12]
155	Scylla	$38.41_{-0.54}^{+0.54}$	16_{-5}^{+15}	XFC	2.860–3.252	MBA	[5]
167	Urda	$41.5_{-0.8}^{+0.8}$	115_{-5}^{+5}	S	2.8	MBA	[12]
171	Ophelia	$103.816_{-4.869}^{+5.667}$	30_{-11}^{+15}	C	3.1301	MBA	[10]
188	Menippe	$36.0_{-1.1}^{+1.1}$	13_{-7}^{+7}	S	3.2	MBA	[12]
193	Ambrosia	$30.1_{-0.8}^{+0.8}$	52_{-17}^{+17}	Sk	3.3	MBA	[12]
195	Eurykleia	87_{-9}^{+11}	15_{-15}^{+55}	Ch	2.85	MBA	[13]
220	Stephania	$29.8_{-0.6}^{+0.6}$	2_{-2}^{+2}	XC	2.8	MBA	[12]
222	Lucia	$61.729_{-4.518}^{+4.332}$	70_{-20}^{+22}	B	3.1430	MBA	[10]
226	Weringia	$31.5_{-0.3}^{+0.3}$	30_{-10}^{+10}	S	3.1	MBA	[12]
263	Dresda	$23.7_{-1.0}^{+1.0}$	25_{-25}^{+25}	S	2.8	MBA	[12]
271	Penthesilea	$65.05_{-2.30}^{+2.30}$	16_{-16}^{+33}	PC	3.278–3.306	MBA	[5]
272	Antonia	$30.5_{-1.1}^{+1.1}$	75_{-10}^{+10}	X	2.9	MBA	[12]
274	Philagoria	$28.9_{-0.9}^{+0.9}$	90_{-10}^{+10}	–	2.7	MBA	[12]
277	Elvira	38_{-2}^{+2}	250_{-150}^{+150}	S	2.6	MBA	[8]
281	Lucretia	$11.3_{-0.2}^{+0.2}$	45_{-10}^{+10}	SU	2.5	MBA	[12]
283	Emma	135_{-14}^{+14}	105_{-100}^{+100}	P	2.6	MBA	[7]
290	Bruna	$9.9_{-0.3}^{+0.3}$	12_{-12}^{+12}	–	2.9	MBA	[12]
295	Theresia	$30.50_{-1.23}^{+1.23}$	24_{-17}^{+38}	S	3.122–3.257	MBA	[5]
301	Bavaria	55_{-2}^{+2}	45_{-30}^{+60}	C	2.65	MBA	[13]
306	Unitas	56_{-1}^{+1}	180_{-80}^{+80}	S	2.2	MBA	[8]
311	Claudia	$25.8_{-0.8}^{+0.8}$	9_{-9}^{+9}	S	2.9	MBA	[12]
322	Phaeo	$59.66_{-1.29}^{+1.29}$	12_{-7}^{+11}	X	3.281–3.445	MBA	[5]
340	Eduarda	$27.3_{-0.3}^{+0.3}$	30_{-14}^{+14}	S	2.9	MBA	[12]
343	Ostara	$19.65_{-1.38}^{+1.38}$	140_{-60}^{+120}	CSGU	2.678–2.916	MBA	[5]
349	Dembowska	$155.8_{-6.2}^{+7.5}$	20_{-7}^{+12}	R	2.719–3.170	MBA	[15]
351	Yrsa	$42.3_{-1.6}^{+1.6}$	47_{-17}^{+17}	S	3.2	MBA	[12]
352	Gisela	$24.8_{-0.6}^{+0.6}$	17_{-17}^{+17}	S	2.3	MBA	[12]
355	Gabriela	$24.8_{-0.8}^{+0.8}$	35_{-5}^{+5}	S	2.3	MBA	[12]
378	Holmia	$29.0_{-0.6}^{+0.6}$	13_{-12}^{+12}	S	2.8	MBA	[12]
380	Fiducia	72_{-5}^{+9}	10_{-10}^{+140}	C	2.50	MBA	[13]
382	Dodona	75_{-1}^{+1}	80_{-65}^{+65}	M	2.6	MBA	[8]
390	Alma	$24.3_{-0.4}^{+0.4}$	29_{-21}^{+21}	DT	2.4	MBA	[12]

Table 3 continued

Table 3 (continued)

Asteroid	D (km)	Γ ($\text{J m}^{-2} \text{s}^{-0.5} \text{K}^{-1}$)	Taxonomy	r_h (au)	Orbit	Reference	
394	Arduina	$30.6^{+0.6}_{-0.6}$	90^{+10}_{-10}	S	2.9	MBA	[12]
400	Ducrosa	$35.2^{+1.1}_{-1.1}$	42^{+12}_{-12}	–	3.4	MBA	[12]
413	Edburga	$34.6^{+0.8}_{-0.8}$	110^{+50}_{-50}	M	2.9	MBA	[12]
423	Diotima	200^{+3}_{-4}	40^{+30}_{-20}	C	3.07	MBA	[2]
430	Hybris	$32.9^{+0.5}_{-0.5}$	52^{+2}_{-2}	–	3.5	MBA	[12]
433	Eros	17.8^{+1}_{-1}	150^{+50}_{-50}	S	1.6	AMO	[16]
444	Gyptis	$162.3^{+22.9}_{-22.9}$	74^{+74}_{-74}	C	2.925–3.150	MBA	[5]
463	Lola	$20.27^{+1.48}_{-1.48}$	70^{+30}_{-30}	X	2.903–2.904	MBA	[5]
464	Megaira	$69.56^{+6.38}_{-6.38}$	120^{+120}_{-120}	FXU:	3.320–3.371	MBA	[5]
468	Lina	69^{+11}_{-4}	20^{+280}_{-20}	CPF	3.00	MBA	[13]
468	Lina	$66.915^{+2.372}_{-1.552}$	5^{+23}_{-5}	C	3.1332	MBA	[10]
478	Tergeste	81^{+5}_{-4}	26^{+25}_{-25}	S	3.05	MBA	[14]
482	Petrina	$44.2^{+1.0}_{-1.0}$	12^{+12}_{-12}	S	3.3	MBA	[12]
483	Seppina	73^{+5}_{-2}	17^{+23}_{-12}	S	3.45	OMB	[14]
484	Pittsburghia	$29.2^{+0.7}_{-0.7}$	6^{+5}_{-5}	S	2.8	MBA	[12]
493	Griseldis	$40.86^{+1.13}_{-1.13}$	56^{+25}_{-32}	–	3.487–3.621	MBA	[5]
497	Iva	$37.6^{+0.7}_{-0.7}$	67^{+22}_{-22}	M	3.6	MBA	[12]
500	Selinur	$41.15^{+0.37}_{-0.37}$	16^{+7}_{-8}	–	2.785–2.951	MBA	[5]
501	Urhixidur	82^{+2}_{-4}	13^{+30}_{-11}	–	3.20	MBA	[14]
509	Iolanda	$55.2^{+1.4}_{-1.4}$	8^{+8}_{-8}	S	3.3	MBA	[12]
511	Davida	307^{+7}_{-4}	35^{+15}_{-17}	C	3.35	MBA	[2]
512	Taurinensis	$18.0^{+0.7}_{-0.7}$	4^{+4}_{-4}	S	2.2	MCA	[12]
520	Franziska	$28.9^{+0.9}_{-0.9}$	28^{+16}_{-16}	CGU	3.3	MBA	[12]
520	Franziska	$27.42^{+1.00}_{-1.00}$	12^{+24}_{-5}	CGU	3.207–3.305	MBA	[5]
526	Jena	$55.120^{+4.046}_{-3.098}$	10^{+16}_{-10}	B	3.1208	MBA	[10]
532	Herculina	203^{+14}_{-14}	10^{+10}_{-10}	S	2.772	MBA	[1]
537	Pauly	$41.4^{+0.9}_{-0.9}$	5^{+5}_{-5}	DU:	3.5	MBA	[12]
537	Pauly	47^{+1}_{-2}	11^{+30}_{-10}	DU:	2.96	MBA	[14]
538	Friederike	76^{+5}_{-2}	20^{+25}_{-20}	C	3.50	MBA	[13]
538	Friederike	$66.45^{+1.42}_{-1.42}$	35^{+12}_{-11}	–	3.403–3.586	MBA	[5]
544	Jetta	$27.5^{+1.3}_{-1.3}$	27^{+17}_{-17}	–	3.0	MBA	[12]
550	Senta	$37.3^{+0.7}_{-0.7}$	22^{+22}_{-22}	S	3.1	MBA	[12]
552	Sigelinde	88^{+10}_{-5}	3^{+55}_{-2}	–	3.26	MBA	[14]
556	Phyllis	$35.600^{+0.883}_{-0.901}$	30^{+12}_{-11}	S	2.215–2.718	MBA	[11]
558	Carmen	$59.71^{+3.15}_{-3.15}$	$7.7^{+26.9}_{-7.7}$	M	2.937–3.000	MBA	[5]
562	Salome	$33.4^{+0.8}_{-0.8}$	0^{+0}_{-0}	S	3.2	MBA	[12]
562	Salome	$36.99^{+1.90}_{-1.90}$	23^{+12}_{-20}	S	3.095–3.225	MBA	[5]
567	Eleutheria	$87.45^{+7.81}_{-7.81}$	19^{+30}_{-11}	CFB:	2.835–2.871	MBA	[5]
573	Recha	$40.1^{+1.1}_{-1.1}$	45^{+15}_{-15}	–	2.7	MBA	[12]
583	Klotilde	$80.78^{+6.25}_{-6.25}$	30^{+12}_{-19}	C	2.771–3.016	MBA	[5]

Table 3 continued

Table 3 (continued)

Asteroid		D	Γ	Taxonomy	r_h	Orbit	Reference
		(km)	($\text{J m}^{-2} \text{s}^{-0.5} \text{K}^{-1}$)		(au)		
590	Tomyris	$32.3^{+1.2}_{-1.2}$	22^{+22}_{-22}	–	3.1	MBA	[12]
617	Patroclus	106^{+11}_{-11}	20^{+15}_{-15}	P	5.9	TJN	[17]
624	Hektor	170^{+20}_{-20}	5^{+5}_{-5}	D	5.3	TJN	[18]
631	Philippina	$46.6^{+3.2}_{-3.2}$	0^{+0}_{-0}	S	2.8	MBA	[12]
644	Cosima	$19.5^{+0.4}_{-0.4}$	42^{+17}_{-17}	S	3.0	MBA	[12]
651	Antikleia	$34.07^{+1.92}_{-1.92}$	37^{+16}_{-26}	S	3.306–3.312	MBA	[5]
653	Berenike	46^{+4}_{-2}	40^{+120}_{-40}	K	3.00	MBA	[13]
656	Beagle	$55.14^{+3.02}_{-3.02}$	32^{+14}_{-14}	–	2.824–3.031	MBA	[5]
662	Newtonia	$24.04^{+1.41}_{-1.41}$	35^{+23}_{-25}	–	2.289–2.681	MBA	[5]
667	Denise	83^{+4}_{-2}	13^{+17}_{-8}	–	3.36	MBA	[14]
668	Dora	$23.18^{+0.48}_{-0.48}$	52^{+8}_{-8}	Ch	2.895–3.219	MBA	[5]
669	Kypria	$31.1^{+1.3}_{-1.3}$	45^{+10}_{-10}	S	3.2	MBA	[12]
670	Ottegebe	$35.08^{+0.76}_{-0.76}$	44^{+14}_{-18}	S	3.206–3.332	MBA	[5]
673	Edda	38^{+6}_{-2}	3^{+33}_{-3}	S	2.82	MBA	[13]
687	Tinette	$22.2^{+0.5}_{-0.5}$	50^{+15}_{-15}	X	3.2	MBA	[12]
688	Melanie	$38.44^{+2.49}_{-2.49}$	41^{+44}_{-19}	C	2.566–2.808	MBA	[5]
694	Ekard	$109.5^{+1.5}_{-1.5}$	120^{+20}_{-20}	–	1.8	MBA	[8]
720	Bohlinia	41^{+1}_{-1}	135^{+65}_{-65}	S	2.9	MBA	[8]
731	Sorga	$36.9^{+1.3}_{-1.3}$	62^{+22}_{-22}	CD	3.3	MBA	[12]
734	Benda	$66.30^{+2.75}_{-2.75}$	13^{+8}_{-13}	–	3.237–3.363	MBA	[5]
735	Marghanna	$65.09^{+3.93}_{-3.93}$	17^{+88}_{-17}	C	2.873–3.313	MBA	[5]
749	Malzovia	$12.8^{+0.4}_{-0.4}$	50^{+15}_{-15}	S	2.2	MBA	[12]
756	Lilliana	$60.0^{+0.8}_{-0.8}$	11^{+5}_{-5}	–	3.5	MBA	[12]
757	Portlandia	$33.1^{+0.5}_{-0.5}$	62^{+2}_{-2}	XF	2.5	MBA	[12]
767	Bondia	$50.546^{+4.776}_{-3.720}$	65^{+30}_{-17}	C	3.1220	MBA	[10]
771	Libera	33^{+3}_{-3}	90^{+60}_{-60}	X	2.8	MBA	[18]
784	Pickeringia	$80.0^{+1.4}_{-1.4}$	30^{+10}_{-10}	C	3.7	MBA	[12]
787	Moskva	$31.3^{+0.6}_{-0.6}$	37^{+7}_{-7}	–	2.9	MBA	[12]
789	Lena	$22.5^{+0.3}_{-0.3}$	47^{+7}_{-7}	X	2.7	MBA	[12]
793	Arizona	$26.94^{+1.33}_{-1.33}$	32^{+16}_{-13}	DU:	2.871–3.046	MBA	[5]
802	Epyaxa	$7.2^{+0.5}_{-0.5}$	62^{+7}_{-7}	–	2.3	MBA	[12]
808	Merxia	$29.3^{+0.5}_{-0.5}$	115^{+25}_{-25}	Sq	2.9	MBA	[12]
810	Atossa	$8.0^{+0.2}_{-0.2}$	65^{+30}_{-30}	–	2.5	MBA	[12]
816	Juliana	$48.0^{+0.7}_{-0.7}$	23^{+17}_{-17}	–	2.8	MBA	[12]
826	Henrika	$23.11^{+0.97}_{-0.97}$	45^{+16}_{-21}	C	2.230–2.547	MBA	[5]
829	Academia	$37.20^{+1.49}_{-1.49}$	15^{+7}_{-15}	–	2.797–2.835	MBA	[5]
834	Burnhamia	67^{+8}_{-6}	22^{+30}_{-20}	GS:	2.75	MBA	[13]
852	Wladilena	$26.3^{+0.3}_{-0.3}$	45^{+15}_{-15}	–	2.7	MBA	[12]
857	Glazenappia	$12.0^{+0.2}_{-0.2}$	47^{+22}_{-22}	MU	2.3	MBA	[12]
867	Kovacia	$25.0^{+0.8}_{-0.8}$	23^{+17}_{-17}	–	3.4	MBA	[12]

Table 3 continued

Table 3 (continued)

Asteroid		D	Γ	Taxonomy	r_h	Orbit	Reference
		(km)	($\text{J m}^{-2} \text{s}^{-0.5} \text{K}^{-1}$)		(au)		
873	Mechthild	$32.4^{+0.4}_{-0.4}$	17^{+17}_{-17}	PC	2.6	MBA	[12]
874	Rotraut	$51.2^{+0.6}_{-0.6}$	45^{+10}_{-10}	–	3.3	MBA	[12]
883	Matterania	$7.60^{+0.81}_{-0.81}$	36^{+37}_{-24}	S	2.261–2.571	MBA	[5]
890	Waltraut	$28.9^{+1.0}_{-1.0}$	80^{+20}_{-20}	CTGU:	3.1	MBA	[12]
900	Rosalinde	$20.4^{+0.6}_{-0.6}$	7^{+6}_{-6}	–	2.8	MBA	[12]
906	Repsolda	$71.08^{+6.05}_{-6.05}$	47^{+115}_{-28}	–	2.864–3.000	MBA	[5]
915	Cosette	$12.3^{+0.2}_{-0.2}$	37^{+37}_{-37}	–	2.5	MBA	[12]
918	Itha	$21.59^{+0.37}_{-0.37}$	37^{+10}_{-10}	–	3.058–3.286	MBA	[5]
923	Herluga	$36.2^{+0.4}_{-1.5}$	37^{+15}_{-36}	–	2.73	MBA	[14]
934	Thuringia	$52.3^{+1.0}_{-1.0}$	5^{+5}_{-5}	Ch	3.3	MBA	[12]
936	Kunigunde	$40.391^{+8.462}_{-9.113}$	65^{+20}_{-25}	B	3.1323	MBA	[10]
956	Elisa	$10.4^{+0.8}_{-0.8}$	90^{+60}_{-60}	–	1.8	MBA	[19]
958	Asplinda	$46.8^{+0.6}_{-0.6}$	2^{+2}_{-2}	–	3.7	OMB	[12]
972	Cohnia	$73.12^{+0.79}_{-0.79}$	19^{+38}_{-13}	–	3.426–3.662	MBA	[5]
977	Philippa	$76.87^{+6.35}_{-6.35}$	27^{+84}_{-21}	C	3.038–3.072	MBA	[5]
984	Gretia	$33.2^{+0.7}_{-0.7}$	14^{+6}_{-6}	Sr	3.2	MBA	[12]
987	Wallia	$43.05^{+1.91}_{-1.91}$	46^{+64}_{-46}	–	2.992–3.365	MBA	[5]
996	Hilaritas	$27.560^{+1.767}_{-1.925}$	50^{+16}_{-26}	B	3.0901	MBA	[10]
998	Bodea	$28.6^{+0.6}_{-0.6}$	9^{+6}_{-6}	–	3.6	MBA	[12]
998	Bodea	$31.14^{+1.87}_{-1.87}$	20^{+16}_{-7}	–	3.560–3.727	MBA	[5]
1013	Tombecka	$34.5^{+0.8}_{-0.8}$	55^{+15}_{-15}	XSC	3.1	MBA	[12]
1017	Jacqueline	$37.6^{+1.7}_{-1.7}$	57^{+12}_{-12}	C	2.8	MBA	[12]
1018	Arnolda	$16.31^{+1.74}_{-1.74}$	43^{+47}_{-43}	–	2.439–2.858	MBA	[5]
1036	Ganymed	36^{+3}_{-3}	54^{+46}_{-46}	S	3.9	AMO	[18]
1047	Geisha	$10.53^{+0.41}_{-0.41}$	35^{+58}_{-14}	S	2.637–2.651	MBA	[5]
1051	Merope	$53.46^{+1.81}_{-1.81}$	48^{+81}_{-25}	–	3.259–3.396	OMB	[5]
1056	Azalea	$11.4^{+0.3}_{-0.3}$	4^{+3}_{-3}	S	2.5	MBA	[12]
1076	Viola	$22.22^{+1.49}_{-1.49}$	24^{+44}_{-24}	F	2.503–2.729	MBA	[5]
1077	Campanula	$10.12^{+0.80}_{-0.80}$	56^{+40}_{-34}	–	2.678–2.850	MBA	[5]
1082	Pirola	$41.054^{+1.651}_{-1.972}$	45^{+14}_{-12}	C	3.1241	MBA	[10]
1083	Salvia	$11.22^{+1.12}_{-1.12}$	54^{+17}_{-30}	–	2.018–2.361	MBA	[5]
1087	Arabis	$34.3^{+0.4}_{-0.4}$	0^{+0}_{-0}	S	3.2	MBA	[12]
1095	Tulipa	$31.05^{+1.36}_{-1.36}$	23^{+13}_{-13}	–	2.951–2.970	MBA	[5]
1102	Pepita	$34.9^{+0.6}_{-0.6}$	10^{+10}_{-10}	C	3.3	MBA	[12]
1109	Tata	$64.10^{+2.59}_{-2.59}$	10^{+46}_{-10}	FC	2.894–2.987	OMB	[5]
1119	Euboea	$30.6^{+0.5}_{-0.5}$	9^{+6}_{-6}	–	2.5	MBA	[12]
1123	Shapleya	$11.97^{+0.55}_{-0.55}$	14^{+33}_{-14}	–	2.518–2.566	MBA	[5]
1125	China	$26.87^{+1.09}_{-1.09}$	34^{+8}_{-7}	–	3.187–3.500	MBA	[5]
1127	Mimi	$46.9^{+0.8}_{-0.8}$	8^{+2}_{-2}	CX	3.3	MBA	[12]
1130	Skuld	$9.8^{+0.3}_{-0.3}$	2^{+2}_{-2}	–	2.2	MBA	[12]

Table 3 continued

Table 3 (continued)

Asteroid		D	Γ	Taxonomy	r_h	Orbit	Reference
		(km)	($\text{J m}^{-2} \text{s}^{-0.5} \text{K}^{-1}$)		(au)		
1136	Mercedes	$24.66^{+1.81}_{-1.81}$	54^{+81}_{-34}	–	2.745–3.079	MBA	[5]
1140	Crimea	$29.4^{+0.6}_{-0.6}$	5^{+5}_{-5}	S	3.0	MBA	[12]
1142	Aetolia	$23.91^{+1.28}_{-1.28}$	$8.0^{+29.7}_{-8.0}$	–	2.900–2.944	MBA	[5]
1152	Pawona	$17.47^{+0.90}_{-0.90}$	26^{+35}_{-14}	SI	2.324–2.344	MBA	[5]
1162	Larissa	$41.15^{+2.27}_{-2.27}$	19^{+15}_{-19}	P	3.514–3.610	OMB	[5]
1173	Anchises	136^{+15}_{-15}	62^{+37}_{-37}	P	5.0	TJN	[20]
1188	Gothlandia	$13.0^{+0.4}_{-0.4}$	57^{+12}_{-12}	S	2.6	MBA	[12]
1210	Morosovia	$36.5^{+1.2}_{-1.2}$	30^{+30}_{-30}	–	2.9	MBA	[12]
1224	Fantasia	$13.65^{+0.22}_{-0.22}$	58^{+16}_{-12}	S	2.652–2.761	MBA	[5]
1241	Dysona	$78.4^{+2.2}_{-2.2}$	10^{+10}_{-10}	PDC	3.5	MBA	[12]
1258	Sicilia	$44.05^{+2.62}_{-2.62}$	61^{+76}_{-31}	–	3.283–3.303	MBA	[5]
1276	Uccia	$35.7^{+0.6}_{-0.6}$	55^{+10}_{-10}	–	3.1	MBA	[12]
1281	Jeanne	$24.38^{+0.94}_{-0.94}$	90^{+44}_{-25}	–	2.195–2.567	MBA	[5]
1288	Santa	$30.68^{+1.27}_{-1.27}$	15^{+23}_{-5}	–	2.993–3.052	MBA	[5]
1291	Phryne	$25.3^{+1.0}_{-1.0}$	19^{+16}_{-16}	–	3.1	MBA	[12]
1296	Andree	$23.28^{+2.12}_{-2.12}$	40^{+74}_{-12}	–	2.310–2.571	MBA	[5]
1299	Mertona	$15.22^{+1.18}_{-1.18}$	15^{+29}_{-8}	–	3.006–3.230	MBA	[5]
1301	Yvonne	$21.2^{+0.9}_{-0.9}$	1^{+1}_{-1}	C	3.2	MBA	[12]
1310	Villigera	$14.63^{+1.28}_{-1.28}$	40^{+23}_{-30}	S	2.170–2.778	MCA	[5]
1316	Kasan	$6.54^{+0.50}_{-0.50}$	10^{+34}_{-10}	Sr	3.022–3.175	MCA	[5]
1325	Inanda	$11.42^{+1.57}_{-1.57}$	76^{+50}_{-36}	–	2.915–3.145	MBA	[5]
1335	Demoulina	$7.65^{+0.78}_{-0.78}$	130^{+90}_{-100}	–	2.560–2.565	MBA	[5]
1339	Desagneauxa	$26.0^{+1.2}_{-1.2}$	60^{+20}_{-20}	S	3.1	MBA	[12]
1352	Wawel	$21.72^{+1.68}_{-1.68}$	97^{+28}_{-71}	X	2.950–2.951	MBA	[5]
1360	Tarka	$29.4^{+0.4}_{-0.4}$	40^{+5}_{-5}	Ch	3.2	MBA	[12]
1375	Alfreda	$14.46^{+0.55}_{-0.55}$	30^{+48}_{-18}	–	2.501–2.599	MBA	[5]
1386	Storeria	$10.4^{+0.7}_{-0.7}$	20^{+19}_{-19}	Ch	3.0	MBA	[12]
1388	Aphrodite	$21.1^{+0.6}_{-0.6}$	67^{+22}_{-22}	–	3.2	MBA	[12]
1401	Lavonne	$9.3^{+0.5}_{-0.5}$	65^{+45}_{-45}	S	2.6	MBA	[12]
1412	Lagrula	$9.13^{+0.50}_{-0.50}$	37^{+23}_{-9}	–	2.258–2.427	MBA	[5]
1419	Danzig	$14.6^{+0.9}_{-0.9}$	75^{+10}_{-10}	–	2.0	MBA	[12]
1424	Sundmania	$61.3^{+2.4}_{-2.4}$	15^{+15}_{-15}	X	3.2	MBA	[12]
1436	Salonta	$55.4^{+1.1}_{-1.1}$	4^{+4}_{-4}	–	3.3	MBA	[12]
1443	Ruppina	$16.68^{+1.03}_{-1.03}$	40^{+18}_{-14}	–	2.933–3.029	MBA	[5]
1452	Hunnia	$21.22^{+1.99}_{-1.99}$	24^{+34}_{-20}	–	2.849–3.183	MBA	[5]
1472	Muonio	$9.1^{+0.2}_{-0.2}$	44^{+45}_{-45}	–	2.7	MBA	[18]
1495	Helsinki	$12.1^{+0.2}_{-0.2}$	1^{+1}_{-1}	–	2.4	MBA	[12]
1501	Baade	$11.48^{+0.88}_{-0.88}$	34^{+48}_{-34}	–	2.962–3.142	MBA	[5]
1508	Kemi	$14.6^{+0.2}_{-0.2}$	17^{+7}_{-7}	BCF	3.7	MCA	[12]
1517	Beograd	$34.21^{+2.25}_{-2.25}$	19^{+55}_{-5}	X	2.645–2.718	MBA	[5]

Table 3 continued

Table 3 (continued)

Asteroid		D	Γ	Taxonomy	r_h	Orbit	Reference
		(km)	($\text{J m}^{-2} \text{s}^{-0.5} \text{K}^{-1}$)		(au)		
1536	Pielinen	$8.53^{+0.19}_{-0.19}$	74^{+23}_{-35}	–	2.534–2.634	MBA	[5]
1542	Schalen	$46.48^{+1.54}_{-1.54}$	10^{+15}_{-10}	D	3.406–3.439	MBA	[5]
1545	Therhoe	$17.0^{+0.5}_{-0.5}$	6^{+6}_{-6}	K	3.1	MBA	[12]
1565	Lemaitre	$8.44^{+0.96}_{-0.96}$	24^{+53}_{-24}	Sq	2.690–3.092	MCA	[5]
1567	Alikoski	$71.15^{+4.24}_{-4.24}$	$7.2^{+73.4}_{-7.2}$	PU	2.951–3.027	OMB	[5]
1568	Aisleen	$11.8^{+0.3}_{-0.3}$	55^{+5}_{-5}	–	2.9	MBA	[12]
1573	Vaisala	$10.31^{+0.64}_{-0.64}$	130^{+120}_{-80}	–	2.704–2.901	MBA	[5]
1576	Fabiola	$27.796^{+2.471}_{-2.018}$	10^{+27}_{-10}	B	3.1429	MBA	[10]
1577	Reiss	$5.72^{+0.57}_{-0.57}$	25^{+36}_{-20}	–	2.516–2.599	MBA	[5]
1580	Betulia	$4.57^{+0.46}_{-0.46}$	180^{+50}_{-50}	C	1.1	AMO	[16]
1607	Mavis	$13.5^{+0.5}_{-0.5}$	62^{+22}_{-22}	–	3.2	MBA	[12]
1618	Dawn	$16.5^{+0.4}_{-0.4}$	5^{+5}_{-5}	S	2.9	MBA	[12]
1620	Geographos	$5.04^{+0.07}_{-0.07}$	340^{+120}_{-120}	S	1.1	APO	[21]
1627	Ivar	$7.7^{+0.6}_{-0.6}$	140^{+80}_{-80}	S	2.1	AMO	[18]
1628	Strobel	$53.71^{+1.21}_{-1.21}$	47^{+12}_{-30}	–	2.983–3.093	MBA	[5]
1633	Chimay	$47.849^{+3.993}_{-3.431}$	30^{+18}_{-13}	S	3.1929	MBA	[10]
1644	Rafita	$13.49^{+0.84}_{-0.84}$	28^{+25}_{-14}	S	2.394–2.676	MBA	[5]
1651	Behrens	$10.09^{+0.46}_{-0.46}$	59^{+29}_{-19}	–	2.041–2.147	MBA	[5]
1655	Comas Sola	$35.09^{+1.30}_{-1.30}$	40^{+37}_{-30}	XFU	2.951–3.258	MBA	[5]
1672	Gezelle	$25.0^{+0.9}_{-0.9}$	10^{+10}_{-10}	–	3.3	MBA	[12]
1685	Toro	$3.5^{+0.4}_{-0.4}$	260^{+130}_{-130}	Sv	1.9	APO	[22]
1687	Glarona	$34.852^{+1.442}_{-0.941}$	15^{+23}_{-10}	S	3.1688	MBA	[10]
1691	Oort	$36.8^{+0.7}_{-0.7}$	22^{+22}_{-22}	CU	3.6	MBA	[12]
1691	Oort	$34.844^{+2.595}_{-2.121}$	10^{+19}_{-10}	C	3.1636	MBA	[10]
1701	Okavango	$18.9^{+0.4}_{-0.4}$	16^{+13}_{-13}	–	2.6	MBA	[12]
1702	Kalahari	$34.16^{+1.23}_{-1.23}$	28^{+40}_{-9}	D	3.009–3.182	MBA	[5]
1704	Wachmann	$6.6^{+0.1}_{-0.1}$	120^{+40}_{-40}	–	2.0	MBA	[12]
1723	Klemola	$31.4^{+0.5}_{-0.5}$	32^{+7}_{-7}	S	3.0	MBA	[12]
1723	Klemola	$33.77^{+0.91}_{-0.91}$	30^{+11}_{-10}	S	2.919–2.990	MBA	[5]
1734	Zhongolovich	$25.33^{+0.71}_{-0.71}$	35^{+31}_{-10}	Ch	3.112–3.345	MBA	[5]
1738	Oosterhoff	$7.9^{+0.1}_{-0.1}$	77^{+32}_{-32}	S	2.2	MBA	[12]
1741	Giclas	$13.17^{+0.56}_{-0.56}$	33^{+20}_{-10}	–	3.050–3.082	MBA	[5]
1742	Schaifers	$15.5^{+0.3}_{-0.3}$	97^{+12}_{-12}	–	3.1	MBA	[12]
1759	Kienle	$7.73^{+1.17}_{-1.17}$	52^{+88}_{-52}	–	3.079–3.387	MBA	[5]
1768	Appenzella	$18.91^{+0.59}_{-0.59}$	31^{+18}_{-12}	F	2.766–2.886	MBA	[5]
1789	Dobrovolsky	$8.7^{+0.1}_{-0.1}$	13^{+7}_{-7}	–	2.2	MBA	[12]
1807	Slovakia	$9.83^{+1.19}_{-1.19}$	200^{+240}_{-50}	S	2.511–2.622	MBA	[5]
1820	Lohmann	$6.1^{+0.3}_{-0.3}$	120^{+20}_{-20}	–	2.5	MBA	[12]
1837	Osita	$7.2^{+0.2}_{-0.2}$	110^{+20}_{-20}	–	2.0	MBA	[12]
1862	Apollo	$1.55^{+0.07}_{-0.07}$	140^{+100}_{-100}	Q	1.0	APO	[23]

Table 3 continued

Table 3 (continued)

Asteroid		D	Γ	Taxonomy	r_h	Orbit	Reference
		(km)	($\text{J m}^{-2} \text{s}^{-0.5} \text{K}^{-1}$)		(au)		
1896	Beer	$5.07^{+0.96}_{-0.96}$	80^{+335}_{-80}	–	2.674–2.872	MBA	[5]
1902	Shaposhnikov	$79.7^{+2.9}_{-2.9}$	0^{+0}_{-0}	X	4.8	OMB	[12]
1906	Naef	$7.728^{+0.407}_{-0.211}$	70^{+19}_{-16}	V	2.077–2.337	MBA	[11]
1930	Lucifer	$31.6^{+1.2}_{-1.2}$	80^{+30}_{-30}	Cgh	3.3	MBA	[12]
1936	Lugano	$24.03^{+0.27}_{-0.27}$	120^{+70}_{-80}	Ch	2.357–2.577	MBA	[5]
1979	Sakharov	$4.69^{+0.77}_{-0.77}$	58^{+269}_{-27}	–	2.542–2.611	MBA	[5]
1980	Tezcatlipoca	$5.1^{+0.1}_{-0.1}$	310^{+300}_{-300}	SI	2.3	AMO	[18]
1987	Kaplan	$13.0^{+0.2}_{-0.2}$	35^{+10}_{-10}	–	2.9	MBA	[12]
2005	Hencke	$8.99^{+0.95}_{-0.95}$	40^{+48}_{-34}	–	3.019–3.055	MBA	[5]
2060	Chiron	142^{+10}_{-10}	4^{+4}_{-4}	B/Cb	8–15	CEN	[24]
2060	Chiron	218^{+20}_{-20}	5^{+5}_{-5}	B/Cb	13	CEN	[25]
2072	Kosmodemyanskaya	$4.74^{+1.44}_{-1.44}$	19^{+129}_{-19}	–	2.695–2.840	MBA	[5]
2106	Hugo	$16.15^{+1.50}_{-1.50}$	22^{+36}_{-9}	C	2.931–2.964	MBA	[5]
2111	Tselina	$24.05^{+2.19}_{-2.19}$	47^{+36}_{-24}	S	3.273–3.294	MBA	[5]
2123	Vltava	$16.05^{+0.68}_{-0.68}$	56^{+37}_{-22}	–	3.067–3.069	MBA	[5]
2140	Kemerovo	$33.56^{+2.05}_{-2.05}$	20^{+39}_{-14}	–	3.144–3.145	MBA	[5]
2144	Marietta	$17.26^{+0.45}_{-0.45}$	53^{+10}_{-8}	–	3.014–3.049	MBA	[5]
2177	Oliver	$19.52^{+0.50}_{-0.50}$	42^{+10}_{-10}	–	3.101–3.259	MBA	[5]
2203	van Rhijn	$22.31^{+1.08}_{-1.08}$	55^{+55}_{-27}	–	3.575–3.673	MBA	[5]
2204	Lyyli	$25.05^{+0.95}_{-0.95}$	90^{+36}_{-50}	X	2.289–2.974	MCA	[5]
2214	Carol	$26.28^{+1.60}_{-1.60}$	21^{+15}_{-9}	–	2.744–3.187	MBA	[5]
2239	Paracelsus	$37.53^{+2.48}_{-2.48}$	18^{+7}_{-18}	–	3.482–3.516	MBA	[5]
2268	Szmytowna	$15.18^{+1.46}_{-1.46}$	30^{+32}_{-30}	S	3.137–3.246	MBA	[5]
2275	Cuitlahuac	$7.29^{+0.19}_{-0.19}$	13^{+24}_{-13}	–	2.329–2.596	MBA	[5]
2297	Daghestan	$25.06^{+0.89}_{-0.89}$	58^{+23}_{-18}	–	2.749–2.870	MBA	[5]
2306	Bauschinger	$19.24^{+0.97}_{-0.97}$	18^{+14}_{-10}	X	2.793–2.872	MBA	[5]
2332	Kalm	$36.52^{+2.55}_{-2.55}$	77^{+15}_{-48}	–	3.055–3.149	MBA	[5]
2347	Vinata	$23.63^{+1.27}_{-1.27}$	35^{+20}_{-14}	–	3.701–3.741	MBA	[5]
2363	Cebriones	82^{+5}_{-5}	7^{+7}_{-7}	D	5.2	TJN	[26]
2365	Interkosmos	$16.62^{+1.41}_{-1.41}$	41^{+10}_{-41}	–	2.351–2.561	MBA	[5]
2375	Radek	$32.19^{+1.60}_{-1.60}$	11^{+14}_{-11}	D	2.528–2.537	MBA	[5]
2446	Lunacharsky	$12.43^{+0.31}_{-0.31}$	33^{+12}_{-10}	B	1.997–2.255	MBA	[5]
2463	Sterpin	$11.93^{+0.69}_{-0.69}$	17^{+43}_{-17}	–	2.672–2.895	MBA	[5]
2500	Alascattalo	$7.99^{+0.27}_{-0.27}$	41^{+18}_{-28}	–	2.029–2.076	MBA	[5]
2511	Patterson	$9.034^{+0.997}_{-1.128}$	90^{+58}_{-43}	V	2.093–2.534	MBA	[11]
2528	Mohler	$16.826^{+1.088}_{-0.654}$	35^{+15}_{-28}	C	3.1472	MBA	[10]
2556	Louise	$5.96^{+0.55}_{-0.55}$	61^{+37}_{-33}	–	2.119–2.192	MBA	[5]
2567	Elba	$18.40^{+1.27}_{-1.27}$	50^{+11}_{-36}	Xc	2.894–3.058	MBA	[5]
2592	Hunan	$18.958^{+0.963}_{-1.177}$	40^{+46}_{-40}	C	3.1205	MBA	[10]
2606	Odesa	18^{+3}_{-3}	125^{+75}_{-75}	X	3.5	MBA	[18]

Table 3 continued

Table 3 (continued)

Asteroid		D	Γ	Taxonomy	r_h	Orbit	Reference
		(km)	($\text{J m}^{-2} \text{s}^{-0.5} \text{K}^{-1}$)		(au)		
2617	Jiangxi	$50.7_{-2.3}^{+2.3}$	0_{-0}^{+0}	–	2.7	MBA	[12]
2659	Millis	$27.2_{-0.6}^{+0.6}$	35_{-19}^{+19}	B	3.5	MBA	[12]
2659	Millis	$27.463_{-2.328}^{+1.674}$	35_{-16}^{+19}	B	3.1317	MBA	[10]
2673	Lossignol	$14.005_{-0.865}^{+1.376}$	15_{-15}^{+29}	C	3.2055	OMB	[10]
2687	Tortali	$14.91_{-0.21}^{+0.21}$	59_{-10}^{+16}	–	2.424–2.644	MBA	[5]
2708	Burns	$20.492_{-1.731}^{+2.003}$	65_{-48}^{+25}	B	3.0821	MBA	[10]
2718	Handley	$24.431_{-0.849}^{+1.924}$	30_{-30}^{+16}	C	3.1201	MBA	[10]
2786	Grinevia	$11.07_{-0.98}^{+0.98}$	12_{-12}^{+19}	–	2.998–3.063	MBA	[5]
2803	Vilho	$27.757_{-2.389}^{+0.394}$	110_{-29}^{+12}	C	3.1410	MBA	[10]
2855	Bastian	$8.78_{-0.57}^{+0.57}$	17_{-7}^{+42}	SI	2.431–2.706	MBA	[5]
2867	Steins	$4.92_{-0.4}^{+0.4}$	150_{-60}^{+60}	E	2.1	MBA	[27]
2867	Steins	5.2_{-1}^{+1}	210_{-30}^{+30}	E	2.1	MBA	[28]
2870	Haupt	$15.51_{-2.28}^{+2.28}$	130_{-130}^{+180}	–	2.639–2.862	MBA	[5]
2947	Kippenhahn	$7.80_{-0.29}^{+0.29}$	32_{-11}^{+18}	–	2.392–2.562	MBA	[5]
2985	Shakespeare	$10.64_{-0.92}^{+0.92}$	41_{-13}^{+49}	–	2.843–2.912	MBA	[5]
3036	Krat	$41.41_{-1.28}^{+1.28}$	15_{-9}^{+57}	–	3.303–3.428	OMB	[5]
3051	Nantong	$16.79_{-1.60}^{+1.60}$	27_{-14}^{+28}	–	2.969–3.210	MBA	[5]
3063	Makhaon	116_{-4}^{+4}	15_{-15}^{+15}	D	4.7	TJN	[26]
3144	Brosche	$4.80_{-0.53}^{+0.53}$	59_{-45}^{+56}	–	2.197–2.554	MBA	[5]
3162	Nostalgia	$28.88_{-1.48}^{+1.48}$	29_{-15}^{+51}	–	3.229–3.444	MBA	[5]
3200	Phaethon	$5.1_{-0.2}^{+0.2}$	600_{-200}^{+200}	B	1.1	APO	[29]
3200	Phaethon	$4.6_{-0.3}^{+0.2}$	880_{-330}^{+580}	B	1.0067–2.3170	APO	[30]
3249	Musashino	$6.44_{-1.22}^{+1.22}$	93_{-73}^{+132}	S	2.890–2.898	MBA	[5]
3267	Glo	$7.37_{-1.28}^{+1.28}$	23_{-13}^{+43}	–	2.505–2.882	MCA	[5]
3281	Maupertuis	$5.509_{-0.270}^{+0.447}$	60_{-31}^{+58}	V	2.132–2.194	MBA	[11]
3305	Ceadaams	$10.37_{-0.12}^{+0.12}$	21_{-3}^{+6}	–	2.286–2.540	MBA	[5]
3411	Debetencourt	$5.18_{-0.21}^{+0.21}$	22_{-12}^{+83}	–	2.062–2.289	MBA	[5]
3428	Roberts	$17.1_{-0.2}^{+0.2}$	62_{-17}^{+17}	–	3.1	MBA	[12]
3438	Inarradas	$25.18_{-0.68}^{+0.68}$	54_{-15}^{+15}	–	3.274–3.512	MBA	[5]
3483	Svetlov	$2.96_{-0.48}^{+0.48}$	110_{-50}^{+400}	–	2.043–2.172	IMB	[5]
3509	Sanshui	$9.93_{-0.84}^{+0.84}$	62_{-34}^{+27}	–	2.830–2.972	MBA	[5]
3536	Schleicher	$3.67_{-1.14}^{+1.14}$	32_{-10}^{+182}	V	2.354–2.436	MBA	[5]
3544	Borodino	$8.3_{-0.2}^{+0.2}$	60_{-20}^{+20}	–	2.3	MBA	[12]
3544	Borodino	$9.29_{-0.81}^{+0.81}$	72_{-45}^{+14}	–	2.065–2.485	MBA	[5]
3554	Amun	$2.71_{-0.02}^{+0.02}$	1400_{-200}^{+700}	–	1.081–1.219	ATE	[5]
3560	Chenqian	$22.84_{-0.56}^{+0.56}$	44_{-10}^{+22}	–	3.296–3.362	MBA	[5]
3628	Boznemcova	$8.07_{-0.80}^{+0.80}$	32_{-32}^{+23}	O	2.923–3.215	MBA	[5]
3678	Mongmanwai	$8.5_{-0.3}^{+0.3}$	72_{-17}^{+17}	S	2.9	MBA	[12]
3751	Kiang	$22.38_{-0.68}^{+0.68}$	62_{-16}^{+20}	–	2.920–3.072	MBA	[5]
3823	Yorii	$13.66_{-1.47}^{+1.47}$	49_{-49}^{+22}	–	2.779–3.201	MBA	[5]

Table 3 continued

Table 3 (continued)

Asteroid		D	Γ	Taxonomy	r_h	Orbit	Reference
		(km)	($\text{J m}^{-2} \text{s}^{-0.5} \text{K}^{-1}$)		(au)		
3907	Kilmartin	$8.16^{+1.12}_{-1.12}$	26^{+47}_{-26}	–	3.096–3.126	MBA	[5]
3915	Fukushima	$22.18^{+0.39}_{-0.39}$	22^{+13}_{-7}	–	2.419–2.491	MBA	[5]
3935	Toatenmongakkai	$12.02^{+0.82}_{-0.82}$	120^{+90}_{-60}	–	3.016–3.130	MBA	[5]
3936	Elst	$5.00^{+0.68}_{-0.68}$	22^{+56}_{-22}	–	2.200–2.430	MBA	[5]
4003	Schumann	$31.92^{+0.41}_{-0.41}$	32^{+35}_{-11}	–	3.236–3.388	OMB	[5]
4006	Sandler	$16.89^{+0.64}_{-0.64}$	36^{+7}_{-11}	–	2.904–2.976	MBA	[5]
4008	Corbin	$6.18^{+0.31}_{-0.31}$	67^{+37}_{-25}	–	1.967–2.357	MBA	[5]
4029	Bridges	$7.87^{+0.62}_{-0.62}$	32^{+26}_{-18}	–	2.202–2.261	MBA	[5]
4077	Asuka	$19.4^{+0.4}_{-0.4}$	9^{+3}_{-3}	–	3.3	MBA	[12]
4142	Dersu-Uzala	$6.31^{+0.52}_{-0.52}$	110^{+140}_{-30}	A	1.709–2.020	MCA	[5]
4150	Starr	$6.93^{+0.39}_{-0.39}$	29^{+16}_{-14}	–	2.244–2.509	MBA	[5]
4255	Spacewatch	$15.71^{+0.45}_{-0.45}$	24^{+22}_{-17}	–	3.389–3.532	OMB	[5]
4264	Karljosephine	$6.37^{+1.83}_{-1.83}$	110^{+300}_{-110}	–	2.980–3.104	MBA	[5]
4265	Kani	$14.3^{+0.3}_{-0.3}$	6^{+6}_{-6}	C	2.9	MBA	[12]
4294	Horatius	$8.07^{+0.66}_{-0.66}$	12^{+77}_{-12}	–	2.850–2.861	MBA	[5]
4352	Kyoto	$11.33^{+1.31}_{-1.31}$	47^{+64}_{-32}	S	3.226–3.306	MBA	[5]
4359	Berlage	$4.98^{+0.69}_{-0.69}$	40^{+71}_{-26}	–	2.342–2.502	MBA	[5]
4363	Sergej	$5.48^{+0.48}_{-0.48}$	27^{+94}_{-27}	–	2.638–2.877	MBA	[5]
4383	Suruga	$6.79^{+1.03}_{-1.03}$	37^{+53}_{-17}	–	2.554–2.575	MBA	[5]
4528	Berg	$10.45^{+0.96}_{-0.96}$	26^{+20}_{-26}	–	2.331–2.571	MBA	[5]
4565	Grossman	$7.57^{+0.37}_{-0.37}$	51^{+36}_{-12}	–	2.253–2.281	MBA	[5]
4569	Baerbel	$9.21^{+0.73}_{-0.73}$	48^{+45}_{-9}	–	2.425–2.490	MBA	[5]
4606	Saheki	$7.1^{+0.3}_{-0.3}$	8^{+8}_{-8}	–	2.4	MBA	[12]
4613	Mamoru	$11.96^{+1.48}_{-1.48}$	$9.4^{+22.6}_{-9.4}$	–	3.307–3.464	MBA	[5]
4713	Steel	$6.58^{+0.18}_{-0.18}$	40^{+28}_{-13}	A	1.784–1.885	IMB	[5]
4771	Hayashi	$13.32^{+0.96}_{-0.96}$	61^{+37}_{-29}	–	2.663–2.919	MBA	[5]
4800	Veveri	$13.3^{+0.4}_{-0.4}$	40^{+10}_{-10}	–	2.7	MBA	[12]
4898	Nishiizumi	$2.46^{+0.22}_{-0.22}$	34^{+445}_{-34}	–	1.801–1.940	IMB	[5]
4899	Candace	$7.17^{+0.57}_{-0.57}$	79^{+104}_{-60}	–	1.946–2.212	MBA	[5]
4908	Ward	$4.91^{+0.71}_{-0.71}$	12^{+68}_{-12}	–	2.384–2.657	MBA	[5]
5035	Swift	$10.22^{+1.06}_{-1.06}$	26^{+35}_{-20}	–	2.501–2.774	MBA	[5]
5052	Nancyruth	$4.66^{+0.78}_{-0.78}$	10^{+72}_{-10}	–	2.618–2.700	MBA	[5]
5080	Oja	$7.98^{+0.53}_{-0.53}$	26^{+50}_{-17}	–	2.324–2.491	MBA	[5]
5088	Tancredi	$16.17^{+1.02}_{-1.02}$	40^{+12}_{-19}	–	3.133–3.363	MBA	[5]
5104	Skripnichenko	$9.49^{+0.48}_{-0.48}$	41^{+31}_{-22}	–	2.332–2.345	MBA	[5]
5111	Jacliff	$5.302^{+0.237}_{-0.397}$	0^{+15}_{-0}	R	2.055–2.359	MBA	[11]
5226	Pollack	$5.74^{+1.03}_{-1.03}$	24^{+51}_{-18}	–	2.416–2.532	MBA	[5]
5333	Kanaya	$13.86^{+1.32}_{-1.32}$	23^{+32}_{-7}	Ch	1.980–2.272	MBA	[5]
5378	Ellyett	$2.77^{+0.25}_{-0.25}$	75^{+455}_{-62}	–	1.936–2.076	IMB	[5]
5427	Jensmartin	$3.13^{+0.14}_{-0.14}$	19^{+76}_{-19}	–	1.844–1.995	IMB	[5]

Table 3 continued

Table 3 (continued)

Asteroid		D	Γ	Taxonomy	r_h	Orbit	Reference
		(km)	($\text{J m}^{-2} \text{s}^{-0.5} \text{K}^{-1}$)		(au)		
5489	Oberkochen	$14.1_{-0.2}^{+0.2}$	17_{-17}^{+17}	–	2.9	MBA	[12]
5527	1991 UQ3	$5.30_{-0.56}^{+0.56}$	120_{-80}^{+130}	–	2.007–2.247	MBA	[5]
5574	Seagrave	$9.72_{-1.05}^{+1.05}$	34_{-34}^{+34}	–	2.425–2.613	MBA	[5]
5592	Oshima	$23.91_{-1.16}^{+1.16}$	34_{-27}^{+23}	–	3.215–3.302	MBA	[5]
5604	1992 FE	$0.67_{-0.01}^{+0.01}$	1100_{-600}^{+2200}	V	1.068–1.238	ATE	[5]
5682	Beresford	$5.37_{-1.83}^{+1.83}$	29_{-29}^{+152}	–	2.736–2.965	MCA	[5]
5712	Funke	$7.22_{-1.60}^{+1.60}$	33_{-33}^{+50}	–	2.967–3.158	MBA	[5]
6091	Mitsuru	$4.94_{-0.75}^{+0.75}$	45_{-13}^{+25}	–	1.869–2.314	MBA	[5]
6121	Plachinda	$5.83_{-0.82}^{+0.82}$	56_{-34}^{+63}	–	2.433–2.655	MBA	[5]
6136	Gryphon	$15.3_{-0.5}^{+0.5}$	40_{-15}^{+15}	–	3.0	MBA	[12]
6139	Naomi	$10.68_{-0.36}^{+0.36}$	66_{-36}^{+31}	–	2.255–2.401	MBA	[5]
6170	Levasseur	$5.57_{-0.63}^{+0.63}$	76_{-56}^{+161}	–	1.881–2.497	MCA	[5]
6185	Mitsuma	$10.36_{-1.00}^{+1.00}$	66_{-45}^{+61}	–	2.415–2.472	MBA	[5]
6261	Chione	$3.91_{-0.56}^{+0.56}$	41_{-41}^{+52}	–	2.120–2.735	MCA	[5]
6361	Koppel	$3.59_{-0.19}^{+0.19}$	20_{-20}^{+172}	–	2.059–2.087	MBA	[5]
6572	Carson	$8.56_{-1.21}^{+1.21}$	21_{-15}^{+33}	–	2.610–2.998	MBA	[5]
6635	Zuber	$3.6_{-0.1}^{+0.1}$	85_{-15}^{+15}	–	2.1	IMB	[12]
6838	Okuda	$11.88_{-0.28}^{+0.28}$	47_{-10}^{+13}	–	2.378–2.694	MBA	[5]
6870	1991 OM1	$2.80_{-0.66}^{+0.66}$	59_{-59}^{+330}	–	2.114–2.122	IMB	[5]
6901	Roybishop	$5.05_{-0.44}^{+0.44}$	59_{-40}^{+83}	–	2.046–2.158	IMB	[5]
6905	Miyazaki	$14.30_{-0.73}^{+0.73}$	26_{-26}^{+66}	–	2.719–2.992	MBA	[5]
6911	Nancygreen	$2.90_{-0.32}^{+0.32}$	210_{-180}^{+1220}	–	1.996–2.103	IMB	[5]
7001	Neother	$5.923_{-0.378}^{+0.167}$	20_{-20}^{+21}	–	2.058–2.348	MBA	[11]
7476	Ogilsbie	$18.41_{-1.21}^{+1.21}$	70_{-20}^{+30}	–	2.440–2.496	MBA	[5]
7783	1994JD	$2.78_{-0.33}^{+0.33}$	170_{-110}^{+190}	–	1.830–1.990	IMB	[5]
7829	Jaroff	$2.55_{-0.50}^{+0.50}$	32_{-32}^{+176}	–	1.965–2.087	IMB	[5]
7832	1993 FA27	$3.55_{-0.53}^{+0.53}$	46_{-46}^{+160}	–	2.013–2.430	MBA	[5]
7949	1992 SU	$18.26_{-1.36}^{+1.36}$	37_{-27}^{+28}	–	3.284–3.595	MBA	[5]
8213	1995 FE	$4.80_{-1.02}^{+1.02}$	36_{-18}^{+167}	–	2.095–2.506	MBA	[5]
8359	1989 WD	$8.1_{-0.4}^{+0.4}$	57_{-12}^{+12}	–	2.5	MBA	[12]
8405	Asbolus	66_{-4}^{+4}	5_{-5}^{+5}	–	7.9	CEN	[31]
8862	Takayukiota	$7.76_{-2.35}^{+2.35}$	43_{-43}^{+195}	–	3.038–3.105	MBA	[5]
8887	Scheeres	$7.56_{-0.81}^{+0.81}$	21_{-21}^{+52}	–	2.495–2.717	MBA	[5]
9158	Plate	$4.113_{-0.134}^{+0.137}$	10_{-10}^{+19}	SQp	2.258–2.265	MBA	[11]
9297	Marchuk	$9.55_{-0.57}^{+0.57}$	22_{-22}^{+120}	–	2.318–2.540	MBA	[5]
10199	Chariklo	236_{-12}^{+12}	1_{-1}^{+1}	D	13	CEN	[24]
10199	Chariklo	248_{-18}^{+18}	16_{-14}^{+14}	D	13	CEN	[23]
10936	1998 FN11	$11.75_{-0.50}^{+0.50}$	13_{-13}^{+22}	–	3.063–3.079	MBA	[5]
11549	1992 YY	$10.30_{-0.44}^{+0.44}$	30_{-5}^{+18}	–	2.311–2.352	MBA	[5]
11780	Thunder Bay	$7.82_{-2.43}^{+2.43}$	130_{-130}^{+450}	–	2.941–3.193	MBA	[5]

Table 3 continued

Table 3 (continued)

Asteroid		D	Γ	Taxonomy	r_h	Orbit	Reference
		(km)	($\text{J m}^{-2} \text{s}^{-0.5} \text{K}^{-1}$)		(au)		
12088	Macalintal	$3.591^{+0.293}_{-0.499}$	70^{+68}_{-53}	V	2.459–2.460	MBA	[11]
12376	Cochabamba	$5.93^{+0.97}_{-0.97}$	120^{+60}_{-110}	–	1.961–2.111	MBA	[5]
12753	Povenmire	$8.00^{+0.19}_{-0.19}$	17^{+23}_{-11}	–	2.269–2.273	MBA	[5]
13474	V'yus	$6.63^{+1.41}_{-1.41}$	64^{+123}_{-44}	–	3.158–3.359	MBA	[5]
13856	1999 XZ105	$14.79^{+1.23}_{-1.23}$	20^{+12}_{-10}	–	3.138–3.172	MBA	[5]
14342	Iglik	$16.22^{+1.11}_{-1.11}$	24^{+8}_{-14}	–	3.237–3.500	MBA	[5]
14950	1996 BE2	$6.66^{+1.01}_{-1.01}$	54^{+49}_{-34}	–	2.034–2.130	MBA	[5]
15032	Alexlevin	$2.832^{+0.154}_{-0.093}$	20^{+15}_{-20}	V	2.140–2.142	MBA	[11]
15362	1996 ED	$4.95^{+1.01}_{-1.01}$	110^{+120}_{-110}	–	2.393–2.597	MBA	[5]
15430	1998 UR31	$3.78^{+0.43}_{-0.43}$	72^{+127}_{-63}	–	1.863–1.985	MBA	[5]
15499	Cloyd	$9.67^{+1.25}_{-1.25}$	33^{+36}_{-33}	–	3.151–3.249	MBA	[5]
15914	1997 UM3	$4.20^{+0.95}_{-0.95}$	88^{+188}_{-72}	–	2.634–2.829	MBA	[5]
16681	1994 EV7	$3.94^{+0.34}_{-0.34}$	63^{+74}_{-30}	–	1.984–2.005	IMB	[5]
16886	1998 BC26	$7.11^{+0.78}_{-0.78}$	33^{+49}_{-18}	–	1.983–2.005	MBA	[5]
17681	Tweedledum	$2.48^{+0.31}_{-0.31}$	130^{+320}_{-110}	–	1.823–1.875	IMB	[5]
17822	1998 FM135	$10.92^{+1.43}_{-1.43}$	79^{+53}_{-52}	–	3.206–3.394	MBA	[5]
18487	1996 AU3	$7.78^{+0.79}_{-0.79}$	46^{+36}_{-26}	–	2.595–2.893	MBA	[5]
19251	Totziens	$6.24^{+2.14}_{-2.14}$	32^{+121}_{-32}	–	3.066–3.319	MBA	[5]
19848	Yeungchuchiu	$11.4^{+0.9}_{-0.9}$	18^{+17}_{-17}	–	2.8	MBA	[12]
20378	1998 KZ46	$7.78^{+0.80}_{-0.80}$	34^{+23}_{-14}	–	2.850–2.905	MBA	[5]
20932	2258 T-1	$5.76^{+1.32}_{-1.32}$	41^{+111}_{-41}	–	2.746–2.999	MBA	[5]
21594	1998 VP31	$10.30^{+0.26}_{-0.26}$	44^{+16}_{-12}	–	2.145–2.324	MBA	[5]
23200	2000 SH3	$7.20^{+1.10}_{-1.10}$	17^{+66}_{-17}	–	2.713–2.899	MBA	[5]
23276	2000 YT101	$7.01^{+0.96}_{-0.96}$	27^{+30}_{-27}	–	2.841–3.053	MBA	[5]
24101	Cassini	$7.40^{+1.43}_{-1.43}$	15^{+38}_{-15}	–	3.177–3.418	MBA	[5]
25143	Itokawa	$0.32^{+0.03}_{-0.03}$	700^{+100}_{-100}	S	1.1	APO	[16]
25143	Itokawa	$0.320^{+0.029}_{-0.029}$	700^{+200}_{-200}	S	1.1	APO	[32]
27851	1994 VG2	$10.43^{+0.98}_{-0.98}$	11^{+14}_{-11}	–	2.713–2.439	MBA	[5]
28126	Nydegger	$2.63^{+0.76}_{-0.76}$	33^{+205}_{-33}	–	2.183–2.387	MBA	[5]
29075	1950 DA	$1.30^{+0.13}_{-0.13}$	24^{+20}_{-20}	M	1.7	APO	[33]
30470	2000 OR19	$9.42^{+0.28}_{-0.28}$	45^{+43}_{-22}	–	2.550–2.879	MBA	[5]
32802	1990 SK	$4.27^{+1.76}_{-1.76}$	20^{+162}_{-20}	–	2.664–2.884	MBA	[5]
33342	1998 WT24	$0.35^{+0.04}_{-0.04}$	200^{+100}_{-100}	E	1.0	ATE	[16]
33916	2000 LF19	$4.08^{+0.41}_{-0.41}$	38^{+51}_{-38}	–	2.129–2.582	MBA	[5]
41044	1999 VW6	$5.79^{+1.58}_{-1.58}$	14^{+157}_{-14}	–	2.833–3.024	MBA	[5]
41223	1999 XD16	$11.61^{+1.15}_{-1.15}$	23^{+43}_{-23}	–	3.417–3.616	MCA	[5]
41288	1999 XD107	$4.22^{+0.98}_{-0.98}$	41^{+86}_{-34}	–	2.249–2.450	MBA	[5]
42265	2001 QL69	$7.07^{+1.35}_{-1.35}$	25^{+89}_{-25}	–	2.910–2.980	MBA	[5]
42946	1999 TU95	$4.74^{+0.79}_{-0.79}$	37^{+60}_{-37}	–	2.380–2.449	MBA	[5]
44892	1999 VJ8	$7.80^{+1.66}_{-1.66}$	32^{+93}_{-32}	–	2.912–3.148	MBA	[5]

Table 3 continued

Table 3 (*continued*)

Asteroid		D	Γ	Taxonomy	r_h	Orbit	Reference
		(km)	($\text{J m}^{-2} \text{s}^{-0.5} \text{K}^{-1}$)		(au)		
45436	2000 AD176	$3.89^{+1.54}_{-1.54}$	75^{+482}_{-75}	–	2.252–2.455	MBA	[5]
50000	Quaoar	1082^{+67}_{-67}	6^{+4}_{-4}	–	43	TNO	[25]
54509	YORP	$0.092^{+0.010}_{-0.010}$	700^{+500}_{-500}	S	1.1	APO	[16]
55565	2002 AW197	700^{+50}_{-50}	10^{+10}_{-10}	–	47	TNO	[34]
68216	2001 CV26	$1.24^{+0.05}_{-0.05}$	430^{+1210}_{-280}	–	1.102–1.698	APO	[5]
69350	1993 YP	$2.87^{+0.69}_{-0.69}$	240^{+490}_{-150}	–	1.939–2.076	MCA	[5]
72675	2001 FP54	$3.77^{+1.32}_{-1.32}$	29^{+367}_{-29}	–	2.533–2.571	MBA	[5]
90377	Sedna	995^{+80}_{-80}	$0.1^{+0.1}_{-0.1}$	–	87	TNO	[35]
90482	Orcus	968^{+63}_{-63}	1^{+1}_{-1}	–	48	TNO	[25]
90698	Kosciuszko	$3.55^{+0.25}_{-0.25}$	16^{+49}_{-16}	–	1.970–2.470	MBA	[5]
99942	Apophis	$0.375^{+0.014}_{-0.010}$	600^{+200}_{-350}	Sq	1.05	ATE	[36]
99942	Apophis	$0.378^{+0.027}_{-0.029}$	100^{+240}_{-100}	Sq	1.036–1.093	ATE	[37]
101955	Bennu	$0.495^{+0.015}_{-0.015}$	650^{+300}_{-300}	B	1.1	APO	[38]
101955	Bennu	$0.49^{+0.02}_{-0.02}$	310^{+70}_{-70}	B	1.1	APO	[39]
101955	Bennu	$0.510^{+0.006}_{-0.040}$	240^{+440}_{-60}	B	0.991–1.143	APO	[40]
136108	Haumea	1240^{+70}_{-70}	$0.3^{+0.2}_{-0.2}$	–	51	TNO	[41]
161989	Cacus	$1.00^{+0.20}_{-0.20}$	650^{+150}_{-150}	S	1.3	APO	[42]
162173	Ryugu	$0.87^{+0.03}_{-0.03}$	400^{+200}_{-200}	C	1.4	APO	[43]
162173	Ryugu	$0.865^{+0.015}_{-0.015}$	225^{+75}_{-75}	C	1.4	APO	[44]
175706	1996 FG3	$1.71^{+0.07}_{-0.07}$	120^{+50}_{-50}	C	1.4	APO	[45]
175706	1996 FG3	$1.69^{+0.05}_{-0.02}$	80^{+40}_{-40}	C	1.053–1.377	APO	[46]
208996	2003 AZ84	480^{+20}_{-20}	$1.2^{+0.6}_{-0.6}$	–	45	TNO	[41]
308635	2005 YU55	$0.306^{+0.006}_{-0.006}$	575^{+225}_{-225}	C	1.0	APO	[47]
341843	2008 EV5	$0.370^{+0.006}_{-0.006}$	450^{+60}_{-60}	C	1.0	ATE	[48]
341843	2008 EV5	$0.431^{+0.006}_{-0.033}$	110^{+40}_{-12}	C	1.032–1.038	ATE	[49]

Table 3 *continued*

Table 3 (continued)

Asteroid	D	Γ	Taxonomy	r_h	Orbit	Reference
	(km)	($\text{J m}^{-2} \text{s}^{-0.5} \text{K}^{-1}$)		(au)		

References—[1] Mueller & Lagerros (1998); [2] Alí-Lagoa et al. (2020); [3] Leyrat et al. (2012); [4] Matter et al. (2013); [5] MacLennan & Emery (2021); [6] O’Rourke et al. (2012); [7] Marchis et al. (2012); [8] Delbo’ & Tanga (2009); [9] Matter et al. (2011); [10] Jiang & Ji (2021); [11] Jiang et al. (2020); [12] Hanuš et al. (2018a); [13] Marciniak et al. (2019); [14] Marciniak et al. (2021); [15] Yu et al. (2017b); [16] Mueller (2012); [17] Mueller et al. (2010); [18] Hanuš et al. (2015); [19] Lim et al. (2011); [20] Horner et al. (2012); [21] Rozitis & Green (2014); [22] Ďurech et al. (2018b); [23] Rozitis et al. (2013); [24] Groussin et al. (2004); [25] Fornasier et al. (2013); [26] Fernández et al. (2003); [27] Lamy et al. (2008); [28] Leyrat et al. (2011); [29] Hanuš et al. (2016a); [30] Masiero et al. (2019); [31] Fernández et al. (2002); [32] Müller et al. (2014a); [33] Rozitis et al. (2014); [34] Cruikshank et al. (2005); [35] Pál et al. (2012); [36] Müller et al. (2014b); [37] Yu et al. (2017a); [38] Müller et al. (2012); [39] Emery et al. (2014); [40] Yu & Ji (2015); [41] Lellouch et al. (2013); [42] Ďurech et al. (2017); [43] Müller et al. (2011); [44] Müller et al. (2017); [45] Wolters et al. (2011); [46] Yu et al. (2014); [47] Müller et al. (2013); [48] Alí-Lagoa et al. (2014); [49] Jiang et al. (2019)

NOTE—This table contains a compilation of previously published values for thermophysical properties diameter D and thermal inertia Γ , taxonomic class, heliocentric distance r_h of the thermal infrared data used for the thermal inertia determination, and orbital classification, adapted from Table 2 in Delbo’ et al. (2015) and Tables A.2 and A.3 from Hanuš et al. (2018a) and updated with recent literature results. The taxonomical classes are taken from the Tholen (1984) or SMASS II (Bus & Binzel 2002) taxonomy where available or adopted directly from the referenced publication. The heliocentric distances of the observations used are not reported in Mueller & Lagerros (1998) and Jiang & Ji (2021), thus r_h is assumed to be equal to the semimajor axis of the orbit. The orbital classification is sourced from the JPL Small-Body Database as one of the following: inner or outer MBAs (IMB: $a < 2.0$ au, MBA: $2.0 < a < 3.2$ au, OMB: $3.2 < a < 4.6$ au), Jupiter Trojans (TJN), Aten, Apollo, or Amor NEAs (ATE, APO, AMO), Mars crossers (MCA), or trans-Neptunian objects (TNO). The Marciniak et al. (2021) results do not include the eight asteroids where only an upper limit was found for the thermal inertia.

Table 4. Final Sample TPM-derived Properties

Asteroid	D_{WISE} (km)	D (km)	Γ ($\text{J m}^{-2} \text{s}^{-0.5} \text{K}^{-1}$)	A	p_V	$\bar{\theta}$ °	χ^2_{red}	Model ID
5 Astraea*	108.3±3.7	104.8 ^{+7.8} _{-6.2}	45 ⁺⁵⁸ ₋₄₀	0.106 ^{+0.015} _{-0.015}	0.271 ^{+0.038} _{-0.038}	55.4	6.7	D1
		102.4 ^{+4.8} _{-2.1}	10 ⁺¹⁹ ₋₁₀	0.113 ^{+0.004} _{-0.010}	0.288 ^{+0.010} _{-0.025}	55.4	2.1	R1
		105.2 ^{+4.3} _{-2.9}	14 ⁺²⁰ ₋₁₄	0.107 ^{+0.005} _{-0.008}	0.272 ^{+0.013} _{-0.021}	55.4	2.1	R2
14 Irene*	140.8±8.4	132.6 ^{+6.6} _{-0.0}	0 ⁺²⁹ ₋₀	0.113 ^{+0.000} _{-0.010}	0.287 ^{+0.000} _{-0.025}	55.4	10.0	D1
		134.3 ^{+5.9} _{-0.0}	0 ⁺²¹ ₋₀	0.110 ^{+0.000} _{-0.009}	0.279 ^{+0.000} _{-0.022}	55.4	9.9	R2
17 Thetis*	84.9±2.0	73.1 ^{+1.0} _{-0.0}	0 ⁺²⁸ ₋₀	0.096 ^{+0.000} _{-0.002}	0.244 ^{+0.000} _{-0.006}	55.4	1.2	D1
		72.6 ^{+1.3} _{-0.0}	0 ⁺³⁰ ₋₀	0.096 ^{+0.000} _{-0.003}	0.249 ^{+0.000} _{-0.007}	55.4	1.1	R1
		72.6 ^{+1.6} _{-0.0}	0 ⁺⁴³ ₋₀	0.096 ^{+0.000} _{-0.004}	0.244 ^{+0.000} _{-0.009}	55.4	1.3	R2
21 Lutetia*	99.5±27.1	93.4 ^{+5.6} _{-3.6}	2 ⁺²⁸ ₋₂	0.079 ^{+0.007} _{-0.008}	0.216 ^{+0.018} _{-0.022}	46.8	3.0	D1
		91.8 ^{+4.4} _{-3.5}	0 ⁺²⁸ ₋₀	0.083 ^{+0.007} _{-0.007}	0.227 ^{+0.018} _{-0.019}	46.8	2.6	R1
		89.9 ^{+4.4} _{-1.8}	6 ⁺²² ₋₆	0.087 ^{+0.003} _{-0.008}	0.238 ^{+0.008} _{-0.021}	55.4	2.2	R2
22 Kalliope*	167.5±3.1	137.4 ^{+6.4} _{-0.0}	0 ⁺¹⁷ ₋₀	0.099 ^{+0.000} _{-0.008}	0.229 ^{+0.000} _{-0.019}	55.4	8.5	D1
		136.3 ^{+5.5} _{-0.0}	0 ⁺¹³ ₋₀	0.101 ^{+0.000} _{-0.007}	0.232 ^{+0.000} _{-0.017}	55.4	8.7	R1
24 Themis*	195.5±4.4	169.3 ^{+9.0} _{-0.0}	0 ⁺¹⁷ ₋₀	0.036 ^{+0.000} _{-0.003}	0.087 ^{+0.000} _{-0.007}	55.4	9.3	D1
		170.3 ^{+10.9} _{-0.0}	0 ⁺²¹ ₋₀	0.036 ^{+0.000} _{-0.004}	0.086 ^{+0.000} _{-0.010}	55.4	9.2	D2
26 Proserpina*	83.0±2.1	83.4 ^{+4.3} _{-4.8}	11 ⁺⁵⁷ ₋₁₁	0.103 ^{+0.011} _{-0.010}	0.263 ^{+0.029} _{-0.025}	35.8	3.0	D1
		82.7 ^{+2.6} _{-3.2}	19 ⁺¹² ₋₁₉	0.095 ^{+0.008} _{-0.006}	0.242 ^{+0.020} _{-0.014}	26.7	1.4	R1
27 Euterpe*	114.1±4.5	95.6 ^{+7.5} _{-0.5}	1 ⁺⁶² ₋₁	0.114 ^{+0.000} _{-0.016}	0.289 ^{+0.001} _{-0.042}	55.4	9.7	D1
30 Urania*	92.8±2.0	80.0 ^{+4.2} _{-0.2}	1 ⁺⁴³ ₋₁	0.094 ^{+0.000} _{-0.009}	0.240 ^{+0.001} _{-0.023}	55.4	5.8	D1
		79.3 ^{+4.2} _{-0.8}	1 ⁺⁵⁴ ₋₁	0.096 ^{+0.000} _{-0.009}	0.244 ^{+0.001} _{-0.023}	55.4	6.2	D2
		79.6 ^{+2.0} _{-0.0}	0 ⁺²¹ ₋₀	0.093 ^{+0.000} _{-0.004}	0.238 ^{+0.000} _{-0.010}	55.4	4.2	R1
		79.6 ^{+2.0} _{-1.4}	1 ⁺²⁴ ₋₁	0.093 ^{+0.000} _{-0.004}	0.238 ^{+0.001} _{-0.011}	55.4	4.7	R2
35 Leukothea*	103.1±1.2	97.6 ^{+3.4} _{-0.0}	0 ⁺¹⁶ ₋₀	0.027 ^{+0.000} _{-0.001}	0.069 ^{+0.000} _{-0.003}	55.4	7.1	D1
		98.0 ^{+3.9} _{-0.5}	1 ⁺²⁸ ₋₁	0.027 ^{+0.000} _{-0.002}	0.069 ^{+0.000} _{-0.005}	55.4	7.4	D2
		97.9 ^{+3.1} _{-0.0}	0 ⁺¹⁸ ₋₀	0.027 ^{+0.000} _{-0.001}	0.068 ^{+0.000} _{-0.003}	55.4	5.8	R1
		98.0 ^{+2.5} _{-0.0}	0 ⁺¹⁴ ₋₀	0.027 ^{+0.000} _{-0.001}	0.068 ^{+0.000} _{-0.003}	55.4	6.1	R2
56 Melete*	120.3±1.4	104.7 ^{+1.7} _{-0.3}	1 ⁺⁴⁰ ₋₁	0.029 ^{+0.000} _{-0.001}	0.073 ^{+0.000} _{-0.002}	55.4	2.9	D1
		104.6 ^{+1.8} _{-0.0}	0 ⁺⁴⁹ ₋₀	0.029 ^{+0.000} _{-0.001}	0.073 ^{+0.000} _{-0.002}	55.4	3.2	D2
		104.9 ^{+1.4} _{-0.3}	1 ⁺³⁴ ₋₁	0.029 ^{+0.000} _{-0.001}	0.073 ^{+0.000} _{-0.002}	55.4	2.5	R1
64 Angelina*	58.3±1.1	46.0 ^{+2.8} _{-0.2}	6 ⁺¹²⁷⁵ ₋₆	0.408 ^{+0.003} _{-0.047}	0.659 ^{+0.004} _{-0.075}	55.4	1.8	D1
		47.6 ^{+1.2} _{-1.8}	471 ⁺⁹⁰⁹ ₋₄₇₁	0.383 ^{+0.029} _{-0.020}	0.619 ^{+0.046} _{-0.032}	55.4	1.7	D2
		46.1 ^{+2.1} _{-0.1}	3 ⁺⁷⁶⁰ ₋₃	0.410 ^{+0.001} _{-0.019}	0.662 ^{+0.001} _{-0.031}	55.4	1.0	R1
		46.0 ^{+1.9} _{-0.1}	3 ⁺⁷¹² ₋₃	0.410 ^{+0.001} _{-0.019}	0.664 ^{+0.001} _{-0.030}	55.4	1.0	R2
68 Leto*	122.5±3.1	102.7 ^{+5.6} _{-0.3}	1 ⁺⁵⁴ ₋₁	0.096 ^{+0.000} _{-0.009}	0.295 ^{+0.001} _{-0.029}	55.4	5.6	D1
69 Hesperia*	131.1±32.2	102.8 ^{+7.0} _{-0.0}	0 ⁺¹⁴ ₋₀	0.101 ^{+0.000} _{-0.012}	0.240 ^{+0.000} _{-0.029}	55.4	3.0	D1
		102.0 ^{+4.8} _{-0.0}	0 ⁺³ ₋₀	0.100 ^{+0.000} _{-0.008}	0.239 ^{+0.000} _{-0.018}	55.4	2.5	D2
		103.5 ^{+5.0} _{-0.0}	0 ⁺¹⁰ ₋₀	0.099 ^{+0.000} _{-0.008}	0.236 ^{+0.000} _{-0.020}	55.4	2.2	R1
		102.4 ^{+5.8} _{-0.0}	0 ⁺⁹ ₋₀	0.099 ^{+0.000} _{-0.008}	0.236 ^{+0.000} _{-0.020}	55.4	2.3	R2

Table 4 continued

Table 4 (continued)

Asteroid		D_{WISE}	D	Γ	A	pv	$\bar{\theta}$	χ^2_{red}	Model ID
		(km)	(km)	($\text{J m}^{-2} \text{s}^{-0.5} \text{K}^{-1}$)			°		
71	Niobe*	82.1±2.6	74.2 ^{+1.4} _{-3.3}	1 ⁺⁷⁶ ₋₁	0.201 ^{+0.018} _{-0.007}	0.356 ^{+0.033} _{-0.013}	46.8	1.1	D1
			72.9 ^{+2.9} _{-1.7}	41 ⁺⁵⁵ ₋₄₁	0.209 ^{+0.010} _{-0.016}	0.370 ^{+0.017} _{-0.028}	55.4	1.1	R1
72	Feronia*	78.8±2.0	73.5 ^{+1.9} _{-0.5}	1 ⁺²⁵ ₋₁	0.032 ^{+0.000} _{-0.002}	0.081 ^{+0.000} _{-0.004}	55.4	9.1	D1
			72.3 ^{+1.7} _{-0.0}	0 ⁺¹⁹ ₋₀	0.032 ^{+0.000} _{-0.001}	0.082 ^{+0.000} _{-0.003}	55.4	7.8	R1
			74.5 ^{+1.5} _{-0.5}	1 ⁺¹⁸ ₋₁	0.031 ^{+0.000} _{-0.001}	0.078 ^{+0.000} _{-0.003}	55.4	7.8	R2
73	Klytia	44.6±0.9	44.3 ^{+3.5} _{-1.6}	13 ⁺³¹ ₋₉	0.079 ^{+0.005} _{-0.011}	0.202 ^{+0.014} _{-0.028}	26.7	2.1	D1
			42.6 ^{+2.7} _{-1.7}	13 ⁺²⁰ ₋₁₃	0.089 ^{+0.007} _{-0.010}	0.228 ^{+0.017} _{-0.026}	26.7	2.1	D2
			45.3 ^{+1.9} _{-3.0}	26 ⁺¹⁵ ₋₂₁	0.078 ^{+0.011} _{-0.006}	0.200 ^{+0.029} _{-0.015}	26.7	1.9	R1
			44.3 ^{+1.4} _{-1.7}	28 ⁺³³ ₋₁₂	0.084 ^{+0.007} _{-0.005}	0.213 ^{+0.017} _{-0.014}	26.7	1.1	R2
76	Freia*	145.4±1.3	152.0 ^{+6.3} _{-7.0}	3 ⁺¹⁶ ₋₃	0.020 ^{+0.002} _{-0.002}	0.050 ^{+0.005} _{-0.004}	46.8	1.3	D1
			150.8 ^{+6.3} _{-7.3}	4 ⁺¹⁵ ₋₄	0.020 ^{+0.002} _{-0.002}	0.051 ^{+0.005} _{-0.004}	46.8	1.5	D2
79	Eurynome*	63.5±1.0	65.4 ^{+4.5} _{-2.7}	55 ⁺⁴⁸ ₋₃₃	0.114 ^{+0.012} _{-0.014}	0.247 ^{+0.026} _{-0.030}	55.4	3.4	D1
			64.9 ^{+4.4} _{-3.1}	56 ⁺⁴⁷ ₋₃₄	0.116 ^{+0.014} _{-0.014}	0.251 ^{+0.030} _{-0.030}	55.4	3.9	D2
			64.9 ^{+2.1} _{-0.5}	1 ⁺⁹ ₋₁	0.117 ^{+0.001} _{-0.007}	0.254 ^{+0.002} _{-0.015}	16.5	1.1	R1
			64.9 ^{+1.9} _{-1.2}	2 ⁺⁹ ₋₂	0.117 ^{+0.005} _{-0.006}	0.253 ^{+0.010} _{-0.014}	16.5	1.0	R2
80	Sappho*	68.6±1.0	66.7 ^{+4.6} _{-0.8}	1 ⁺⁹³ ₋₁	0.092 ^{+0.001} _{-0.012}	0.235 ^{+0.001} _{-0.031}	55.4	8.0	R1
94	Aurora*	173.8±4.2	157.6 ^{+7.0} _{-0.0}	0 ⁺⁹ ₋₀	0.025 ^{+0.000} _{-0.002}	0.064 ^{+0.000} _{-0.005}	55.4	9.8	D1
			159.5 ^{+5.4} _{-0.0}	0 ⁺⁸ ₋₀	0.025 ^{+0.000} _{-0.001}	0.063 ^{+0.000} _{-0.003}	55.4	9.4	R1
			158.1 ^{+6.7} _{-0.0}	0 ⁺⁹ ₋₀	0.025 ^{+0.000} _{-0.002}	0.063 ^{+0.000} _{-0.004}	55.4	9.8	R2
95	Arethusa*	148.0±5.1	131.1 ^{+5.2} _{-4.5}	1 ⁺⁹ ₋₁	0.023 ^{+0.002} _{-0.002}	0.059 ^{+0.004} _{-0.004}	26.7	5.5	D1
98	Ianthé*	102.5±4.0	94.7 ^{+2.5} _{-0.0}	0 ⁺³⁰ ₋₀	0.021 ^{+0.000} _{-0.001}	0.053 ^{+0.000} _{-0.002}	55.4	4.9	D1
			94.4 ^{+1.8} _{-0.2}	1 ⁺²⁶ ₋₁	0.021 ^{+0.000} _{-0.001}	0.054 ^{+0.000} _{-0.002}	55.4	4.1	R1
			94.8 ^{+2.3} _{-0.0}	0 ⁺⁴⁵ ₋₀	0.021 ^{+0.000} _{-0.001}	0.053 ^{+0.000} _{-0.003}	55.4	5.2	R2
99	Dike	67.4±0.4	66.2 ^{+4.1} _{-3.0}	56 ⁺³² ₋₅₆	0.025 ^{+0.003} _{-0.003}	0.065 ^{+0.007} _{-0.007}	55.4	3.0	D1
			63.6 ^{+2.4} _{-1.3}	6 ⁺²⁰ ₋₆	0.027 ^{+0.001} _{-0.002}	0.070 ^{+0.002} _{-0.005}	26.7	1.2	R1
			62.9 ^{+2.7} _{-1.2}	5 ⁺²³ ₋₅	0.028 ^{+0.001} _{-0.002}	0.071 ^{+0.002} _{-0.006}	26.7	1.1	R2
100	Hekate*	85.7±2.0	79.9 ^{+5.1} _{-0.0}	0 ⁺³⁹ ₋₀	0.085 ^{+0.000} _{-0.009}	0.217 ^{+0.000} _{-0.024}	55.4	4.8	D1
			81.5 ^{+5.3} _{-0.0}	0 ⁺⁴⁴ ₋₀	0.083 ^{+0.000} _{-0.009}	0.212 ^{+0.000} _{-0.024}	55.4	3.9	D2
			80.5 ^{+3.1} _{-0.4}	1 ⁺²⁵ ₋₁	0.088 ^{+0.000} _{-0.006}	0.225 ^{+0.001} _{-0.016}	55.4	2.4	R1
103	Hera*	83.9±2.1	75.1 ^{+2.3} _{-0.0}	0 ⁺³³ ₋₀	0.097 ^{+0.000} _{-0.005}	0.247 ^{+0.000} _{-0.013}	55.4	8.1	D1
			74.7 ^{+2.3} _{-0.0}	0 ⁺¹⁹ ₋₀	0.097 ^{+0.000} _{-0.003}	0.247 ^{+0.000} _{-0.007}	55.4	7.5	D2
			75.0 ^{+1.5} _{-0.0}	0 ⁺²⁴ ₋₀	0.097 ^{+0.000} _{-0.004}	0.247 ^{+0.000} _{-0.009}	55.4	7.2	R1
			75.2 ^{+2.1} _{-0.0}	0 ⁺²⁹ ₋₀	0.097 ^{+0.000} _{-0.004}	0.246 ^{+0.000} _{-0.011}	55.4	7.2	R2
107	Camilla*	210.4±8.3	199.9 ^{+12.3} _{-8.6}	14 ⁺¹¹ ₋₉	0.021 ^{+0.002} _{-0.002}	0.062 ^{+0.006} _{-0.007}	55.4	3.1	D1
			196.3 ^{+10.9} _{-7.3}	12 ⁺⁷ ₋₉	0.022 ^{+0.002} _{-0.002}	0.064 ^{+0.005} _{-0.006}	55.4	2.1	R1
109	Felicita*	82.6±0.6	79.4 ^{+3.8} _{-2.9}	0 ⁺⁴² ₋₀	0.027 ^{+0.002} _{-0.002}	0.084 ^{+0.007} _{-0.007}	46.8	2.6	D1
			78.2 ^{+3.6} _{-3.1}	1 ⁺⁴⁷ ₋₁	0.028 ^{+0.002} _{-0.002}	0.087 ^{+0.007} _{-0.007}	46.8	2.1	D2
			78.3 ^{+5.7} _{-2.1}	10 ⁺⁴² ₋₁₀	0.027 ^{+0.001} _{-0.004}	0.086 ^{+0.004} _{-0.012}	55.4	2.8	R1
110	Lydia*	88.2±2.7	90.7 ^{+4.3} _{-5.1}	112 ⁺⁸³ ₋₇₁	0.065 ^{+0.008} _{-0.005}	0.151 ^{+0.018} _{-0.012}	55.4	4.3	D1
			88.2 ^{+3.5} _{-3.4}	128 ⁺⁷⁶ ₋₅₁	0.069 ^{+0.006} _{-0.005}	0.161 ^{+0.013} _{-0.011}	55.4	2.9	D2

Table 4 continued

Table 4 (continued)

Asteroid	D_{WISE}	D	Γ	A	pv	$\bar{\theta}$	χ^2_{red}	Model ID
	(km)	(km)	($\text{J m}^{-2} \text{s}^{-0.5} \text{K}^{-1}$)			°		
112 Iphigenia*	69.8±1.8	61.6 ^{+1.5} _{-0.0}	0 ⁺²⁵ ₋₀	0.019 ^{+0.000} _{-0.001}	0.049 ^{+0.000} _{-0.002}	55.4	2.3	D1
		68.0 ^{+3.0} _{-0.0}	0 ⁺¹⁷ ₋₀	0.014 ^{+0.000} _{-0.001}	0.036 ^{+0.000} _{-0.003}	55.4	8.6	D2
119 Althaea*	59.3±1.5	60.4 ^{+2.2} _{-4.0}	1 ⁺³³ ₋₁	0.066 ^{+0.009} _{-0.004}	0.169 ^{+0.023} _{-0.011}	35.8	4.5	D1
		55.7 ^{+1.7} _{-0.4}	1 ⁺¹⁵ ₋₁	0.086 ^{+0.000} _{-0.005}	0.218 ^{+0.001} _{-0.012}	35.8	2.6	D2
		56.0 ^{+1.7} _{-1.2}	5 ⁺¹⁵ ₋₅	0.083 ^{+0.002} _{-0.005}	0.211 ^{+0.006} _{-0.012}	26.7	1.1	R1
		55.4 ^{+1.3} _{-1.4}	7 ⁺¹³ ₋₇	0.086 ^{+0.003} _{-0.004}	0.220 ^{+0.008} _{-0.010}	26.7	1.3	R2
121 Hermione*	166.2±8.8	165.4 ^{+8.8} _{-0.0}	0 ⁺⁷ ₋₀	0.026 ^{+0.000} _{-0.002}	0.066 ^{+0.000} _{-0.005}	55.4	6.9	D1
		163.3 ^{+5.9} _{-2.7}	1 ⁺⁷ ₋₁	0.028 ^{+0.000} _{-0.002}	0.070 ^{+0.001} _{-0.004}	55.4	2.7	R1
		158.9 ^{+5.8} _{-0.0}	0 ⁺⁵ ₋₀	0.029 ^{+0.000} _{-0.002}	0.073 ^{+0.000} _{-0.004}	55.4	2.8	R2
122 Gerda	70.7±0.9	74.6 ^{+3.8} _{-5.2}	49 ⁺²⁴ ₋₄₃	0.082 ^{+0.014} _{-0.007}	0.209 ^{+0.036} _{-0.018}	55.4	3.3	D1
		72.3 ^{+5.6} _{-3.1}	12 ⁺⁵⁹ ₋₁₁	0.089 ^{+0.008} _{-0.013}	0.220 ^{+0.020} _{-0.033}	26.7	3.5	D2
		73.5 ^{+1.5} _{-2.7}	29 ⁺¹¹ ₋₈	0.086 ^{+0.007} _{-0.003}	0.218 ^{+0.017} _{-0.008}	46.8	0.7	R1
		72.2 ^{+2.9} _{-1.2}	12 ⁺⁸ ₋₆	0.089 ^{+0.003} _{-0.007}	0.226 ^{+0.008} _{-0.017}	26.7	0.7	R2
125 Liberatrix	48.4±0.5	51.4 ^{+2.1} _{-2.6}	83 ⁺⁶⁰ ₋₄₉	0.079 ^{+0.009} _{-0.006}	0.152 ^{+0.018} _{-0.012}	46.8	2.0	D1
		50.7 ^{+2.5} _{-2.2}	43 ⁺⁴⁰ ₋₁₄	0.081 ^{+0.007} _{-0.009}	0.157 ^{+0.014} _{-0.017}	16.5	2.8	D2
		50.3 ^{+1.3} _{-1.3}	61 ⁺¹⁴ ₋₁₁	0.081 ^{+0.004} _{-0.004}	0.159 ^{+0.007} _{-0.007}	26.7	0.8	R1
155 Scylla	39.6±0.2	39.4 ^{+2.0} _{-1.8}	18 ⁺²⁹ ₋₁₅	0.011 ^{+0.001} _{-0.001}	0.029 ^{+0.003} _{-0.003}	26.7	4.7	D1
		39.9 ^{+2.0} _{-1.9}	80 ⁺⁵⁵ ₋₃₀	0.011 ^{+0.001} _{-0.001}	0.028 ^{+0.003} _{-0.003}	55.4	4.7	D2
157 Dejanira	18.3±3.2	19.8 ^{+2.0} _{-1.1}	127 ⁺⁶⁹ ₋₅₁	0.055 ^{+0.006} _{-0.009}	0.141 ^{+0.016} _{-0.023}	46.8	3.3	D1
		19.0 ^{+1.7} _{-2.0}	73 ⁺⁴⁴ ₋₇₃	0.059 ^{+0.015} _{-0.009}	0.150 ^{+0.038} _{-0.024}	26.7	5.2	D2
159 Aemilia*	125.2±1.2	126.0 ^{+3.1} _{-6.6}	0 ⁺²⁹ ₋₀	0.023 ^{+0.003} _{-0.001}	0.059 ^{+0.007} _{-0.002}	35.8	2.1	D1
		121.5 ^{+7.8} _{-3.9}	0 ⁺³¹ ₋₀	0.025 ^{+0.002} _{-0.003}	0.064 ^{+0.005} _{-0.007}	46.8	2.1	D2
		118.8 ^{+5.8} _{-5.0}	5 ⁺³¹ ₋₅	0.027 ^{+0.002} _{-0.002}	0.069 ^{+0.006} _{-0.006}	46.8	1.8	R1
		120.8 ^{+6.2} _{-4.9}	3 ⁺³² ₋₃	0.026 ^{+0.002} _{-0.002}	0.066 ^{+0.006} _{-0.006}	46.8	1.7	R2
162 Laurentia*	97.0±0.5	91.3 ^{+5.9} _{-5.8}	3 ⁺⁴⁸ ₋₃	0.022 ^{+0.003} _{-0.003}	0.057 ^{+0.008} _{-0.007}	27.3	4.2	D1
		91.2 ^{+4.9} _{-2.0}	0 ⁺¹³ ₋₀	0.023 ^{+0.001} _{-0.002}	0.058 ^{+0.003} _{-0.005}	26.7	2.7	D2
		91.4 ^{+3.7} _{-2.0}	2 ⁺¹⁴ ₋₂	0.023 ^{+0.001} _{-0.002}	0.059 ^{+0.003} _{-0.004}	26.7	1.1	R1
		92.1 ^{+3.0} _{-2.4}	26 ⁺¹³ ₋₉	0.022 ^{+0.001} _{-0.001}	0.057 ^{+0.003} _{-0.003}	55.4	1.0	R2
166 Rhodope*	52.4±0.2	50.5 ^{+2.1} _{-2.0}	48 ⁺¹¹⁵ ₋₄₈	0.028 ^{+0.002} _{-0.002}	0.070 ^{+0.006} _{-0.005}	55.4	2.0	D1
		48.9 ^{+1.4} _{-2.4}	2 ⁺⁵¹ ₋₂	0.029 ^{+0.003} _{-0.002}	0.075 ^{+0.007} _{-0.004}	26.7	1.9	D2
		47.9 ^{+1.9} _{-2.3}	12 ⁺⁷¹ ₋₁₂	0.030 ^{+0.003} _{-0.002}	0.078 ^{+0.007} _{-0.006}	46.8	1.7	R1
		48.3 ^{+1.5} _{-2.2}	0 ⁺⁵⁸ ₋₀	0.030 ^{+0.003} _{-0.002}	0.077 ^{+0.008} _{-0.004}	26.7	1.7	R2
167 Urda	39.9±0.3	40.8 ^{+2.0} _{-1.8}	61 ⁺⁸⁶ ₋₂₃	0.082 ^{+0.007} _{-0.007}	0.210 ^{+0.019} _{-0.019}	26.7	3.0	D1
		40.6 ^{+3.3} _{-1.5}	52 ⁺¹³⁵ ₋₂₂	0.083 ^{+0.007} _{-0.011}	0.211 ^{+0.019} _{-0.029}	26.7	3.8	D2
171 Ophelia*	105.0±3.5	95.0 ^{+3.0} _{-5.5}	0 ⁺³² ₋₀	0.032 ^{+0.004} _{-0.002}	0.082 ^{+0.010} _{-0.004}	26.7	2.6	R1
		96.2 ^{+2.8} _{-5.4}	0 ⁺²⁸ ₋₀	0.032 ^{+0.004} _{-0.001}	0.081 ^{+0.010} _{-0.004}	26.7	3.1	R2
174 Phaedra	64.8±0.4	60.8 ^{+0.9} _{-2.3}	27 ⁺⁵⁷ ₋₂₇	0.070 ^{+0.006} _{-0.002}	0.179 ^{+0.015} _{-0.005}	35.8	1.1	D1
		63.1 ^{+1.4} _{-2.4}	10 ⁺⁴⁶ ₋₁₀	0.066 ^{+0.005} _{-0.003}	0.168 ^{+0.013} _{-0.007}	35.8	1.5	R1
		64.5 ^{+1.5} _{-1.3}	0 ⁺¹⁵ ₋₀	0.063 ^{+0.003} _{-0.002}	0.161 ^{+0.007} _{-0.005}	35.8	1.1	R2
176 Iduna*	107.0±1.1	110.7 ^{+4.3} _{-8.0}	1 ⁺¹⁹ ₋₁	0.027 ^{+0.004} _{-0.002}	0.069 ^{+0.010} _{-0.005}	16.5	3.6	D1

Table 4 continued

Table 4 (continued)

Asteroid	D_{WISE}	D	Γ	A	pv	$\bar{\theta}$	χ^2_{red}	Model ID	
	(km)	(km)	($\text{J m}^{-2} \text{s}^{-0.5} \text{K}^{-1}$)			°			
180	Garumna	23.4±0.4	119.0 ^{+4.6} _{-7.3}	9 ⁺⁸ ₋₉	0.022 ^{+0.002} _{-0.002}	0.056 ^{+0.006} _{-0.004}	26.7	3.5	D2
			108.7 ^{+7.1} _{-2.7}	4 ⁺¹¹ ₋₄	0.037 ^{+0.002} _{-0.004}	0.093 ^{+0.004} _{-0.011}	26.7	1.9	R1
			104.8 ^{+6.0} _{-4.6}	9 ⁺¹⁴ ₋₈	0.041 ^{+0.003} _{-0.004}	0.104 ^{+0.008} _{-0.011}	26.7	3.8	R2
			22.7 ^{+0.7} _{-0.5}	0 ⁺¹¹ ₋₀	0.091 ^{+0.004} _{-0.004}	0.232 ^{+0.010} _{-0.011}	12.6	3.3	D1
184	Dejopeja	62.5±0.3	22.7 ^{+0.8} _{-0.2}	1 ⁺¹³ ₋₁	0.093 ^{+0.001} _{-0.006}	0.236 ^{+0.002} _{-0.016}	16.5	2.4	D2
			62.5 ^{+4.7} _{-3.1}	6 ⁺³⁸ ₋₆	0.081 ^{+0.008} _{-0.011}	0.206 ^{+0.021} _{-0.028}	0	6.7	D1
			63.0 ^{+7.5} _{-3.6}	7 ⁺⁹⁰ ₋₇	0.080 ^{+0.010} _{-0.018}	0.204 ^{+0.025} _{-0.045}	0	8.0	D2
			64.7 ^{+5.1} _{-4.7}	26 ⁺¹¹¹ ₋₂₄	0.076 ^{+0.012} _{-0.011}	0.194 ^{+0.031} _{-0.029}	3.9	4.7	R1
187	Lamberta*	129.9±2.4	63.2 ^{+9.5} _{-3.4}	6 ⁺²⁶⁵ ₋₆	0.079 ^{+0.008} _{-0.020}	0.201 ^{+0.021} _{-0.051}	0	5.9	R2
			119.5 ^{+5.9} _{-0.0}	0 ⁺¹⁵ ₋₀	0.025 ^{+0.000} _{-0.002}	0.063 ^{+0.000} _{-0.005}	55.4	10.0	D1
			119.8 ^{+5.2} _{-0.0}	0 ⁺¹³ ₋₀	0.025 ^{+0.000} _{-0.002}	0.066 ^{+0.000} _{-0.004}	55.4	8.9	D2
			129.3 ^{+3.8} _{-1.4}	1 ⁺⁹ ₋₁	0.021 ^{+0.000} _{-0.001}	0.053 ^{+0.000} _{-0.003}	55.4	7.4	R1
189	Phthia	38.5±0.3	124.3 ^{+3.7} _{-1.2}	0 ⁺⁹ ₋₀	0.023 ^{+0.000} _{-0.001}	0.059 ^{+0.000} _{-0.003}	55.4	8.2	R2
			36.5 ^{+3.3} _{-1.6}	22 ⁺⁸⁹ ₋₂₂	0.089 ^{+0.008} _{-0.015}	0.228 ^{+0.019} _{-0.038}	26.7	4.6	D1
			37.0 ^{+2.0} _{-1.8}	44 ⁺⁷⁴ ₋₄₄	0.088 ^{+0.009} _{-0.009}	0.223 ^{+0.023} _{-0.024}	26.7	3.4	D2
			35.0 ^{+3.9} _{-1.5}	22 ⁺¹⁰³ ₋₂₂	0.097 ^{+0.008} _{-0.020}	0.248 ^{+0.021} _{-0.050}	26.7	6.9	R1
192	Nausikaa*	98.8±1.2	35.1 ^{+4.0} _{-1.3}	22 ⁺¹⁰⁸ ₋₂₁	0.098 ^{+0.007} _{-0.020}	0.248 ^{+0.019} _{-0.051}	26.7	5.2	R2
			88.1 ^{+4.3} _{-2.8}	21 ⁺²¹ ₋₁₅	0.093 ^{+0.006} _{-0.008}	0.299 ^{+0.019} _{-0.027}	26.7	2.3	D1
			87.4 ^{+2.9} _{-3.6}	27 ⁺¹⁷ ₋₂₀	0.093 ^{+0.008} _{-0.006}	0.301 ^{+0.026} _{-0.018}	26.7	2.3	R1
			88.5 ^{+3.6} _{-2.8}	20 ⁺¹⁹ ₋₁₅	0.092 ^{+0.006} _{-0.007}	0.295 ^{+0.020} _{-0.022}	26.7	2.2	R2
193	Ambrosia	26.3±0.2	31.1 ^{+2.1} _{-1.6}	35 ⁺¹⁸ ₋₁₅	0.082 ^{+0.009} _{-0.012}	0.208 ^{+0.022} _{-0.030}	26.7	4.2	D1
			32.5 ^{+1.2} _{-2.2}	38 ⁺¹³ ₋₁₂	0.075 ^{+0.011} _{-0.007}	0.192 ^{+0.029} _{-0.017}	16.5	1.6	D2
			33.1 ^{+2.2} _{-3.3}	95 ⁺⁷² ₋₇₀	0.072 ^{+0.018} _{-0.008}	0.184 ^{+0.047} _{-0.020}	55.4	4.9	R1
			34.1 ^{+3.0} _{-7.9}	100 ⁺¹⁰² ₋₁₀₀	0.067 ^{+0.046} _{-0.010}	0.172 ^{+0.118} _{-0.026}	55.4	8.7	R2
195	Eurykleia*	85.4±2.5	76.7 ^{+1.8} _{-1.3}	0 ⁺⁷ ₋₀	0.028 ^{+0.001} _{-0.001}	0.070 ^{+0.003} _{-0.002}	26.7	2.1	D1
			79.6 ^{+1.7} _{-4.5}	0 ⁺¹⁸ ₋₀	0.026 ^{+0.003} _{-0.001}	0.065 ^{+0.008} _{-0.002}	26.7	2.4	D2
			79.5 ^{+1.4} _{-4.3}	0 ⁺¹⁴ ₋₀	0.026 ^{+0.002} _{-0.001}	0.066 ^{+0.005} _{-0.002}	26.7	1.7	R1
			77.2 ^{+2.5} _{-4.2}	0 ⁺²⁸ ₋₀	0.028 ^{+0.003} _{-0.001}	0.071 ^{+0.008} _{-0.004}	26.7	2.0	R2
196	Philomela*	144.6±4.1	129.7 ^{+3.6} _{-0.0}	0 ⁺¹⁴ ₋₀	0.093 ^{+0.000} _{-0.004}	0.237 ^{+0.000} _{-0.010}	55.4	6.1	D1
			130.4 ^{+2.7} _{-0.0}	0 ⁺¹² ₋₀	0.093 ^{+0.000} _{-0.003}	0.237 ^{+0.000} _{-0.008}	55.4	6.4	D2
			129.0 ^{+2.5} _{-0.8}	1 ⁺¹⁴ ₋₁	0.094 ^{+0.000} _{-0.004}	0.240 ^{+0.001} _{-0.009}	55.4	5.8	R1
			129.0 ^{+2.5} _{-0.0}	0 ⁺¹² ₋₀	0.094 ^{+0.000} _{-0.003}	0.239 ^{+0.000} _{-0.008}	55.4	6.1	R2
199	Byblis*	76.1±0.6	65.8 ^{+2.2} _{-0.6}	60 ⁺¹¹⁷⁸ ₋₆₀	0.061 ^{+0.001} _{-0.004}	0.154 ^{+0.003} _{-0.010}	55.4	1.6	D1
			66.2 ^{+2.1} _{-0.8}	43 ⁺⁷⁰⁰ ₋₄₃	0.060 ^{+0.001} _{-0.004}	0.153 ^{+0.003} _{-0.009}	55.4	1.5	D2
208	Lacrimosa	40.1±0.6	39.9 ^{+1.3} _{-1.3}	36 ⁺²² ₋₃₁	0.103 ^{+0.007} _{-0.007}	0.261 ^{+0.017} _{-0.019}	26.7	3.0	D1
			39.9 ^{+1.6} _{-1.2}	38 ⁺²⁹ ₋₁₅	0.103 ^{+0.006} _{-0.009}	0.262 ^{+0.016} _{-0.022}	26.7	3.1	D2
			38.7 ^{+3.1} _{-2.1}	52 ⁺¹¹⁹ ₋₄₃	0.110 ^{+0.014} _{-0.015}	0.280 ^{+0.035} _{-0.039}	26.7	4.9	R1
			39.1 ^{+3.2} _{-1.6}	52 ⁺¹⁹⁸ ₋₃₂	0.108 ^{+0.011} _{-0.015}	0.276 ^{+0.027} _{-0.039}	26.7	4.8	R2
218	Bianca*	57.3±1.6	54.3 ^{+2.7} _{-3.0}	19 ⁺⁵⁶ ₋₁₉	0.106 ^{+0.013} _{-0.010}	0.208 ^{+0.025} _{-0.019}	26.7	4.1	D1
			52.6 ^{+2.5} _{-2.5}	1 ⁺⁵⁴ ₋₁	0.107 ^{+0.011} _{-0.009}	0.210 ^{+0.021} _{-0.018}	26.7	2.7	R1

Table 4 continued

Table 4 (continued)

Asteroid	D_{WISE}	D	Γ	A	pv	$\bar{\theta}$	χ^2_{red}	Model ID	
	(km)	(km)	($\text{J m}^{-2} \text{s}^{-0.5} \text{K}^{-1}$)			°			
220	Stephania	31.7±0.2	53.6 ^{+2.6} _{-2.0}	0 ⁺⁴⁰ ₋₀	0.102 ^{+0.009} _{-0.008}	0.200 ^{+0.017} _{-0.017}	26.7	2.8	R2
			30.6 ^{+1.0} _{-0.6}	0 ⁺⁶¹ ₋₀	0.022 ^{+0.001} _{-0.001}	0.055 ^{+0.003} _{-0.002}	12.6	1.2	D1
			29.6 ^{+1.3} _{-0.0}	0 ⁺³⁰ ₋₀	0.024 ^{+0.000} _{-0.002}	0.060 ^{+0.000} _{-0.004}	16.5	1.5	D2
			30.1 ^{+1.3} _{-1.3}	55 ⁺¹⁰¹ ₋₃₉	0.028 ^{+0.003} _{-0.002}	0.071 ^{+0.007} _{-0.006}	26.7	3.0	R1
221	Eos*	91.2±2.2	30.5 ^{+1.1} _{-1.6}	58 ⁺¹¹¹ ₋₃₄	0.027 ^{+0.003} _{-0.002}	0.069 ^{+0.008} _{-0.005}	26.7	2.8	R2
			85.6 ^{+5.7} _{-1.2}	4 ⁺²⁸ ₋₄	0.076 ^{+0.002} _{-0.009}	0.200 ^{+0.004} _{-0.024}	55.4	3.2	D1
222	Lucia	55.4±1.0	85.8 ^{+5.0} _{-1.8}	5 ⁺²⁷ ₋₅	0.075 ^{+0.002} _{-0.008}	0.199 ^{+0.006} _{-0.021}	55.4	2.7	D2
			56.5 ^{+3.2} _{-2.4}	75 ⁺⁸⁰ ₋₃₁	0.044 ^{+0.004} _{-0.004}	0.113 ^{+0.009} _{-0.011}	27.3	2.0	D1
226	Weringia	31.5±0.3	57.1 ^{+3.8} _{-5.1}	134 ⁺¹⁰⁷ ₋₉₀	0.043 ^{+0.009} _{-0.005}	0.110 ^{+0.022} _{-0.012}	55.4	5.1	D2
			55.9 ^{+5.2} _{-3.2}	69 ⁺¹⁵² ₋₄₃	0.046 ^{+0.006} _{-0.007}	0.117 ^{+0.016} _{-0.018}	26.7	3.5	R1
			56.3 ^{+5.5} _{-3.6}	68 ⁺¹⁶⁸ ₋₄₃	0.045 ^{+0.007} _{-0.007}	0.114 ^{+0.018} _{-0.018}	26.7	4.5	R2
242	Kriemhild	40.8±0.3	28.5 ^{+0.4} _{-0.4}	42 ⁺²⁵ ₋₁₉	0.086 ^{+0.003} _{-0.003}	0.218 ^{+0.007} _{-0.007}	26.7	0.5	D1
			27.8 ^{+1.0} _{-0.3}	11 ⁺⁶¹ ₋₁₁	0.109 ^{+0.002} _{-0.008}	0.277 ^{+0.005} _{-0.019}	26.7	1.3	R1
245	Vera*	75.9±2.6	43.0 ^{+2.5} _{-1.9}	31 ⁺²³ ₋₂₆	0.066 ^{+0.006} _{-0.008}	0.169 ^{+0.016} _{-0.021}	12.6	3.0	D1
			43.5 ^{+2.0} _{-1.9}	36 ⁺³⁷ ₋₂₂	0.065 ^{+0.006} _{-0.007}	0.165 ^{+0.015} _{-0.017}	12.6	2.1	D2
			43.6 ^{+2.5} _{-2.1}	34 ⁺⁷⁵ ₋₁₂	0.071 ^{+0.007} _{-0.008}	0.181 ^{+0.019} _{-0.020}	12.6	2.5	R1
254	Augusta	12.5±0.1	44.1 ^{+2.6} _{-1.8}	42 ⁺¹³⁶ ₋₁₆	0.070 ^{+0.006} _{-0.008}	0.179 ^{+0.016} _{-0.020}	16.5	2.0	R2
			69.4 ^{+5.2} _{-4.0}	11 ⁺⁹⁹ ₋₁₁	0.099 ^{+0.012} _{-0.014}	0.253 ^{+0.030} _{-0.036}	46.8	8.5	D1
260	Huberta	101.5±0.9	68.8 ^{+5.7} _{-3.7}	45 ⁺⁸⁶ ₋₄₅	0.102 ^{+0.012} _{-0.014}	0.260 ^{+0.030} _{-0.036}	55.4	7.9	D2
			10.8 ^{+1.9} _{-0.4}	0 ⁺² ₋₀	0.072 ^{+0.006} _{-0.003}	0.185 ^{+0.017} _{-0.007}	16.5	8.1	D1
264	Libussa*	63.0±0.4	12.1 ^{+1.2} _{-1.1}	114 ⁺¹⁴⁵ ₋₇₇	0.060 ^{+0.014} _{-0.010}	0.153 ^{+0.035} _{-0.025}	55.4	5.4	D2
			91.8 ^{+5.2} _{-4.8}	43 ⁺²³ ₋₁₇	0.020 ^{+0.002} _{-0.002}	0.050 ^{+0.006} _{-0.006}	55.4	4.8	D1
			90.9 ^{+3.3} _{-5.3}	27 ⁺¹⁶ ₋₈	0.020 ^{+0.003} _{-0.001}	0.051 ^{+0.006} _{-0.004}	46.8	2.1	D2
			87.8 ^{+4.0} _{-3.7}	11 ⁺²² ₋₉	0.021 ^{+0.002} _{-0.002}	0.054 ^{+0.005} _{-0.004}	26.7	2.5	R1
270	Anahita*	51.4±1.5	87.0 ^{+3.9} _{-4.2}	10 ⁺¹⁵ ₋₁₀	0.022 ^{+0.002} _{-0.002}	0.056 ^{+0.005} _{-0.005}	26.7	2.9	R2
			52.4 ^{+2.4} _{-1.7}	9 ⁺¹⁴⁹¹ ₋₉	0.097 ^{+0.007} _{-0.009}	0.248 ^{+0.017} _{-0.022}	46.8	1.5	D1
			53.3 ^{+1.8} _{-2.6}	598 ⁺⁶⁵⁷ ₋₅₉₈	0.095 ^{+0.010} _{-0.006}	0.242 ^{+0.025} _{-0.015}	46.8	1.5	D2
			52.4 ^{+2.2} _{-1.7}	8 ⁺⁶⁰³ ₋₈	0.098 ^{+0.006} _{-0.008}	0.249 ^{+0.016} _{-0.020}	46.8	1.4	R1
271	Penthesilea	65.9±0.2	52.9 ^{+1.9} _{-2.3}	630 ⁺⁶³¹ ₋₆₃₀	0.096 ^{+0.009} _{-0.007}	0.244 ^{+0.023} _{-0.017}	46.8	1.4	R2
			46.5 ^{+1.9} _{-1.8}	54 ⁺⁹⁷ ₋₁₈	0.094 ^{+0.007} _{-0.007}	0.239 ^{+0.019} _{-0.019}	26.7	3.8	D1
272	Antonia	26.9±0.3	46.5 ^{+1.1} _{-2.6}	55 ⁺⁶⁸ ₋₂₄	0.093 ^{+0.011} _{-0.004}	0.237 ^{+0.028} _{-0.010}	26.7	4.0	D2
			63.2 ^{+2.7} _{-1.9}	30 ⁺³² ₋₁₈	0.019 ^{+0.001} _{-0.002}	0.050 ^{+0.003} _{-0.004}	26.7	2.5	D1
274	Philagoria	27.3±0.4	63.0 ^{+3.3} _{-2.5}	33 ⁺⁷⁷ ₋₁₇	0.019 ^{+0.001} _{-0.002}	0.050 ^{+0.004} _{-0.005}	26.7	3.4	D2
			32.7 ^{+1.6} _{-2.5}	58 ⁺³³ ₋₂₄	0.033 ^{+0.006} _{-0.003}	0.083 ^{+0.015} _{-0.007}	26.7	4.3	D1
276	Adelheid*	114.7±3.3	32.0 ^{+1.2} _{-1.5}	103 ⁺⁵⁴ ₋₅₆	0.031 ^{+0.003} _{-0.002}	0.079 ^{+0.008} _{-0.005}	55.4	3.0	R1
			31.4 ^{+1.4} _{-1.1}	77 ⁺³¹ ₋₄₇	0.059 ^{+0.004} _{-0.005}	0.149 ^{+0.010} _{-0.013}	55.4	2.1	D1
281	Lucretia	11.0±0.1	29.2 ^{+1.6} _{-1.2}	44 ⁺⁹³ ₋₄₂	0.074 ^{+0.008} _{-0.008}	0.189 ^{+0.019} _{-0.019}	26.7	3.0	D2
			101.9 ^{+6.1} _{-0.0}	0 ⁺³ ₋₀	0.021 ^{+0.002} _{-0.002}	0.053 ^{+0.005} _{-0.005}	46.8	5.7	D1
			102.6 ^{+8.0} _{-4.9}	1 ⁺²⁴ ₋₁	0.021 ^{+0.002} _{-0.003}	0.054 ^{+0.005} _{-0.007}	46.8	4.5	D2
			11.3 ^{+0.4} _{-0.5}	55 ⁺¹⁷ ₋₂₈	0.096 ^{+0.012} _{-0.006}	0.199 ^{+0.025} _{-0.013}	35.8	1.5	D1

Table 4 continued

Table 4 (continued)

Asteroid	D_{WISE}	D	Γ	A	pv	$\bar{\theta}$	χ^2_{red}	Model ID
	(km)	(km)	($\text{J m}^{-2} \text{s}^{-0.5} \text{K}^{-1}$)			°		
287 Nephthys*	59.6±1.3	11.2 ^{+0.5} _{-0.5}	59 ⁺²¹ ₋₁₈	0.097 ^{+0.012} _{-0.008}	0.202 ^{+0.025} _{-0.017}	27.3	1.2	D2
		10.7 ^{+0.9} _{-0.4}	42 ⁺²³ ₋₂₂	0.110 ^{+0.009} _{-0.018}	0.227 ^{+0.020} _{-0.038}	26.7	2.6	R1
		11.4 ^{+0.4} _{-0.4}	38 ⁺²⁵ ₋₁₄	0.096 ^{+0.007} _{-0.007}	0.199 ^{+0.014} _{-0.014}	16.5	1.2	R2
		57.1 ^{+2.1} _{-1.7}	5 ⁺¹¹ ₋₅	0.105 ^{+0.006} _{-0.007}	0.239 ^{+0.015} _{-0.017}	26.7	1.3	D1
		56.6 ^{+3.4} _{-2.7}	20 ⁺⁴⁷ ₋₂₀	0.107 ^{+0.011} _{-0.013}	0.243 ^{+0.025} _{-0.028}	46.8	3.9	D2
		57.1 ^{+1.3} _{-0.6}	1 ⁺⁶ ₋₁	0.104 ^{+0.001} _{-0.004}	0.237 ^{+0.002} _{-0.010}	26.7	2.0	R1
290 Bruna	9.8±0.1	54.4 ^{+1.6} _{-0.0}	0 ⁺⁸ ₋₀	0.115 ^{+0.000} _{-0.006}	0.262 ^{+0.000} _{-0.013}	26.7	2.4	R2
		9.8 ^{+0.6} _{-0.6}	12 ⁺²⁶ ₋₁₂	0.104 ^{+0.015} _{-0.012}	0.264 ^{+0.038} _{-0.030}	12.0	5.5	D1
		9.7 ^{+0.2} _{-0.1}	1 ⁺⁷ ₋₁	0.106 ^{+0.001} _{-0.005}	0.269 ^{+0.002} _{-0.012}	16.5	3.1	D2
293 Brasilia*	57.5±1.4	50.0 ^{+2.0} _{-2.1}	40 ⁺⁶⁸ ₋₄₀	0.026 ^{+0.002} _{-0.002}	0.067 ^{+0.005} _{-0.005}	55.4	2.9	D1
		49.4 ^{+2.7} _{-2.0}	29 ⁺⁸⁶ ₋₂₉	0.027 ^{+0.002} _{-0.003}	0.069 ^{+0.004} _{-0.007}	55.4	4.6	D2
296 Phaetusa	8.2±0.1	8.7 ^{+0.2} _{-0.3}	56 ⁺⁴³ ₋₃₀	0.073 ^{+0.006} _{-0.003}	0.185 ^{+0.015} _{-0.009}	12.0	1.6	D1
		8.7 ^{+0.3} _{-0.3}	52 ⁺⁴⁰ ₋₃₁	0.073 ^{+0.006} _{-0.004}	0.186 ^{+0.014} _{-0.011}	12.6	1.8	D2
301 Bavaria*	53.0±0.4	51.8 ^{+1.6} _{-1.9}	10 ⁺³² ₋₁₀	0.019 ^{+0.001} _{-0.001}	0.048 ^{+0.003} _{-0.004}	46.8	1.6	D1
		51.8 ^{+1.9} _{-1.7}	6 ⁺³⁸ ₋₆	0.018 ^{+0.001} _{-0.001}	0.047 ^{+0.003} _{-0.003}	46.8	1.6	D2
		51.1 ^{+1.5} _{-2.9}	0 ⁺⁶¹ ₋₀	0.023 ^{+0.003} _{-0.001}	0.059 ^{+0.008} _{-0.002}	27.3	2.5	R1
310 Margarita	33.7±0.2	30.6 ^{+1.1} _{-1.0}	0 ⁺¹³⁴ ₋₀	0.061 ^{+0.004} _{-0.004}	0.156 ^{+0.011} _{-0.010}	26.7	2.2	D1
		30.9 ^{+0.9} _{-0.9}	5 ⁺¹⁰² ₋₅	0.061 ^{+0.004} _{-0.004}	0.156 ^{+0.009} _{-0.009}	26.7	1.8	D2
		31.1 ^{+0.9} _{-0.0}	0 ⁺⁴⁴ ₋₀	0.051 ^{+0.000} _{-0.002}	0.129 ^{+0.000} _{-0.006}	26.7	1.6	R1
		30.6 ^{+0.9} _{-0.1}	2 ⁺⁶⁰ ₋₂	0.051 ^{+0.000} _{-0.003}	0.131 ^{+0.001} _{-0.007}	26.7	2.0	R2
311 Claudia	26.3±0.4	29.4 ^{+2.6} _{-2.0}	80 ⁺⁴⁸ ₋₃₄	0.072 ^{+0.011} _{-0.012}	0.184 ^{+0.028} _{-0.030}	26.7	9.8	D1
		28.6 ^{+2.9} _{-2.0}	81 ⁺⁵³ ₋₄₉	0.077 ^{+0.012} _{-0.014}	0.195 ^{+0.030} _{-0.035}	46.8	7.9	D2
		27.5 ^{+0.7} _{-0.8}	22 ⁺⁸ ₋₁₁	0.090 ^{+0.006} _{-0.004}	0.229 ^{+0.015} _{-0.011}	16.5	1.6	R1
		27.2 ^{+1.0} _{-0.9}	23 ⁺¹⁰ ₋₁₂	0.094 ^{+0.007} _{-0.006}	0.240 ^{+0.017} _{-0.016}	16.5	2.2	R2
		49.5 ^{+2.7} _{-2.9}	64 ⁺⁴⁷ ₋₃₁	0.071 ^{+0.010} _{-0.007}	0.182 ^{+0.025} _{-0.019}	26.7	4.2	D1
312 Pierretta	46.2±0.4	48.2 ^{+2.4} _{-2.4}	42 ⁺⁴² ₋₄₂	0.076 ^{+0.008} _{-0.007}	0.194 ^{+0.021} _{-0.019}	35.8	3.3	D2
		45.2 ^{+3.2} _{-2.1}	12 ⁺²⁹ ₋₁₂	0.086 ^{+0.006} _{-0.011}	0.219 ^{+0.015} _{-0.028}	26.7	3.5	R1
		45.5 ^{+0.9} _{-1.5}	0 ⁺⁴ ₋₀	0.084 ^{+0.007} _{-0.002}	0.215 ^{+0.018} _{-0.005}	16.5	3.2	R2
		7.4 ^{+0.6} _{-0.4}	8 ⁺²² ₋₈	0.101 ^{+0.012} _{-0.015}	0.257 ^{+0.030} _{-0.038}	16.5	2.3	D1
315 Constantia	6.5±0.1	6.8 ^{+1.0} _{-0.3}	9 ⁺⁵⁵ ₋₉	0.129 ^{+0.010} _{-0.032}	0.327 ^{+0.024} _{-0.082}	26.7	4.7	D2
		18.4 ^{+0.4} _{-0.6}	74 ⁺²⁷ ₋₂₅	0.179 ^{+0.012} _{-0.009}	0.455 ^{+0.030} _{-0.022}	12.6	1.9	D1
317 Roxane	18.6±0.2	18.3 ^{+0.5} _{-0.8}	44 ⁺³¹ ₋₂₀	0.181 ^{+0.016} _{-0.012}	0.461 ^{+0.040} _{-0.030}	12.6	3.3	D2
		28.6 ^{+0.8} _{-0.5}	32 ⁺⁸ ₋₁₀	0.069 ^{+0.003} _{-0.004}	0.175 ^{+0.007} _{-0.009}	16.5	0.7	D1
321 Florentina	28.0±0.1	28.7 ^{+0.5} _{-0.4}	32 ⁺⁸ ₋₇	0.068 ^{+0.002} _{-0.002}	0.173 ^{+0.005} _{-0.006}	16.5	0.6	D2
		29.3 ^{+0.7} _{-0.7}	23 ⁺¹⁰ ₋₈	0.068 ^{+0.003} _{-0.003}	0.173 ^{+0.008} _{-0.007}	16.5	1.1	R1
		69.2 ^{+3.4} _{-1.5}	10 ⁺⁴⁰ ₋₁₀	0.020 ^{+0.001} _{-0.002}	0.051 ^{+0.001} _{-0.004}	55.4	3.7	D1
329 Svea*	74.1±2.4	65.6 ^{+2.5} _{-0.7}	5 ⁺³² ₋₅	0.021 ^{+0.000} _{-0.002}	0.055 ^{+0.001} _{-0.004}	55.4	2.0	R1
		66.0 ^{+3.4} _{-0.0}	0 ⁺³³ ₋₀	0.021 ^{+0.000} _{-0.002}	0.053 ^{+0.000} _{-0.004}	55.4	1.9	R2
335 Roberta*	88.4±1.2	85.2 ^{+6.1} _{-5.6}	1 ⁺⁵⁶ ₋₁	0.024 ^{+0.004} _{-0.003}	0.061 ^{+0.009} _{-0.008}	35.8	5.0	D1
		84.0 ^{+5.8} _{-5.3}	1 ⁺⁵¹ ₋₁	0.025 ^{+0.004} _{-0.003}	0.063 ^{+0.009} _{-0.008}	35.8	4.7	D2

Table 4 continued

Table 4 (continued)

Asteroid	D_{WISE}	D	Γ	A	pv	$\bar{\theta}$	χ^2_{red}	Model ID
	(km)	(km)	($\text{J m}^{-2} \text{s}^{-0.5} \text{K}^{-1}$)			°		
		$84.5^{+4.3}_{-4.3}$	1^{+49}_{-1}	$0.025^{+0.002}_{-0.003}$	$0.063^{+0.006}_{-0.007}$	26.7	2.7	R1
		$84.1^{+3.7}_{-4.3}$	1^{+35}_{-1}	$0.025^{+0.003}_{-0.002}$	$0.063^{+0.007}_{-0.005}$	35.8	2.4	R2
349 Dembowska*	138.4 ± 7.9	$133.9^{+10.1}_{-7.4}$	20^{+20}_{-20}	$0.213^{+0.025}_{-0.028}$	$0.392^{+0.046}_{-0.052}$	55.4	6.1	D1
350 Ornamenta*	128.7 ± 1.2	$114.5^{+5.5}_{-3.1}$	19^{+17}_{-16}	$0.023^{+0.001}_{-0.002}$	$0.058^{+0.003}_{-0.005}$	55.4	2.2	D1
		$116.0^{+3.1}_{-3.7}$	21^{+13}_{-16}	$0.022^{+0.001}_{-0.001}$	$0.056^{+0.004}_{-0.003}$	55.4	1.6	R1
351 Yrsa	39.7 ± 0.4	$43.1^{+1.8}_{-3.3}$	0^{+21}_{-0}	$0.088^{+0.015}_{-0.006}$	$0.225^{+0.039}_{-0.015}$	3.9	4.6	D1
		$44.3^{+2.1}_{-4.2}$	44^{+33}_{-43}	$0.084^{+0.017}_{-0.009}$	$0.214^{+0.044}_{-0.023}$	35.8	3.7	D2
		$43.2^{+2.1}_{-4.1}$	43^{+23}_{-43}	$0.088^{+0.019}_{-0.009}$	$0.224^{+0.049}_{-0.024}$	27.3	3.1	R1
352 Gisela	26.7 ± 0.8	$25.1^{+1.4}_{-1.2}$	39^{+36}_{-32}	$0.099^{+0.010}_{-0.011}$	$0.251^{+0.025}_{-0.028}$	27.3	4.3	D1
		$25.0^{+1.7}_{-1.1}$	43^{+41}_{-35}	$0.100^{+0.009}_{-0.013}$	$0.254^{+0.023}_{-0.033}$	27.3	5.0	D2
		$23.8^{+0.8}_{-1.1}$	29^{+21}_{-28}	$0.106^{+0.010}_{-0.007}$	$0.270^{+0.026}_{-0.018}$	26.7	3.3	R1
		$23.6^{+1.4}_{-0.6}$	8^{+35}_{-8}	$0.110^{+0.004}_{-0.012}$	$0.280^{+0.009}_{-0.031}$	26.7	4.1	R2
355 Gabriella	24.0 ± 0.3	$26.8^{+0.6}_{-1.0}$	11^{+7}_{-10}	$0.079^{+0.006}_{-0.003}$	$0.201^{+0.015}_{-0.008}$	12.0	2.7	D1
		$23.5^{+1.1}_{-0.8}$	55^{+13}_{-30}	$0.080^{+0.007}_{-0.007}$	$0.203^{+0.017}_{-0.018}$	46.8	2.3	R1
360 Carlova*	129.1 ± 2.8	$113.2^{+5.2}_{-0.8}$	1^{+17}_{-1}	$0.020^{+0.000}_{-0.002}$	$0.050^{+0.000}_{-0.004}$	55.4	6.4	D1
		$113.2^{+3.3}_{-0.7}$	1^{+13}_{-1}	$0.021^{+0.000}_{-0.001}$	$0.053^{+0.000}_{-0.003}$	55.4	3.8	R1
		$115.0^{+3.3}_{-0.0}$	0^{+9}_{-0}	$0.019^{+0.000}_{-0.001}$	$0.050^{+0.000}_{-0.002}$	55.4	3.8	R2
364 Isara	27.2 ± 0.7	$28.3^{+3.3}_{-0.8}$	0^{+91}_{-0}	$0.091^{+0.006}_{-0.017}$	$0.232^{+0.016}_{-0.044}$	16.5	5.9	D1
		$28.5^{+0.9}_{-1.6}$	0^{+43}_{-0}	$0.090^{+0.011}_{-0.004}$	$0.228^{+0.029}_{-0.011}$	3.9	4.3	D2
365 Corduba*	86.8 ± 0.4	$85.2^{+3.9}_{-3.3}$	0^{+28}_{-0}	$0.018^{+0.002}_{-0.001}$	$0.047^{+0.004}_{-0.003}$	35.8	3.8	D1
		$86.1^{+3.7}_{-3.7}$	0^{+31}_{-0}	$0.018^{+0.002}_{-0.001}$	$0.046^{+0.005}_{-0.003}$	35.8	3.2	D2
		$84.4^{+0.7}_{-0.0}$	0^{+3}_{-0}	$0.019^{+0.002}_{-0.000}$	$0.048^{+0.006}_{-0.000}$	26.7	2.5	R1
		$82.6^{+3.5}_{-3.6}$	11^{+17}_{-11}	$0.020^{+0.001}_{-0.002}$	$0.051^{+0.004}_{-0.004}$	55.4	2.1	R2
371 Bohemia*	53.0 ± 0.6	$48.2^{+2.2}_{-2.6}$	27^{+771}_{-27}	$0.089^{+0.011}_{-0.008}$	$0.226^{+0.027}_{-0.019}$	26.7	2.8	D1
		$49.1^{+2.4}_{-2.4}$	27^{+546}_{-26}	$0.086^{+0.009}_{-0.008}$	$0.218^{+0.023}_{-0.020}$	26.7	2.5	D2
		$48.6^{+1.8}_{-0.8}$	11^{+51}_{-11}	$0.088^{+0.002}_{-0.007}$	$0.224^{+0.005}_{-0.017}$	26.7	2.4	R1
		$47.5^{+2.4}_{-0.0}$	0^{+62}_{-0}	$0.090^{+0.002}_{-0.007}$	$0.228^{+0.004}_{-0.017}$	26.7	2.4	R2
372 Palma*	186.5 ± 6.3	$165.6^{+7.7}_{-9.4}$	0^{+21}_{-0}	$0.023^{+0.003}_{-0.002}$	$0.059^{+0.008}_{-0.004}$	26.7	3.9	D1
		$168.1^{+9.2}_{-10.3}$	18^{+15}_{-18}	$0.023^{+0.003}_{-0.002}$	$0.058^{+0.008}_{-0.005}$	55.4	3.8	D2
376 Geometria*	35.5 ± 0.1	$32.8^{+1.8}_{-1.3}$	0^{+59}_{-0}	$0.095^{+0.009}_{-0.005}$	$0.241^{+0.022}_{-0.013}$	12.6	3.0	D1
		$33.2^{+1.0}_{-1.0}$	37^{+64}_{-37}	$0.096^{+0.006}_{-0.006}$	$0.244^{+0.016}_{-0.015}$	26.7	1.8	D2
377 Campania*	90.3 ± 0.6	$90.4^{+5.3}_{-3.3}$	0^{+21}_{-0}	$0.022^{+0.002}_{-0.002}$	$0.055^{+0.004}_{-0.005}$	46.8	6.1	D1
		$90.2^{+5.9}_{-4.3}$	1^{+28}_{-1}	$0.022^{+0.002}_{-0.003}$	$0.056^{+0.005}_{-0.006}$	46.8	6.6	D2
378 Holmia	27.8 ± 0.4	$29.1^{+1.2}_{-2.0}$	17^{+31}_{-17}	$0.093^{+0.013}_{-0.007}$	$0.236^{+0.034}_{-0.018}$	16.5	1.9	D1
		$28.3^{+1.9}_{-1.0}$	7^{+17}_{-6}	$0.098^{+0.006}_{-0.012}$	$0.250^{+0.015}_{-0.030}$	16.5	1.9	D2
380 Fiducia*	67.5 ± 2.5	$69.3^{+5.1}_{-3.1}$	26^{+39}_{-26}	$0.022^{+0.002}_{-0.003}$	$0.057^{+0.005}_{-0.007}$	55.4	7.7	D1
		$69.0^{+5.3}_{-2.9}$	0^{+60}_{-0}	$0.022^{+0.002}_{-0.002}$	$0.058^{+0.005}_{-0.006}$	26.7	6.4	D2
		$71.6^{+2.6}_{-2.7}$	0^{+23}_{-0}	$0.021^{+0.002}_{-0.001}$	$0.054^{+0.004}_{-0.003}$	46.8	2.4	R1
		$73.1^{+2.4}_{-3.0}$	15^{+19}_{-15}	$0.021^{+0.001}_{-0.001}$	$0.052^{+0.003}_{-0.004}$	55.4	1.8	R2
381 Myrrha*	117.6 ± 2.8	$108.6^{+5.8}_{-4.0}$	16^{+23}_{-15}	$0.028^{+0.002}_{-0.003}$	$0.071^{+0.005}_{-0.007}$	55.4	8.4	D1

Table 4 continued

Table 4 (continued)

Asteroid	D_{WISE}	D	Γ	A	pv	$\bar{\theta}$	χ^2_{red}	Model ID
	(km)	(km)	($\text{J m}^{-2} \text{s}^{-0.5} \text{K}^{-1}$)			°		
390 Alma	25.7±0.2	108.0 ^{+5.6} _{-2.7}	10 ⁺¹⁹ ₋₉	0.028 ^{+0.001} _{-0.003}	0.072 ^{+0.003} _{-0.007}	55.4	5.9	D2
		111.4 ^{+4.8} _{-4.2}	18 ⁺¹⁵ ₋₁₄	0.026 ^{+0.002} _{-0.002}	0.067 ^{+0.005} _{-0.005}	55.4	4.7	R1
		111.3 ^{+4.9} _{-3.6}	17 ⁺¹⁵ ₋₁₂	0.026 ^{+0.002} _{-0.002}	0.067 ^{+0.005} _{-0.005}	55.4	4.3	R2
		25.4 ^{+1.9} _{-1.2}	71 ⁺⁴⁶ ₋₄₃	0.067 ^{+0.007} _{-0.009}	0.170 ^{+0.017} _{-0.023}	46.8	4.1	D1
		25.2 ^{+1.2} _{-1.6}	64 ⁺⁴⁴ ₋₄₀	0.068 ^{+0.010} _{-0.006}	0.174 ^{+0.025} _{-0.016}	35.8	4.2	D2
		24.6 ^{+1.5} _{-0.8}	38 ⁺²⁴ ₋₃₄	0.072 ^{+0.005} _{-0.008}	0.184 ^{+0.012} _{-0.020}	26.7	2.5	R1
391 Ingeborg	17.3±3.7	24.5 ^{+1.0} _{-0.8}	51 ⁺²⁰ ₋₃₁	0.074 ^{+0.006} _{-0.006}	0.188 ^{+0.015} _{-0.015}	27.3	1.5	R2
		18.3 ^{+0.9} _{-0.6}	87 ⁺³⁸ ₋₅₁	0.093 ^{+0.006} _{-0.008}	0.238 ^{+0.015} _{-0.021}	27.3	3.0	D1
394 Arduina	30.0±0.3	31.5 ^{+1.3} _{-1.0}	99 ⁺³⁴ ₋₂₇	0.086 ^{+0.006} _{-0.006}	0.220 ^{+0.016} _{-0.016}	55.4	1.8	D1
400 Ducrosa	36.0±0.4	32.8 ^{+1.2} _{-1.3}	42 ⁺⁶³ ₋₁₉	0.080 ^{+0.006} _{-0.006}	0.205 ^{+0.016} _{-0.017}	26.7	2.0	D2
		32.3 ^{+2.3} _{-1.7}	19 ⁺¹⁸ ₋₁₆	0.038 ^{+0.004} _{-0.005}	0.097 ^{+0.011} _{-0.012}	12.6	3.8	D1
		34.6 ^{+1.6} _{-2.2}	42 ⁺¹⁹ ₋₂₂	0.033 ^{+0.004} _{-0.004}	0.083 ^{+0.011} _{-0.009}	27.3	2.1	D2
		33.6 ^{+2.2} _{-2.1}	34 ⁺¹⁷ ₋₂₉	0.049 ^{+0.007} _{-0.007}	0.128 ^{+0.017} _{-0.017}	26.7	3.6	R1
402 Chloe*	55.4±1.8	33.9 ^{+4.5} _{-3.1}	34 ⁺¹⁶ ₋₃₄	0.048 ^{+0.010} _{-0.011}	0.122 ^{+0.024} _{-0.028}	26.7	4.2	R2
		57.3 ^{+4.3} _{-5.1}	85 ⁺⁵⁹ ₋₈₅	0.050 ^{+0.010} _{-0.007}	0.126 ^{+0.026} _{-0.018}	55.4	8.3	D1
404 Arsinoe*	95.0±1.0	53.9 ^{+6.0} _{-3.4}	1 ⁺¹⁰⁹ ₋₁	0.055 ^{+0.008} _{-0.011}	0.141 ^{+0.020} _{-0.028}	16.5	9.0	D2
		88.9 ^{+3.5} _{-0.8}	0 ⁺⁸ ₋₀	0.020 ^{+0.000} _{-0.001}	0.050 ^{+0.001} _{-0.003}	27.3	1.3	D1
406 Erna*	46.0±0.8	91.6 ^{+3.4} _{-2.3}	26 ⁺¹⁷ ₋₇	0.019 ^{+0.001} _{-0.001}	0.048 ^{+0.002} _{-0.003}	55.4	1.2	R1
		42.2 ^{+2.2} _{-1.7}	1 ⁺¹¹ ₋₁	0.026 ^{+0.002} _{-0.002}	0.064 ^{+0.005} _{-0.006}	35.8	2.6	D1
416 Vaticana	54.9±0.5	42.6 ^{+2.6} _{-0.8}	0 ⁺¹¹ ₋₀	0.025 ^{+0.001} _{-0.002}	0.063 ^{+0.003} _{-0.006}	35.8	1.9	D2
		77.1 ^{+5.8} _{-4.5}	33 ⁺²⁶ ₋₃₃	0.082 ^{+0.011} _{-0.011}	0.192 ^{+0.025} _{-0.025}	46.8	2.7	D1
		75.7 ^{+4.9} _{-3.0}	7 ⁺²⁸ ₋₇	0.086 ^{+0.006} _{-0.010}	0.201 ^{+0.014} _{-0.024}	16.5	1.5	R1
417 Suevia	54.9±0.5	48.2 ^{+1.1} _{-0.3}	1 ⁺²⁶ ₋₁	0.052 ^{+0.000} _{-0.002}	0.132 ^{+0.000} _{-0.005}	26.7	1.0	D1
		48.8 ^{+1.1} _{-0.0}	0 ⁺³⁰ ₋₀	0.051 ^{+0.000} _{-0.002}	0.129 ^{+0.000} _{-0.005}	26.7	1.2	D2
		47.6 ^{+0.6} _{-0.0}	0 ⁺¹⁹ ₋₀	0.053 ^{+0.000} _{-0.001}	0.134 ^{+0.000} _{-0.003}	26.7	0.8	R1
		45.4 ^{+0.6} _{-0.2}	1 ⁺²³ ₋₁	0.057 ^{+0.000} _{-0.002}	0.144 ^{+0.001} _{-0.004}	27.3	0.8	R2
423 Diotima*	175.9±3.9	154.3 ^{+9.9} _{-2.1}	1 ⁺¹² ₋₁	0.036 ^{+0.000} _{-0.004}	0.091 ^{+0.001} _{-0.010}	55.4	6.6	D1
		156.1 ^{+9.4} _{-0.0}	0 ⁺⁹ ₋₀	0.034 ^{+0.000} _{-0.003}	0.086 ^{+0.000} _{-0.008}	55.4	5.8	R1
		153.3 ^{+8.7} _{-0.0}	0 ⁺⁹ ₋₀	0.035 ^{+0.000} _{-0.003}	0.090 ^{+0.000} _{-0.008}	55.4	5.5	R2
436 Patricia	58.6±0.5	60.7 ^{+3.9} _{-4.4}	112 ⁺⁹⁰ ₋₇₁	0.017 ^{+0.003} _{-0.002}	0.044 ^{+0.007} _{-0.005}	55.4	5.3	D2
441 Bathilde*	65.5±2.4	66.5 ^{+2.1} _{-2.7}	35 ⁺²⁶ ₋₂₇	0.057 ^{+0.005} _{-0.004}	0.144 ^{+0.012} _{-0.010}	26.7	1.8	D1
		66.8 ^{+2.8} _{-2.7}	40 ⁺⁹⁴ ₋₂₆	0.055 ^{+0.005} _{-0.005}	0.140 ^{+0.012} _{-0.012}	26.7	2.4	D2
		66.3 ^{+2.5} _{-2.2}	28 ⁺³⁸ ₋₂₂	0.058 ^{+0.004} _{-0.004}	0.147 ^{+0.010} _{-0.011}	26.7	1.3	R1
		66.7 ^{+2.4} _{-2.6}	28 ⁺²⁷ ₋₂₅	0.057 ^{+0.005} _{-0.004}	0.145 ^{+0.012} _{-0.011}	26.7	1.7	R2
450 Brigitta	37.0±0.1	30.5 ^{+0.7} _{-0.8}	57 ⁺²⁰³ ₋₅₁	0.062 ^{+0.003} _{-0.003}	0.157 ^{+0.008} _{-0.007}	26.7	1.1	D1
		30.7 ^{+1.2} _{-1.1}	96 ⁺¹⁷⁵⁷ ₋₇₅	0.061 ^{+0.005} _{-0.005}	0.156 ^{+0.012} _{-0.012}	26.7	1.2	D2
		30.3 ^{+0.8} _{-0.9}	183 ⁺¹⁰⁶⁴ ₋₁₆₁	0.053 ^{+0.003} _{-0.003}	0.135 ^{+0.008} _{-0.007}	46.8	0.9	R1
468 Lina*	65.3±1.0	30.6 ^{+1.2} _{-0.8}	373 ⁺¹³⁶⁵ ₋₃₄₃	0.052 ^{+0.003} _{-0.004}	0.134 ^{+0.007} _{-0.010}	46.8	1.0	R2
		66.3 ^{+2.3} _{-3.0}	12 ⁺⁶⁵ ₋₁₂	0.017 ^{+0.002} _{-0.001}	0.044 ^{+0.004} _{-0.003}	35.8	2.9	D1
		65.7 ^{+2.6} _{-2.7}	6 ⁺⁶³ ₋₆	0.018 ^{+0.002} _{-0.001}	0.045 ^{+0.004} _{-0.003}	35.8	3.1	D2

Table 4 continued

Table 4 (continued)

Asteroid	D_{WISE}	D	Γ	A	pv	$\bar{\theta}$	χ^2_{red}	Model ID		
	(km)	(km)	($\text{J m}^{-2} \text{s}^{-0.5} \text{K}^{-1}$)			$^{\circ}$				
474 Prudentia*	41.0±1.4	61.8 ^{+2.8} _{-0.0}	0 ⁺²⁶ ₋₀	0.019 ^{+0.000} _{-0.001}	0.049 ^{+0.000} _{-0.003}	26.7	4.1	R1		
		63.0 ^{+3.2} _{-0.0}	0 ⁺³⁴ ₋₀	0.019 ^{+0.000} _{-0.002}	0.048 ^{+0.000} _{-0.004}	26.7	3.6	R2		
		36.8 ^{+0.6} _{-2.2}	1 ⁺⁷ ₋₁	0.020 ^{+0.003} _{-0.001}	0.050 ^{+0.007} _{-0.001}	12.6	5.2	D1		
		37.5 ^{+1.9} _{-2.6}	1 ⁺⁸ ₋₁	0.019 ^{+0.003} _{-0.002}	0.048 ^{+0.007} _{-0.004}	12.0	6.7	D2		
		34.3 ^{+2.4} _{-0.0}	0 ⁺³ ₋₀	0.028 ^{+0.000} _{-0.002}	0.071 ^{+0.000} _{-0.006}	26.7	4.7	R1		
478 Tergeste	80.7±1.0	38.1 ^{+1.0} _{-0.0}	0 ⁺⁴ ₋₀	0.022 ^{+0.000} _{-0.001}	0.057 ^{+0.000} _{-0.002}	26.7	7.0	R2		
		77.3 ^{+2.2} _{-1.1}	1 ⁺⁷ ₋₁	0.069 ^{+0.001} _{-0.003}	0.175 ^{+0.002} _{-0.009}	16.5	2.5	D1		
		76.1 ^{+2.1} _{-3.5}	25 ⁺⁹ ₋₂₅	0.073 ^{+0.007} _{-0.004}	0.186 ^{+0.018} _{-0.009}	26.7	1.6	D2		
482 Petrina	45.8±0.3	76.9 ^{+1.9} _{-1.1}	1 ⁺⁶ ₋₁	0.070 ^{+0.001} _{-0.003}	0.180 ^{+0.002} _{-0.008}	16.5	1.7	R1		
		44.3 ^{+1.6} _{-1.8}	29 ⁺²⁹ ₋₂₉	0.095 ^{+0.008} _{-0.007}	0.241 ^{+0.020} _{-0.017}	35.8	3.0	D1		
		43.3 ^{+2.8} _{-2.6}	6 ⁺⁷⁷ ₋₆	0.098 ^{+0.013} _{-0.012}	0.250 ^{+0.033} _{-0.030}	16.5	4.9	D2		
487 Venetia*	59.0±0.5	60.4 ^{+2.0} _{-2.0}	1 ⁺²³ ₋₁	0.095 ^{+0.006} _{-0.006}	0.241 ^{+0.015} _{-0.015}	35.8	2.0	D1		
		58.4 ^{+1.1} _{-2.2}	0 ⁺⁴ ₋₀	0.102 ^{+0.008} _{-0.001}	0.260 ^{+0.021} _{-0.003}	16.5	2.0	D2		
		61.7 ^{+1.6} _{-1.5}	23 ⁺¹⁶ ₋₁₅	0.095 ^{+0.005} _{-0.004}	0.241 ^{+0.012} _{-0.011}	26.7	2.1	R1		
495 Eulalia	37.3±0.1	58.9 ^{+2.2} _{-1.3}	82 ⁺³³ ₋₂₈	0.106 ^{+0.004} _{-0.007}	0.270 ^{+0.011} _{-0.019}	55.4	1.8	R2		
		31.6 ^{+1.2} _{-1.1}	73 ⁺²³⁶ ₋₇₃	0.028 ^{+0.002} _{-0.002}	0.071 ^{+0.005} _{-0.005}	26.7	1.2	D1		
		32.5 ^{+1.5} _{-1.1}	74 ⁺³²⁷ ₋₇₄	0.028 ^{+0.002} _{-0.002}	0.072 ^{+0.005} _{-0.006}	26.7	1.4	D2		
		32.7 ^{+0.4} _{-0.8}	0 ⁺¹² ₋₀	0.029 ^{+0.002} _{-0.001}	0.074 ^{+0.004} _{-0.001}	16.5	0.5	R1		
		32.3 ^{+0.5} _{-1.3}	0 ⁺¹⁵ ₋₀	0.029 ^{+0.003} _{-0.000}	0.075 ^{+0.006} _{-0.001}	16.5	0.7	R2		
497 Iva	40.9±0.3	38.2 ^{+0.6} _{-1.4}	100 ⁺²⁵ ₋₂₈	0.039 ^{+0.003} _{-0.001}	0.107 ^{+0.008} _{-0.003}	12.0	0.6	D1		
		37.0 ^{+0.5} _{-0.5}	75 ⁺²⁰ ₋₁₅	0.041 ^{+0.001} _{-0.001}	0.112 ^{+0.003} _{-0.003}	12.6	0.7	D2		
		38.7 ^{+1.9} _{-1.2}	94 ⁺⁵⁵ ₋₃₄	0.038 ^{+0.002} _{-0.003}	0.103 ^{+0.007} _{-0.009}	16.5	2.1	R1		
		39.4 ^{+2.1} _{-1.7}	97 ⁺¹¹⁷ ₋₃₆	0.036 ^{+0.003} _{-0.003}	0.098 ^{+0.009} _{-0.009}	16.5	2.1	R2		
		19.2 ^{+0.9} _{-0.8}	134 ⁺²⁹⁴ ₋₇₆	0.084 ^{+0.007} _{-0.008}	0.219 ^{+0.019} _{-0.020}	26.7	3.1	D1		
502 Sigune	15.8±1.2	19.7 ^{+0.7} _{-0.6}	109 ⁺⁶⁹ ₋₅₂	0.079 ^{+0.005} _{-0.005}	0.201 ^{+0.013} _{-0.013}	26.7	1.6	R1		
		18.6 ^{+0.6} _{-0.7}	133 ⁺⁷⁴ ₋₆₉	0.091 ^{+0.007} _{-0.005}	0.233 ^{+0.018} _{-0.014}	55.4	2.5	R2		
		28.3 ^{+2.0} _{-1.4}	19 ⁺³³ ₋₁₄	0.044 ^{+0.005} _{-0.006}	0.112 ^{+0.012} _{-0.014}	16.5	3.7	D1		
		27.9 ^{+1.2} _{-1.3}	22 ⁺³⁹ ₋₁₆	0.046 ^{+0.004} _{-0.004}	0.118 ^{+0.011} _{-0.010}	16.5	2.8	D2		
		25.7 ^{+2.9} _{-1.6}	0 ⁺⁶⁵ ₋₀	0.053 ^{+0.007} _{-0.010}	0.134 ^{+0.018} _{-0.025}	16.5	7.8	R1		
520 Franziska	25.2±0.2	27.7 ^{+1.9} _{-1.8}	37 ⁺³² ₋₂₇	0.045 ^{+0.007} _{-0.006}	0.115 ^{+0.017} _{-0.016}	26.7	6.0	R2		
		92.0±0.4	92.1 ^{+7.9} _{-5.2}	21 ⁺⁵² ₋₁₆	0.016 ^{+0.002} _{-0.003}	0.040 ^{+0.005} _{-0.007}	26.7	5.7	D1	
		94.1 ^{+7.7} _{-5.3}	70 ⁺⁴⁹ ₋₄₇	0.015 ^{+0.002} _{-0.002}	0.039 ^{+0.005} _{-0.005}	55.4	3.4	D2		
528 Rezia	92.0±0.4	14.0 ^{+0.8} _{-0.4}	24 ⁺⁴⁸ ₋₂₄	0.051 ^{+0.003} _{-0.005}	0.130 ^{+0.007} _{-0.014}	26.7	3.3	D1		
		14.3 ^{+0.4} _{-0.4}	35 ⁺²⁷ ₋₂₅	0.059 ^{+0.003} _{-0.003}	0.151 ^{+0.009} _{-0.008}	26.7	1.4	R1		
531 Zerlina	17.8±0.2	75.5 ^{+2.3} _{-2.7}	19 ⁺¹⁸ ₋₁₅	0.018 ^{+0.001} _{-0.001}	0.045 ^{+0.003} _{-0.003}	26.7	1.8	D1		
		72.6 ^{+2.1} _{-2.2}	12 ⁺¹⁷ ₋₁₂	0.020 ^{+0.001} _{-0.001}	0.050 ^{+0.003} _{-0.003}	26.7	2.1	D2		
538 Friederike	69.3±0.7	19.2±0.1	19.2 ^{+2.1} _{-0.4}	0 ⁺¹ ₋₀	0.082 ^{+0.003} _{-0.015}	0.208 ^{+0.009} _{-0.037}	12.6	4.0	D1	
		19.9 ^{+0.1} _{-0.4}	0 ⁺⁰ ₋₀	0.072 ^{+0.003} _{-0.000}	0.182 ^{+0.008} _{-0.000}	12.6	3.7	D2		
540 Rosamunde	19.2±0.1	544 Jetta	27.6±0.2	27.6 ^{+1.6} _{-1.2}	46 ⁺²² ₋₂₁	0.081 ^{+0.009} _{-0.008}	0.205 ^{+0.023} _{-0.021}	26.7	2.6	D1
		29.1 ^{+1.2} _{-1.0}	89 ⁺²⁷ ₋₂₉	0.076 ^{+0.005} _{-0.006}	0.194 ^{+0.012} _{-0.015}	55.4	1.2	D2		

Table 4 continued

Table 4 (continued)

Asteroid	D_{WISE}	D	Γ	A	pv	$\bar{\theta}$	χ^2_{red}	Model ID
	(km)	(km)	($\text{J m}^{-2} \text{s}^{-0.5} \text{K}^{-1}$)			°		
550 Senta	37.4±0.2	27.4 ^{+0.9} _{-1.4}	19 ⁺²⁸ ₋₁₅	0.094 ^{+0.011} _{-0.005}	0.239 ^{+0.027} _{-0.014}	16.5	2.0	R1
		28.2 ^{+1.5} _{-1.1}	10 ⁺³¹ ₋₉	0.088 ^{+0.007} _{-0.009}	0.223 ^{+0.018} _{-0.022}	16.5	2.1	R2
		39.3 ^{+1.3} _{-1.8}	36 ⁺⁶⁵ ₋₂₃	0.074 ^{+0.007} _{-0.005}	0.188 ^{+0.018} _{-0.014}	26.7	2.4	D1
		36.3 ^{+2.8} _{-0.0}	0 ⁺³² ₋₀	0.086 ^{+0.000} _{-0.011}	0.219 ^{+0.000} _{-0.029}	26.7	4.7	D2
		37.5 ^{+2.2} _{-0.0}	0 ⁺²³ ₋₀	0.081 ^{+0.000} _{-0.008}	0.206 ^{+0.000} _{-0.019}	26.7	3.1	R1
553 Kundry	9.0±0.1	39.5 ^{+1.6} _{-1.4}	22 ⁺²⁰ ₋₁₈	0.073 ^{+0.005} _{-0.006}	0.187 ^{+0.013} _{-0.014}	26.7	2.6	R2
		9.5 ^{+0.5} _{-0.4}	84 ⁺⁵⁸ ₋₅₈	0.088 ^{+0.007} _{-0.009}	0.225 ^{+0.017} _{-0.023}	26.7	2.1	D1
556 Phyllis	36.3±0.4	9.4 ^{+0.7} _{-0.6}	39 ⁺¹⁴¹ ₋₃₉	0.090 ^{+0.012} _{-0.013}	0.230 ^{+0.032} _{-0.032}	16.5	4.2	D2
		33.1 ^{+1.9} _{-0.9}	2 ⁺⁴⁸ ₋₂	0.087 ^{+0.007} _{-0.008}	0.222 ^{+0.017} _{-0.020}	16.5	2.7	D1
562 Salome	32.7±0.1	35.2 ^{+1.3} _{-1.4}	37 ⁺⁵³ ₋₁₇	0.080 ^{+0.006} _{-0.006}	0.202 ^{+0.015} _{-0.016}	26.7	2.0	D2
		33.6 ^{+0.7} _{-1.9}	1 ⁺²¹ ₋₁	0.086 ^{+0.009} _{-0.004}	0.219 ^{+0.024} _{-0.009}	16.5	3.2	R1
		32.8 ^{+0.9} _{-1.3}	1 ⁺¹² ₋₁	0.088 ^{+0.007} _{-0.004}	0.224 ^{+0.019} _{-0.011}	16.5	2.6	R2
		34.4 ^{+0.6} _{-1.4}	10 ⁺⁶ ₋₈	0.057 ^{+0.004} _{-0.003}	0.146 ^{+0.010} _{-0.006}	12.6	1.9	D1
567 Eleutheria*	80.0±2.5	34.4 ^{+1.6} _{-0.9}	10 ⁺¹¹ ₋₉	0.056 ^{+0.003} _{-0.005}	0.144 ^{+0.007} _{-0.013}	16.5	3.4	D2
		32.9 ^{+0.9} _{-0.0}	0 ⁺¹ ₋₀	0.060 ^{+0.000} _{-0.003}	0.153 ^{+0.000} _{-0.007}	16.5	3.9	R1
		32.8 ^{+1.7} _{-2.2}	21 ⁺¹⁹ ₋₁₉	0.061 ^{+0.009} _{-0.006}	0.156 ^{+0.022} _{-0.015}	26.7	5.8	R2
		86.9 ^{+3.1} _{-3.3}	22 ⁺¹³ ₋₁₃	0.018 ^{+0.002} _{-0.001}	0.047 ^{+0.004} _{-0.003}	55.4	2.8	D1
573 Recha	47.6±0.5	86.3 ^{+2.9} _{-4.1}	21 ⁺¹² ₋₁₆	0.019 ^{+0.002} _{-0.001}	0.048 ^{+0.005} _{-0.003}	55.4	3.6	D2
		87.4 ^{+3.6} _{-4.8}	21 ⁺¹⁵ ₋₂₁	0.018 ^{+0.002} _{-0.001}	0.046 ^{+0.005} _{-0.004}	55.4	3.7	R1
		83.1 ^{+5.4} _{-3.2}	8 ⁺¹⁸ ₋₈	0.020 ^{+0.001} _{-0.002}	0.052 ^{+0.003} _{-0.006}	55.4	3.7	R2
		43.8 ^{+1.3} _{-2.8}	43 ⁺⁵⁷ ₋₂₅	0.055 ^{+0.008} _{-0.003}	0.140 ^{+0.019} _{-0.009}	26.7	3.9	D1
590 Tomyris	30.6±0.2	44.1 ^{+1.6} _{-1.9}	49 ⁺¹⁰⁰ ₋₁₈	0.045 ^{+0.004} _{-0.003}	0.115 ^{+0.010} _{-0.007}	26.7	3.2	R1
		31.9 ^{+1.8} _{-1.9}	0 ⁺¹¹ ₋₀	0.065 ^{+0.009} _{-0.006}	0.167 ^{+0.022} _{-0.016}	16.5	9.0	D1
595 Polyxena*	90.6±1.4	32.7 ^{+1.8} _{-1.0}	3 ⁺¹¹ ₋₃	0.063 ^{+0.002} _{-0.008}	0.161 ^{+0.005} _{-0.020}	16.5	6.7	D2
		33.6 ^{+1.6} _{-1.2}	7 ⁺¹⁸ ₋₇	0.060 ^{+0.004} _{-0.005}	0.152 ^{+0.010} _{-0.013}	16.5	4.2	R1
		32.0 ^{+1.0} _{-0.0}	0 ⁺¹ ₋₀	0.064 ^{+0.000} _{-0.003}	0.163 ^{+0.000} _{-0.008}	16.5	3.0	R2
		89.5 ^{+3.5} _{-6.1}	0 ⁺⁶⁴ ₋₀	0.055 ^{+0.008} _{-0.004}	0.141 ^{+0.021} _{-0.009}	26.7	3.9	D1
596 Scheila*	118.0±6.0	89.1 ^{+1.9} _{-6.0}	0 ⁺²⁶ ₋₀	0.054 ^{+0.008} _{-0.002}	0.139 ^{+0.021} _{-0.005}	26.7	2.5	D2
		87.9 ^{+5.7} _{-3.8}	29 ⁺⁴⁹ ₋₂₉	0.053 ^{+0.005} _{-0.006}	0.135 ^{+0.012} _{-0.017}	55.4	2.9	R1
		89.8 ^{+2.6} _{-5.9}	1 ⁺⁶⁶ ₋₁	0.050 ^{+0.007} _{-0.003}	0.128 ^{+0.018} _{-0.007}	26.7	2.5	R2
		100.6 ^{+3.8} _{-2.2}	176 ⁺¹¹³⁴ ₋₁₅₆	0.018 ^{+0.001} _{-0.001}	0.045 ^{+0.002} _{-0.003}	55.4	1.7	D1
600 Musa	25.1±0.2	100.2 ^{+3.0} _{-2.4}	904 ⁺⁶¹⁰ ₋₈₂₄	0.017 ^{+0.001} _{-0.001}	0.043 ^{+0.002} _{-0.003}	55.4	1.7	D2
		25.2 ^{+1.4} _{-0.9}	9 ⁺³⁴ ₋₉	0.084 ^{+0.004} _{-0.009}	0.214 ^{+0.010} _{-0.022}	16.5	2.8	D1
608 Adolfine	20.4±0.1	26.7 ^{+0.6} _{-1.0}	48 ⁺¹⁶ ₋₂₁	0.072 ^{+0.007} _{-0.003}	0.184 ^{+0.017} _{-0.007}	26.7	1.9	D2
		24.6 ^{+1.5} _{-0.5}	0 ⁺³⁷ ₋₀	0.086 ^{+0.004} _{-0.007}	0.218 ^{+0.009} _{-0.019}	12.6	2.8	R1
		25.3 ^{+2.0} _{-1.2}	28 ⁺²⁷ ₋₂₈	0.082 ^{+0.008} _{-0.011}	0.209 ^{+0.021} _{-0.029}	26.7	2.9	R2
		21.7 ^{+1.4} _{-0.5}	0 ⁺¹⁴ ₋₀	0.055 ^{+0.003} _{-0.007}	0.145 ^{+0.008} _{-0.017}	12.6	2.1	D1
		20.9 ^{+0.9} _{-1.6}	1 ⁺¹⁸ ₋₁	0.063 ^{+0.010} _{-0.005}	0.161 ^{+0.025} _{-0.013}	16.5	4.3	D2
		22.9 ^{+1.5} _{-1.4}	0 ⁺¹⁷ ₋₀	0.067 ^{+0.009} _{-0.006}	0.170 ^{+0.023} _{-0.016}	3.9	7.9	R1
		22.9 ^{+3.0} _{-2.4}	17 ⁺⁶⁹ ₋₁₇	0.068 ^{+0.017} _{-0.015}	0.174 ^{+0.042} _{-0.037}	12.0	9.3	R2

Table 4 continued

Table 4 (continued)

Asteroid		D_{WISE}	D	Γ	A	pv	$\bar{\theta}$	χ^2_{red}	Model ID
		(km)	(km)	($\text{J m}^{-2} \text{s}^{-0.5} \text{K}^{-1}$)			°		
616	Elly	21.2±0.2	22.7 ^{+0.9} _{-1.2}	30 ⁺⁴⁶ ₋₂₂	0.068 ^{+0.008} _{-0.005}	0.174 ^{+0.020} _{-0.014}	12.0	1.9	D1
			22.6 ^{+1.2} _{-1.4}	0 ⁺³¹ ₋₀	0.067 ^{+0.010} _{-0.005}	0.170 ^{+0.026} _{-0.013}	3.9	3.6	D2
			23.1 ^{+1.8} _{-1.7}	0 ⁺⁶⁵ ₋₀	0.063 ^{+0.011} _{-0.009}	0.160 ^{+0.027} _{-0.022}	3.9	3.5	R1
			22.5 ^{+2.0} _{-1.4}	53 ⁺¹⁰² ₋₂₅	0.067 ^{+0.011} _{-0.010}	0.172 ^{+0.027} _{-0.025}	26.7	3.7	R2
624	Hektor	147.4±2.3	170.3 ^{+9.1} _{-2.9}	3 ⁺⁵ ₋₂	0.027 ^{+0.001} _{-0.003}	0.069 ^{+0.002} _{-0.007}	26.7	1.8	D1
			168.8 ^{+6.0} _{-2.3}	2 ⁺⁴ ₋₁	0.021 ^{+0.001} _{-0.001}	0.053 ^{+0.001} _{-0.003}	26.7	1.8	R1
			167.5 ^{+4.0} _{-3.2}	2 ⁺³ ₋₁	0.021 ^{+0.001} _{-0.001}	0.054 ^{+0.002} _{-0.002}	26.7	2.0	R2
628	Christine*	48.2±0.2	51.0 ^{+3.0} _{-3.6}	164 ⁺¹⁴¹ ₋₈₆	0.049 ^{+0.008} _{-0.005}	0.124 ^{+0.019} _{-0.013}	55.4	9.6	D2
631	Philippina	50.5±0.8	49.5 ^{+1.6} _{-0.9}	5 ⁺⁷ ₋₅	0.086 ^{+0.003} _{-0.005}	0.220 ^{+0.007} _{-0.013}	16.5	1.0	D1
			48.7 ^{+2.4} _{-1.2}	16 ⁺¹³ ₋₁₆	0.088 ^{+0.004} _{-0.008}	0.224 ^{+0.011} _{-0.021}	26.7	1.3	R1
			46.8 ^{+1.3} _{-1.0}	20 ⁺¹³ ₋₈	0.096 ^{+0.004} _{-0.005}	0.243 ^{+0.011} _{-0.012}	26.7	1.3	R2
632	Pyrrha	14.4±0.2	14.9 ^{+1.8} _{-1.5}	150 ⁺³³⁷ ₋₁₁₀	0.076 ^{+0.018} _{-0.016}	0.193 ^{+0.045} _{-0.040}	27.3	5.2	D1
			15.7 ^{+1.6} _{-1.7}	256 ⁺³⁹³ ₋₂₀₈	0.067 ^{+0.017} _{-0.012}	0.171 ^{+0.043} _{-0.032}	46.8	4.3	D2
639	Latona*	78.5±1.2	68.7 ^{+4.7} _{-2.7}	0 ⁺⁵⁰ ₋₀	0.068 ^{+0.006} _{-0.008}	0.172 ^{+0.015} _{-0.021}	46.8	3.5	D1
644	Cosima	17.0±0.2	72.0 ^{+3.2} _{-2.8}	0 ⁺¹⁵ ₋₀	0.062 ^{+0.005} _{-0.003}	0.159 ^{+0.013} _{-0.007}	35.8	3.8	D2
			19.2 ^{+1.3} _{-1.4}	32 ⁺⁵⁰ ₋₁₃	0.061 ^{+0.010} _{-0.008}	0.155 ^{+0.024} _{-0.021}	16.5	4.1	D1
			19.4 ^{+1.2} _{-1.3}	56 ⁺⁴³ ₋₂₈	0.059 ^{+0.010} _{-0.006}	0.150 ^{+0.025} _{-0.016}	27.3	3.4	D2
			18.8 ^{+1.0} _{-0.8}	41 ⁺²⁰ ₋₁₇	0.063 ^{+0.006} _{-0.007}	0.160 ^{+0.014} _{-0.017}	26.7	4.1	R1
653	Berenike	49.8±0.4	18.8 ^{+1.1} _{-0.7}	42 ⁺²⁴ ₋₁₆	0.063 ^{+0.005} _{-0.008}	0.161 ^{+0.013} _{-0.020}	26.7	3.4	R2
			46.2 ^{+2.6} _{-1.6}	26 ⁺⁶⁴ ₋₂₆	0.058 ^{+0.004} _{-0.006}	0.147 ^{+0.010} _{-0.015}	26.7	3.7	D1
			49.1 ^{+1.9} _{-2.2}	41 ⁺⁶⁴ ₋₃₅	0.052 ^{+0.005} _{-0.004}	0.133 ^{+0.013} _{-0.010}	26.7	1.8	D2
			48.9 ^{+1.6} _{-1.5}	80 ⁺⁴³ ₋₂₈	0.057 ^{+0.004} _{-0.004}	0.144 ^{+0.009} _{-0.009}	55.4	1.4	R1
660	Crescentia*	42.3±0.4	41.6 ^{+1.1} _{-1.0}	1239 ⁺⁴¹² ₋₅₆₆	0.080 ^{+0.004} _{-0.004}	0.203 ^{+0.011} _{-0.011}	55.4	3.3	D2
673	Edda	37.6±0.4	37.5 ^{+0.5} _{-0.3}	1 ⁺⁴ ₋₁	0.038 ^{+0.000} _{-0.001}	0.097 ^{+0.001} _{-0.002}	16.5	0.9	D1
			36.5 ^{+1.3} _{-1.1}	10 ⁺¹⁴ ₋₁₀	0.039 ^{+0.002} _{-0.003}	0.100 ^{+0.006} _{-0.007}	26.7	1.2	D2
			36.4 ^{+2.4} _{-0.4}	2 ⁺²³ ₋₂	0.039 ^{+0.001} _{-0.004}	0.100 ^{+0.001} _{-0.011}	26.7	1.5	R1
			37.6 ^{+1.7} _{-0.4}	2 ⁺¹⁹ ₋₂	0.036 ^{+0.001} _{-0.003}	0.091 ^{+0.001} _{-0.008}	26.7	1.4	R2
679	Pax	63.0±0.4	58.5 ^{+2.1} _{-2.1}	10 ⁺⁹⁹ ₋₁₀	0.049 ^{+0.004} _{-0.003}	0.124 ^{+0.009} _{-0.008}	46.8	1.7	D1
			55.3 ^{+2.1} _{-0.7}	52 ⁺³²⁷ ₋₅₂	0.054 ^{+0.001} _{-0.004}	0.137 ^{+0.003} _{-0.009}	46.8	1.1	D2
687	TINETTE	21.5±0.5	22.4 ^{+1.2} _{-1.6}	36 ⁺¹⁸ ₋₁₈	0.026 ^{+0.004} _{-0.003}	0.067 ^{+0.010} _{-0.008}	26.7	3.1	D1
			21.5 ^{+2.1} _{-1.0}	9 ⁺⁴⁵ ₋₉	0.029 ^{+0.002} _{-0.005}	0.073 ^{+0.006} _{-0.012}	16.5	2.8	D2
692	Hippodamia	42.8±0.6	41.6 ^{+1.5} _{-0.0}	0 ⁺⁴ ₋₀	0.077 ^{+0.000} _{-0.005}	0.196 ^{+0.000} _{-0.012}	16.5	2.0	D1
699	Hela	42.8±0.6	12.8 ^{+0.6} _{-2.0}	74 ⁺⁷³ ₋₆₁	0.076 ^{+0.030} _{-0.007}	0.194 ^{+0.076} _{-0.017}	35.8	2.1	D2
			12.3 ^{+1.5} _{-1.2}	9 ⁺⁵⁷ ₋₉	0.086 ^{+0.017} _{-0.017}	0.218 ^{+0.044} _{-0.043}	12.6	1.7	R1
			12.9 ^{+0.5} _{-1.4}	85 ⁺⁸² ₋₅₈	0.076 ^{+0.020} _{-0.005}	0.193 ^{+0.051} _{-0.013}	35.8	1.6	R2
725	Amanda	23.7±0.2	25.2 ^{+1.2} _{-1.4}	19 ⁺¹⁵ ₋₁₉	0.019 ^{+0.002} _{-0.002}	0.048 ^{+0.005} _{-0.004}	3.9	3.9	D1
			24.7 ^{+0.8} _{-0.9}	41 ⁺¹¹ ₋₂₄	0.020 ^{+0.001} _{-0.001}	0.051 ^{+0.004} _{-0.003}	35.8	1.5	D2
			21.9 ^{+0.4} _{-0.4}	0 ⁺⁵ ₋₀	0.024 ^{+0.001} _{-0.000}	0.061 ^{+0.002} _{-0.001}	12.6	4.1	R2
731	Sorga	34.6±0.4	37.2 ^{+2.4} _{-4.3}	34 ⁺¹⁹ ₋₃₄	0.065 ^{+0.017} _{-0.009}	0.166 ^{+0.044} _{-0.023}	16.5	5.2	D1
			37.5 ^{+1.8} _{-2.4}	36 ⁺²⁶ ₋₁₁	0.064 ^{+0.009} _{-0.007}	0.162 ^{+0.023} _{-0.017}	16.5	2.5	D2

Table 4 continued

Table 4 (continued)

Asteroid	D_{WISE}	D	Γ	A	pv	$\bar{\theta}$	χ^2_{red}	Model ID
	(km)	(km)	($\text{J m}^{-2} \text{s}^{-0.5} \text{K}^{-1}$)			°		
742 Edisona	47.1±0.4	41.1 ^{+2.6} _{-3.1}	172 ⁺¹⁵⁰ ₋₈₀	0.053 ^{+0.009} _{-0.006}	0.134 ^{+0.022} _{-0.016}	55.4	6.7	R1
		34.3 ^{+5.8} _{-1.7}	8 ⁺⁵⁹ ₋₈	0.077 ^{+0.007} _{-0.022}	0.197 ^{+0.017} _{-0.055}	16.5	5.8	R2
		41.3 ^{+1.6} _{-2.1}	12 ⁺⁴⁷ ₋₁₂	0.055 ^{+0.006} _{-0.004}	0.139 ^{+0.015} _{-0.010}	12.0	2.8	D1
		41.2 ^{+1.7} _{-2.2}	40 ⁺⁶² ₋₃₆	0.054 ^{+0.006} _{-0.004}	0.137 ^{+0.015} _{-0.011}	16.5	2.9	D2
		39.7 ^{+1.2} _{-0.0}	0 ⁺¹³ ₋₀	0.059 ^{+0.000} _{-0.003}	0.150 ^{+0.000} _{-0.007}	16.5	2.4	R1
746 Marlu	74.3±1.1	40.0 ^{+0.6} _{-1.7}	0 ⁺²¹ ₋₀	0.057 ^{+0.005} _{-0.001}	0.146 ^{+0.013} _{-0.002}	16.5	3.4	R2
		75.1 ^{+2.4} _{-4.9}	77 ⁺⁴⁵ ₋₄₄	0.011 ^{+0.002} _{-0.001}	0.028 ^{+0.004} _{-0.002}	55.4	2.9	D1
749 Malzovia	11.1±0.1	72.0 ^{+4.7} _{-3.9}	81 ⁺⁷⁶ ₋₈₀	0.012 ^{+0.001} _{-0.001}	0.031 ^{+0.004} _{-0.004}	55.4	4.2	D2
		12.5 ^{+0.6} _{-0.6}	55 ⁺⁴⁴ ₋₃₅	0.077 ^{+0.007} _{-0.007}	0.197 ^{+0.019} _{-0.017}	35.8	2.7	D1
756 Lilliana	64.8±0.5	12.6 ^{+0.6} _{-0.5}	64 ⁺³³ ₋₃₄	0.076 ^{+0.007} _{-0.007}	0.195 ^{+0.019} _{-0.019}	27.3	2.4	D2
		11.9 ^{+0.8} _{-0.6}	1 ⁺⁴⁰ ₋₁	0.084 ^{+0.007} _{-0.009}	0.213 ^{+0.018} _{-0.024}	12.6	3.6	R1
		11.9 ^{+1.2} _{-0.8}	0 ⁺¹⁷ ₋₀	0.084 ^{+0.013} _{-0.014}	0.214 ^{+0.032} _{-0.035}	3.9	3.4	R2
		61.3 ^{+2.0} _{-1.4}	6 ⁺¹⁰ ₋₅	0.019 ^{+0.001} _{-0.001}	0.048 ^{+0.002} _{-0.003}	26.7	1.2	D1
757 Portlandia	32.9±0.2	59.6 ^{+3.6} _{-0.9}	4 ⁺¹² ₋₄	0.020 ^{+0.000} _{-0.002}	0.050 ^{+0.001} _{-0.006}	26.7	3.4	D2
		59.0 ^{+1.9} _{-0.0}	0 ⁺¹² ₋₀	0.026 ^{+0.000} _{-0.001}	0.065 ^{+0.000} _{-0.003}	26.7	2.2	R1
		59.0 ^{+0.6} _{-0.0}	0 ⁺¹ ₋₀	0.026 ^{+0.000} _{-0.000}	0.065 ^{+0.000} _{-0.000}	26.7	2.4	R2
		33.7 ^{+0.9} _{-1.1}	36 ⁺³⁸ ₋₁₀	0.047 ^{+0.003} _{-0.003}	0.119 ^{+0.007} _{-0.007}	26.7	1.2	D1
758 Mancunia	89.0±0.6	33.2 ^{+1.1} _{-1.5}	28 ⁺¹⁴ ₋₁₁	0.048 ^{+0.004} _{-0.003}	0.123 ^{+0.009} _{-0.008}	26.7	1.8	D2
		32.3 ^{+1.8} _{-0.4}	1 ⁺¹² ₋₁	0.049 ^{+0.000} _{-0.005}	0.125 ^{+0.001} _{-0.012}	26.7	5.0	R1
		29.5 ^{+1.4} _{-0.0}	0 ⁺⁸ ₋₀	0.059 ^{+0.000} _{-0.005}	0.150 ^{+0.000} _{-0.013}	26.7	5.0	R2
		89.7 ^{+5.7} _{-4.2}	94 ⁺⁹⁰ ₋₈₈	0.045 ^{+0.005} _{-0.005}	0.115 ^{+0.012} _{-0.013}	55.4	2.6	D1
771 Libera	29.3±0.2	92.4 ^{+4.6} _{-5.2}	43 ⁺⁶⁴ ₋₄₃	0.043 ^{+0.005} _{-0.004}	0.110 ^{+0.013} _{-0.011}	46.8	2.5	D2
		30.8 ^{+1.0} _{-1.9}	74 ⁺²² ₋₃₉	0.043 ^{+0.006} _{-0.003}	0.109 ^{+0.014} _{-0.008}	35.8	2.7	D1
775 Lumiere	32.0±0.1	29.3 ^{+1.8} _{-1.8}	72 ⁺³⁰ ₋₂₅	0.047 ^{+0.006} _{-0.005}	0.120 ^{+0.015} _{-0.014}	27.3	4.0	R1
		32.4 ^{+1.4} _{-1.1}	49 ⁺²⁶ ₋₂₂	0.047 ^{+0.004} _{-0.004}	0.119 ^{+0.010} _{-0.009}	26.7	1.4	D1
776 Berbericia*	151.7±0.9	32.0 ^{+1.2} _{-1.3}	66 ⁺⁶⁰ ₋₂₆	0.048 ^{+0.004} _{-0.003}	0.121 ^{+0.011} _{-0.009}	26.7	1.7	D2
		134.0 ^{+4.1} _{-0.6}	1 ⁺¹⁹ ₋₁	0.041 ^{+0.000} _{-0.002}	0.079 ^{+0.000} _{-0.004}	55.4	5.5	D1
787 Moskva	32.0±0.8	136.0 ^{+5.2} _{-0.0}	0 ⁺¹³ ₋₀	0.040 ^{+0.000} _{-0.002}	0.076 ^{+0.000} _{-0.005}	55.4	4.7	R2
		30.7 ^{+1.5} _{-1.0}	33 ⁺²⁵ ₋₁₅	0.087 ^{+0.006} _{-0.008}	0.222 ^{+0.014} _{-0.020}	27.3	1.6	D1
		29.7 ^{+1.4} _{-1.1}	57 ⁺²⁶ ₋₃₅	0.093 ^{+0.008} _{-0.008}	0.237 ^{+0.020} _{-0.020}	35.8	2.0	D2
792 Metcalfia*	61.8±0.4	30.9 ^{+1.2} _{-0.9}	29 ⁺¹⁷ ₋₁₁	0.069 ^{+0.004} _{-0.006}	0.177 ^{+0.009} _{-0.015}	26.7	2.5	R1
		53.4 ^{+2.1} _{-2.0}	4 ⁺¹¹¹ ₋₄	0.017 ^{+0.001} _{-0.001}	0.042 ^{+0.003} _{-0.003}	46.8	1.4	D1
		53.7 ^{+2.2} _{-1.6}	3 ⁺⁵⁶ ₋₃	0.016 ^{+0.001} _{-0.001}	0.041 ^{+0.002} _{-0.003}	46.8	1.2	D2
		53.3 ^{+1.8} _{-1.7}	0 ⁺³³ ₋₀	0.016 ^{+0.001} _{-0.001}	0.042 ^{+0.003} _{-0.002}	46.8	1.1	R1
798 Ruth	30.9±0.2	52.6 ^{+2.0} _{-1.7}	0 ⁺²⁴ ₋₀	0.017 ^{+0.001} _{-0.001}	0.042 ^{+0.003} _{-0.003}	46.8	1.2	R2
		43.4 ^{+1.9} _{-1.7}	118 ⁺⁶² ₋₄₀	0.049 ^{+0.004} _{-0.004}	0.126 ^{+0.011} _{-0.009}	55.4	1.9	D1
		41.6 ^{+1.7} _{-1.8}	27 ⁺¹¹ ₋₂₇	0.062 ^{+0.005} _{-0.005}	0.152 ^{+0.012} _{-0.012}	26.7	1.5	R1
802 Epyaxa	7.4±0.2	42.6 ^{+1.3} _{-2.5}	16 ⁺²¹ ₋₁₆	0.059 ^{+0.007} _{-0.003}	0.149 ^{+0.018} _{-0.008}	16.5	1.4	R2
		8.1 ^{+0.7} _{-1.4}	61 ⁺¹⁹⁴ ₋₃₇	0.072 ^{+0.031} _{-0.012}	0.184 ^{+0.078} _{-0.030}	16.5	3.3	D1
808 Merxia	30.9±0.2	30.0 ^{+1.6} _{-1.2}	138 ⁺⁸¹ ₋₆₆	0.080 ^{+0.007} _{-0.007}	0.202 ^{+0.018} _{-0.018}	55.4	2.8	D1

Table 4 continued

Table 4 (continued)

Asteroid	D_{WISE}	D	Γ	A	pv	$\bar{\theta}$	χ^2_{red}	Model ID
	(km)	(km)	($\text{J m}^{-2} \text{s}^{-0.5} \text{K}^{-1}$)			$^{\circ}$		
812 Adele	12.4±0.1	30.5 ^{+1.3} _{-1.0}	148 ⁺⁶⁸ ₋₄₄	0.078 ^{+0.005} _{-0.006}	0.198 ^{+0.013} _{-0.015}	55.4	2.5	D2
		30.0 ^{+1.6} _{-0.0}	0 ⁺³⁷ ₋₀	0.088 ^{+0.000} _{-0.008}	0.224 ^{+0.000} _{-0.020}	26.7	2.6	R1
		29.8 ^{+1.0} _{-1.1}	31 ⁺²⁵ ₋₃₁	0.089 ^{+0.006} _{-0.006}	0.227 ^{+0.017} _{-0.016}	26.7	3.0	R2
		13.4 ^{+0.6} _{-1.1}	73 ⁺¹²⁰ ₋₄₅	0.066 ^{+0.012} _{-0.006}	0.167 ^{+0.030} _{-0.016}	16.5	4.4	D1
		13.2 ^{+0.9} _{-0.9}	32 ⁺²²⁰ ₋₂₇	0.067 ^{+0.011} _{-0.009}	0.172 ^{+0.027} _{-0.023}	16.5	3.8	D2
816 Juliana	50.7±0.2	13.2 ^{+0.7} _{-0.5}	36 ⁺⁸⁴ ₋₁₄	0.089 ^{+0.006} _{-0.010}	0.227 ^{+0.016} _{-0.025}	16.5	2.3	R1
		13.4 ^{+0.6} _{-0.7}	37 ⁺⁷³ ₋₁₆	0.086 ^{+0.009} _{-0.008}	0.219 ^{+0.024} _{-0.020}	16.5	2.2	R2
		49.5 ^{+1.2} _{-2.8}	17 ⁺³² ₋₁₄	0.017 ^{+0.002} _{-0.001}	0.044 ^{+0.005} _{-0.002}	26.7	2.4	D1
832 Karin	15.8±0.1	48.8 ^{+1.8} _{-1.1}	39 ⁺²⁷ ₋₁₃	0.018 ^{+0.001} _{-0.001}	0.046 ^{+0.002} _{-0.003}	55.4	1.8	D2
		16.1 ^{+1.6} _{-1.3}	312 ⁺⁴⁴² ₋₁₇₆	0.082 ^{+0.015} _{-0.013}	0.209 ^{+0.037} _{-0.034}	46.8	5.8	D1
834 Burnhamia	61.3±0.3	16.6 ^{+0.7} _{-1.7}	175 ⁺¹⁶⁶ ₋₁₂₇	0.076 ^{+0.018} _{-0.006}	0.195 ^{+0.046} _{-0.016}	35.8	3.6	D2
		15.5 ^{+0.9} _{-0.6}	33 ⁺⁶⁹ ₋₂₂	0.087 ^{+0.007} _{-0.010}	0.222 ^{+0.018} _{-0.025}	16.5	2.1	R1
		16.4 ^{+0.8} _{-0.9}	41 ⁺⁴⁷ ₋₂₆	0.077 ^{+0.008} _{-0.007}	0.196 ^{+0.021} _{-0.019}	16.5	2.2	R2
		65.5 ^{+3.1} _{-4.1}	26 ⁺³⁵ ₋₂₆	0.027 ^{+0.004} _{-0.002}	0.069 ^{+0.009} _{-0.006}	26.7	3.5	D1
		63.5 ^{+4.8} _{-3.2}	15 ⁺⁴³ ₋₁₅	0.028 ^{+0.003} _{-0.004}	0.072 ^{+0.007} _{-0.010}	26.7	3.5	D2
849 Ara*	80.8±1.1	63.4 ^{+2.1} _{-2.4}	4 ⁺²⁸ ₋₄	0.029 ^{+0.002} _{-0.002}	0.074 ^{+0.006} _{-0.004}	16.5	1.4	R1
		64.7 ^{+2.7} _{-2.3}	19 ⁺¹⁴ ₋₁₉	0.027 ^{+0.002} _{-0.002}	0.070 ^{+0.005} _{-0.005}	26.7	1.4	R2
		72.1 ^{+1.4} _{-1.8}	24 ⁺¹² ₋₁₂	0.070 ^{+0.004} _{-0.003}	0.179 ^{+0.009} _{-0.007}	26.7	1.0	D1
852 Wladilena	26.5±0.2	72.1 ^{+1.7} _{-2.3}	23 ⁺¹⁶ ₋₁₇	0.071 ^{+0.004} _{-0.003}	0.181 ^{+0.011} _{-0.008}	26.7	1.1	R1
		26.8 ^{+1.3} _{-1.6}	24 ⁺⁹⁶ ₋₂₄	0.091 ^{+0.012} _{-0.009}	0.232 ^{+0.030} _{-0.024}	16.5	3.2	D1
		26.4 ^{+0.8} _{-1.1}	15 ⁺³⁰ ₋₁₄	0.093 ^{+0.008} _{-0.005}	0.238 ^{+0.021} _{-0.013}	16.5	1.7	D2
		26.5 ^{+0.7} _{-0.9}	16 ⁺²⁵ ₋₁₂	0.102 ^{+0.007} _{-0.005}	0.260 ^{+0.018} _{-0.012}	16.5	1.1	R1
857 Glasenappia	13.6±0.6	26.7 ^{+1.3} _{-1.4}	23 ⁺⁷⁰ ₋₂₃	0.101 ^{+0.011} _{-0.010}	0.257 ^{+0.029} _{-0.025}	16.5	2.5	R2
		12.1 ^{+0.3} _{-0.7}	15 ⁺⁵⁷ ₋₁₅	0.116 ^{+0.015} _{-0.005}	0.295 ^{+0.038} _{-0.014}	16.5	3.5	D1
		12.0 ^{+0.2} _{-0.2}	36 ⁺²⁸ ₋₂₅	0.115 ^{+0.004} _{-0.004}	0.292 ^{+0.010} _{-0.011}	26.7	1.8	D2
		12.6 ^{+0.3} _{-0.3}	13 ⁺¹⁷ ₋₁₂	0.107 ^{+0.004} _{-0.005}	0.273 ^{+0.010} _{-0.012}	16.5	1.3	R1
		12.3 ^{+0.3} _{-0.4}	14 ⁺³⁸ ₋₁₄	0.108 ^{+0.007} _{-0.004}	0.276 ^{+0.018} _{-0.011}	16.5	2.0	R2
872 Holda	34.4±0.3	31.4 ^{+0.5} _{-0.7}	51 ⁺⁵⁵ ₋₃₂	0.070 ^{+0.003} _{-0.002}	0.177 ^{+0.008} _{-0.005}	26.7	0.7	D1
		30.9 ^{+1.7} _{-0.6}	12 ⁺²³ ₋₁₂	0.071 ^{+0.003} _{-0.007}	0.182 ^{+0.006} _{-0.018}	26.7	1.0	D2
873 Mechthild	34.5±0.1	33.1 ^{+1.3} _{-1.9}	62 ⁺⁵⁰ ₋₃₁	0.015 ^{+0.002} _{-0.001}	0.037 ^{+0.005} _{-0.003}	26.7	3.7	D1
		34.7 ^{+1.6} _{-1.5}	119 ⁺⁴³ ₋₄₀	0.013 ^{+0.001} _{-0.001}	0.034 ^{+0.004} _{-0.002}	55.4	3.8	D2
874 Rotraut	58.3±0.2	53.4 ^{+1.8} _{-1.6}	21 ⁺²⁵ ₋₁₈	0.020 ^{+0.001} _{-0.001}	0.051 ^{+0.003} _{-0.003}	26.7	1.1	D1
		54.0 ^{+1.9} _{-2.4}	22 ⁺¹⁹ ₋₂₂	0.020 ^{+0.002} _{-0.001}	0.050 ^{+0.004} _{-0.003}	26.7	3.0	D2
		54.1 ^{+1.9} _{-1.6}	97 ⁺⁵⁸ ₋₃₇	0.022 ^{+0.002} _{-0.001}	0.056 ^{+0.004} _{-0.003}	55.4	0.9	R1
		52.6 ^{+2.4} _{-1.8}	66 ⁺⁵¹ ₋₆₁	0.023 ^{+0.002} _{-0.002}	0.055 ^{+0.005} _{-0.005}	55.4	1.8	R2
875 Nymphe	14.1±0.3	16.2 ^{+1.2} _{-1.6}	168 ⁺²⁸⁹ ₋₁₁₉	0.075 ^{+0.017} _{-0.010}	0.190 ^{+0.042} _{-0.026}	27.3	4.5	D1
		17.1 ^{+1.6} _{-1.9}	312 ⁺⁴⁵⁴ ₋₂₆₃	0.068 ^{+0.018} _{-0.011}	0.174 ^{+0.045} _{-0.028}	55.4	6.0	D2
890 Waltraut	28.4±0.2	28.3 ^{+3.0} _{-0.0}	0 ⁺³⁸ ₋₀	0.036 ^{+0.000} _{-0.006}	0.091 ^{+0.000} _{-0.015}	26.7	9.1	D1
		30.0 ^{+2.4} _{-2.1}	30 ⁺⁹⁵ ₋₃₀	0.033 ^{+0.005} _{-0.005}	0.084 ^{+0.012} _{-0.013}	26.7	4.2	D2
898 Hildegard	11.7±0.2	12.1 ^{+1.4} _{-1.4}	5 ⁺³⁷ ₋₅	0.100 ^{+0.028} _{-0.019}	0.254 ^{+0.070} _{-0.048}	12.6	5.2	D1

Table 4 continued

Table 4 (continued)

Asteroid		D_{WISE}	D	Γ	A	pv	$\bar{\theta}$	χ^2_{red}	Model ID
		(km)	(km)	($\text{J m}^{-2} \text{s}^{-0.5} \text{K}^{-1}$)			°		
908	Buda	30.7±0.5	11.7 ^{+1.6} _{-1.2}	4 ⁺⁴⁴ ₋₄	0.107 ^{+0.025} _{-0.024}	0.273 ^{+0.063} _{-0.060}	16.5	5.5	D2
			25.6 ^{+0.6} _{-1.0}	1 ⁺⁴⁸ ₋₁	0.051 ^{+0.004} _{-0.003}	0.131 ^{+0.010} _{-0.006}	35.8	1.2	D1
			24.6 ^{+1.7} _{-0.6}	0 ⁺³⁶ ₋₀	0.056 ^{+0.003} _{-0.007}	0.142 ^{+0.007} _{-0.017}	26.7	3.4	D2
918	Itha	21.6±0.1	23.0 ^{+1.0} _{-0.8}	17 ⁺⁹ ₋₈	0.070 ^{+0.005} _{-0.006}	0.177 ^{+0.012} _{-0.015}	16.5	2.1	D1
951	Gaspra	13.2±0.1	12.3 ^{+0.4} _{-0.2}	698 ⁺⁵⁷⁵ ₋₅₂₁	0.109 ^{+0.003} _{-0.007}	0.278 ^{+0.008} _{-0.018}	26.7	0.8	D1
			12.7 ^{+0.2} _{-0.2}	661 ⁺⁵¹⁹ ₋₄₁₁	0.104 ^{+0.004} _{-0.004}	0.264 ^{+0.010} _{-0.010}	35.8	0.6	D2
			12.6 ^{+0.2} _{-0.2}	610 ⁺⁵⁵¹ ₋₄₀₇	0.105 ^{+0.004} _{-0.004}	0.267 ^{+0.010} _{-0.010}	35.8	0.7	R1
			12.3 ^{+0.2} _{-0.2}	798 ⁺⁴⁵³ ₋₅₀₈	0.109 ^{+0.004} _{-0.005}	0.278 ^{+0.011} _{-0.012}	35.8	0.5	R2
958	Asplinda	45.1±0.4	46.0 ^{+3.6} _{-0.0}	0 ⁺¹⁵ ₋₀	0.015 ^{+0.000} _{-0.002}	0.038 ^{+0.000} _{-0.005}	26.7	4.1	D2
			45.1 ^{+1.4} _{-0.0}	0 ⁺⁶ ₋₀	0.015 ^{+0.000} _{-0.001}	0.037 ^{+0.000} _{-0.002}	26.7	8.8	R1
			44.5 ^{+1.2} _{-0.0}	0 ⁺⁵ ₋₀	0.015 ^{+0.000} _{-0.001}	0.037 ^{+0.000} _{-0.001}	26.7	8.3	R2
984	Gretia	32.0±0.6	33.8 ^{+1.3} _{-2.2}	4 ⁺⁷ ₋₄	0.131 ^{+0.005} _{-0.009}	0.333 ^{+0.013} _{-0.024}	16.5	4.2	D1
			34.5 ^{+2.7} _{-1.4}	24 ⁺⁷³ ₋₁₀	0.127 ^{+0.010} _{-0.019}	0.324 ^{+0.026} _{-0.048}	26.7	5.4	R1
986	Amelia	48.7±0.2	47.9 ^{+1.8} _{-1.1}	5 ⁺³¹ ₋₅	0.048 ^{+0.002} _{-0.003}	0.123 ^{+0.006} _{-0.009}	16.5	1.5	D1
			46.4 ^{+1.7} _{-0.0}	0 ⁺¹⁶ ₋₀	0.050 ^{+0.000} _{-0.003}	0.127 ^{+0.000} _{-0.008}	16.5	1.5	D2
			46.9 ^{+2.3} _{-1.5}	23 ⁺²⁴ ₋₂₃	0.051 ^{+0.003} _{-0.004}	0.129 ^{+0.008} _{-0.011}	26.7	1.8	R1
			47.9 ^{+1.2} _{-0.9}	6 ⁺¹⁰ ₋₆	0.049 ^{+0.001} _{-0.002}	0.124 ^{+0.003} _{-0.006}	16.5	0.8	R2
1010	Marlene	46.9±0.2	43.3 ^{+1.3} _{-1.5}	217 ⁺¹⁸⁵ ₋₁₀₀	0.017 ^{+0.001} _{-0.001}	0.044 ^{+0.003} _{-0.003}	55.4	3.3	D1
			41.9 ^{+1.1} _{-1.5}	151 ⁺¹²² ₋₇₉	0.019 ^{+0.001} _{-0.001}	0.047 ^{+0.003} _{-0.003}	55.4	2.6	D2
1021	Flammario*	100.8±1.6	93.7 ^{+3.3} _{-5.8}	40 ⁺²⁰ ₋₃₀	0.019 ^{+0.003} _{-0.002}	0.049 ^{+0.006} _{-0.004}	55.4	2.5	D1
			91.2 ^{+2.5} _{-2.3}	0 ⁺⁹ ₋₀	0.020 ^{+0.001} _{-0.001}	0.051 ^{+0.003} _{-0.002}	26.7	2.4	D2
1036	Ganymed	37.7±0.4	35.2 ^{+1.9} _{-1.4}	32 ⁺²² ₋₁₃	0.110 ^{+0.009} _{-0.012}	0.223 ^{+0.018} _{-0.025}	26.7	1.7	D1
			35.6 ^{+1.6} _{-1.5}	35 ⁺¹⁹ ₋₁₄	0.107 ^{+0.009} _{-0.010}	0.217 ^{+0.018} _{-0.021}	26.7	1.6	R1
1080	Orchis	22.9±0.2	21.1 ^{+0.5} _{-0.9}	1 ⁺⁶² ₋₁	0.019 ^{+0.002} _{-0.001}	0.049 ^{+0.004} _{-0.002}	3.9	3.2	D1
			21.1 ^{+0.8} _{-0.9}	24 ⁺⁴³ ₋₂₄	0.019 ^{+0.002} _{-0.001}	0.049 ^{+0.005} _{-0.003}	12.6	4.0	D2
1095	Tulipa	27.9±0.4	30.1 ^{+1.7} _{-2.1}	64 ⁺¹⁹⁷ ₋₂₇	0.049 ^{+0.007} _{-0.005}	0.126 ^{+0.019} _{-0.013}	27.3	4.6	D1
			29.3 ^{+1.4} _{-1.3}	46 ⁺⁸⁸ ₋₁₄	0.052 ^{+0.006} _{-0.004}	0.132 ^{+0.015} _{-0.011}	27.3	2.3	D2
			29.7 ^{+1.1} _{-1.3}	46 ⁺⁵⁵ ₋₁₅	0.050 ^{+0.006} _{-0.003}	0.126 ^{+0.014} _{-0.008}	26.7	2.3	R1
			28.9 ^{+0.9} _{-0.8}	41 ⁺¹⁴ ₋₉	0.054 ^{+0.003} _{-0.004}	0.137 ^{+0.008} _{-0.009}	26.7	1.4	R2
1103	Sequoia	6.7±0.1	7.0 ^{+0.4} _{-0.5}	110 ⁺²¹⁸ ₋₆₄	0.165 ^{+0.029} _{-0.017}	0.421 ^{+0.074} _{-0.044}	35.8	2.8	D1
1111	Reinmuthia		28.5 ^{+1.3} _{-1.8}	78 ⁺⁴² ₋₂₉	0.040 ^{+0.005} _{-0.003}	0.101 ^{+0.013} _{-0.009}	12.0	4.2	R1
			27.2 ^{+1.0} _{-1.3}	75 ⁺³⁰ ₋₂₄	0.044 ^{+0.004} _{-0.003}	0.112 ^{+0.011} _{-0.008}	12.0	3.5	R2
1117	Reginita	10.2±0.2	11.1 ^{+1.0} _{-1.0}	122 ⁺¹³⁸ ₋₉₇	0.109 ^{+0.025} _{-0.017}	0.278 ^{+0.063} _{-0.043}	55.4	2.8	D1
			11.1 ^{+0.8} _{-0.7}	105 ⁺⁸² ₋₆₇	0.110 ^{+0.015} _{-0.014}	0.280 ^{+0.037} _{-0.035}	55.4	1.8	D2
			10.5 ^{+1.0} _{-0.7}	44 ⁺⁸⁸ ₋₁₉	0.100 ^{+0.013} _{-0.018}	0.254 ^{+0.034} _{-0.046}	16.5	2.1	R1
			10.4 ^{+1.3} _{-0.6}	39 ⁺¹³⁵ ₋₁₄	0.104 ^{+0.014} _{-0.022}	0.264 ^{+0.036} _{-0.056}	16.5	2.0	R2
1125	China	26.1±0.2	25.8 ^{+4.2} _{-1.6}	25 ⁺⁶⁶ ₋₉	0.022 ^{+0.003} _{-0.006}	0.055 ^{+0.007} _{-0.015}	26.7	8.3	D1
			27.0 ^{+2.4} _{-3.1}	58 ⁺³² ₋₄₃	0.020 ^{+0.006} _{-0.003}	0.050 ^{+0.015} _{-0.008}	55.4	7.3	D2
1130	Skuld	10.1±0.1	9.8 ^{+0.3} _{-0.6}	82 ⁺¹¹⁵ ₋₄₅	0.105 ^{+0.015} _{-0.006}	0.267 ^{+0.038} _{-0.016}	16.5	2.2	D1
			9.5 ^{+0.4} _{-0.5}	66 ⁺⁹⁶ ₋₄₂	0.110 ^{+0.013} _{-0.009}	0.279 ^{+0.034} _{-0.022}	16.5	2.0	D2

Table 4 continued

Table 4 (continued)

Asteroid	D_{WISE} (km)	D (km)	Γ ($\text{J m}^{-2} \text{s}^{-0.5} \text{K}^{-1}$)	A	p_V	$\bar{\theta}$ °	χ_{red}^2	Model ID
1140 Crimea	29.2±0.2	9.8 ^{+0.1} _{-0.1}	146 ⁺⁵⁴ ₋₄₀	0.096 ^{+0.003} _{-0.002}	0.243 ^{+0.006} _{-0.006}	35.8	0.7	R1
		29.6 ^{+1.7} _{-2.5}	5 ⁺²³ ₋₅	0.054 ^{+0.010} _{-0.006}	0.137 ^{+0.025} _{-0.014}	16.5	9.5	D1
		28.0 ^{+0.5} _{-0.6}	0 ⁺³ ₋₀	0.062 ^{+0.003} _{-0.001}	0.158 ^{+0.008} _{-0.003}	12.6	2.7	D2
		31.0 ^{+1.0} _{-1.5}	27 ⁺³⁶ ₋₁₃	0.051 ^{+0.005} _{-0.004}	0.129 ^{+0.014} _{-0.009}	16.5	2.4	R1
		28.3 ^{+1.4} _{-1.1}	3 ⁺²³ ₋₃	0.060 ^{+0.004} _{-0.006}	0.153 ^{+0.010} _{-0.014}	12.6	3.3	R2
1148 Rarahu	27.5±0.4	28.1 ^{+2.2} _{-1.6}	37 ⁺⁵⁷ ₋₂₄	0.067 ^{+0.008} _{-0.009}	0.170 ^{+0.021} _{-0.024}	26.7	3.4	D1
		29.1 ^{+2.1} _{-2.3}	67 ⁺⁷² ₋₄₉	0.061 ^{+0.011} _{-0.008}	0.156 ^{+0.029} _{-0.020}	26.7	7.6	D2
1175 Margo	24.3±0.3	25.2 ^{+0.5} _{-1.2}	120 ⁺¹⁰⁵ ₋₄₂	0.102 ^{+0.010} _{-0.004}	0.259 ^{+0.026} _{-0.010}	46.8	0.9	D1
		25.3 ^{+0.6} _{-0.7}	244 ⁺¹⁵⁰ ₋₉₈	0.102 ^{+0.005} _{-0.005}	0.260 ^{+0.013} _{-0.013}	55.4	0.9	D2
1188 Gothlandia	12.7±0.1	13.2 ^{+0.8} _{-0.8}	41 ⁺¹⁷ ₋₁₇	0.084 ^{+0.011} _{-0.010}	0.213 ^{+0.027} _{-0.025}	12.0	3.5	D1
		12.7 ^{+0.4} _{-0.6}	37 ⁺¹³ ₋₁₂	0.083 ^{+0.008} _{-0.007}	0.212 ^{+0.020} _{-0.018}	12.6	2.0	R1
		12.7 ^{+0.6} _{-0.3}	38 ⁺¹⁰ ₋₁₀	0.083 ^{+0.004} _{-0.009}	0.212 ^{+0.010} _{-0.022}	16.5	1.6	R2
1210 Morosovia	33.7±0.3	35.1 ^{+1.0} _{-0.0}	0 ⁺¹ ₋₀	0.054 ^{+0.000} _{-0.002}	0.138 ^{+0.000} _{-0.006}	16.5	3.5	D1
		34.8 ^{+1.4} _{-1.9}	88 ⁺³⁰ ₋₅₀	0.056 ^{+0.006} _{-0.005}	0.143 ^{+0.017} _{-0.012}	55.4	2.6	D2
1241 Dysona	79.2±0.7	77.1 ^{+3.5} _{-4.5}	0 ⁺¹⁸ ₋₀	0.017 ^{+0.002} _{-0.001}	0.044 ^{+0.006} _{-0.003}	16.5	5.1	D1
		74.5 ^{+3.6} _{-2.6}	14 ⁺¹³ ₋₁₄	0.019 ^{+0.001} _{-0.002}	0.049 ^{+0.004} _{-0.004}	26.7	2.2	D2
1249 Rutherfordia	13.1±0.1	11.7 ^{+0.3} _{-0.5}	0 ⁺² ₋₀	0.103 ^{+0.011} _{-0.004}	0.264 ^{+0.027} _{-0.010}	16.5	7.0	R1
		11.9 ^{+0.2} _{-0.2}	0 ⁺⁸ ₋₀	0.101 ^{+0.004} _{-0.001}	0.256 ^{+0.009} _{-0.003}	12.6	4.5	R2
1251 Hedera	13.2±0.1	11.8 ^{+1.2} _{-0.8}	44 ⁺⁷⁶ ₋₃₆	0.287 ^{+0.041} _{-0.057}	0.732 ^{+0.105} _{-0.144}	26.7	5.1	D1
		12.1 ^{+1.7} _{-1.0}	66 ⁺¹⁶⁰ ₋₅₀	0.269 ^{+0.055} _{-0.061}	0.685 ^{+0.139} _{-0.156}	26.7	4.9	D2
1310 Villigera		12.9 ^{+0.4} _{-0.7}	23 ⁺⁵⁰ ₋₁₈	0.102 ^{+0.012} _{-0.007}	0.261 ^{+0.031} _{-0.017}	16.5	2.7	D1
		12.6 ^{+0.5} _{-0.1}	23 ⁺²⁰ ₋₆	0.104 ^{+0.002} _{-0.007}	0.266 ^{+0.005} _{-0.018}	16.5	1.5	D2
1317 Silvretta	26.4±0.4	29.1 ^{+2.1} _{-3.6}	234 ⁺²⁹⁰ ₋₂₀₆	0.082 ^{+0.025} _{-0.011}	0.210 ^{+0.063} _{-0.028}	55.4	7.9	D1
		29.5 ^{+2.0} _{-3.4}	219 ⁺²¹⁴ ₋₂₁₅	0.078 ^{+0.022} _{-0.009}	0.199 ^{+0.057} _{-0.024}	55.4	5.7	D2
1320 Impala	37.3±0.2	37.9 ^{+2.5} _{-3.5}	6 ⁺³⁰ ₋₆	0.019 ^{+0.004} _{-0.002}	0.049 ^{+0.010} _{-0.006}	16.5	7.7	D1
		38.9 ^{+2.7} _{-2.0}	27 ⁺¹⁴ ₋₁₅	0.018 ^{+0.002} _{-0.002}	0.047 ^{+0.005} _{-0.006}	26.7	6.4	D2
1332 Marconia	46.8±0.1	45.5 ^{+2.5} _{-1.1}	16 ⁺⁵¹ ₋₁₅	0.017 ^{+0.001} _{-0.002}	0.044 ^{+0.002} _{-0.005}	26.7	1.6	D1
		45.8 ^{+2.6} _{-1.4}	87 ⁺⁶⁹ ₋₆₄	0.017 ^{+0.001} _{-0.002}	0.044 ^{+0.003} _{-0.005}	55.4	1.6	D2
1333 Cevenola	15.3±0.2	15.2 ^{+0.7} _{-0.7}	184 ⁺¹⁰⁵ ₋₆₅	0.066 ^{+0.006} _{-0.006}	0.168 ^{+0.016} _{-0.015}	55.4	2.8	D1
		15.4 ^{+0.6} _{-0.8}	315 ⁺²³⁹ ₋₁₂₈	0.065 ^{+0.007} _{-0.005}	0.166 ^{+0.018} _{-0.012}	55.4	3.4	D2
1339 Desagneuxa	24.4±0.2	25.9 ^{+2.1} _{-2.2}	21 ⁺¹³⁴ ₋₁₉	0.043 ^{+0.008} _{-0.007}	0.110 ^{+0.021} _{-0.017}	16.5	9.2	D2
1352 Wawel	20.0±0.1	19.8 ^{+1.9} _{-0.9}	616 ⁺⁴³⁶ ₋₄₅₅	0.057 ^{+0.005} _{-0.010}	0.146 ^{+0.013} _{-0.025}	55.4	8.1	D1
		20.5 ^{+1.8} _{-1.2}	684 ⁺⁴⁴⁹ ₋₅₃₂	0.052 ^{+0.007} _{-0.008}	0.133 ^{+0.017} _{-0.021}	55.4	7.7	D2
1353 Maartje	39.0±0.5	39.9 ^{+1.9} _{-2.2}	178 ⁺¹¹⁵ ₋₈₆	0.042 ^{+0.005} _{-0.004}	0.107 ^{+0.013} _{-0.010}	55.4	3.8	D1
		36.8 ^{+1.9} _{-1.3}	174 ⁺¹¹¹ ₋₁₃₀	0.050 ^{+0.004} _{-0.005}	0.128 ^{+0.009} _{-0.012}	55.4	2.6	D2
1360 Tarka	33.3±0.1	31.1 ^{+1.2} _{-1.8}	74 ⁺⁵⁰ ₋₄₀	0.016 ^{+0.002} _{-0.001}	0.040 ^{+0.005} _{-0.003}	55.4	2.5	D1
1364 Safara	21.2±0.2	21.5 ^{+2.0} _{-1.0}	29 ⁺¹⁵ ₋₁₉	0.067 ^{+0.006} _{-0.011}	0.171 ^{+0.017} _{-0.028}	26.7	3.4	D1
		21.5 ^{+1.9} _{-0.9}	29 ⁺²¹ ₋₁₇	0.069 ^{+0.006} _{-0.011}	0.175 ^{+0.015} _{-0.028}	26.7	2.5	D2
1386 Storeria	10.6±0.2	10.6 ^{+0.5} _{-0.4}	22 ⁺⁸ ₋₁₂	0.021 ^{+0.002} _{-0.002}	0.053 ^{+0.005} _{-0.004}	27.3	0.8	D1
		12.1 ^{+1.0} _{-1.4}	39 ⁺³⁶ ₋₃₉	0.015 ^{+0.004} _{-0.002}	0.039 ^{+0.010} _{-0.006}	26.7	9.0	D2

Table 4 continued

Table 4 (continued)

Asteroid	D_{WISE} (km)	D (km)	Γ ($\text{J m}^{-2} \text{s}^{-0.5} \text{K}^{-1}$)	A	pv	$\bar{\theta}$ °	χ_{red}^2	Model ID
1388 Aphrodite	21.4±0.3	22.1 ^{+0.9} _{-1.6}	32 ⁺⁷¹ ₋₁₄	0.057 ^{+0.009} _{-0.005}	0.145 ^{+0.024} _{-0.012}	16.5	1.7	D1
		20.4 ^{+1.5} _{-0.8}	18 ⁺³⁸ ₋₁₅	0.066 ^{+0.006} _{-0.010}	0.169 ^{+0.014} _{-0.025}	16.5	2.1	D2
1401 Lavonne	9.3±0.1	9.3 ^{+0.4} _{-0.5}	24 ⁺³⁹ ₋₂₃	0.092 ^{+0.010} _{-0.007}	0.235 ^{+0.026} _{-0.018}	12.6	1.3	D1
		9.2 ^{+0.4} _{-0.4}	26 ⁺²³ ₋₂₀	0.093 ^{+0.007} _{-0.008}	0.238 ^{+0.019} _{-0.021}	16.5	1.3	D2
1430 Somalia	9.4±0.1	9.8 ^{+0.8} _{-1.9}	40 ⁺²⁰⁹ ₋₄₀	0.094 ^{+0.047} _{-0.015}	0.240 ^{+0.119} _{-0.039}	16.5	7.1	D1
		9.3 ^{+0.9} _{-0.8}	40 ⁺⁷⁸ ₋₄₀	0.106 ^{+0.021} _{-0.018}	0.271 ^{+0.055} _{-0.047}	26.7	5.2	D2
1432 Ethiopia	6.9±0.1	6.0 ^{+0.7} _{-0.5}	90 ⁺⁶⁹⁷ ₋₉₀	0.258 ^{+0.042} _{-0.053}	0.657 ^{+0.108} _{-0.136}	26.7	6.3	D2
		6.4 ^{+0.4} _{-0.3}	13 ⁺⁵³⁹ ₋₁₂	0.314 ^{+0.036} _{-0.039}	0.800 ^{+0.091} _{-0.098}	16.5	1.9	R1
		6.5 ^{+0.3} _{-0.4}	13 ⁺²⁸⁸ ₋₁₃	0.313 ^{+0.045} _{-0.029}	0.796 ^{+0.115} _{-0.074}	12.0	2.0	R2
1436 Salonta	53.8±0.3	54.3 ^{+3.9} _{-3.3}	0 ⁺⁴⁶ ₋₀	0.016 ^{+0.002} _{-0.002}	0.041 ^{+0.006} _{-0.005}	16.5	8.0	D1
		55.0 ^{+4.1} _{-3.2}	0 ⁺¹¹ ₋₀	0.015 ^{+0.002} _{-0.002}	0.039 ^{+0.005} _{-0.004}	12.0	5.3	D2
		56.3 ^{+3.0} _{-2.1}	5 ⁺¹² ₋₅	0.015 ^{+0.001} _{-0.001}	0.038 ^{+0.002} _{-0.004}	26.7	3.2	R1
		53.6 ^{+5.4} _{-1.0}	1 ⁺²¹ ₋₁	0.017 ^{+0.000} _{-0.003}	0.042 ^{+0.001} _{-0.007}	26.7	2.3	R2
1446 Sillanpaa	8.2±0.2	8.0 ^{+0.6} _{-0.5}	26 ⁺⁴⁹ ₋₂₆	0.086 ^{+0.012} _{-0.013}	0.218 ^{+0.031} _{-0.033}	16.5	6.0	D1
		7.9 ^{+1.0} _{-0.7}	38 ⁺¹¹⁵ ₋₃₈	0.087 ^{+0.017} _{-0.020}	0.222 ^{+0.042} _{-0.050}	16.5	8.2	D2
1449 Virtanen	9.3±0.1	10.4 ^{+0.4} _{-0.6}	0 ⁺¹² ₋₀	0.090 ^{+0.011} _{-0.007}	0.229 ^{+0.028} _{-0.017}	3.9	2.2	D1
		9.8 ^{+0.7} _{-0.3}	0 ⁺¹¹ ₋₀	0.099 ^{+0.005} _{-0.012}	0.252 ^{+0.014} _{-0.031}	12.6	4.0	D2
1472 Muonio	8.4±0.1	9.6 ^{+1.1} _{-2.4}	374 ⁺⁶⁶⁴ ₋₂₆₄	0.084 ^{+0.020} _{-0.017}	0.214 ^{+0.050} _{-0.043}	55.4	6.2	D1
		8.5 ^{+0.6} _{-0.7}	1 ⁺³² ₋₁	0.106 ^{+0.020} _{-0.012}	0.270 ^{+0.050} _{-0.031}	3.9	3.1	D2
1486 Marilyn	6.4±0.1	7.4 ^{+0.5} _{-0.7}	124 ⁺¹³⁴ ₋₇₃	0.084 ^{+0.020} _{-0.009}	0.213 ^{+0.051} _{-0.022}	26.7	7.8	D1
		7.3 ^{+0.6} _{-0.8}	167 ⁺¹⁶⁹ ₋₁₂₁	0.086 ^{+0.021} _{-0.012}	0.220 ^{+0.053} _{-0.031}	55.4	9.5	D2
		7.0 ^{+0.6} _{-0.5}	95 ⁺¹⁵⁰ ₋₄₉	0.079 ^{+0.015} _{-0.011}	0.200 ^{+0.039} _{-0.028}	26.7	7.1	R1
		6.8 ^{+0.7} _{-0.3}	91 ⁺¹⁰⁰ ₋₃₄	0.085 ^{+0.008} _{-0.015}	0.217 ^{+0.021} _{-0.039}	26.7	6.2	R2
1495 Helsinki	12.2±0.1	11.6 ^{+1.0} _{-0.0}	0 ⁺³² ₋₀	0.125 ^{+0.000} _{-0.017}	0.318 ^{+0.000} _{-0.043}	16.5	3.7	D1
		13.3 ^{+0.3} _{-0.6}	81 ⁺²⁶ ₋₂₁	0.081 ^{+0.007} _{-0.004}	0.206 ^{+0.018} _{-0.011}	35.8	1.0	R1
1518 Rovaniemi	8.5±0.2	8.4 ^{+0.6} _{-0.7}	114 ⁺¹⁷³ ₋₅₇	0.096 ^{+0.020} _{-0.011}	0.245 ^{+0.050} _{-0.028}	26.7	3.1	D1
		8.2 ^{+0.9} _{-0.4}	159 ⁺¹³³ ₋₉₁	0.100 ^{+0.010} _{-0.019}	0.256 ^{+0.025} _{-0.048}	55.4	3.2	D2
1546 Izsak	26.4±0.1	26.6 ^{+2.4} _{-2.7}	118 ⁺¹⁶³ ₋₆₁	0.045 ^{+0.011} _{-0.007}	0.115 ^{+0.028} _{-0.017}	27.3	7.5	D1
		27.2 ^{+2.2} _{-2.5}	132 ⁺³⁰³ ₋₆₂	0.044 ^{+0.009} _{-0.006}	0.112 ^{+0.023} _{-0.016}	26.7	7.2	D2
1627 Ivar	8.4±0.1	7.5 ^{+0.2} _{-0.4}	81 ⁺⁶⁵ ₋₃₀	0.099 ^{+0.010} _{-0.004}	0.141 ^{+0.014} _{-0.006}	3.9	1.0	D1
		7.5 ^{+0.1} _{-0.1}	133 ⁺⁶² ₋₄₄	0.099 ^{+0.004} _{-0.003}	0.141 ^{+0.006} _{-0.004}	12.0	0.8	R1
1633 Chimay	37.4±0.5	46.9 ^{+2.4} _{-3.3}	65 ⁺¹⁰⁰ ₋₃₀	0.014 ^{+0.002} _{-0.001}	0.035 ^{+0.006} _{-0.003}	26.7	2.9	D1
		43.0 ^{+4.6} _{-2.6}	119 ⁺¹¹⁹ ₋₅₄	0.018 ^{+0.002} _{-0.003}	0.045 ^{+0.006} _{-0.008}	55.4	5.0	D2
1635 Bohrmann	17.1±0.2	18.1 ^{+1.7} _{-1.5}	53 ⁺¹⁴⁰ ₋₂₄	0.075 ^{+0.015} _{-0.012}	0.192 ^{+0.039} _{-0.030}	16.5	3.2	D1
		16.6 ^{+2.1} _{-1.4}	34 ⁺¹³¹ ₋₃₁	0.089 ^{+0.017} _{-0.020}	0.227 ^{+0.043} _{-0.051}	16.5	6.5	D2
		18.5 ^{+1.5} _{-1.6}	68 ⁺¹⁰³ ₋₄₄	0.066 ^{+0.014} _{-0.010}	0.168 ^{+0.036} _{-0.025}	16.5	3.7	R1
		18.3 ^{+1.6} _{-1.3}	58 ⁺⁹² ₋₃₇	0.068 ^{+0.012} _{-0.010}	0.172 ^{+0.030} _{-0.026}	16.5	3.3	R2
1672 Gezelle	26.2±0.2	26.8 ^{+4.3} _{-0.9}	10 ⁺¹²⁶ ₋₁₀	0.019 ^{+0.002} _{-0.004}	0.047 ^{+0.005} _{-0.011}	26.7	8.3	D1
1685 Toro	3.8±0.0	3.6 ^{+0.2} _{-0.1}	210 ⁺⁸⁵ ₋₅₅	0.099 ^{+0.007} _{-0.009}	0.253 ^{+0.018} _{-0.023}	0	1.8	R1
1719 Jens	19.9±0.1	20.9 ^{+1.2} _{-1.4}	1 ⁺⁷³ ₋₁	0.031 ^{+0.004} _{-0.003}	0.079 ^{+0.011} _{-0.009}	3.9	5.8	D1

Table 4 continued

Table 4 (continued)

Asteroid		D_{WISE}	D	Γ	A	pv	$\bar{\theta}$	χ^2_{red}	Model ID
		(km)	(km)	($\text{J m}^{-2} \text{s}^{-0.5} \text{K}^{-1}$)			°		
1723	Klemola	33.5±0.2	22.0 ^{+1.5} _{-1.5}	40 ⁺¹¹⁵ ₋₃₉	0.027 ^{+0.004} _{-0.004}	0.068 ^{+0.010} _{-0.009}	16.5	6.0	D2
			32.9 ^{+0.8} _{-1.6}	12 ⁺²³ ₋₇	0.054 ^{+0.006} _{-0.002}	0.138 ^{+0.015} _{-0.006}	16.5	1.9	D1
			32.7 ^{+1.0} _{-1.4}	12 ⁺²⁶ ₋₇	0.055 ^{+0.005} _{-0.003}	0.140 ^{+0.013} _{-0.008}	16.5	2.9	D2
			32.1 ^{+1.9} _{-0.8}	29 ⁺¹⁷ ₋₂₃	0.057 ^{+0.003} _{-0.006}	0.145 ^{+0.007} _{-0.016}	26.7	2.9	R1
1730	Marceline	15.2±0.1	33.0 ^{+0.7} _{-2.0}	13 ⁺²³ ₋₈	0.053 ^{+0.007} _{-0.002}	0.136 ^{+0.018} _{-0.005}	16.5	2.5	R2
			15.8 ^{+2.4} _{-1.6}	119 ⁺³²⁴ ₋₇₁	0.041 ^{+0.009} _{-0.010}	0.105 ^{+0.024} _{-0.025}	16.5	8.9	D1
			15.7 ^{+1.2} _{-1.8}	103 ⁺¹⁰¹ ₋₅₆	0.041 ^{+0.011} _{-0.005}	0.104 ^{+0.029} _{-0.013}	12.6	6.6	D2
1741	Giclas	12.5±0.2	14.5 ^{+3.4} _{-1.2}	57 ⁺⁴⁸² ₋₃₄	0.072 ^{+0.015} _{-0.024}	0.183 ^{+0.038} _{-0.061}	16.5	9.4	R1
			13.0 ^{+0.8} _{-0.6}	159 ⁺²³⁵ ₋₉₃	0.103 ^{+0.011} _{-0.011}	0.263 ^{+0.028} _{-0.028}	55.4	1.0	D1
			13.1 ^{+0.7} _{-0.8}	67 ⁺²⁴³ ₋₂₇	0.101 ^{+0.013} _{-0.011}	0.258 ^{+0.033} _{-0.027}	26.7	1.2	D2
1789	Dobrovolsky	7.9±0.1	12.8 ^{+0.7} _{-0.5}	21 ⁺¹⁴⁸ ₋₂₀	0.131 ^{+0.010} _{-0.015}	0.334 ^{+0.026} _{-0.037}	16.5	0.8	R1
			12.9 ^{+0.7} _{-0.5}	22 ⁺¹⁷⁷ ₋₂₂	0.130 ^{+0.010} _{-0.013}	0.330 ^{+0.026} _{-0.034}	16.5	0.8	R2
			8.7 ^{+0.5} _{-0.6}	77 ⁺⁴³ ₋₃₁	0.049 ^{+0.008} _{-0.005}	0.125 ^{+0.019} _{-0.014}	12.6	2.2	R1
1865	Cerberus	1.6±0.0	8.7 ^{+0.4} _{-0.6}	64 ⁺²⁸ ₋₂₉	0.049 ^{+0.009} _{-0.004}	0.125 ^{+0.022} _{-0.010}	12.6	2.4	R2
			1.2 ^{+0.0} _{-0.0}	809 ⁺²¹⁹ ₋₁₃₄	0.061 ^{+0.000} _{-0.001}	0.155 ^{+0.001} _{-0.002}	3.9	1.6	R2
1925	Franklin-Adams	8.9±0.1	8.5 ^{+0.8} _{-0.8}	0 ⁺¹⁵ ₋₀	0.121 ^{+0.026} _{-0.019}	0.309 ^{+0.067} _{-0.048}	0	4.5	D1
			8.5 ^{+2.8} _{-0.9}	0 ⁺¹⁴ ₋₀	0.120 ^{+0.027} _{-0.053}	0.306 ^{+0.069} _{-0.136}	0	6.0	D2
1930	Lucifer	34.4±0.2	31.7 ^{+1.9} _{-2.8}	38 ⁺⁹¹ ₋₃₈	0.024 ^{+0.005} _{-0.003}	0.062 ^{+0.012} _{-0.007}	26.7	9.4	D1
			29.6 ^{+2.3} _{-0.0}	0 ⁺²⁵ ₋₀	0.031 ^{+0.000} _{-0.004}	0.079 ^{+0.000} _{-0.010}	26.7	6.4	R1
			30.5 ^{+2.4} _{-0.7}	10 ⁺³⁵ ₋₁₀	0.030 ^{+0.001} _{-0.004}	0.076 ^{+0.003} _{-0.011}	26.7	5.2	R2
1963	Bezovec	35.5±0.2	35.2 ^{+1.0} _{-1.2}	55 ⁺²⁸ ₋₂₉	0.022 ^{+0.002} _{-0.001}	0.056 ^{+0.004} _{-0.003}	55.4	1.3	R1
			32.6 ^{+1.5} _{-0.3}	0 ⁺⁴¹ ₋₀	0.025 ^{+0.001} _{-0.002}	0.064 ^{+0.002} _{-0.005}	46.8	1.1	R2
1987	Kaplan	13.0±0.2	12.9 ^{+0.6} _{-0.3}	39 ⁺²⁵ ₋₁₀	0.096 ^{+0.004} _{-0.009}	0.244 ^{+0.011} _{-0.024}	26.7	2.4	D1
			12.2 ^{+0.3} _{-0.5}	50 ⁺¹⁶ ₋₂₂	0.113 ^{+0.011} _{-0.006}	0.287 ^{+0.028} _{-0.015}	26.7	2.7	R1
2001	Einstein	4.0±0.2	3.7 ^{+0.3} _{-0.2}	8 ⁺⁴⁶ ₋₈	0.342 ^{+0.047} _{-0.054}	0.870 ^{+0.119} _{-0.137}	16.5	2.0	D1
2110	Moore-Sitterly	5.7±0.2	5.6 ^{+0.6} _{-0.5}	116 ⁺¹¹⁷ ₋₇₀	0.088 ^{+0.019} _{-0.015}	0.223 ^{+0.048} _{-0.039}	27.3	2.3	D1
			5.8 ^{+0.6} _{-0.4}	81 ⁺¹⁰³ ₋₃₀	0.082 ^{+0.011} _{-0.014}	0.209 ^{+0.028} _{-0.036}	16.5	1.6	D2
			6.0 ^{+0.4} _{-0.4}	64 ⁺⁶⁰ ₋₄₀	0.054 ^{+0.008} _{-0.006}	0.137 ^{+0.020} _{-0.016}	12.6	1.2	R1
2306	Bauschinger	19.4±0.1	17.7 ^{+0.5} _{-0.7}	15 ⁺²⁴ ₋₁₄	0.026 ^{+0.002} _{-0.001}	0.066 ^{+0.005} _{-0.004}	12.6	2.8	D1
			18.5 ^{+0.5} _{-0.8}	56 ⁺²³ ₋₂₄	0.023 ^{+0.002} _{-0.001}	0.059 ^{+0.006} _{-0.003}	35.8	2.0	D2
			16.8 ^{+1.1} _{-0.3}	5 ⁺³⁶ ₋₅	0.059 ^{+0.002} _{-0.007}	0.151 ^{+0.004} _{-0.018}	26.7	5.9	R1
2381	Landi	13.1±0.1	13.6 ^{+1.1} _{-1.1}	83 ⁺⁸⁰ ₋₃₇	0.067 ^{+0.012} _{-0.010}	0.172 ^{+0.031} _{-0.026}	35.8	9.0	D1
			13.0 ^{+1.0} _{-0.6}	44 ⁺²⁶ ₋₂₃	0.096 ^{+0.009} _{-0.015}	0.243 ^{+0.022} _{-0.037}	26.7	2.8	R1
			13.5 ^{+0.6} _{-0.7}	35 ⁺²² ₋₁₄	0.089 ^{+0.010} _{-0.009}	0.226 ^{+0.025} _{-0.023}	16.5	2.0	R2
2384	Schulhof	11.5±0.2	12.1 ^{+0.4} _{-0.3}	42 ⁺¹⁵ ₋₁₂	0.077 ^{+0.005} _{-0.006}	0.197 ^{+0.012} _{-0.015}	12.6	0.7	D1
			12.4 ^{+0.5} _{-0.7}	61 ⁺¹⁰⁵ ₋₁₈	0.072 ^{+0.009} _{-0.006}	0.183 ^{+0.022} _{-0.015}	16.5	1.5	D2
			12.2 ^{+0.7} _{-0.6}	95 ⁺¹¹¹ ₋₄₈	0.056 ^{+0.006} _{-0.006}	0.143 ^{+0.016} _{-0.016}	26.7	1.9	R1
2455	Somville	16.1±0.2	13.4 ^{+0.6} _{-0.7}	97 ⁺³⁹ ₋₄₇	0.044 ^{+0.005} _{-0.003}	0.112 ^{+0.013} _{-0.008}	27.3	1.3	R2
			15.9 ^{+0.9} _{-0.8}	219 ⁺²³² ₋₁₂₉	0.049 ^{+0.005} _{-0.005}	0.125 ^{+0.012} _{-0.012}	16.5	3.0	D1
			15.8 ^{+1.4} _{-1.0}	602 ⁺⁷⁶³ ₋₄₁₉	0.050 ^{+0.007} _{-0.008}	0.127 ^{+0.017} _{-0.021}	26.7	4.7	D2

Table 4 continued

Table 4 (continued)

Asteroid		D_{WISE}	D	Γ	A	pv	$\bar{\theta}$	χ^2_{red}	Model ID
		(km)	(km)	($\text{J m}^{-2} \text{s}^{-0.5} \text{K}^{-1}$)			°		
2606	Odessa	15.9±0.2	15.5 ^{+2.0} _{-1.6}	78 ⁺⁴⁹ ₋₃₀	0.052 ^{+0.011} _{-0.011}	0.132 ^{+0.029} _{-0.029}	12.6	6.1	D1
2659	Millis	27.9±0.3	26.9 ^{+2.7} _{-2.0}	12 ⁺¹²³ ₋₁₀	0.020 ^{+0.003} _{-0.004}	0.051 ^{+0.008} _{-0.009}	16.5	6.2	D1
			27.4 ^{+2.3} _{-2.4}	31 ⁺⁹⁹ ₋₂₈	0.019 ^{+0.004} _{-0.003}	0.049 ^{+0.010} _{-0.007}	35.8	5.7	D2
2839	Annette	7.3±0.1	6.6 ^{+0.4} _{-0.5}	189 ⁺⁵⁸⁶ ₋₁₁₇	0.096 ^{+0.016} _{-0.011}	0.245 ^{+0.040} _{-0.028}	26.7	2.6	D1
			6.5 ^{+0.5} _{-0.4}	196 ⁺⁴³⁶ ₋₁₁₄	0.099 ^{+0.012} _{-0.013}	0.252 ^{+0.032} _{-0.032}	26.7	1.9	D2
2957	Tatsuo	22.5±0.1	24.6 ^{+0.9} _{-1.1}	65 ⁺⁴⁰ ₋₃₅	0.048 ^{+0.005} _{-0.004}	0.123 ^{+0.013} _{-0.009}	46.8	1.3	D1
			24.3 ^{+0.8} _{-1.1}	20 ⁺⁴⁹ ₋₂₀	0.051 ^{+0.005} _{-0.003}	0.131 ^{+0.013} _{-0.009}	12.0	1.4	D2
3478	Fanale	7.0±0.1	6.7 ^{+0.4} _{-0.2}	0 ⁺¹⁹ ₋₀	0.117 ^{+0.006} _{-0.013}	0.299 ^{+0.015} _{-0.032}	0	7.3	D1
3544	Borodino	8.5±0.1	8.5 ^{+0.6} _{-0.4}	39 ⁺³⁷ ₋₂₀	0.090 ^{+0.008} _{-0.012}	0.229 ^{+0.020} _{-0.031}	16.5	6.0	D2
			8.8 ^{+0.5} _{-0.6}	40 ⁺⁵³ ₋₂₀	0.077 ^{+0.011} _{-0.009}	0.196 ^{+0.027} _{-0.023}	16.5	5.7	R1
			8.4 ^{+0.5} _{-0.6}	40 ⁺⁸³ ₋₁₉	0.085 ^{+0.014} _{-0.010}	0.217 ^{+0.035} _{-0.026}	16.5	5.7	R2
3722	Urata	7.9±0.2	6.5 ^{+0.4} _{-0.4}	1576 ⁺²⁶⁶ ₋₁₄₉₉	0.106 ^{+0.016} _{-0.012}	0.269 ^{+0.040} _{-0.030}	55.4	1.7	D1
			6.6 ^{+0.4} _{-0.4}	1 ⁺¹¹⁸⁶ ₋₁	0.107 ^{+0.015} _{-0.013}	0.272 ^{+0.039} _{-0.032}	26.7	2.8	D2
3786	Yamada	15.8±1.0	16.7 ^{+0.6} _{-0.7}	29 ⁺²¹ ₋₁₆	0.077 ^{+0.007} _{-0.006}	0.196 ^{+0.017} _{-0.016}	12.6	1.9	D1
			15.9 ^{+0.2} _{-0.4}	0 ⁺¹¹ ₋₀	0.086 ^{+0.003} _{-0.002}	0.218 ^{+0.008} _{-0.005}	0	2.9	D2
4077	Asuka	19.5±0.2	19.9 ^{+1.3} _{-2.0}	27 ⁺¹⁹ ₋₂₂	0.056 ^{+0.013} _{-0.007}	0.142 ^{+0.034} _{-0.019}	3.9	8.0	D2
			19.7 ^{+0.6} _{-1.3}	20 ⁺⁸ ₋₁₃	0.044 ^{+0.006} _{-0.002}	0.111 ^{+0.017} _{-0.006}	12.0	2.0	R1
			19.2 ^{+1.1} _{-0.5}	26 ⁺¹¹ ₋₇	0.046 ^{+0.002} _{-0.005}	0.118 ^{+0.006} _{-0.012}	16.5	1.5	R2
4265	Kani	14.2±0.2	15.0 ^{+1.0} _{-1.1}	11 ⁺¹⁵ ₋₁₁	0.016 ^{+0.003} _{-0.002}	0.041 ^{+0.007} _{-0.005}	12.0	6.0	D1
			14.0 ^{+1.1} _{-0.6}	14 ⁺¹⁰ ₋₁₄	0.019 ^{+0.002} _{-0.003}	0.048 ^{+0.004} _{-0.007}	12.0	4.7	D2
			12.9 ^{+0.5} _{-1.2}	1 ⁺¹⁰ ₋₁	0.027 ^{+0.005} _{-0.002}	0.069 ^{+0.012} _{-0.004}	16.5	9.6	R1
			13.1 ^{+0.4} _{-1.0}	0 ⁺⁵ ₋₀	0.026 ^{+0.005} _{-0.001}	0.067 ^{+0.012} _{-0.004}	16.5	9.5	R2
4606	Saheki	6.7±0.0	6.4 ^{+0.5} _{-0.5}	1 ⁺²² ₋₁	0.094 ^{+0.015} _{-0.012}	0.239 ^{+0.038} _{-0.032}	16.5	4.5	D1
			6.6 ^{+0.7} _{-0.6}	0 ⁺²⁷ ₋₀	0.085 ^{+0.017} _{-0.015}	0.216 ^{+0.043} _{-0.039}	12.6	8.4	D2
			6.8 ^{+0.5} _{-0.5}	16 ⁺²⁵ ₋₁₆	0.113 ^{+0.019} _{-0.014}	0.288 ^{+0.049} _{-0.035}	16.5	2.1	R1
			6.7 ^{+0.4} _{-0.5}	19 ⁺¹⁸ ₋₁₆	0.117 ^{+0.020} _{-0.013}	0.299 ^{+0.051} _{-0.033}	16.5	1.9	R2
4905	Hiromi	8.4±0.6	10.0 ^{+1.1} _{-0.9}	44 ⁺¹⁴⁶ ₋₃₉	0.080 ^{+0.014} _{-0.016}	0.205 ^{+0.035} _{-0.040}	26.7	5.1	D1
			10.2 ^{+0.4} _{-0.6}	31 ⁺⁴⁸ ₋₂₀	0.091 ^{+0.011} _{-0.007}	0.231 ^{+0.027} _{-0.017}	16.5	1.5	R1
5489	Oberkochen	13.1±0.1	14.0 ^{+0.5} _{-0.7}	1 ⁺⁹ ₋₁	0.082 ^{+0.009} _{-0.005}	0.209 ^{+0.022} _{-0.014}	3.9	2.7	D1
			14.9 ^{+0.5} _{-0.7}	21 ⁺¹¹ ₋₁₂	0.071 ^{+0.007} _{-0.004}	0.181 ^{+0.018} _{-0.010}	12.0	1.2	D2
6262	Javid	7.8±0.2	7.7 ^{+1.0} _{-0.8}	56 ⁺⁴⁶ ₋₅₆	0.087 ^{+0.023} _{-0.019}	0.222 ^{+0.059} _{-0.048}	35.8	1.9	D1
7043	Godart	5.7±0.1	6.0 ^{+0.6} _{-0.6}	55 ⁺³⁹ ₋₃₁	0.080 ^{+0.018} _{-0.014}	0.204 ^{+0.045} _{-0.036}	27.3	1.6	D1
			5.2 ^{+1.6} _{-0.3}	0 ⁺¹¹⁴ ₋₀	0.092 ^{+0.037} _{-0.024}	0.233 ^{+0.095} _{-0.062}	16.5	3.5	D2
			5.3 ^{+0.6} _{-0.3}	0 ⁺⁶³ ₋₀	0.160 ^{+0.022} _{-0.029}	0.407 ^{+0.055} _{-0.075}	16.5	1.8	R1
			5.5 ^{+0.8} _{-0.4}	1 ⁺²¹ ₋₁	0.150 ^{+0.021} _{-0.037}	0.382 ^{+0.052} _{-0.093}	16.5	1.6	R2
7517	Alisondoane	9.1±0.2	9.2 ^{+1.0} _{-0.7}	1031 ⁺⁴⁶⁹ ₋₄₈₁	0.019 ^{+0.004} _{-0.004}	0.049 ^{+0.009} _{-0.009}	55.4	4.4	D1
			8.0 ^{+0.8} _{-0.3}	122 ⁺⁸⁴ ₋₅₁	0.045 ^{+0.004} _{-0.008}	0.115 ^{+0.009} _{-0.020}	26.7	1.9	R1
7660	Alexanderwilson	3.2±0.5	3.7 ^{+0.1} _{-0.2}	0 ⁺⁴⁷ ₋₀	0.075 ^{+0.009} _{-0.003}	0.192 ^{+0.024} _{-0.007}	16.5	3.3	R2
8359	1989 WD	8.2±0.1	9.6 ^{+0.9} _{-1.5}	115 ⁺⁹⁹ ₋₆₅	0.026 ^{+0.006} _{-0.004}	0.067 ^{+0.016} _{-0.010}	55.4	4.5	D1
			8.7 ^{+0.9} _{-0.9}	207 ⁺²⁴⁰ ₋₁₀₆	0.037 ^{+0.009} _{-0.006}	0.093 ^{+0.022} _{-0.017}	46.8	4.7	D2

Table 4 continued

Table 4 (continued)

Asteroid		D_{WISE}	D	Γ	A	p_V	$\bar{\theta}$	χ_{red}^2	Model ID
		(km)	(km)	($\text{J m}^{-2} \text{s}^{-0.5} \text{K}^{-1}$)			$^\circ$		
14197	1998 XK72	8.1±0.2	7.3 ^{+1.3} _{-0.8}	94 ⁺¹⁶³ ₋₄₂	0.042 ^{+0.011} _{-0.011}	0.106 ^{+0.027} _{-0.028}	26.7	2.7	D1
			7.7 ^{+1.2} _{-0.9}	83 ⁺⁸² ₋₃₉	0.036 ^{+0.010} _{-0.009}	0.092 ^{+0.025} _{-0.023}	26.7	2.5	D2
28736	2000 GE133	6.4±1.5	9.2 ^{+0.6} _{-0.7}	65 ⁺³⁷ ₋₃₆	0.020 ^{+0.004} _{-0.002}	0.050 ^{+0.009} _{-0.006}	26.7	6.5	D1
			9.3 ^{+1.0} _{-0.7}	24 ⁺⁶⁷ ₋₂₄	0.018 ^{+0.003} _{-0.003}	0.045 ^{+0.007} _{-0.008}	16.5	9.9	D2
28887	2000 KQ58	4.4±0.1	4.4 ^{+0.6} _{-0.4}	0 ⁺⁵⁴ ₋₀	0.100 ^{+0.018} _{-0.022}	0.255 ^{+0.047} _{-0.056}	12.6	2.6	D1
			4.3 ^{+0.6} _{-0.5}	8 ⁺⁸³ ₋₈	0.099 ^{+0.024} _{-0.024}	0.253 ^{+0.060} _{-0.062}	16.5	3.9	D2
33116	1998 BO12	4.4±0.1	4.8 ^{+0.3} _{-0.2}	192 ⁺¹²² ₋₇₄	0.091 ^{+0.009} _{-0.010}	0.232 ^{+0.023} _{-0.025}	55.4	1.7	D1
			5.2 ^{+0.3} _{-0.3}	255 ⁺²¹² ₋₁₀₄	0.078 ^{+0.010} _{-0.010}	0.198 ^{+0.026} _{-0.025}	55.4	2.7	D2
44612	1999 RP27	2.0±0.3	2.5 ^{+0.4} _{-0.4}	368 ⁺⁷¹⁶ ₋₂₄₆	0.061 ^{+0.027} _{-0.015}	0.156 ^{+0.069} _{-0.039}	27.3	0.5	D2
55760	1992 BL1		5.4 ^{+0.3} _{-0.1}	95 ⁺⁸⁷ ₋₃₆	0.107 ^{+0.006} _{-0.010}	0.273 ^{+0.015} _{-0.025}	26.7	3.2	D1

* $W3$ band thermal flux measurements used in the TPM fit are partially saturated.

NOTE—Thermophysical properties of a portion of our final 1847 asteroid sample. Here we limit the sample to the 270 asteroids with the most reliable shape models, as defined in §4.2. The full table can be found online. The parameters relevant to the TPM inputs as well as the IDs corresponding to the shape models used are given in Table 5. The Mainzer et al. (2019) NEATM-derived diameter D_{WISE} is given where available as a basis for comparison. The volume equivalent diameter D , thermal inertia Γ , Bond albedo A , visual geometric albedo p_V , Hapke mean surface slope $\bar{\theta}$, and reduced chi-square χ_{red}^2 are all outputs of the best-fit TPM solution. While we find the extremely high qualitative roughness of $\bar{\theta} = 55.4^\circ$ preferred for many TPM fits, the majority of such cases are subject to partial saturation in the $W3$ band flux measurements, which may be corrupting the TPM fit.

Table 5. Shape Models and Thermal Infrared Observations

Asteroid	λ (deg)	β (deg)	P (hr)	Shape Reference(s)	Mod. ID	Den. LC	Tot. LC	N_{W3}	$W3$ Sat.	N_{W4}	$W4$ Sat.	r_{hel} (au)	H (mag)	G	Taxonomy T1 T2	Orbit	
5 Astraea	126	40	16.80061	[1,2,3]	D1	7	25	14	0.171	14	0.000	2.896	6.8	0.15	S	S	MBA
	320	45	16.80062	Revised	R1	7	29										
	122	43	16.80061	Revised	R2	7	29										
14 Irene	95	-11	15.02986	[3,4]	D1	27	33	8	0.238	8	0.167	2.812	6.3	0.15	S	S	MBA
	265	-22	15.02990	Revised	R2	27	37										
17 Thetis	236	19	12.26603	[1,2]	D1	14	53	12	0.158	12	0.000	2.799	7.8	0.15	S	SI	MBA
	240	24	12.26603	Revised	R1	14	57										
	57	12	12.26604	Revised	R2	14	57										
21 Lutetia	54	-7	8.16827	[5]	D1	32	50	10	0.170	10	0.000	2.770	7.3	0.11	M	Xk	MBA
	233	-3	8.16827	Revised	R1	32	54										
	54	-7	8.16827	Revised	R2	32	54										
22 Kalliope	196	3	4.14820	[2,6]	D1	58	102	10	0.219	10	0.167	2.925	6.5	0.21	M	X	MBA
	196	4	4.14820	Revised	R1	58	106										
24 Themis	331	52	8.37419	[7]	D1	23	47	8	0.196	7	0.080	3.418	7.1	0.19	C	B	MBA
	137	59	8.37419	[7]	D2	23	47										
26 Proserpina	88	-52	13.10977	[7]	D1	26	30	15	0.273	15	0.000	2.671	7.5	0.15	S	S	MBA
	86	-48	13.10977	Revised	R1	26	34										
27 Euterpe	258	-42	10.40828	[8]	D1	40	55	5	0.212	6	0.000	2.690	7.0	0.15	S	S	MBA
	107	23	13.68717	[1,3]	D1	3	12	16	0.178	17	0.000	2.644	7.6	0.15	S	SI	MBA
30 Urania	284	20	13.68717	[1,3]	D2	3	12										
	110	24	13.68717	Revised	R1	3	16										
	286	24	13.68717	Revised	R2	3	16										
35 Leukothea	196	0	31.90100	[7]	D1	33	53	12	0.201	13	0.000	2.745	8.5	0.15	C	C	MBA
	15	7	31.90090	[7]	D2	33	53										
	16	8	31.90093	Revised	R1	33	57										
56 Melete	196	1	31.90100	Revised	R2	33	57										
	103	-27	18.14817	[7]	D1	25	38	14	0.166	14	0.000	3.214	8.3	0.15	P	Xk	MBA
	282	-5	18.14817	[7]	D2	25	38										
64 Angelina	102	-24	18.14807	Revised	R1	25	42										
	317	17	8.75032	[2]	D1	2	22	13	0.250	13	0.000	2.375	7.7	0.48	E	Xe	MBA
	138	14	8.75033	[2]	D2	2	22										
68 Leto	319	-1	8.75158	Revised	R1	2	26										
	139	-1	8.75159	Revised	R2	2	26										
69 Hesperia	103	43	14.84547	[2,3,4]	D1	4	16	11	0.192	12	0.000	2.854	6.8	0.05	S	-	MBA
	250	17	5.65534	[3,4]	D1	3	38	14	0.208	14	0.122	2.575	7.0	0.19	M	X	MBA
	71	-2	5.65534	[3,4]	D2	3	38										

Table 5 continued

Table 5 (continued)

Asteroid	λ (deg)	β (deg)	P (hr)	Shape Reference(s)	Mod. ID	Den. LC	Tot. LC	N_{W3}	$W3$ Sat.	N_{W4}	$W4$ Sat.	r_{hel} (au)	H (mag)	G	Taxonomy	Orbit
															T1	T2
	250	16	5.65534	Revised	R1	3	42									
	71	-4	5.65534	Revised	R2	3	42									
71 Niobe	88	-33	35.85210	[7]	D1	15	50	14	0.160	12	0.000	2.867	7.3	0.40	S	Xe MBA
	89	-33	35.85206	Revised	R1	15	54									
72 Feronia	102	-55	8.09068	[3,9]	D1	3	23	15	0.198	15	0.000	2.407	8.9	0.15	TDG	- MBA
	101	-54	8.09068	Revised	R1	3	27									
	285	-46	8.09068	Revised	R2	3	27									
73 Klytia	44	83	8.28307	[4,10]	D1	7	26	13	0.000	13	0.000	2.759	9.0	0.15	S	- MBA
	266	68	8.28307	[4,10]	D2	7	26									
	46	80	8.28307	Revised	R1	7	30									
	229	74	8.28307	Revised	R2	7	30									
76 Freia	140	14	9.97306	[11]	D1	22	38	8	0.105	8	0.000	3.751	7.9	0.15	P	X OMB
	320	17	9.97306	[11]	D2	22	38									
79 Eurynome	54	24	5.97772	[9]	D1	16	39	11	0.125	11	0.000	2.657	8.0	0.25	S	S MBA
	228	30	5.97772	[9]	D2	16	39									
	54	25	5.97773	Revised	R1	16	43									
	227	30	5.97773	Revised	R2	16	43									
80 Sappho	194	-2	14.02949	Revised	R1	8	24	22	0.172	22	0.000	2.360	8.0	0.15	S	S MBA
94 Aurora	58	16	7.22619	[12]	D1	10	22	14	0.202	15	0.136	3.218	7.6	0.15	GP	C MBA
	240	-2	7.22619	Revised	R1	10	26									
	59	9	7.22619	Revised	R2	10	26									
95 Arethusa	149	33	8.70221	[2]	D1	2	5	22	0.153	22	0.000	3.490	7.8	0.15	C	Ch MBA
98 Ianthe	286	18	16.48013	[7]	D1	5	10	11	0.169	11	0.000	2.929	8.8	0.15	CG	Ch MBA
	282	14	16.48017	Revised	R1	5	14									
	112	39	16.48018	Revised	R2	5	14									
99 Dike	233	50	18.11914	[7]	D1	14	30	12	0.000	12	0.000	3.163	9.4	0.15	C	Xk MBA
	230	48	18.11915	Revised	R1	14	34									
	21	42	18.11910	Revised	R2	14	34									
100 Hekate	306	52	27.07030	[13]	D1	29	62	14	0.170	15	0.000	2.612	7.7	0.15	S	S MBA
	104	51	27.07030	[13]	D2	29	62									
	104	50	27.07027	Revised	R1	29	66									
103 Hera	85	24	23.74265	[7]	D1	9	30	14	0.189	14	0.000	2.483	7.7	0.15	S	S MBA
	270	40	23.74266	[7]	D2	9	30									
	270	39	23.74265	Revised	R1	9	34									
	85	24	23.74265	Revised	R2	9	34									
107 Camilla	73	54	4.84393	[2,3,5,14]	D1	5	34	12	0.168	12	0.021	3.738	7.1	0.08	C	X OMB
	71	52	4.84393	Revised	R1	5	38									
109 Felicitas	252	-49	13.19058	[13]	D1	16	62	10	0.043	10	0.000	3.247	8.8	0.04	GC	Ch MBA
	77	-26	13.19055	[13]	D2	16	62									

Table 5 continued

Table 5 (continued)

Asteroid	λ (deg)	β (deg)	P (hr)	Shape Reference(s)	Mod. ID	Den. LC	Tot. LC	N_{W3}	$W3$ Sat.	N_{W4}	$W4$ Sat.	r_{hel} (au)	H (mag)	G	Taxonomy	Orbit
	250	-57	13.19059	Revised	R1	16	66									
110 Lydia	149	-55	10.92580	[15,16]	D1	20	26	13	0.200	13	0.000	2.907	7.8	0.20	M	X MBA
	331	-61	10.92580	[15,16]	D2	20	26									
112 Iphigenia	286	-50	31.46260	[7]	D1	6	8	9	0.179	9	0.000	2.372	9.8	0.15	DCX	Ch MBA
	101	-66	31.46250	[7]	D2	6	8									
119 Althaea	339	-67	11.46514	[4]	D1	1	7	12	0.107	12	0.000	2.503	8.4	0.15	S	SI MBA
	181	-61	11.46514	[4]	D2	1	7									
	339	-62	11.46514	Revised	R1	1	11									
	181	-63	11.46514	Revised	R2	1	11									
121 Hermione	359	8	5.55088	[17]	D1	37	48	8	0.180	11	0.043	3.298	7.3	0.15	C	Ch OMB
	2	12	5.55088	Revised	R1	37	52									
	185	32	5.55087	Revised	R2	37	52									
122 Gerda	23	20	10.68724	[7]	D1	7	18	9	0.000	9	0.000	3.299	7.9	0.15	ST	L OMB
	201	22	10.68724	[7]	D2	7	18									
	201	21	10.68724	Revised	R1	7	22									
	23	20	10.68725	Revised	R2	7	22									
125 Liberatrix	95	68	3.96820	[15]	D1	6	34	14	0.000	14	0.000	2.949	9.0	0.33	M	X MBA
	280	74	3.96820	[15]	D2	6	34									
	290	83	3.96820	Revised	R1	6	38									
155 Scylla	201	69	7.95880	[7]	D1	6	10	29	0.000	29	0.000	3.251	11.4	0.15	XFC	- MBA
	356	53	7.95879	[7]	D2	6	10									
157 Dejanira	146	-33	15.82860	[9]	D1	11	17	8	0.000	8	0.000	2.886	10.6	0.15	-	- MBA
	319	-64	15.82870	[9]	D2	11	17									
159 Aemilia	139	68	24.47869	[18]	D1	17	45	11	0.118	11	0.000	3.416	8.1	0.15	C	Ch MBA
	348	59	24.47866	[18]	D2	17	45									
	344	60	24.47871	Revised	R1	17	49									
	137	71	24.47869	Revised	R2	17	49									
162 Laurentia	139	64	11.86917	[4]	D1	1	7	12	0.174	12	0.000	3.282	8.8	0.15	STU	Ch MBA
	313	51	11.86918	[4]	D2	1	7									
	323	46	11.86918	Revised	R1	1	11									
	147	60	11.86917	Revised	R2	1	11									
166 Rhodope	173	-3	4.71480	[9]	D1	2	9	15	0.080	15	0.000	2.705	9.9	0.15	GC;	Xe MBA
	345	-22	4.71479	[9]	D2	2	9									
	346	-17	4.71478	Revised	R1	2	13									
	170	2	4.71478	Revised	R2	2	13									
167 Urda	107	-69	13.06133	[2,19,20]	D1	7	20	24	0.000	24	0.000	2.842	9.2	0.15	S	Sk MBA
	249	-68	13.06133	[2,19,20]	D2	7	20									
171 Ophelia	149	25	6.66543	Revised	R1	27	42	10	0.158	10	0.000	2.879	8.3	0.15	C	C MBA
	330	24	6.66544	Revised	R2	27	42									

Table 5 continued

Table 5 (continued)

Asteroid	λ (deg)	β (deg)	P (hr)	Shape Reference(s)	Mod. ID	Den. LC	Tot. LC	N_{W3}	W3 Sat.	N_{W4}	W4 Sat.	τ_{hel} (au)	H (mag)	G	Taxonomy	Orbit	
														T1	T2		
174 Phaedra	266	5	5.75025	[12]	D1	18	36	11	0.000	11	0.000	3.219	8.5	0.15	S	S	MBA
	266	4	5.75025	Revised	R1	18	40										
	89	26	5.75025	Revised	R2	18	40										
176 Iduna	85	29	11.28783	[21,22]	D1	7	11	12	0.021	12	0.000	3.608	7.9	0.15	G	Ch	MBA
	156	79	11.28783	[21,22]	D2	7	11										
	87	29	11.28783	Revised	R1	7	15										
	2	88	11.28784	Revised	R2	7	15										
180 Garumna	41	-64	23.85920	[7]	D1	12	24	11	0.000	11	0.000	3.157	10.3	0.15	S	Sq	MBA
	196	-64	23.85920	[7]	D2	12	24										
184 Dejopeja	200	52	6.44111	[3,23]	D1	10	17	10	0.000	11	0.000	3.159	8.3	0.15	X	X	MBA
	18	54	6.44111	[3,23]	D2	10	17										
	196	50	6.44111	Revised	R1	10	21										
	16	53	6.44111	Revised	R2	10	21										
187 Lamberta	328	-62	10.66703	[7]	D1	7	21	13	0.207	13	0.000	2.885	8.2	0.15	C	Ch	MBA
	153	-56	10.66703	[7]	D2	7	21										
	134	-65	10.66703	Revised	R1	7	25										
	352	-79	10.66703	Revised	R2	7	25										
189 Phthia	197	45	22.34154	[7]	D1	11	17	11	0.000	12	0.000	2.471	9.3	0.15	S	Sa	MBA
	26	35	22.34156	[7]	D2	11	17										
	11	36	22.34164	Revised	R1	11	21										
	185	34	22.34162	Revised	R2	11	21										
192 Nausikaa	139	-45	13.62523	[6,24]	D1	16	23	15	0.167	18	0.000	2.928	7.1	0.03	S	Sl	MBA
	340	-48	13.62524	Revised	R1	16	31										
	138	-46	13.62523	Revised	R2	16	31										
193 Ambrosia	141	-11	6.58167	[9]	D1	15	21	8	0.000	8	0.000	3.256	9.7	0.15	-	Sk	MBA
	328	-17	6.58167	[9]	D2	15	21										
	140	-10	6.58168	Revised	R1	15	25										
	326	-16	6.58168	Revised	R2	15	25										
195 Eurykleia	101	71	16.52178	[13]	D1	26	51	14	0.150	14	0.000	2.760	9.0	0.15	C	Ch	MBA
	352	83	16.52179	[13]	D2	26	51										
	20	86	16.52179	Revised	R1	26	55										
	274	66	16.52179	Revised	R2	26	55										
196 Philomela	111	-41	8.33283	[15]	D1	16	28	13	0.191	14	0.000	3.171	6.5	0.15	S	S	MBA
	276	-49	8.33283	[15]	D2	16	28										
	112	-41	8.33283	Revised	R1	16	32										
	276	-49	8.33283	Revised	R2	16	32										
199 Byblis	165	9	5.22063	[9]	D1	12	24	15	0.167	15	0.000	2.958	8.3	0.15	-	X	MBA
	344	-24	5.22063	[9]	D2	12	24										
208 Lacrimosa	202	61	14.08574	[2,19,25]	D1	9	20	20	0.000	20	0.000	2.902	9.0	0.15	S	Sk	MBA

Table 5 continued

Table 5 (continued)

Asteroid	λ (deg)	β (deg)	P (hr)	Shape Reference(s)	Mod. ID	Den. LC	Tot. LC	N_{W3}	$W3$ Sat.	N_{W4}	$W4$ Sat.	r_{hel} (au)	H (mag)	G	Taxonomy	Orbit
	16	60	14.08574	[2,19,25]	D2	9	20									
	212	48	14.08574	Revised	R1	9	28									
	23	51	14.08575	Revised	R2	9	28									
218 Bianca	305	17	6.33717	[15]	D1	35	50	15	0.103	14	0.000	2.358	8.6	0.32	S	MBA
	298	-24 ^a	6.33646	Revised	R1	35	54									
	137	-49 ^a	6.33646	Revised	R2	35	54									
220 Stephania	26	-50	18.20870	[9]	D1	4	12	12	0.000	12	0.000	2.792	11.0	0.15	XC	MBA
	223	-62	18.20880	[9]	D2	4	12									
	32	-42	18.20866	Revised	R1	4	16									
	224	-57	18.20871	Revised	R2	4	16									
221 Eos	289	-23	10.44212	[26]	D1	14	29	16	0.160	16	0.000	2.693	7.7	0.13	S	K MBA
	119	-37	10.44213	[26]	D2	14	29									
222 Lucia	293	49	7.83670	[9]	D1	5	12	14	0.000	14	0.000	2.868	9.1	0.15	BU	MBA
	106	50	7.83671	[9]	D2	5	12									
	109	50	7.83670	Revised	R1	5	16									
	290	49	7.83670	Revised	R2	5	16									
226 Weringia	284	-14	11.14849	[7]	D1	12	25	11	0.000	11	0.000	3.126	9.7	0.15	-	S MBA
	288	-17	11.14846	Revised	R1	12	29									
242 Kriemhild	284	-15	4.54518	[9]	D1	15	27	17	0.000	17	0.000	2.923	9.2	0.15	-	Xc MBA
	100	-40	4.54517	[9]	D2	15	27									
	283	-19	4.54518	Revised	R1	15	31									
	98	-47	4.54518	Revised	R2	15	31									
245 Vera	96	-50	14.35651	[7]	D1	2	4	13	0.085	13	0.000	2.925	7.8	0.15	S	S MBA
	265	-51	14.35651	[7]	D2	2	4									
254 Augusta	25	-53	5.89505	[7]	D1	4	7	14	0.000	14	0.000	1.929	12.1	0.15	S	MBA
	179	-52	5.89505	[7]	D2	4	7									
260 Huberta	206	-19	8.29055	[9]	D1	3	9	12	0.000	12	0.000	3.640	9.0	0.15	CX:	OMB
	23	-28	8.29055	[9]	D2	3	9									
	214	-25	8.29056	Revised	R1	3	13									
	28	-32	8.29058	Revised	R2	3	13									
264 Libussa	157	18	9.22794	[4]	D1	17	22	14	0.032	13	0.000	3.109	8.4	0.15	S	MBA
	338	-9	9.22795	[4]	D2	17	22									
	159	15	9.22795	Revised	R1	17	26									
	339	-8	9.22796	Revised	R2	17	26									
270 Anahita	15	-50	15.05906	[7]	D1	1	13	22	0.147	22	0.000	2.254	8.8	0.15	S	MBA
	207	-59	15.05907	[7]	D2	1	13									
271 Penthesilea	225	49	18.78750	[7]	D1	6	10	24	0.000	24	0.000	3.309	9.8	0.15	PC	MBA
	42	53	18.78740	[7]	D2	6	10									
272 Antonia	293	-90	3.85480	[9]	D1	6	10	12	0.000	12	0.000	2.858	10.7	0.15	-	X MBA

Table 5 continued

Table 5 (continued)

Asteroid	λ (deg)	β (deg)	P (hr)	Shape Reference(s)	Mod. ID	Den. LC	Tot. LC	N_{W3}	W3 Sat.	N_{W4}	W4 Sat.	r_{hel} (au)	H (mag)	G	Taxonomy	Orbit
	38	-88	3.85480	Revised	R1	6	14									
274 Philagoria	274	-78	17.94082	[7]	D1	5	7	13	0.000	13	0.000	2.677	10.1	0.15	-	MBA
	114	-66	17.94072	[7]	D2	5	7									
276 Adelheid	9	-4	6.31920	[2,3,23]	D1	17	31	17	0.075	17	0.000	3.307	8.6	0.15	X	MBA
	199	-20	6.31920	[2,3,23]	D2	17	31									
281 Lucretia	128	-49	4.34971	[9]	D1	3	10	9	0.000	9	0.000	2.471	12.0	0.28	SU	S MBA
	309	-61	4.34971	[9]	D2	3	10									
	140	-43	4.34971	Revised	R1	3	14									
	349	-64	4.34971	Revised	R2	3	14									
287 Nephthys	356	36	7.60411	[7]	D1	2	10	13	0.146	13	0.000	2.405	8.3	0.22	S	MBA
	158	39	7.60410	[7]	D2	2	10									
	358	46	7.60411	Revised	R1	2	14									
	159	38	7.60411	Revised	R2	2	14									
290 Bruna	37	-74	13.80556	[9]	D1	8	11	26	0.000	25	0.000	2.302	11.5	0.15	-	MBA
	286	-80	13.80554	[9]	D2	8	11									
293 Brasilia	274	-34	8.17409	[7]	D1	3	5	12	0.148	12	0.000	2.561	9.9	0.15	CX	MBA
	103	-7	8.17410	[7]	D2	3	5									
296 Phaetusa	146	53	4.53809	[7]	D1	4	6	22	0.000	23	0.000	1.912	12.6	0.15	S	MBA
	330	52	4.53809	[7]	D2	4	6									
301 Bavaria	226	70	12.24090	[13]	D1	16	30	13	0.067	12	0.000	2.587	10.1	0.15	-	MBA
	46	61	12.24090	[13]	D2	16	30									
310 Margarita	218	62	12.24092	Revised	R1	16	34									
	225	-35	12.07098	[4]	D1	12	30	13	0.000	13	0.000	2.469	10.3	0.15	-	MBA
	42	-33	12.07095	[4]	D2	12	30									
	227	-33	12.07097	Revised	R1	12	34									
	41	-32	12.07106	Revised	R2	12	34									
311 Claudia	30	40	7.53138	[4,19]	D1	3	27	14	0.000	14	0.000	2.913	9.9	0.15	S	MBA
	214	43	7.53138	[4,19]	D2	3	27									
	25	49	7.53139	Revised	R1	3	31									
	211	41	7.53139	Revised	R2	3	31									
312 Pierretta	82	-39	10.20764	[4]	D1	1	7	14	0.000	14	0.000	2.756	8.9	0.15	S	Sk MBA
	256	-58	10.20765	[4]	D2	1	7									
	83	-38	10.20765	Revised	R1	1	11									
	253	-53	10.20765	Revised	R2	1	11									
315 Constantia	162	56	5.34750	[7]	D1	1	6	13	0.000	13	0.000	2.484	13.2	0.15	-	MBA
	353	45	5.34749	[7]	D2	1	6									
317 Roxane	220	-62	8.16961	[7]	D1	8	17	15	0.000	15	0.000	2.283	10.0	0.15	E	Xe MBA
	40	-70	8.16961	[7]	D2	8	17									
321 Florentina	95	-60	2.87087	[19]	D1	10	29	15	0.000	15	0.000	2.765	10.0	0.15	S	S MBA

Table 5 continued

Table 5 (continued)

Asteroid	λ (deg)	β (deg)	P (hr)	Shape Reference(s)	Mod. ID	Den. LC	Tot. LC	N_{W3}	W3 Sat.	N_{W4}	W4 Sat.	r_{hel} (au)	H (mag)	G	Taxonomy	Orbit
	267	-66	2.87087	[19]	D2	10	29									
	267	-69	2.87087	Revised	R1	10	33									
329 Svea	33	51	22.76703	[18]	D1	19	60	17	0.162	17	0.000	2.457	9.7	0.15	C	MBA
	204	-24 ^a	22.77573	Revised	R1	19	64									
	357	-26 ^a	22.77576	Revised	R2	19	64									
335 Roberta	105	48	12.02713	[13]	D1	23	52	12	0.170	12	0.000	2.700	9.0	0.15	FP	B MBA
	297	54	12.02713	[13]	D2	23	52									
	106	50	12.02713	Revised	R1	23	56									
	301	54	12.02714	Revised	R2	23	56									
349 Dembowska	322	18	4.70120	[3,5]	D1	13	40	18	0.183	18	0.000	3.131	5.9	0.37	R	R MBA
350 Ornamenta	184	-29	9.18041	[27]	D1	21	37	28	0.150	28	0.000	3.511	8.4	0.15	C	MBA
	184	-32	9.18041	Revised	R1	21	45									
351 Yrsa	193	-41	13.31198	[9]	D1	1	5	11	0.000	11	0.000	3.148	9.0	0.15	S	MBA
	20	-70	13.31195	[9]	D2	1	5									
	194	-39	13.31194	Revised	R1	1	9									
352 Gisela	24	-21	7.48008	[9]	D1	1	8	16	0.000	16	0.000	2.284	10.0	0.15	S	SI MBA
	206	-28	7.48008	[9]	D2	1	8									
	207	-35	7.48008	Revised	R1	1	12									
	24	-30	7.48008	Revised	R2	1	12									
355 Gabriella	341	83	4.82899	[4,11]	D1	6	16	24	0.000	24	0.000	2.273	10.4	0.15	-	S MBA
	177	89	4.82899	Revised	R1	6	20									
360 Carlota	350	55	6.18959	[1]	D1	4	9	26	0.182	26	0.000	2.956	8.5	0.15	C	MBA
	106	50	6.18959	Revised	R1	4	13									
	354	61	6.18959	Revised	R2	4	13									
364 Isara	67	59	9.15753	[28]	D1	3	6	9	0.000	10	0.000	2.401	9.9	0.15	S	MBA
	283	44	9.15751	[28]	D2	3	6									
365 Corduba	80	4	12.70548	[7]	D1	20	50	23	0.174	23	0.000	3.063	9.2	0.15	X	C MBA
	255	33	12.70544	[7]	D2	20	50									
	254	30	12.70543	Revised	R1	20	54									
	78	1	12.70543	Revised	R2	20	54									
371 Bohemia	93	49	10.73965	[9]	D1	15	33	10	0.069	10	0.000	2.559	8.7	0.15	QSV	S MBA
	256	43	10.73965	[9]	D2	15	33									
	258	43	10.73964	Revised	R1	15	37									
	99	51	10.73964	Revised	R2	15	37									
372 Palma	221	-47	8.58189	[2,4]	D1	3	31	16	0.153	16	0.000	3.740	7.2	0.15	BFC	B MBA
	44	17	8.58191	[2,4]	D2	3	31									
376 Geometria	239	45	7.71097	[4,29]	D1	4	40	13	0.101	13	0.000	2.110	9.5	0.15	S	SI MBA
	63	53	7.71098	[4,29]	D2	4	40									
377 Campania	47	67	11.66440	[10]	D1	11	34	16	0.158	16	0.000	2.832	8.9	0.15	PD	Ch MBA

Table 5 continued

Table 5 (continued)

Asteroid	λ (deg)	β (deg)	P (hr)	Shape Reference(s)	Mod. ID	Den. LC	Tot. LC	N_{W3}	$W3$ Sat.	N_{W4}	$W4$ Sat.	τ_{hel} (au)	H (mag)	G	Taxonomy	Orbit
															T1	T2
378 Holmia	196	66	11.66440	[10]	D2	11	34									
	130	60	4.44043	[10]	D1	6	13	12	0.000	13	0.000	2.763	9.8	0.15	S	S MBA
	286	76	4.44043	[10]	D2	6	13									
380 Fiducia	202	44	13.71720	[13]	D1	16	37	12	0.158	12	0.000	2.474	9.4	0.15	C	– MBA
	21	34	13.71720	[13]	D2	16	37									
	208	44	13.71726	Revised	R1	16	41									
	24	34	13.71726	Revised	R2	16	41									
381 Myrrha	31	44	6.57195	[7]	D1	5	11	36	0.164	37	0.000	3.031	8.2	0.15	C	Cb OMB
	228	79	6.57195	[7]	D2	5	11									
	175	75	6.57195	Revised	R1	5	19									
	12	50	6.57195	Revised	R2	5	19									
390 Alma	275	-76	3.74117	[9]	D1	4	7	14	0.000	14	0.000	2.422	10.4	0.15	DT	– MBA
	53	-50	3.74117	[9]	D2	4	7									
	58	-59	3.74117	Revised	R1	4	11									
	260	-71	3.74117	Revised	R2	4	11									
391 Ingeborg	354	-65	26.41460	[7]	D1	8	25	26	0.000	26	0.000	2.284	10.1	0.15	S	S MCA
394 Arduina	195	-61	16.62174	[7]	D1	1	9	11	0.000	11	0.000	2.893	9.7	0.15	S	S MBA
	56	-79	16.62174	[7]	D2	1	9									
400 Ducrosa	328	56	6.86788	[4]	D1	1	4	12	0.000	11	0.000	3.375	10.1	0.15	–	– MBA
	158	62	6.86789	[4]	D2	1	4									
	153	55	6.86789	Revised	R1	1	8									
	302	53	6.86790	Revised	R2	1	8									
402 Chloe	160	-37	10.66844	[7]	D1	9	14	13	0.089	14	0.000	2.425	9.0	0.15	S	K MBA
	312	-49	10.66844	[7]	D2	9	14									
404 Arsinoe	25	57	8.88766	[9]	D1	36	51	10	0.205	10	0.000	3.093	9.0	0.15	C	MBA
	27	58	8.88766	Revised	R1	36	55									
406 Erna	357	-49	8.79079	[9]	D1	4	10	13	0.125	14	0.000	2.404	10.4	0.15	P	– MBA
	161	-60	8.79078	[9]	D2	4	10									
416 Vaticana	291	12	5.37160	[1]	D1	9	25	5	0.000	6	0.000	3.183	7.9	0.20	S	SI MBA
	289	14	5.37160	Revised	R1	9	29									
417 Suevia	13	23	7.01849	[11]	D1	22	37	14	0.000	14	0.000	3.153	9.3	0.15	X	Xk MBA
	186	20	7.01849	[11]	D2	22	37									
	187	16	7.01849	Revised	R1	22	41									
	13	19	7.01848	Revised	R2	22	41									
423 Diotima	351	4	4.77538	[3,15,24]	D1	38	58	12	0.202	12	0.134	3.183	7.2	0.15	C	C MBA
	349	1	4.77538	Revised	R1	38	62									
	173	30	4.77538	Revised	R2	38	62									
436 Patricia	339	-58	16.13200	[4]	D2	3	8	11	0.000	12	0.000	3.398	9.8	0.15	–	– OMB
441 Bathilde	122	43	10.44313	[9]	D1	15	34	15	0.080	15	0.000	2.935	8.5	0.15	M	Xk MBA

Table 5 continued

Table 5 (continued)

Asteroid	λ (deg)	β (deg)	P (hr)	Shape Reference(s)	Mod. ID	Den. LC	Tot. LC	N_{W3}	W3 Sat.	N_{W4}	W4 Sat.	r_{hel} (au)	H (mag)	G	Taxonomy	Orbit
															T1	T2
	285	55	10.44313	[9]	D2	15	34									
	121	42	10.44313	Revised	R1	15	38									
	286	54	10.44313	Revised	R2	15	38									
450 Brigitta	203	-26	10.76437	[26]	D1	4	12	13	0.000	13	0.000	2.790	10.3	0.15	CSU	MBA
	32	-16	10.76437	[26]	D2	4	12									
	203	-22	10.76439	Revised	R1	4	16									
	32	-14	10.76437	Revised	R2	4	16									
468 Lina	74	68	16.47838	[13]	D1	15	40	17	0.250	18	0.000	2.514	9.8	0.15	CPF	MBA
	255	68	16.47838	[13]	D2	15	40									
	92	49	16.47838	Revised	R1	15	44									
	273	51	16.47838	Revised	R2	15	44									
474 Prudentia	135	-65	8.57228	[7]	D1	3	6	16	0.171	17	0.000	1.929	10.6	0.15	-	MBA
	301	-51	8.57227	[7]	D2	3	6									
	130	-73	8.57226	Revised	R1	3	10									
	288	-67	8.57227	Revised	R2	3	10									
478 Tergeste	2	-42	16.10310	[18]	D1	17	48	10	0.000	10	0.000	3.266	8.0	0.15	S	L MBA
	216	-56	16.10311	[18]	D2	17	48									
	0	-50	16.10310	Revised	R1	17	52									
482 Petrina	281	61	11.79214	[7]	D1	37	43	12	0.000	12	0.000	3.284	8.8	0.15	S	MBA
	94	24	11.79210	[7]	D2	37	43									
487 Venetia	78	3	13.34133	[18]	D1	20	34	24	0.042	24	0.000	2.906	8.1	0.15	S	MBA
	252	3	13.34135	[18]	D2	20	34									
	260	2	13.34137	Revised	R1	20	42									
	70	-4	13.34134	Revised	R2	20	42									
495 Eulalia	212	46	28.96590	[30]	D1	18	44	11	0.000	11	0.000	2.801	10.8	0.15	-	MBA
	38	35	28.96590	[30]	D2	18	44									
	38	28	28.96572	Revised	R1	18	48									
	215	29	28.96569	Revised	R2	18	48									
497 Iva	303	-32	4.62085	[7]	D1	3	9	15	0.000	15	0.000	3.580	10.0	0.11	M	MBA
	121	-22	4.62085	[7]	D2	3	9									
	120	-34	4.62085	Revised	R1	3	13									
	304	-45	4.62085	Revised	R2	3	13									
502 Sigune	178	-36	10.92666	[7]	D1	15	24	18	0.000	18	0.000	2.008	10.8	0.15	S	MBA
	184	-39	10.92666	Revised	R1	15	28									
	285	-45	10.92666	Revised	R2	15	28									
520 Franziska	282	-79	16.50448	[7]	D1	6	10	25	0.000	24	0.000	3.307	10.6	0.15	CGU	MBA
	114	-45	16.50449	[7]	D2	6	10									
	278	-65	16.50451	Revised	R1	6	18									
	109	-43	16.50449	Revised	R2	6	18									

Table 5 continued

Table 5 (continued)

Asteroid	λ (deg)	β (deg)	P (hr)	Shape Reference(s)	Mod. ID	Den. LC	Tot. LC	N_{W3}	$W3$ Sat.	N_{W4}	$W4$ Sat.	τ_{hel} (au)	H (mag)	G	Taxonomy	Orbit	
															T1	T2	
528 Rezia	176	-59	7.33797	[9]	D1	2	8	12	0.000	12	0.000	3.461	9.1	0.15	-	-	OMB
	46	-66	7.33797	[9]	D2	2	8										
531 Zerlina	78	-84	16.70730	[9]	D1	21	30	14	0.000	14	0.000	3.071	11.8	0.15	-	-	MBA
	78	-84	16.70728	Revised	R1	21	34										
538 Friederike	328	-59	46.73990	[13]	D1	1	98	23	0.000	23	0.000	3.587	9.3	0.15	-	-	MBA
	168	-58	46.73930	[13]	D2	1	98										
540 Rosamunde	127	62	9.34779	[28]	D1	2	5	16	0.000	16	0.000	2.368	10.8	0.15	S	-	MBA
	301	81	9.34779	[28]	D2	2	5										
544 Jetta	21	-71	7.74528	[4]	D1	1	5	13	0.000	13	0.000	2.992	9.9	0.15	-	-	MBA
	267	-89	7.74528	[4]	D2	1	5										
	360	-61	7.74529	Revised	R1	1	9										
	90	-88	7.74529	Revised	R2	1	9										
550 Senta	63	-40	20.57260	[28]	D1	6	11	28	0.000	29	0.000	3.149	9.4	0.15	S	-	MBA
	258	-58	20.57270	[28]	D2	6	11										
	52	-44	20.57264	Revised	R1	6	15										
	263	-64	20.57261	Revised	R2	6	15										
553 Kundry	359	64	12.60244	[28]	D1	4	7	16	0.000	16	0.000	2.371	12.2	0.15	-	-	MBA
	197	73	12.60247	[28]	D2	4	7										
556 Phyllis	209	41	4.29262	[23]	D1	7	19	25	0.000	25	0.000	2.500	9.6	0.15	S	S	MBA
	34	54	4.29262	[23]	D2	7	19										
	33	49	4.29262	Revised	R1	7	23										
	210	40	4.29262	Revised	R2	7	23										
562 Salome	268	44	6.35032	[7,26]	D1	13	27	28	0.000	28	0.000	3.098	9.9	0.15	S	-	MBA
	54	56	6.35032	[7,26]	D2	13	27										
	277	41	6.35031	Revised	R1	13	35										
	77	39	6.35031	Revised	R2	13	35										
567 Eleutheria	317	33	7.71743	[7]	D1	14	20	22	0.160	24	0.000	2.873	9.2	0.15	CFB:	-	MBA
	131	53	7.71743	[7]	D2	14	20										
	316	35	7.71743	Revised	R1	14	28										
	132	53	7.71744	Revised	R2	14	28										
573 Recha	76	-26	7.16585	[4,26]	D1	8	12	16	0.000	16	0.000	2.659	9.6	0.15	-	-	MBA
	77	-28	7.16585	Revised	R1	8	16										
590 Tomyris	274	-30	5.55248	[4,26]	D1	1	8	14	0.000	14	0.000	3.061	9.9	0.15	-	-	MBA
	113	-35	5.55248	[4,26]	D2	1	8										
	272	-35	5.55248	Revised	R1	1	12										
	111	-30	5.55248	Revised	R2	1	12										
595 Polyxena	42	8	11.79416	[31]	D1	6	10	12	0.101	12	0.000	3.068	8.0	0.15	-	-	OMB
	222	-4	11.79416	[31]	D2	6	10										
	42	6	11.79416	Revised	R1	6	14										

Table 5 continued

Table 5 (continued)

Asteroid	λ (deg)	β (deg)	P (hr)	Shape Reference(s)	Mod. ID	Den. LC	Tot. LC	N_{W3}	W3 Sat.	N_{W4}	W4 Sat.	τ_{hel} (au)	H (mag)	G	Taxonomy	Orbit
	222	-3	11.79416	Revised	R2	6	14									
596 Scheila	264	-18	15.86660	[7]	D1	5	9	11	0.152	12	0.000	3.395	8.9	0.15	PCD	T MBA
	89	-9	15.86660	[7]	D2	5	9									
600 Musa	208	-46	5.88638	[9]	D1	14	26	10	0.000	10	0.000	2.528	10.2	0.15	-	S MBA
	360	-74	5.88638	[9]	D2	14	26									
	213	-47	5.88638	Revised	R1	14	30									
	10	-74	5.88638	Revised	R2	14	30									
608 Adolfin	172	30	8.34487	[21]	D1	9	12	11	0.000	11	0.000	3.243	10.6	0.15	-	MBA
	343	43	8.34489	[21]	D2	9	12									
	347	40	8.34492	Revised	R1	9	16									
	170	12	8.34495	Revised	R2	9	16									
616 Elly	353	86	5.29770	[21,22]	D1	16	21	14	0.000	14	0.000	2.518	10.7	0.15	S	- MBA
	263	55	5.29770	[21,22]	D2	16	21									
	263	54	5.29770	Revised	R1	16	25									
	355	85	5.29770	Revised	R2	16	25									
624 Hektor	333	-31	6.92051	[32,33]	D1	11	21	11	0.000	11	0.000	5.269	7.5	0.15	D	- T,JN
	333	-32	6.92051	Revised	R1	11	25									
	134	-18	6.92051	Revised	R2	11	25									
628 Christine	209	-34	16.17290	[1]	D2	3	7	24	0.042	24	0.000	2.659	9.2	0.15	SD	- MBA
631 Philippina	183	-2	5.90220	[4]	D1	1	8	22	0.000	24	0.000	2.782	8.7	0.15	S	S MBA
	182	-1	5.90221	Revised	R1	1	12									
	12	29 ^a	5.90220	Revised	R2	1	12									
632 Pyrrha	253	-74	4.11686	[7]	D1	4	6	13	0.000	13	0.000	3.075	11.6	0.15	-	MBA
	74	-72	4.11686	[7]	D2	4	6									
639 Latona	25	12	6.19127	[7]	D1	4	7	12	0.042	12	0.000	3.327	8.2	0.15	S	- MBA
	204	10	6.19127	[7]	D2	4	7									
644 Cosima	100	-30	7.55709	[7]	D1	12	17	21	0.000	21	0.000	2.997	11.1	0.15	S	- MBA
	278	-31	7.55709	[7]	D2	12	17									
	279	-34	7.55710	Revised	R1	12	25									
	100	-30	7.55709	Revised	R2	12	25									
653 Berenike	147	18	12.48356	[13]	D1	16	39	8	0.000	9	0.000	3.015	9.2	0.15	S	K MBA
	335	9	12.48357	[13]	D2	16	39									
	340	37	12.48393	Revised	R1	16	43									
660 Crescentia	68	11	7.91036	[7]	D2	14	19	29	0.059	29	0.000	2.295	9.1	0.15	S	- MBA
673 Edda	66	64	22.33410	[13]	D1	16	49	15	0.000	15	0.000	2.811	10.2	0.15	S	S MBA
	236	63	22.33410	[13]	D2	16	49									
	61	64	22.33414	Revised	R1	16	53									
	229	71	22.33414	Revised	R2	16	53									
679 Pax	42	-5	8.45602	[12]	D1	23	42	36	0.000	37	0.000	3.214	9.0	0.15	I	K MBA

Table 5 continued

Table 5 (continued)

Asteroid	λ (deg)	β (deg)	P (hr)	Shape Reference(s)	Mod. ID	Den. LC	Tot. LC	N_{W3}	$W3$ Sat.	N_{W4}	$W4$ Sat.	r_{hel} (au)	H (mag)	G	Taxonomy	Orbit	
														T1	T2		
687 Tinette	220	32	8.45602	[12]	D2	23	42	12	0.000	12	0.000	3.249	11.7	0.15	X	X	MBA
	100	43	7.39710	[7]	D1	2	4	12	0.000	12	0.000	3.249	11.7	0.15	X	X	MBA
	271	18	7.39710	[7]	D2	2	4	12	0.000	12	0.000	3.249	11.7	0.15	X	X	MBA
692 Hippodamia	233	-53	8.99690	[7]	D1	2	4	12	0.000	11	0.000	3.850	9.2	0.15	S	-	OMB
699 Hela	197	31	3.39623	-	D2	6	21	13	0.000	13	0.000	3.671	11.7	0.15	S	Sq	MCA
	45	46	3.39623	Revised	R1	6	24	13	0.000	13	0.000	3.671	11.7	0.15	S	Sq	MCA
	197	31	3.39623	Revised	R2	6	24	13	0.000	13	0.000	3.671	11.7	0.15	S	Sq	MCA
725 Amanda	320	-70	3.74311	[9]	D1	6	20	13	0.000	13	0.000	2.099	11.8	0.15	CSU	-	MBA
	145	-63	3.74311	[9]	D2	6	20	13	0.000	13	0.000	2.099	11.8	0.15	CSU	-	MBA
	320	-68	3.74311	Revised	R2	6	24	13	0.000	13	0.000	2.099	11.8	0.15	CSU	-	MBA
731 Sorgia	274	21	8.18632	[9]	D1	5	12	13	0.000	13	0.000	3.293	9.6	0.15	CD	Xe	MBA
	83	42	8.18632	[9]	D2	5	12	13	0.000	13	0.000	3.293	9.6	0.15	CD	Xe	MBA
	78	51	8.18634	Revised	R1	5	16	16	0.000	16	0.000	3.293	9.6	0.15	CD	Xe	MBA
	274	26	8.18632	Revised	R2	5	16	16	0.000	16	0.000	3.293	9.6	0.15	CD	Xe	MBA
742 Edisona	9	-64	18.58330	[7,26]	D1	12	23	16	0.000	16	0.000	2.650	9.6	0.15	S	K	MBA
	170	-39	18.58320	[7,26]	D2	12	23	16	0.000	16	0.000	2.650	9.6	0.15	S	K	MBA
	173	-39	18.58327	Revised	R1	12	27	16	0.000	16	0.000	2.650	9.6	0.15	S	K	MBA
	364	-64	18.58326	Revised	R2	12	27	16	0.000	16	0.000	2.650	9.6	0.15	S	K	MBA
746 Marlu	202	-66	7.78887	[7]	D1	7	12	10	0.000	10	0.000	3.428	10.0	0.15	P	-	MBA
	64	-27	7.78887	[7]	D2	7	12	10	0.000	10	0.000	3.428	10.0	0.15	P	-	MBA
749 Malzovia	246	55	5.92748	[7]	D1	4	6	12	0.000	14	0.000	2.223	11.8	0.15	S	S	MBA
	55	46	5.92748	[7]	D2	4	6	12	0.000	14	0.000	2.223	11.8	0.15	S	S	MBA
	58	48	5.92748	Revised	R1	4	10	12	0.000	12	0.000	2.223	11.8	0.15	S	S	MBA
	247	50	5.92749	Revised	R2	4	10	12	0.000	12	0.000	2.223	11.8	0.15	S	S	MBA
756 Lilliana	53	36	7.83252	[7]	D1	19	22	12	0.000	12	0.000	3.520	9.6	0.15	-	-	MBA
	201	31	7.83250	[7]	D2	19	22	12	0.000	12	0.000	3.520	9.6	0.15	-	-	MBA
	198	37	7.83251	Revised	R1	19	26	12	0.000	12	0.000	3.520	9.6	0.15	-	-	MBA
	54	36	7.83251	Revised	R2	19	26	12	0.000	12	0.000	3.520	9.6	0.15	-	-	MBA
757 Portlandia	263	-69	6.58112	[7]	D1	7	13	16	0.000	16	0.000	2.513	10.2	0.15	XF	Xk	MBA
	90	-56	6.58112	[7]	D2	7	13	16	0.000	16	0.000	2.513	10.2	0.15	XF	Xk	MBA
	286	-84	6.58112	Revised	R1	7	17	16	0.000	16	0.000	2.513	10.2	0.15	XF	Xk	MBA
	71	-60	6.58111	Revised	R2	7	17	16	0.000	16	0.000	2.513	10.2	0.15	XF	Xk	MBA
758 Mancunia	303	40	12.72013	[7]	D1	10	18	11	0.000	11	0.000	3.576	8.2	0.15	X	-	MBA
	114	52	12.72010	[7]	D2	10	18	11	0.000	11	0.000	3.576	8.2	0.15	X	-	MBA
771 Libera	64	-78	5.89042	[27,32]	D1	8	20	31	0.000	31	0.000	3.111	10.5	0.15	X	X	MBA
	77	-75	5.89042	Revised	R1	8	28	31	0.000	31	0.000	3.111	10.5	0.15	X	X	MBA
775 Lumtete	248	47	6.10301	[21]	D1	4	16	15	0.000	15	0.000	3.217	10.4	0.15	S	-	MBA
	89	55	6.10300	[21]	D2	4	16	15	0.000	15	0.000	3.217	10.4	0.15	S	-	MBA
776 Berbericia	347	12	7.66701	[15]	D1	17	36	13	0.173	13	0.000	3.379	7.7	0.34	C	Cgh	MBA

Table 5 continued

Table 5 (continued)

Asteroid	λ (deg)	β (deg)	P (hr)	Shape Reference(s)	Mod. ID	Den. LC	Tot. LC	N_{W3}	$W3$ Sat.	N_{W4}	$W4$ Sat.	τ_{hel} (au)	H (mag)	G	Taxonomy	Orbit
	171	61 ^d	7.66701	Revised	R2	17	40									
787 Moskva	331	59	6.05581	[9]	D1	8	18	16	0.000	15	0.000	2.871	9.9	0.15	-	MBA
	126	27	6.05580	[9]	D2	8	18									
	336	64	6.05581	Revised	R1	8	22									
792 Metcalfa	274	-13	9.17821	[9]	D1	6	11	12	0.053	12	0.000	2.913	10.3	0.15	-	MBA
	88	-14	9.17821	[9]	D2	6	11									
	87	-16	9.17821	Revised	R1	6	15									
	273	-15	9.17821	Revised	R2	6	15									
798 Ruth	84	27	8.55068	[7]	D1	12	19	10	0.000	10	0.000	3.053	9.4	0.15	M	MBA
	85	34	8.55083	Revised	R1	12	23									
	253	51	8.55083	Revised	R2	12	23									
802 Epyaxa	347	-87	4.39012	[7]	D1	3	6	9	0.000	9	0.000	2.289	12.6	0.15	-	MBA
808 Merxia	26	54	30.62970	[4]	D1	1	7	13	0.000	13	0.000	2.920	9.7	0.15	-	MBA
	192	57	30.62960	[4]	D2	1	7									
	32	62	30.63011	Revised	R1	1	11									
	192	60	30.63006	Revised	R2	1	11									
812 Adele	148	72	5.85745	[9]	D1	1	5	12	0.000	12	0.000	2.615	11.5	0.15	-	MBA
	300	53	5.85745	[9]	D2	1	5									
	292	49	5.85744	Revised	R1	1	9									
	147	75	5.85744	Revised	R2	1	9									
816 Juliana	304	10	10.56277	[9]	D1	9	14	16	0.000	16	0.000	2.759	10.5	0.15	-	MBA
	124	-8	10.56272	[9]	D2	9	14									
832 Karin	242	46	18.35123	[4,32]	D1	2	15	14	0.000	14	0.000	2.886	11.2	0.15	-	MBA
	59	44	18.35121	[4,32]	D2	2	15									
	237	47	18.35127	Revised	R1	2	19									
	67	62	18.35129	Revised	R2	2	19									
834 Burnhamia	77	60	13.87594	[13]	D1	12	32	14	0.000	14	0.000	3.023	9.4	0.15	GS:	MBA
	256	69	13.87593	[13]	D2	12	32									
	76	58	13.87594	Revised	R1	12	36									
	243	72	13.87594	Revised	R2	12	36									
849 Ara	223	-40	4.11639	[1,2,34]	D1	3	23	13	0.174	13	0.000	2.791	8.1	0.15	M	MBA
	222	-39	4.11639	Revised	R1	3	27									
852 Wladilena	46	-53	4.61330	[9]	D1	17	32	14	0.000	14	0.000	2.687	9.9	0.15	-	MBA
	181	-48	4.61330	[9]	D2	17	32									
	187	-49	4.61330	Revised	R1	17	36									
	45	-53	4.61330	Revised	R2	17	36									
857 Glasenappia	38	34	8.20756	[9]	D1	1	7	30	0.000	30	0.000	2.174	11.3	0.15	MU	MBA
	227	48	8.20757	[9]	D2	1	7									
	224	48	8.20758	Revised	R1	1	15									

Table 5 continued

Table 5 (continued)

Asteroid	λ (deg)	β (deg)	P (hr)	Shape Reference(s)	Mod. ID	Den. LC	Tot. LC	N_{W3}	$W3$ Sat.	N_{W4}	$W4$ Sat.	r_{hel} (au)	H (mag)	G	Taxonomy	Orbit
	39	41	8.20758	Revised	R2	1	15									
872 Holda	253	32	5.94052	[7]	D1	5	14	17	0.000	17	0.000	2.930	9.9	0.15	M	X MBA
	77	24	5.94052	[7]	D2	5	14									
873 Mechthild	51	-61	11.00642	[7]	D1	7	10	14	0.000	14	0.000	2.637	11.5	0.15	PC	- MBA
	249	-52	11.00641	[7]	D2	7	10									
874 Rotraut	2	-36	14.30066	[9]	D1	1	5	12	0.000	12	0.000	3.336	10.0	0.15	-	- MBA
	201	-41	14.30065	[9]	D2	1	5									
	202	-27	14.30060	Revised	R1	1	9									
	6	-32	14.30061	Revised	R2	1	9									
875 Nympe	196	41	12.62133	[9]	D1	7	11	14	0.000	15	0.000	2.893	11.5	0.15	-	- MBA
	42	29	12.62133	[9]	D2	7	11									
890 Waltraut	122	72	12.58309	[26]	D1	8	29	12	0.000	12	0.000	3.119	10.8	0.15	CTGU:	- MBA
	30	69	12.58309	[26]	D2	8	29									
898 Hildegard	164	8	24.85440	[7]	D1	3	16	8	0.000	8	0.000	3.404	12.0	0.15	-	SI MBA
	344	27	24.85440	[7]	D2	3	16									
908 Buda	40	5	14.57498	[7]	D1	4	7	9	0.000	9	0.000	2.753	10.7	0.15	-	L MBA
	225	16	14.57504	[7]	D2	4	7									
918 Itha	72	-54	3.47381	[21,22]	D1	4	12	18	0.000	18	0.000	3.061	10.7	0.15	-	- MBA
951 Gaspra	198	15	7.04203	[28]	D1	25	73	17	0.000	17	0.000	2.574	11.5	0.15	S	S MBA
	20	23	7.04203	[28]	D2	25	73									
	20	23	7.04203	Revised	R1	25	77									
	197	15	7.04203	Revised	R2	25	77									
958 Asplinda	226	35	25.30500	[9]	D2	1	4	14	0.000	14	0.000	3.712	10.7	0.15	-	- OMB
	60	31	25.30516	Revised	R1	1	8									
	242	21	25.30515	Revised	R2	1	8									
984 Gretia	245	52	5.77803	[27]	D1	12	28	19	0.000	19	0.000	3.161	9.0	0.15	-	Sr MBA
	242	57	5.77803	Revised	R1	12	36									
986 Amelia	282	30	9.51855	[7]	D1	3	7	10	0.000	12	0.000	3.288	9.4	0.15	-	- MBA
	80	30	9.51856	[7]	D2	3	7									
	86	38	9.51859	Revised	R1	3	11									
	289	26	9.51856	Revised	R2	3	11									
1010 Marlene	106	47	31.06510	[7]	D1	2	9	16	0.000	16	0.000	2.994	10.4	0.15	-	- MBA
	299	42	31.06510	[7]	D2	2	9									
1021 Flammario	216	55	12.15184	[7]	D1	6	11	13	0.086	13	0.000	3.160	9.0	0.15	F	B MBA
	32	22	12.15186	[7]	D2	6	11									
1036 Ganymed	190	-78	10.31284	[6,32]	D1	111	179	23	0.000	23	0.000	3.468	9.4	0.30	S	S AMO
	10	-102	10.31284	Revised	R1	111	187									
1080 Orchis	71	28	16.06590	[7]	D1	8	14	18	0.000	18	0.000	2.088	12.2	0.15	F	- MBA
	255	27	16.06570	[7]	D2	8	14									

Table 5 continued

Table 5 (continued)

Asteroid	λ (deg)	β (deg)	P (hr)	Shape Reference(s)	Mod. ID	Den. LC	Tot. LC	N_{W3}	W3 Sat.	N_{W4}	W4 Sat.	τ_{hel} (au)	H (mag)	G	Taxonomy	Orbit	
															T1	T2	
1095 Tulipa	143	40	2.78715	[21]	D1	5	14	24	0.000	24	0.000	2.973	10.4	0.15	-	-	MBA
	350	56	2.78715	[21]	D2	5	14										
	137	53	2.78715	Revised	R1	5	22										
	340	51	2.78715	Revised	R2	5	22										
1103 Sequoia	60	-59	3.03798	[7]	D1	11	14	13	0.000	13	0.000	2.107	12.2	0.15	E	Xk	IMB
1111 Reinmuthia	29	70	4.00735	Revised	R1	7	20	14	0.000	14	0.000	3.285	10.7	0.15	FXU:	-	MBA
	184	76	4.00735	Revised	R2	7	20										
1117 Reginia	0	43	2.94647	[35]	D1	5	28	12	0.000	12	0.000	2.687	11.9	0.15	-	-	MBA
	174	49	2.94647	[35]	D2	5	28										
	359	34	2.94647	Revised	R1	5	32										
	170	39	2.94647	Revised	R2	5	32										
1125 China	305	-49	5.36863	[7]	D1	1	3	20	0.000	20	0.000	3.500	11.2	0.15	-	-	MBA
	132	-46	5.36863	[7]	D2	1	3										
1130 Skuld	25	42	4.80764	[9]	D1	11	18	12	0.000	12	0.000	2.153	12.1	0.15	-	-	MBA
	200	36	4.80764	[9]	D2	11	18										
1140 Crimea	198	38	4.80764	Revised	R1	11	22								S	S	MBA
	12	-73	9.78693	[4]	D1	2	6	21	0.000	21	0.000	2.990	10.3	0.15	-	-	MBA
	175	-22	9.78694	[4]	D2	2	6										
	358	-68	9.78689	Revised	R1	2	14										
	172	-22	9.78690	Revised	R2	2	14										
1148 Rarahu	146	-3	6.54448	[4,26]	D1	2	7	11	0.000	11	0.000	3.227	10.2	0.15	S	K	MBA
	327	-2	6.54448	[4,26]	D2	2	7										
1175 Margo	353	-17	6.01376	[7]	D1	2	5	14	0.000	14	0.000	3.061	10.2	0.15	-	-	OMB
	184	-43	6.01375	[7]	D2	2	5										
1188 Gothlandia	334	-84	3.49182	[9]	D1	28	38	26	0.000	25	0.000	2.524	11.7	0.15	-	S	MBA
	319	-82	3.49182	Revised	R1	28	46										
	128	-96	3.49182	Revised	R2	28	46										
1210 Morosovia	246	-78	15.26088	[26]	D1	7	14	11	0.000	11	0.000	2.856	9.9	0.15	MU:	-	MBA
	62	-70	15.26088	[26]	D2	7	14										
1241 Dysona	124	-68	8.60738	[9]	D1	3	13	13	0.000	13	0.000	3.521	9.4	0.15	PDC	-	MBA
	20	-23	8.60740	[9]	D2	3	13										
1249 Rutherfordia	365	69	18.21813	Revised	R1	3	12	12	0.000	14	0.000	2.244	11.5	0.15	S	-	MBA
	192	60	18.21815	Revised	R2	3	12										
1251 Hedera	271	-53	19.90200	[22]	D1	7	13	14	0.000	14	0.000	3.135	10.5	0.15	E	X	MBA
	115	-63	19.90200	[22]	D2	7	13										
1310 Villigera	240	26	7.82998	[7]	D1	3	5	21	0.000	21	0.000	2.779	11.4	0.15	S	-	MCA
	2	63	7.83002	[7]	D2	3	5										
1317 Silvretta	161	-46	7.06797	[9]	D1	3	16	16	0.000	16	0.000	2.551	9.9	0.15	CX:	-	OMB
	45	-57	7.06796	[9]	D2	3	16										

Table 5 continued

Table 5 (continued)

Asteroid	λ (deg)	β (deg)	P (hr)	Shape Reference(s)	Mod. ID	Den. LC	Tot. LC	N_{W3}	$W3$ Sat.	N_{W4}	$W4$ Sat.	τ_{hel} (au)	H (mag)	G	Taxonomy	Orbit	
														T1	T2		
1320 Impala	126	-70	6.17082	[21,22]	D1	5	12	14	0.000	14	0.000	3.474	10.4	0.15	-	-	MBA
	186	-43	6.17081	[21,22]	D2	5	12										
1332 Marconia	240	26	32.12000	[22,25]	D1	1	18	13	0.000	13	0.000	3.433	10.2	0.15	-	-	MBA
	59	26	32.12000	[22,25]	D2	1	18										
1333 Cevenola	38	-86	4.87932	[4]	D1	1	5	5	0.000	5	0.000	2.362	11.4	0.15	-	-	MBA
	220	-44	4.87932	[4]	D2	1	5										
1339 Desagneauxa	106	73	9.37509	[22,26]	D2	3	6	28	0.000	28	0.000	3.131	10.8	0.15	S	-	MBA
1352 Wawel	200	59	16.95430	[7]	D1	3	6	22	0.000	22	0.000	2.951	11.1	0.15	-	X	MBA
	32	61	16.95430	[7]	D2	3	6										
1353 Maartje	285	74	22.99240	[26,28]	D1	6	9	14	0.000	14	0.000	2.740	10.4	0.15	-	-	MBA
	120	42	22.99250	[26,28]	D2	6	9										
1360 Tarka	323	-55	8.86606	[7]	D1	6	11	20	0.000	21	0.000	3.198	11.0	0.15	-	Ch	MBA
1364 Safara	11	13	7.14907	[26]	D1	2	6	15	0.000	15	0.000	3.181	10.6	0.15	-	-	MBA
	198	32	7.14908	[26]	D2	2	6										
1386 Storeria	297	-67	8.67793	[9]	D1	7	13	15	0.000	14	0.000	3.036	12.6	0.15	-	Ch	MBA
	227	-67	8.67795	[9]	D2	7	13										
1388 Aphrodite	137	67	11.94393	[26]	D1	5	18	10	0.000	10	0.000	3.202	8.9	0.15	-	-	MBA
	326	35	11.94390	[26]	D2	5	18										
1401 Lavonne	204	23	3.93261	[9]	D1	2	5	13	0.000	14	0.000	2.626	12.2	0.15	S	-	MBA
	27	44	3.93261	[9]	D2	2	5										
1430 Somalia	128	47	6.90907	[7]	D1	5	7	13	0.000	13	0.000	2.647	12.8	0.15	-	-	MBA
	297	42	6.90907	[7]	D2	5	7										
1432 Ethiopia	41	44	9.84425	[9]	D2	4	13	37	0.000	37	0.000	2.699	11.7	0.15	-	-	MBA
	42	42	9.84428	Revised	R1	4	21										
	229	55	9.84426	Revised	R2	4	21										
1436 Salonta	223	18	8.86985	[9]	D1	9	12	13	0.000	13	0.000	3.333	10.3	0.15	-	-	MBA
	57	35	8.86987	[9]	D2	9	12										
	217	32	8.86979	Revised	R1	9	16										
	51	37	8.86984	Revised	R2	9	16										
1446 Sillanpaa	288	63	9.65855	[28]	D1	1	4	13	0.000	13	0.000	2.320	12.7	0.15	-	-	MBA
	129	76	9.65855	[28]	D2	1	4										
1449 Virtanen	307	58	30.50050	[7]	D1	3	12	11	0.000	11	0.000	2.540	12.4	0.15	S	-	MBA
	99	58	30.50060	[7]	D2	3	12										
1472 Muonio	42	62	8.70543	[9,32]	D1	5	8	13	0.000	13	0.000	2.681	12.7	0.15	-	-	MBA
	249	61	8.70543	[9,32]	D2	5	8										
1486 Marilyn	88	-66	4.56695	[7]	D1	4	6	18	0.000	18	0.000	1.959	13.0	0.15	-	-	MBA
	267	-66	4.56695	[7]	D2	4	6										
	90	-57	4.56694	Revised	R1	4	10										
	277	-52	4.56695	Revised	R2	4	10										

Table 5 continued

Table 5 (continued)

Asteroid	λ (deg)	β (deg)	P (hr)	Shape Reference(s)	Mod. ID	Den. LC	Tot. LC	N_{W3}	$W3$ Sat.	N_{W4}	$W4$ Sat.	τ_{hel} (au)	H (mag)	G	Taxonomy	Orbit
														T1	T2	
1495 Helsinki	355	-39	5.33131	[9]	D1	9	16	18	0.000	19	0.000	2.491	11.6	0.15	-	MBA
	-1	-47	5.33126	Revised	R1	9	20									
1518 Rovaniemi	265	45	5.25047	[9]	D1	1	4	9	0.000	9	0.000	2.513	12.3	0.15	-	MBA
	62	60	5.25047	[9]	D2	1	4									
1546 Izsak	124	32	7.33200	[7]	D1	2	5	12	0.000	12	0.000	2.939	10.6	0.15	-	MBA
	322	60	7.33198	[7]	D2	2	5									
1627 Ivar	334	39	4.79517	[32,36]	D1	13	86	13	0.000	13	0.000	2.117	13.2	0.60	S	AMO
	336	42	4.79517	Revised	R1	13	90									
1633 Chimay	116	81	6.59064	[28]	D1	1	5	12	0.000	12	0.000	3.549	10.5	0.15	-	MBA
	322	77	6.59064	[28]	D2	1	5									
1635 Bohrmann	5	-38	5.86427	[4]	D1	1	10	14	0.000	14	0.000	3.022	11.1	0.15	-	MBA
	185	-36	5.86428	[4]	D2	1	10									
	3	-40	5.86429	Revised	R1	1	14									
	187	-43	5.86429	Revised	R2	1	14									
1672 Gezelle	45	79	40.68240	[7]	D1	1	13	14	0.000	14	0.000	3.319	11.1	0.15	-	MBA
1685 Toro	85	-69	10.19780	Revised	R1	67	109	25	0.000	25	0.000	1.863	14.2	0.15	S	APO
1719 Jens	55	-42	5.87017	[9]	D1	2	6	14	0.000	14	0.000	2.474	11.3	0.15	-	MBA
	286	-88	5.87016	[9]	D2	2	6									
1723 Klemola	80	-59	6.25610	[22,26]	D1	10	17	30	0.000	30	0.000	2.991	10.1	0.15	S	MBA
	253	-36	6.25610	[22,26]	D2	10	17									
	252	-38	6.25610	Revised	R1	10	25									
	78	-62	6.25610	Revised	R2	10	25									
1730 Marceline	82	44	3.83654	[7]	D1	1	3	17	0.000	17	0.000	2.537	11.5	0.15	-	MBA
	264	68	3.83654	[7]	D2	1	3									
	68	27	3.83656	Revised	R1	1	7									
1741 Giclas	105	30	2.94252	[37]	D1	24	59	12	0.000	12	0.000	3.084	11.2	0.15	-	MBA
	288	24	2.94252	[37]	D2	24	59									
	287	22	2.94252	Revised	R1	24	62									
	105	27	2.94252	Revised	R2	24	62									
1789 Dobrovolsky	320	-37 ^a	4.81138	Revised	R1	1	8	12	0.000	12	0.000	2.240	13.0	0.15	-	MBA
	141	-34 ^a	4.81138	Revised	R2	1	8									
1865 Cerberus	306	-77	6.80329	Revised	R2	22	52	17	0.000	16	0.000	1.092	16.8	0.15	S	APO
1925 Franklin-Adams	277	57	2.97830	[7]	D1	1	3	15	0.000	15	0.000	2.956	12.0	0.15	-	MBA
	66	48	2.97830	[7]	D2	1	3									
1930 Lucifer	32	17	13.05361	[4]	D1	3	9	14	0.000	14	0.000	3.269	10.9	0.15	-	MBA
	39	17	13.05364	Revised	R1	3	13									
	220	-13	13.05364	Revised	R2	3	13									
1963 Bezevec	222	2	18.16539	Revised	R1	6	18	11	0.000	11	0.000	2.906	10.9	0.15	C	MBA
	73	-65 ^a	18.16563	Revised	R2	6	18									

Table 5 continued

Table 5 (continued)

Asteroid	λ (deg)	β (deg)	P (hr)	Shape Reference(s)	Mod. ID	Den. LC	Tot. LC	N_{W3}	$W3$ Sat.	N_{W4}	$W4$ Sat.	τ_{hel} (au)	H (mag)	G	Taxonomy	Orbit	
															T1	T2	
1987 Kaplan	356	-58	9.45950	[28]	D1	6	10	22	0.000	21	0.000	2.605	11.4	0.15	-	-	MBA
	344	-85	9.45949	Revised	R1	6	18										
2001 Einstein	87	-43	5.48503	[7]	D1	12	14	14	0.000	14	0.000	2.107	12.8	0.15	X	Xe	IMB
2110 Moore-Sitterly	91	-75	3.34473	[37]	D1	35	48	18	0.000	18	0.000	2.348	13.8	0.15	-	-	MBA
	270	-77	3.34473	[37]	D2	35	48										
	354	-89	3.34473	Revised	R1	35	55										
2306 Bauschinger	225	-65	21.67040	[7]	D1	3	7	23	0.000	22	0.000	2.795	11.4	0.15	-	X	MBA
	0	-64	21.67040	[7]	D2	3	7										
	223	-79	21.67048	Revised	R1	3	15										
2381 Landi	220	-36	3.98604	[7]	D1	4	7	12	0.000	13	0.000	2.611	11.4	0.15	-	-	MBA
	36	-67	3.98604	Revised	R1	4	11										
	230	-30	3.98604	Revised	R2	4	11										
2384 Schulhof	172	-76	3.29368	[9,38]	D1	8	25	15	0.000	15	0.000	2.498	12.2	0.15	-	-	MBA
	63	-56	3.29368	[9,38]	D2	8	25										
	62	-53	3.29368	Revised	R1	8	29										
	149	-80	3.29368	Revised	R2	8	29										
2455 Somville	224	-68	2.82868	[39]	D1	4	13	15	0.000	15	0.000	2.510	11.7	0.15	-	C	MBA
	39	-48	2.82868	[39]	D2	4	13										
2606 Odessa	283	-88	8.24446	[9,32]	D1	1	5	13	0.000	13	0.000	3.476	11.3	0.15	-	Xk	MBA
2659 Millis	109	-49	6.12464	[7]	D1	1	3	11	0.000	11	0.000	3.457	11.2	0.15	-	B	MBA
	288	-48	6.12464	[7]	D2	1	3										
2839 Annette	154	-36	10.46090	[9]	D1	3	9	13	0.000	13	0.000	2.458	12.3	0.15	-	-	MBA
	341	-49	10.46091	[9]	D2	3	9										
2957 Tatsuo	81	45	6.82042	[9]	D1	4	15	16	0.000	16	0.000	2.756	10.2	0.15	-	K	MBA
	248	32	6.82038	[9]	D2	4	15										
3478 Fanale	297	62	3.24484	[7]	D1	4	6	14	0.000	14	0.000	2.217	12.8	0.15	-	-	MBA
3544 Borodino	294	-60	5.43460	[7]	D2	6	8	29	0.000	29	0.000	2.068	12.5	0.15	-	-	MBA
	286	-67	5.43460	Revised	R1	6	16										
	154	-69	5.43460	Revised	R2	6	16										
3722 Urata	77	-9	5.56712	[9]	D1	5	11	13	0.000	13	0.000	2.460	12.9	0.15	-	-	MBA
	260	-22	5.56712	[9]	D2	5	11										
3786 Yamada	218	48	4.03295	[7]	D1	1	4	12	0.000	12	0.000	2.364	11.2	0.15	-	-	MBA
	84	52	4.03295	[7]	D2	1	4										
4077 Asuka	57	45	7.92310	[26]	D2	4	10	13	0.000	13	0.000	3.289	11.4	0.15	-	-	MBA
	255	50	7.92310	Revised	R1	4	14										
	46	41	7.92311	Revised	R2	4	14										
4265 Kani	106	60	5.72755	[7]	D1	2	5	12	0.000	12	0.000	2.912	12.8	0.15	-	C	MBA
	310	54	5.72755	[7]	D2	2	5										
	110	1 ^a	5.72857	Revised	R1	2	8										

Table 5 continued

Table 5 (continued)

Asteroid	λ (deg)	β (deg)	P (hr)	Shape Reference(s)	Mod. ID	Den. LC	Tot. LC	N_{W3}	W3 Sat.	N_{W4}	W4 Sat.	τ_{hel} (au)	H (mag)	G	Taxonomy	Orbit
	289	8 ^a	5.72857	Revised	R2	2	8									
4606 Saheki	44	59	4.97347	[28]	D1	1	8	10	0.000	10	0.000	2.430	12.7	0.15	-	MBA
	222	68	4.97347	[28]	D2	1	8									
	190	69	4.97347	Revised	R1	1	12									
	28	69	4.97347	Revised	R2	1	12									
4905 Hiromi	185	-86	6.04484	[37]	D1	13	18	15	0.000	15	0.000	2.385	12.1	0.15	-	MBA
	123	-86	6.04484	Revised	R1	13	22									
5489 Oberkothen	13	-66	5.62440	[7]	D1	2	4	14	0.000	14	0.000	2.857	11.5	0.15	-	MBA
	195	-41	5.62439	[7]	D2	2	4									
6262 Javid	93	76	8.02054	[28]	D1	2	5	11	0.000	11	0.000	3.053	12.9	0.15	-	MBA
7043 Godart	235	80	8.45181	[28]	D1	3	5	12	0.000	12	0.000	2.641	12.8	0.15	-	MBA
	73	62	8.45178	[28]	D2	3	5									
	52	50	8.45184	Revised	R1	3	7									
	210	70	8.45187	Revised	R2	3	7									
7517 Alisondoane	123	-51	9.70943	[9]	D1	3	5	8	0.000	8	0.000	2.995	13.1	0.15	-	MBA
	306	45 ^a	9.70224	Revised	R1	3	7									
7660 Alexanderwilson	273	-58	5.91692	Revised	R2	5	13	26	0.000	26	0.000	1.842	14.2	0.15	-	MCA
8359 1989WD	121	-68	2.89103	[9]	D1	1	8	12	0.000	12	0.000	2.453	12.4	0.15	-	MBA
	274	-68	2.89103	[9]	D2	1	8									
14197 1998 XK72	38	-62	10.64536	[7]	D1	3	5	12	0.000	12	0.000	3.110	13.4	0.15	-	MBA
	192	-74	10.64534	[7]	D2	3	5									
28736 2000 GE133	249	-52	4.65442	[7]	D1	1	4	15	0.000	16	0.000	2.146	13.4	0.15	-	MBA
	134	-84	4.65443	[7]	D2	1	4									
28887 2000 KQ58	182	-35	6.84315	[7]	D1	2	7	15	0.000	15	0.000	2.420	13.4	0.15	-	MBA
	354	-78	6.84316	[7]	D2	2	7									
33116 1998 BO12	244	69	6.34669	[7]	D1	2	5	14	0.000	14	0.000	2.000	13.8	0.15	-	MBA
	45	54	6.34669	[7]	D2	2	5									
44612 1999 RP27	8	-73	4.90706	[37]	D2	20	34	11	0.000	7	0.000	2.224	15.9	0.15	-	MBA
55760 1992 BL1	318	-36	8.08610	[40]	D1	3	5	43	0.000	44	0.000	1.655	12.9	0.15	-	MCA

Table 5 continued

Table 5 (continued)

Asteroid	λ (deg)	β (deg)	P (hr)	Shape Reference(s)	Mod. ID	Den. LC	Tot. LC	N_{W3}	$W3$ Sat.	N_{W4}	$W4$ Sat.	τ_{hel} (au)	H (mag)	G	Taxonomy	Orbit
															T1	T2

^a Shape model has a substantially revised pole ($\Delta\beta > 30^\circ$) compared with the DAMIT shape model(s).

References—[1] Āurech et al. (2009); [2] Āurech et al. (2011); [3] Hanuš et al. (2013a); [4] Hanuš et al. (2011); [5] Torppa et al. (2003); [6] Kaasalainen et al. (2002a); [7] Hanuš et al. (2016b); [8] Stephens et al. (2012); [9] Hanuš et al. (2013b); [10] Marciniak et al. (2008); [11] Marciniak et al. (2012); [12] Marciniak et al. (2011); [13] Marciniak et al. (2019); [14] Polishook (2009); [15] Āurech et al. (2007); [16] Delbo' & Tanga (2009); [17] Descamps et al. (2009); [18] Marciniak et al. (2018); [19] Slihan et al. (2003); [20] Warner et al. (2008); [21] Āurech et al. (2018c); [22] Āurech et al. (2016); [23] Marciniak et al. (2007); [24] Marchis et al. (2006); [25] Āurech et al. (2019); [26] Hanuš et al. (2018b); [27] Marciniak et al. (2009a); [28] Hanuš et al. (2013c); [29] Michałowski et al. (2005); [30] Vokrouhlický et al. (2016a); [31] Warner (2008); [32] Hanuš et al. (2015); [33] Kaasalainen et al. (2002b); [34] Marciniak et al. (2009b); [35] Franco et al. (2019); [36] Kaasalainen et al. (2004); [37] Pravec et al. (2019); [38] Vokrouhlický et al. (2016b); [39] Franco et al. (2015); [40] Āurech et al. (2018a)

NOTE—Shape models and thermal infrared observations used for a portion of our final 1847 asteroid sample in Table 4, limited to the 270 asteroids with the most reliable shape models, as defined in §4.2. The full table can be found online. Shape information is given in four columns, consisting of the pole’s ecliptic coordinates of the shape model used λ and β , the sidereal rotational period P , and the reference(s) given in DAMIT where available. The model ID is given to identify the shape model used in the TPM fits in Table 4; the “D” and “R” designations respectively refer to DAMIT and our revised shape models. We give the number of dense and total lightcurves used in the inversion code to generate the shape model. N_{W3} and N_{W4} are the number of thermal flux measurements in the $W3$ and $W4$ WISE bands respectively. The “Sat.” columns refer to the median saturated pixel fraction over all observations used. τ_{hel} is the corresponding median heliocentric distance. Absolute magnitude H and slope G are referenced from AAMS (Muinonen et al. 2010; Oszkiewicz et al. 2011). The T1 (Tholen 1984) or T2 (SMASS II; Bus & Binzel 2002) taxonomy and the orbital classification are referenced from the JPL Small-Body Database. The orbits are classed as one of the following: inner or outer main-belt asteroids (MBA, IMB, OMB), Jupiter Trojans (TJN), Apollo or Amor NEAs (APO, AMO), or Mars crossers (MCA).

Table 6. Candidates for Yarkovsky Detection

Asteroid		Γ ($\text{J m}^{-2} \text{s}^{-0.5} \text{K}^{-1}$)	D (km)	A	χ_{red}^2	ρ (g cm^{-3})	Dense LC	A_2 ($10^{-15} \text{ au day}^{-2}$)
1685	Toro	210^{+85}_{-55}	$3.6^{+0.2}_{-0.1}$	$0.099^{+0.007}_{-0.009}$	1.8	2.72^a	67	$-2.6^{+0.3}_{-0.2}$
1865	Cerberus	809^{+219}_{-134}	$1.2^{+0.0}_{-0.0}$	$0.061^{+0.000}_{-0.001}$	1.6	2.72^a	22	$-7.2^{+0.8}_{-0.6}$
2818	Juvenalis	57^{+36}_{-57}	$4.7^{+0.3}_{-1.0}$	$0.083^{+0.052}_{-0.010}$	1.8	2.72^a	0	$-2.2^{+2.2}_{-0.6}$
2991	Bilbo	63^{+56}_{-44}	$8.4^{+0.9}_{-1.2}$	$0.031^{+0.012}_{-0.006}$	7.5	1.38^b	0	$2.1^{+0.4}_{-0.4}$
4928	Vermeer	106^{+85}_{-69}	$3.7^{+0.4}_{-0.4}$	$0.085^{+0.025}_{-0.015}$	4.0	2.71^b	0	$-2.0^{+0.6}_{-0.4}$
5240	Kwasan	69^{+206}_{-52}	$6.8^{+0.7}_{-0.9}$	$0.138^{+0.048}_{-0.025}$	6.2	1.93^a	0	$-1.9^{+1.0}_{-0.4}$
5760	Mittlefehldt	61^{+36}_{-27}	$9.9^{+0.6}_{-0.8}$	$0.038^{+0.007}_{-0.004}$	2.3	1.38^b	0	$-2.0^{+0.3}_{-0.2}$
6581	Sobers	55^{+408}_{-53}	$4.7^{+0.7}_{-0.5}$	$0.098^{+0.023}_{-0.023}$	3.1	2.71^b	0	$-2.0^{+1.2}_{-0.4}$
6744	Komoda	54^{+372}_{-54}	$4.2^{+0.8}_{-1.1}$	$0.090^{+0.076}_{-0.026}$	2.3	2.71^b	0	$-1.9^{+1.9}_{-0.8}$
7196	Baroni	53^{+276}_{-48}	$4.2^{+0.9}_{-0.6}$	$0.107^{+0.037}_{-0.034}$	2.4	2.71^b	0	$-2.3^{+1.2}_{-0.6}$
9234	Matsumototaku	42^{+66}_{-41}	$3.1^{+0.2}_{-0.3}$	$0.091^{+0.023}_{-0.012}$	1.8	2.71^b	0	$-2.8^{+2.7}_{-0.8}$
9274	Amylovell	144^{+201}_{-89}	$5.7^{+0.7}_{-0.8}$	$0.022^{+0.008}_{-0.004}$	4.8	1.38^b	0	$-2.6^{+1.3}_{-1.1}$
9566	Rykhlova	65^{+38}_{-33}	$8.8^{+0.4}_{-0.5}$	$0.020^{+0.003}_{-0.002}$	3.2	1.38^b	0	$-2.0^{+0.5}_{-0.2}$
9582	1990 EL7	61^{+127}_{-61}	$4.0^{+0.7}_{-0.6}$	$0.098^{+0.040}_{-0.027}$	3.1	2.71^b	0	$-2.0^{+2.0}_{-0.5}$
11676	1998 CQ2	111^{+36}_{-39}	$5.8^{+0.4}_{-0.5}$	$0.016^{+0.003}_{-0.002}$	1.6	1.38^b	0	$-2.6^{+0.3}_{-0.3}$
12417	1995 TC8	62^{+159}_{-39}	$3.7^{+0.8}_{-0.6}$	$0.086^{+0.037}_{-0.029}$	2.6	2.71^b	0	$2.0^{+0.5}_{-0.9}$
12926	Brianmason	41^{+32}_{-16}	$9.8^{+0.7}_{-0.8}$	$0.037^{+0.007}_{-0.006}$	1.7	1.38^b	0	$2.1^{+0.4}_{-0.5}$
12979	Evgalvasil'ev	93^{+115}_{-69}	$2.8^{+0.4}_{-0.4}$	$0.108^{+0.035}_{-0.023}$	1.3	2.71^b	0	$-3.2^{+1.1}_{-0.6}$
14197	1998 XK72	83^{+82}_{-39}	$7.7^{+1.2}_{-0.9}$	$0.036^{+0.010}_{-0.009}$	2.5	1.38^b	3	$-2.5^{+0.7}_{-0.4}$
15920	1997 UB25	70^{+107}_{-58}	$2.9^{+0.3}_{-0.2}$	$0.126^{+0.024}_{-0.026}$	3.1	2.71^b	0	$-2.4^{+1.7}_{-0.5}$
16669	Rionuevo	78^{+111}_{-41}	$3.9^{+0.3}_{-0.2}$	$0.066^{+0.007}_{-0.010}$	4.5	2.71^b	0	$-2.3^{+0.5}_{-0.1}$
17431	Sainte-Colombe	62^{+98}_{-52}	$3.9^{+0.5}_{-0.5}$	$0.099^{+0.029}_{-0.020}$	2.8	2.71^b	0	$2.1^{+0.4}_{-0.5}$
18997	Mizrahi	61^{+85}_{-61}	$6.8^{+1.4}_{-1.0}$	$0.021^{+0.008}_{-0.007}$	7.6	1.38^b	0	$-2.8^{+2.8}_{-0.5}$
19136	Strassmann	54^{+251}_{-54}	$3.8^{+0.8}_{-0.4}$	$0.057^{+0.016}_{-0.018}$	2.3	2.71^b	0	$-2.3^{+2.3}_{-0.5}$
19876	7637 P-L	50^{+41}_{-48}	$3.4^{+0.2}_{-0.3}$	$0.120^{+0.026}_{-0.012}$	1.3	2.71^b	0	$2.1^{+0.3}_{-1.9}$
19985	1990 GD	60^{+70}_{-42}	$3.0^{+0.3}_{-0.2}$	$0.118^{+0.019}_{-0.018}$	0.6	2.71^b	0	$2.7^{+0.3}_{-0.6}$
20179	1996 XX31	47^{+74}_{-32}	$7.8^{+0.9}_{-0.8}$	$0.034^{+0.009}_{-0.006}$	7.2	1.38^b	0	$-2.4^{+1.3}_{-0.6}$
21041	1990 QO1	38^{+35}_{-31}	$10.2^{+0.7}_{-1.5}$	$0.036^{+0.013}_{-0.005}$	3.3	1.38^b	0	$-2.1^{+1.3}_{-0.4}$
23004	1999 VH114	91^{+525}_{-91}	$6.3^{+0.9}_{-0.9}$	$0.032^{+0.011}_{-0.007}$	2.0	1.38^b	0	$-3.1^{+3.1}_{-0.6}$
25327	1999 JB63	60^{+45}_{-31}	$4.1^{+0.2}_{-0.2}$	$0.071^{+0.008}_{-0.008}$	1.5	2.71^b	0	$-2.3^{+0.6}_{-0.2}$
25887	2000 SU308	70^{+51}_{-38}	$8.9^{+0.9}_{-0.6}$	$0.016^{+0.002}_{-0.003}$	3.5	1.38^b	0	$2.2^{+0.3}_{-0.8}$
26176	1996 GD2	65^{+207}_{-53}	$7.0^{+0.8}_{-1.0}$	$0.022^{+0.009}_{-0.004}$	5.3	1.38^b	0	$-2.2^{+0.6}_{-0.6}$
28575	McQuaid	43^{+80}_{-35}	$4.3^{+0.6}_{-0.5}$	$0.014^{+0.004}_{-0.003}$	1.0	1.38^b	0	$2.1^{+1.2}_{-1.6}$
28736	2000 GE133	65^{+37}_{-36}	$9.2^{+0.6}_{-0.7}$	$0.020^{+0.004}_{-0.002}$	6.5	1.38^b	1	$-2.1^{+0.5}_{-0.2}$

Table 6 continued

Table 6 (continued)

Asteroid		Γ ($\text{J m}^{-2} \text{s}^{-0.5} \text{K}^{-1}$)	D (km)	A	χ_{red}^2	ρ (g cm^{-3})	Dense LC	A_2 ($10^{-15} \text{ au day}^{-2}$)
32507	2001 LR15	45^{+109}_{-40}	$6.5^{+1.3}_{-0.7}$	$0.022^{+0.006}_{-0.006}$	6.8	1.38^b	0	$-2.9^{+0.7}_{-0.6}$
33181	Aalokpatwa	54^{+78}_{-32}	$7.2^{+1.2}_{-0.7}$	$0.021^{+0.005}_{-0.005}$	5.1	1.38^b	0	$-2.4^{+0.6}_{-0.3}$
33974	2000 ND17	26^{+20}_{-18}	$7.1^{+0.3}_{-0.3}$	$0.015^{+0.001}_{-0.001}$	1.6	1.38^b	0	$-2.2^{+1.3}_{-0.6}$
38650	2000 ON17	144^{+112}_{-59}	$7.0^{+0.5}_{-0.6}$	$0.013^{+0.003}_{-0.002}$	5.0	1.38^b	0	$2.0^{+0.6}_{-0.7}$
38950	2000 ST295	130^{+106}_{-86}	$4.1^{+0.5}_{-0.4}$	$0.064^{+0.015}_{-0.012}$	2.2	2.71^b	0	$-2.4^{+0.8}_{-0.5}$
40852	1999 TX105	21^{+54}_{-21}	$6.6^{+0.7}_{-0.4}$	$0.029^{+0.004}_{-0.005}$	3.4	1.38^b	0	$-2.1^{+2.1}_{-0.8}$
42490	1991 SU	71^{+131}_{-71}	$3.9^{+0.4}_{-0.3}$	$0.123^{+0.023}_{-0.022}$	0.8	2.71^b	0	$2.0^{+0.2}_{-2.0}$
44612	1999 RP27	368^{+716}_{-246}	$2.5^{+0.4}_{-0.4}$	$0.061^{+0.027}_{-0.015}$	0.5	2.71^b	20	$-2.2^{+1.4}_{-2.6}$
45898	2000 XQ49	136^{+125}_{-68}	$2.2^{+0.2}_{-0.3}$	$0.272^{+0.081}_{-0.046}$	0.7	2.71^b	0	$2.5^{+0.9}_{-1.1}$
47085	1999 AW2	58^{+93}_{-51}	$6.4^{+0.9}_{-1.2}$	$0.020^{+0.011}_{-0.005}$	2.3	1.38^b	0	$-2.2^{+1.7}_{-0.6}$
48981	1998 QD45	56^{+81}_{-55}	$3.2^{+0.5}_{-0.4}$	$0.119^{+0.034}_{-0.030}$	2.3	2.71^b	0	$-1.9^{+1.8}_{-0.4}$
49088	1998 RS68	117^{+72}_{-49}	$4.5^{+0.3}_{-0.3}$	$0.066^{+0.009}_{-0.007}$	1.2	2.71^b	0	$-2.0^{+0.4}_{-0.2}$
51227	2000 JK25	60^{+79}_{-43}	$8.6^{+1.3}_{-1.0}$	$0.023^{+0.006}_{-0.005}$	5.2	1.38^b	0	$-1.9^{+0.5}_{-0.3}$
57429	2001 SX33	46^{+53}_{-46}	$7.5^{+0.8}_{-0.9}$	$0.018^{+0.006}_{-0.003}$	5.0	1.38^b	0	$-1.9^{+1.9}_{-0.6}$
57458	2001 SX73	65^{+77}_{-64}	$2.5^{+0.3}_{-0.3}$	$0.085^{+0.022}_{-0.020}$	1.8	2.71^b	0	$-3.2^{+0.9}_{-0.5}$
59150	1998 XV90	62^{+33}_{-33}	$7.5^{+0.5}_{-0.9}$	$0.026^{+0.008}_{-0.003}$	2.3	1.38^b	0	$-2.0^{+0.4}_{-0.3}$
68513	2001 UL167	25^{+129}_{-25}	$3.3^{+0.7}_{-0.4}$	$0.050^{+0.014}_{-0.016}$	1.5	2.71^b	0	$-2.2^{+2.2}_{-1.4}$
76516	2000 GX39	64^{+89}_{-42}	$5.6^{+0.6}_{-0.8}$	$0.020^{+0.007}_{-0.004}$	0.9	1.38^b	0	$-3.5^{+0.8}_{-0.6}$
77594	2001 KQ21	82^{+101}_{-60}	$8.1^{+1.2}_{-1.1}$	$0.018^{+0.007}_{-0.004}$	1.5	1.38^b	0	$-2.2^{+0.6}_{-0.4}$
79056	1132 T-3	157^{+202}_{-88}	$1.9^{+0.2}_{-0.1}$	$0.056^{+0.006}_{-0.010}$	1.1	2.71^b	0	$4.1^{+0.5}_{-1.5}$
89932	2002 EV85	38^{+21}_{-35}	$7.0^{+0.5}_{-0.5}$	$0.017^{+0.003}_{-0.002}$	1.4	1.38^b	0	$2.1^{+0.5}_{-1.8}$
92729	2000 QX99	42^{+90}_{-42}	$3.4^{+0.5}_{-0.4}$	$0.023^{+0.007}_{-0.006}$	1.2	1.38^b	0	$-3.4^{+3.4}_{-2.7}$
99028	2001 DC98	36^{+29}_{-28}	$5.0^{+0.8}_{-0.4}$	$0.020^{+0.003}_{-0.005}$	1.5	1.38^b	0	$-3.7^{+2.3}_{-0.6}$

NOTE—Asteroids in our sample with a transverse acceleration parameter A_2 greater than the smallest published value of $A_2 = 1.9 \times 10^{-15} \text{ au day}^{-2}$ for (35107) 1991 VH. We estimate A_2 with the best-fit values for the thermal inertia Γ , the diameter D , and Bond albedo A with Equation 7. χ_{red}^2 refers to that of the TPM fit. The bulk density ρ is either (a) assumed to be equal to the average bulk density of the SMASS II (Bus & Binzel 2002) taxonomic type of the asteroid according to Carry (2012) or (b) assumed to be equal to the Krasinsky et al. (2002) average bulk densities for C-types for $p_V < 0.10$ and S-types for $p_V > 0.10$. Note that a thermal inertia of $0 \text{ J m}^{-2} \text{ s}^{-0.5}$ will drop the A_2 parameter to zero, hence the unconstrained lower bound on A_2 for 11 of these asteroids. While A_2 for (1685) Toro given here is estimated from our derived parameters, we note that it also has a detected Yarkovsky drift of $A_2 = -3.339 \pm 0.6433 \times 10^{-15} \text{ au day}^{-2}$. Further details can be found in §4.4.